PROTEIN ADSORPTION

TO

POLYETHYLENE OXIDE-GRAFTED SURFACES

By

JACQUES GÉRARD ARCHAMBAULT, B.Sc., B.A.Sc.

A Thesis

Submitted to the School of Graduate Studies

In Partial Fulfilment of the Requirements

For the Degree

Doctor of Philosophy

McMaster University

PROTEIN ADSORPTION

TO

POLYETHYLENE OXIDE-GRAFTED SURFACES

DOCTOR OF PHILOSOPHY (2002)
(Chemical Engineering)

McMaster University
Hamilton, ON

TITLE: **Protein Adsorption to Polyethylene Oxide-Grafted Surfaces**

AUTHOR: **Jacques Gérard Archambault, B.Sc., B.A.Sc.**
(University of Ottawa)

SUPERVISOR: **Professor J.L. Brash**

NUMBER OF PAGES: **xx, 253**

ABSTRACT

The objective of this work was to study and gain a better understanding of the mechanisms and factors that mediate how effectively grafted polyethylene oxide chains promote protein repellency.

A polyurethane-urea was used as a substrate to which PEO was grafted. This material was synthesised by conventional methods and characterised using water contact angles, XPS and AFM. A grafting protocol was developed based on methods found in the literature, involving the introduction of isocyanate groups into the polyurethane surface followed by reaction of amine- or hydroxyl-terminated PEO. Surfaces grafted with PEO chains of various lengths were prepared and characterised by water contact angles, XPS and AFM. The data showed that the amine-terminated polyethylene oxide gave higher PEO graft densities than the hydroxy-terminated polyethylene oxide. Direct measurements of the grafting density of PEO via radiolabeling resulted in only qualitative data due to experimental problems associated with the measurements.

Protein adsorption studies were performed with the PEO-grafted surfaces. Several factors anticipated to have an impact on the effectiveness of the PEO-grafted surfaces in repelling proteins were examined. The levels of protein adsorption generally decreased with increasing PEO graft molecular weight. The reduction generally reached a maximum at a PEO MW of 2000. Adsorption levels on surfaces with 5000 and 2000 MW grafts

were usually similar. Adsorption levels on surfaces prepared with amino-terminated PEO were in agreement with the surface characterisation data that indicated higher levels of grafted PEO.

On most of the surfaces, there was little or no effect of protein size on the ability of the PEO grafts to inhibit protein adsorption. However a surface grafted with PEO of MW 550 adsorbed smaller proteins more extensively that larger proteins. The data also showed little or no effect of protein isoelectric point on PEO surfaces with long PEO-grafts probably due to surface charge "masking" by the PEO grafts. Surfaces with shorter PEO grafts, however, showed lower levels of adsorption for the more highly charged proteins. This effect may have been due to electrostatic protein-protein repulsion as protein accumulated at the interface.

Experiments to investigate the effect of temperature on protein repulsion by the PEO-grafted surfaces showed that the properties of the proteins themselves play a large role in determining levels of adsorption and that the solution properties of PEO (inverse temperature dependence) could not explain the effects observed.

Results of experiments using multi-protein systems showed that the PEO-grafted surfaces did not repel proteins selectively: only the total quantity of protein adsorbing to the surfaces was affected.

ACKNOWLEDGEMENTS

I would like to express my gratitude to Dr. John Brash, who provided guidance and encouragement throughout my journey to complete this thesis. His great patience and compassion, especially near the end when I faced many obstacles, was much appreciated. A special thanks to a longtime friend and fellow traveller, Bryan Wickson, with whom I journeyed the longest. I would also like to thank Gary Skarja for his friendship over the years. My memories of the first few years at McMaster with Bryan and Gary were among the very best. I would also like to thank Glenn McClung and Rena Cornelius for their friendship and the valuable assistance they often provided. I was fortunate to meet and befriend many others during my time at McMaster and I would thank them as well: Ying Jun Du, Xiaoling Sun, Akiko Yamazaki, Jiahong Tan, Meghan Price and Larry Unsworth.

I would like to dedicate this thesis to my parents and brothers who offered continuous support and encouragement over the years.

TABLE OF CONTENTS

LIST OF FIGURES

LIST OF TABLES

LIST OF ABBREVIATIONS

AFM	Atomic force microscopy
BCIP	5-Bromo-4-chloro-3-indoyl phosphate p-toluidine salt
C.I.	Confidence interval
DMF	Dimethylformamide
DMSO	Dimethyl sulfoxide
EO	Ethylene oxide
HMDI	Hexamethylene diisocyanate
MDA	Methylene dianiline
MDI	4,4'-Methylenebis(phenyl isocyanate)
MW	Molecular weight
NBT	p-Nitro blue tetrazolium
PAGE	polyacrylamide gel electrophoresis
PEO	Polyethylene oxide
PTMEG	Polytetramethylene ether glycol (also called PTMO)
PTMO	Polytetramethylene oxide (also called PTMEG)
PPP	Platelet poor plasma
PUU	Polyurethaneurea
RF	Radio frequency
SAM	Self-assembled monolayer
SCMF	Single-chain mean field
S.D.	Standard deviation
SDS	Sodium dodecyl sulphate
TEMED	N,N,N',N'-Tetramethylethylenediamine
Tris	Tris(hydroxymethyl)aminomethane
XPS	X-ray photoelectron spectroscopy

1.0 INTRODUCTION

One of the primary goals of research in the field of biomaterials is the development of a material resistant to fouling and able to avoid triggering unwanted biological responses. Such a material does not yet exist. All materials that come into contact with a biological fluid containing proteins invariably show signs of protein adsorption to their surfaces. For this reason, the adsorption of proteins at interfaces remains an area of intense research in the field of biomaterials and in many areas of biotechnology such as food processing, diagnostic systems, biosensors, protein separation and purification.

The study and development of materials that reduce or possibly eliminate protein adsorption is desired to help reduce unfavourable biological responses such as biofouling of implants, blood coagulation and immune responses. An approach that has yielded some success is the grafting of polyethylene oxide (PEO) chains onto materials. This modification has been shown to increase protein "resistance" and may be beneficial to overall biocompatibility.

There has, however, been little systematic research on the nature of the interactions between proteins and grafted PEO chains and the impact of such factors as protein size and charge. The research conducted in this project was intended to provide new knowledge to fill these gaps.

PEO of varying molecular weight was grafted to a polyurethane substrate. The

resulting experimental surfaces were characterised with water contact angles, XPS and AFM. Experiments were performed to measure the graft density of the PEO chains on the surfaces. Protein adsorption studies were performed to examine the impact of several factors on the effectiveness of the grafted PEO layer at repelling proteins. These included the properties of the PEO (MW, hydroxy- versus amino-terminated PEO), and the properties of the proteins (size, isoelectric point). The effects of temperature were also investigated. Multi-protein systems as well as single proteins in buffer were studied.

2.0 LITERATURE REVIEW

2.1 Polyurethanes and polyurethaneureas

Polyurethanes (PUs) and polyurethaneureas (PUUs) have long been used in biomedical applications because of their excellent mechanical properties and relatively good biocompatibility. Both are block copolymers where two alternating blocks are separated by urethane groups (PU) or urethane and urea groups (PUU). One of the alternating blocks, the soft segment, is usually a polyether, a polyester or a polyalkyldiol with a molecular weight between 500 and 5000 [Lelah, M.D. and Cooper, S.L., 1986]. The second alternating block, the hard segment, is created by the reaction of a diisocyanate with a chain extender, often a low molecular weight diamine or diol.

2.1.1 Synthesis

Polyurethane synthesis is usually carried out in two steps. The first step involves the reaction of the soft segment species with a diisocyanate in a 1:2 ratio to form the prepolymer. This attaches an isocyanate group to each end of the soft segment precursor and forms the characteristic urethane bond. This reaction is illustrated in Figure 2.1.

A chain extender is then used to link the prepolymer molecules to form long chains via reaction of the prepolymer molecules with the hydroxyl or amino groups of the chain extender, forming urethane or urea groups respectively [Lelah, M.D. and Cooper, S.L., 1986]. An "ideal" PU or PUU where the two alternating blocks are clearly represented is illustrated in Figure 2.2.

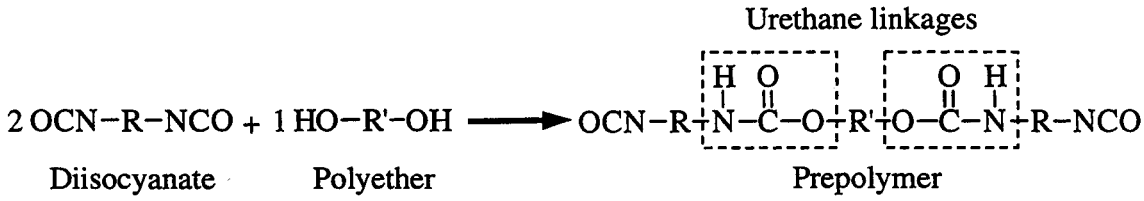

Figure 2.1: Formation of the prepolymer.

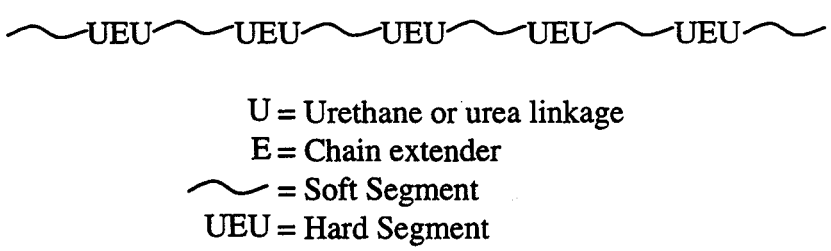

Figure 2.2: Theoretical structure of a polyurethane where the soft segment, diisocyanate and chain extender are reacted in a 1:2:1 ratio. Adapted from [Lelah, M.D. and Cooper, S.L., 1986].

There are several undesirable side-reactions that may arise during polyurethane synthesis. Water can react with isocyanate groups to form amines. Water can therefore transform the diisocyanate into its mono or diamino analogs which could be integrated into the polymer chain, thus disrupting the expected stoichiometry and structure. Ensuring anhydrous reaction conditions is therefore very important.

Other side reactions result from the fact that the urethane and urea groups on the polymer chains can also react with isocyanate groups forming allophanate and biuret groups as illustrated in Figure 2.3.

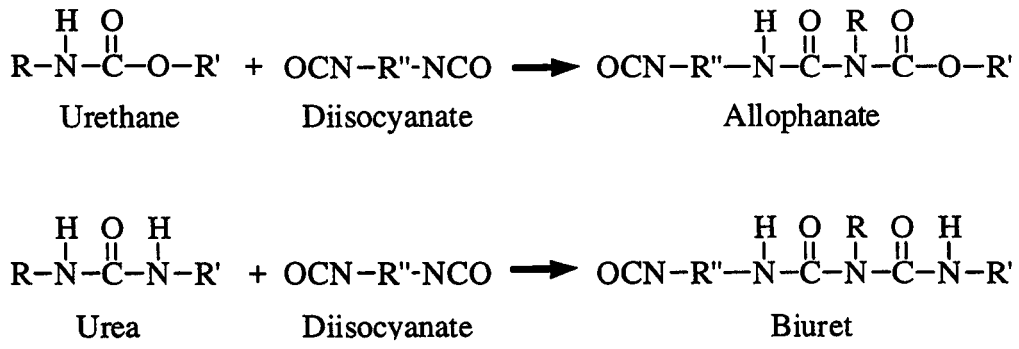

Figure 2.3: Allophanate and biuret side-reactions in polyurethane synthesis.

These reactions lead to branching and cross-linking in the polymer. They also disrupt the stoichiometry and have a negative impact on the mechanical properties of the polymer. However, the occurrence of these reactions can be minimised by keeping reaction temperatures below 100°C during the chain extension reaction [Saunders, J.H., 1969].

2.1.2 Structure and Properties

Polyurethane elastomers exhibit a two-phase microstructure. The relatively stiff hard segments tend to coalesce into discrete semicrystalline "hard" domains. These hard segment domains are generally surrounded by an amorphous or semicrystalline soft segment matrix. This segregation of the hard and soft segments into distinct microphases leads to the excellent physical and mechanical properties characteristic of polyurethanes [Lelah, M.D. and Cooper, S.L., 1986]. The elastic properties of the soft segment matrix coupled with the reinforcing nature of the "hard" domains yields polymers with elasticity and high modulus [Lelah, M.D. and Cooper, S.L., 1986]. These properties make polyurethanes ideal for various applications in the biomedical field. However, although

these materials have reasonable biocompatibility, there is considerable room for improvement [Noshay, A. and McGrath, J.E., 1977].

2.1.3 Surface Modification

The biocompatibility of PUs or PUUs can be improved while maintaining their desirable mechanical properties by chemically altering only the surface of the polymer thereby leaving the bulk unchanged. The literature dealing with surface modification of PUs or PUUs is extensive and diverse. Since the objective of this thesis is to study the effect of PEO grafts, this section of the literature review will be limited to surface modification techniques using PEO.

One technique takes advantage of the urethane functional groups present on the surface of PU films [Han, D.K. et al., 1989]. Films were reacted with HMDI in toluene with the aid of a catalyst, stannous octoate. This reaction forms an allophanate functional group, as illustrated in Figure 2.3, and introduces free isocyanates which can then react with PEO in benzene, again using stannous octoate as a catalyst . Another group used a very similar protocol. However, in their case, both reaction steps were performed in toluene and triethylamine, the catalyst, was used only in the first step [Freij-Larsson, C. and Wesslén, B., 1993].

Another approach involves the use of free radical reactions to graft PEO chains to the polymer surface. In one technique, PU films were first exposed to a hydrogen peroxide solution that introduced peroxide groups into the soft segment [Brinkman, E. et al., 1990]. The films were then exposed to a solution containing ferrous sulphate,

sulphuric acid and methoxy-poly(ethylene glycol) 400 methacrylate. The ferrous ions react with the peroxide groups to generate radicals that initiate the polymerisation of the methacrylate groups . Another free radical technique used by this group involved dipping PU films in a solution of PEO and dicumyl peroxide and allowing to dry. The reaction was initiated by exposing the films to ultraviolet light or by heating. The result was a crosslinked network involving PEO and the PU soft segment (a polyether in this instance) [Brinkman, E. et al., 1989].

Fujimoto et al. used a plasma glow discharge treatment with argon and subsequent exposure to air to introduce surface peroxides into PU films. The films were then placed in an aqueous solution containing methoxy-poly(ethylene glycol) 400 methacrylate. The mixture was heated to initiate polymerisation of the monomer by causing the thermal decomposition of the peroxides [Fujimoto, K. et al., 1993].

2.2 Protein Adsorption

One of the first events to occur upon exposing a surface to a protein-containing fluid, is adsorption of the proteins. Such adsorption occurs to some extent on virtually all surfaces [Andrade, J.D., 1985a]. The surface activity of proteins is due to their large size, amphipathic properties and the variety of interactions that can develop between proteins and surfaces.

2.2.1 Protein Structure

Proteins are macromolecules of biological origin. They are the products of the sequential linking together of 20 different amino acids. The sequence of amino acid

residues constitutes the primary structure of the protein. The peptide group which links the amino acids can, through hydrogen bonding to other protein molecules or to other residues in the same molecule, rearrange the conformation of the polypeptide chain to form complex secondary structures such as the α-helix and the β-sheet. Other intramolecular interactions such as disulphide bonding, salt bridging, ionic and hydrophobic interactions, along with hydrogen bonding, lead to the unique tertiary structure of the protein. In some cases, multiple peptide chains associate to form a protein with a quaternary structure. Many proteins are also glycosylated; i.e. they have polysaccharide chains attached pendant to the polypeptide backbone. Therefore proteins have an almost infinite diversity of chemical structures, and this is the essential reason for the inherent complexity of protein adsorption.

The three dimensional structure of globular proteins, although well defined in the native state, is relatively easily disrupted. Indeed, factors such as pH, ionic strength and temperature have an impact on the conformation of the molecule and hence on the domains that are available for their interactions with surfaces [Andrade, J.D., 1985a]. Figure 2.4 illustrates the multiple-domain structure of the surface of a protein interacting with a hypothetical multi-domain adsorbing surface.

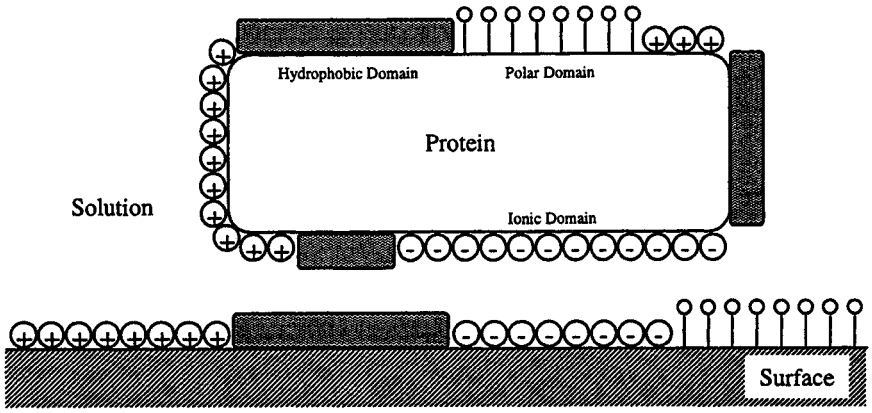

Figure 2.4: Schematic representation of a protein interacting with a surface. Adapted from [Andrade, J.D., 1985a].

2.2.2 Factors Influencing Protein Adsorption

2.2.2.1 Driving Forces for protein Adsorption

The driving forces leading to protein adsorption are important since they influence the adsorption kinetics, the quantity of protein adsorbed and the protein layer structure. Protein adsorption will occur only if the Gibbs free energy of the process is negative. The expression for the Gibbs free energy is:

$$\Delta G = \Delta H - T\Delta S \tag{2.1}$$

The enthalpic contribution to the driving force includes van der Waals, hydrophobic and electrostatic interactions. The entropic contributions include the release of counterions and/or solvation water and the reduction of ordered structure in the protein as a result of conformational changes following adsorption.

The electrostatic and van der Waals interactions occur both intramolecularly within the protein and between the protein and the surface; the former also includes ion coadsorption, and the formation of ion pairs. Depending on the pH and ionic strength of

the solution, as well as the charge distribution on the protein and surface, the adsorption event can be either endothermic or exothermic [Norde, W. and Haynes, C.A., 1995]. In cases where the adsorption is endothermic, the driving force is entropic in nature [Andrade, J.D., 1985a][Norde, W. and Haynes, C.A., 1995][Norde, W., 1992].

The entropic driving force is fuelled by dehydration effects and protein denaturation [Norde, W. and Haynes, C.A., 1995][Norde, W., 1992]. Interactions between hydrophobic regions of the protein and the surface cause a dehydration of these domains, leading to an increase in entropy due to the disruption of the ordered water associated with these domains [Andrade, J.D., 1985a][Norde, W. and Haynes, C.A., 1995][Norde, W., 1992]. In many cases, this contribution dominates the overall driving force for protein adsorption [Norde, W., 1992].

In native proteins, maintenance of structure is favoured by intramolecular hydrophobic interactions in the interior of the protein, and is opposed by intramolecular electrostatic repulsion and conformational entropy loss due to folding [Norde, W. and Haynes, C.A., 1995][Norde, W., 1992]. However, upon adsorption, the protein can modify its conformation and keep its hydrophobic interior regions dehydrated via interaction with hydrophobic domains on the surface [Haynes, C.A. and Norde, W., 1994]. This unfolding may be favoured by a reduction in intramolecular electrostatic repulsion as like charges may be more separated from one another and also by an increase in the entropy of the protein due to greater conformational freedom [Norde, W. and Haynes, C.A., 1995][Duinhoven, S. et al., 1995]. The characteristics of the surface will

determine the extent of conformational change and denaturation upon adsorption [Koutsoukos, P.G. et al., 1982].

2.2.2.2 Other Factors

Size is an important factor in protein adsorption since it is believed that proteins can form multiple contacts with surfaces. Hence the greater the size of the protein, the larger the area capable of interacting with the surface. The widely observed kinetic irreversibility of protein adsorption is thought to derive from the low probability of simultaneously breaking all contacts as required for the protein to dissociate from the surface [Horbett, T.A. and Brash, J.L., 1987].

The chemical properties of the protein will also influence adsorption. The net global charge as well as the charge distribution and the presence of hydrophobic domains will all impact on adsorption behaviour. The conformation of proteins in an aqueous environment will be such that many hydrophobic residues will be oriented toward the interior of the molecule whereas hydrophilic residues will generally be found on the exterior [Norde, W. and Lyklema, J., 1991]. As a result of these energetic considerations, a mosaic of domains with varying chemical identities are found on the protein surface, as is illustrated in Figure 2.4. Proteins are therefore able to interact with a variety of different sites.

The nature of the solvent can also have a significant impact on protein adsorption because of its effect on the structure and stability of the protein in solution. Therefore, pH and ionic strength should be considered. Studies have shown that the maximum

of a protein is typically found near the isoelectric point (IEP) [Norde, W., 1986]. Since the protein net charge is low near the IEP, protein-protein interactions become more favourable due to a decrease in electrostatic repulsion. Increases in ionic strength shields charges and lowers the impact of electrostatic repulsion, leading to increased adsorption as well [Norde, W., 1986].

The conformational stability of a protein is also believed to have an impact on adsorption. So-called "soft" proteins, prone to denaturation, are likely to be more surface active since additional interactions are possible upon unfolding. On the other hand, "hard" proteins, whose structures are stabilised by disulphide bonds or other means, would be less surface active since only limited conformational changes are possible upon adsorption. As well, proteins with quaternary structure could have increased surface activity due to rearrangements in the orientation of non-covalently bound subunits [Horbett, T.A. and Brash, J.L., 1987].

2.2.3 Models for Protein Adsorption

The Langmuir theory, derived for reversible gas adsorption, is frequently applied to model protein adsorption from solution. The Langmuir equation has the form:

$$\theta = \frac{K[P]}{1+K[P]} \tag{2.2}$$

where θ is the fraction of surface sites occupied by adsorbed protein, [P] is the solution protein concentration and K is the adsorption equilibrium constant.

There are problems associated with fitting protein adsorption data to the Langmuir model in that many of the underlying assumptions are not satisfied. The model is based on

There are problems associated with fitting protein adsorption data to the Langmuir model in that many of the underlying assumptions are not satisfied. The model is based on reversible interactions whereas protein adsorption has generally been observed to be at least partly irreversible [Norde, W. and Haynes, C.A., 1995][Brash, J.L. and Horbett, T.A., 1995][Norde, W., 1992]. Other problems include non-negligible lateral interactions between adsorbed proteins, change of protein structure upon adsorption and involvement of multiple sites in a single adsorption event. As a result, some authors have argued that equilibrium constants derived from these analyses are without physical meaning [Norde, W., 1992]. Others believe that these constants can at least provide qualitative information on binding affinity [Brash, J.L. and Horbett, T.A., 1995].

A model that attempts to deal with irreversible adsorption is the random sequential adsorption model (RSA) [Schaaf, P. and Talbot, J., 1989]. In this treatment, adsorbed molecules, represented by spheres or circular disks, are not able to diffuse on the surface, nor can they desorb from it. As a result, the process surface eventually reaches a "jamming limit" at which no further adsorption can occur. The RSA model addresses two shortcomings of the Langmuir model with respect to protein adsorption. First it stipulates irreversible adsorption and second, it replaces the Langmuirian factor for available area, $(1-\theta)$, with a surface availability function, ϕ, that does not limit the proteins to interact with only one adsorption site. Data showing that protein diffusion over the surface does occur [Rabe, T.E. and Tilton, R.D., 1993], argue against the RSA model.

empty sites. Once adsorbed, the protein spreads symmetrically to a larger diameter if no overlap with other proteins would result. The non-linear nature of the surface blockage inherent in this model leads to a slower approach to saturation than for other models with linear surface blockage such as the Langmuir model. This property also ensures that the post-adsorption spreading of the proteins will not be complete. The model also predicts that the extent of spreading decreases with increasing bulk protein concentration. This results from the increased rate of adsorption at higher bulk concentrations causing faster surface blockage thereby limiting the area available for spreading.

Several empirical models can also be used to describe protein adsorption. One is the Freundlich isotherm given by equation (2.3):

$$\theta = k[P]^{\frac{1}{n}} \tag{2.3}$$

where k and n are empirical constants characteristic of the system and temperature. This model can be derived on the assumption that the distribution of binding energies decreases exponentially [Thomson, S.J. and Webb, G., 1968][Adamson, A.W., 1990]. The Temkin isotherm, on the other hand, assumes linearly decreasing binding energy as the surface coverage increases yielding:

$$\theta = -\frac{RT}{\Delta H_0 \alpha}\ln(K[P]) \tag{2.4}$$

where K is the equilibrium binding constant corresponding to the maximum binding energy, ΔH_0 is the maximum heat of adsorption and α is an empirical constant [Thomson, S.J. and Webb, G., 1968][Johnson, R.D. and Arnold, F.H., 1995].

where K is the equilibrium binding constant corresponding to the maximum binding energy, ΔH_0 is the maximum heat of adsorption and α is an empirical constant [Thomson, S.J. and Webb, G., 1968][Johnson, R.D. and Arnold, F.H., 1995].

2.2.4 Multi-Protein Systems

Biological fluids generally contain a number of different proteins. When several proteins are in competition for binding sites, the surface concentration of a given protein will depend on its properties, the surface and the solvent [Andrade, J.D., 1985a]. In addition, the composition of the protein layer is not necessarily fixed; it may undergo time-dependent changes. The proteins present in high concentration are expected to dominate the surface initially. Other proteins with higher surface affinities may eventually displace these proteins. After a long time interval, only the proteins with the highest surface activities will dominate the surface, even if their solution concentrations are low [Andrade, J.D., 1985a][Brash, J.L., 1987].

Adsorption in multi-protein systems will of course be modulated by irreversibilities in protein surface interactions as indicated above. The situation becomes extremely complex in plasma or blood since there are at least 200 proteins competing for the same surface sites. Adsorption of the three most abundant plasma proteins, albumin, IgG and fibrinogen has been studied extensively [Brash, J.L. and Tenhove, P., 1984][Horbett, T.A., 1984]. Protein displacement as described above occurs, for instance, when plasma is exposed to a hydrophilic surface. Initially adsorbed fibrinogen is eventually displaced by other proteins, e.g. high molecular weight kininogen and, to a

lesser extent, factor XII, both of which are present in plasma at substantially lower concentrations than fibrinogen [Vroman, L. and Adams, A.L., 1969].

2.3 Polyethylene Oxide (PEO)

2.3.1 Structure and Properties

Polyethylene oxide (or polyethylene glycol) is a neutral polyether that is soluble in water as well as in many organic solvents. PEO has the following structure:

$$-(CH_2CH_2O)_n-$$

This simple polymer is attractive as a biomaterial for many reasons. PEO is only weakly immunogenic, does not cause denaturation or inactivation of proteins, and is not cytotoxic [Harris, J.M., 1992]. In addition, PEO is a neutral molecule and has only weakly acidic terminal hydroxyl groups and weakly basic ether linkages; there are thus few sites to which proteins can bind [Harris, J.M., 1992][Gölander, C.G. et al., 1986]. Due to its high chain mobility and high excluded volume, PEO also has the propensity to exclude other molecules from its region of influence when in an aqueous environment [Mori, Y. et al., 1982][Horinaka, J. et al., 1998][Ryle, A.P., 1965][Hellsing, K., 1968].

The solution properties of PEO are unusual. For molecular weights above ~2100, a solubility gap exists at higher temperatures [Saeki, S. et al., 1976]; i.e. PEO comes out of solution at the cloud point temperature or lower critical solution temperature and redissolves at the upper critical solution temperature. Also, as the molecular weight of PEO increases, the cloud point temperature decreases.

Unfortunately, PEO as a material lacks the mechanical properties to replace common biomaterials such as PUs or PUUs. Many investigators have speculated that upon coating or attaching PEO to the surface of a substrate with suitable mechanical properties, the underlying material would gain, at its surface, the desired properties of the polyether in aqueous solution. Hence PEO could potentially confer the desirable properties of protein rejection, non-immunogenicity and non-antigenicity to a variety of materials [Harris, J.M., 1992].

A variety of methods have been used to attach PEO to different materials. These include simple adsorption of PEO or PEO containing copolymers onto materials, physical entrapment of the PEO chains, heat-, radiation- or plasma-mediated crosslinking of adsorbed PEO, covalent grafting of PEO chains onto a surface via chemical modification, incorporation of PEO into block copolymers or polymer networks, attachment of PEO via graft copolymerisation or plasma polymerisation, radio frequency plasma deposition of short ethylene oxide oligomers, and chemisorption of thiolated PEOs to gold-coated substrates. In studies where the protein adsorption characteristics of PEO-modified surfaces were examined, most of the methods were successful in enhancing protein resistance to some degree, and in some cases, quite dramatically [Gombotz, W.R. et al., 1991; Lopez, G.P. et al., 1992; Mcpherson, T.B. et al., 1997; Prime, K.L. and Whitesides, G.M., 1993; Wu, Y.J. et al., 2000].

2.3.2 Mechanisms of Protein Repellency

Grafting hydrophilic polymers, particularly PEO, to various substrates remains a common strategy to limit or prevent protein adsorption. There is still debate, however, as to the mechanisms that confer protein resistance on surfaces upon attachment of PEO and in what manner they can best be exploited.

Depending on the graft density, two regimes with different characteristics emerge [De Gennes, P.G., 1987]. The first is called the "mushroom" regime and consists of isolated polymer coils anchored to the surface, where the distance between grafting sites (D) is larger than the Flory radius (R_F), i.e. $D>R_F$. The second regime occurs when $D<R_F$. The grafting sites are close enough that the polymer coils must extend away from the surface forming a "brush". Hence under these conditions, a "brush" regime exists.

Several theoretical treatments investigating protein-surface interactions in the presence of grafted polymer chains have been published. In one study, the model examined van der Waals and hydrophobic attractions in addition to steric repulsion based on scaling concepts developed by de Gennes [De Gennes, P.G., 1979][Jeon, S.I. et al., 1991b][Jeon, S.I. and Andrade, J.D., 1991a]. As a protein diffuses towards the PEO-grafted surface in the "brush" regime, it comes under the influence of van der Waals interactions with the PEO chains. Compression of the PEO chains caused by the approach of the protein results in a loss of entropy which contributes to steric repulsion. Steric repulsion results from osmotic pressure and elastic restoring forces [De Gennes, P.G., 1987]. Van der Waals attraction between the protein and the substrate through the

hydrated PEO layer becomes more important as the protein approaches the surface. Finally, the protein is considered to have a hydrophobic attraction to the substrate.

The first paper [Jeon, S.I. et al., 1991b] used a simplified treatment in which a protein is modelled as an infinitely large plate, shown in Figure 2.5(a). The authors concluded that optimal protein resistance required high surface density and long PEO chains, the former being of greater importance . A subsequent analysis [Jeon, S.I. and Andrade, J.D., 1991a] in which additional hydrophobic interactions between the PEO chains and the protein were considered, used spheres of finite size to model proteins. The model system is shown in Figure 2.5(b). This study showed that the optimal grafting density decreased as the size of the protein increased and that densely packed PEO chains might not necessarily be protein resistant. This conclusion originates from the opposing effects of steric repulsion and the weak hydrophobic interaction between the PEO chains and the protein. The authors also concluded that for a given optimal grafting density, the PEO chain length should be as long as possible .

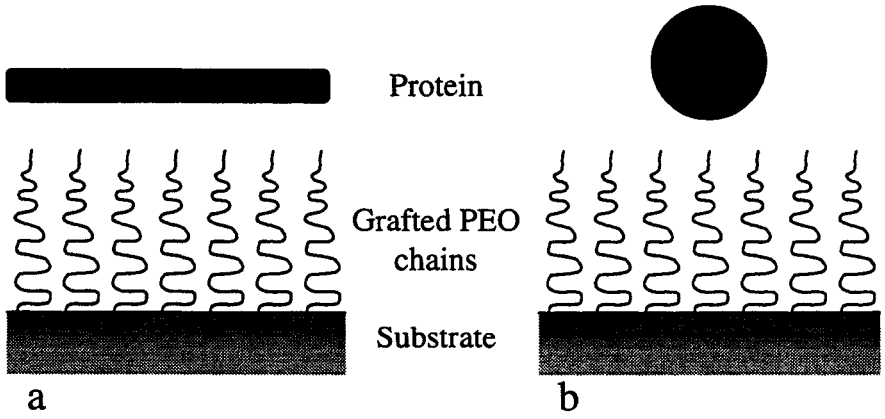

Figure 2.5: (a) Model of PEO-grafted substrate with protein of infinite size. (b) Model of PEO-grafted substrate with protein of finite spherical shape. Adapted from [Jeon, S.I. et al., 1991b] and [Jeon, S.I. and Andrade, J.D., 1991a].

Szleifer developed another theoretical approach based on a generalisation of the single-chain mean-field theory (SCMF) [Szleifer, I., 1997]. The model system consists of a mixture of grafted polymer chains, proteins and solvent molecules, as shown in Figure 2.6. The SCMF framework considers all intramolecular and surface interactions of a grafted polymer chain in an exact fashion and treats intermolecular interactions with a mean-field approximation. The interactions between proteins and the solid surface include electrostatic, van der Waals and hydrophobic components. Interactions between chain segments and the solid surface as well as intramolecular interactions involving chain segments are also considered. All protein-polymer, protein-solvent and polymer-solvent attractive interactions are assumed to be equal. A probability density function provides the probability for each of the system's configurations as a function of the thermodynamic variables. Actual calculations were performed using a spherical model lysozyme and grafted PEO. The results showed that lysozyme adsorption levels decreased as grafting density increased. Increasing the PEO chain length also decreased adsorption levels. When attractive interactions between the polymer segments and the surface were ignored, adsorption reached a minimum at a PEO chain length of 50 and did not decrease further at higher chain lengths. When these attractive interactions were considered, the adsorption minimum occurred at a chain length of 125. The model predicted elimination of adsorption with a grafting density of 4×10^{-3} chains/Å^2 for grafts with a molecular weight of 2200 or greater.

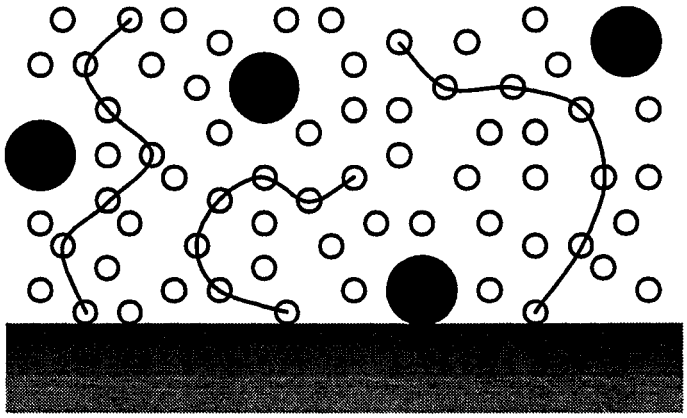

Figure 2.6: Model of the PEO-grafted substrate in contact with a protein solution. The connected circles represent the polymer chains, the small circles are solvent molecules and the large circles are proteins. Adapted from [Szleifer, I., 1997].

Halperin also investigated a polymer brush model in order to identify parameters that may influence adsorption [Halperin, A., 1999]. The analysis modelled polymers as simple flexible chains and proteins as dense, rigid particles. The two parameters with the biggest impact on the effectiveness of the brush in suppressing adsorption are grafting density and layer thickness. The layer thickness is a function of the polymer chain length and graft density. According to this model, proteins approaching a bare surface encounter a purely attractive interaction potential, U_{bare}, shown in Figure 2.7(a). When the proteins enter the brush layer, a purely repulsive interaction potential is encountered, U_{brush}. The effective interaction potential is therefore the sum of these two components giving the curve in Figure 2.7(b). The general shape of this overall potential is characterised by two minima: a primary minimum, U_{in}, close to the surface and a secondary minimum, U_{out}, at the periphery of the brush. These minima give rise to two adsorption modes predicted by the model.

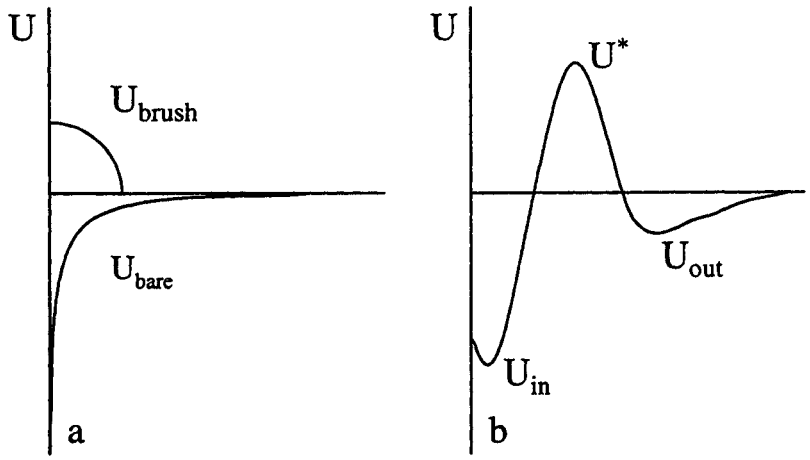

Figure 2.7: (a) Attractive interaction potential between the bare surface and a protein, U_{bare}, and repulsive interaction potential between the brush and a protein, U_{brush}. (b) Effective potential encountered by a protein approaching a surface with a polymer brush, the sum of the potentials in (a). Adapted from [Halperin, A., 1999].

Primary adsorption was found to be important for small proteins capable of penetrating the layer between the polymer chains to adsorb to the surface as shown in Figure 2.8(a). This adsorption mode is suppressed by increasing the density of the polymer brush. Secondary adsorption is important for large proteins and takes place at the outer surface of the brush, as shown in Figure 2.8(b); it is the result of attractive van der Waals interactions between the protein and the surface. This mode of adsorption is suppressed by increasing the thickness of the brush. Therefore, the characteristics of the brush can be tailored to fit specific requirements by using appropriate graft density and chain length when designing the material.

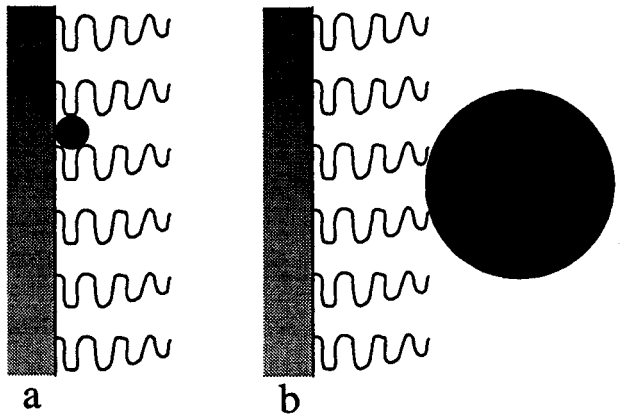

Figure 2.8: (a) Primary adsorption. (b) Secondary adsorption. Adapted from [Halperin, A., 1999].

Another model [Antonsen, K.P. and Hoffman, A.S., 1992] attempts to describe some of the properties of PEO by examining how water associates with PEO chains. The model assumes that for PEO of short chain length, only tightly bound water interacts. As the chain length increases and overlap occurs, intersegmental interactions trap additional loosely bound water molecules thereby "binding together" the polymer coil and making protein interactions more difficult. This transition zone was found to occur at a chain length of about 22.

These theoretical studies, along with the results of other investigations, have led to the widely held theory that the protein rejecting capability of PEO coatings has three origins. First, the electrical neutrality and chemical structure of PEO is generally believed to offer few potential protein binding sites. However recent findings have shown that weak protein binding sites do exist and that, under certain conditions, PEO can behave as a polyelectrolyte [Furness, E.L. et al., 1998][Zhivkova, I.V. et al., 1998]. Second, surfaces coated with PEO cause a reduction of the interfacial energy, thereby reducing the driving

force for protein adsorption [Coleman, D.L. et al., 1982]. Third, the large exclusion volume of PEO results from hydration and the rapid motion of the highly flexible polyether chains [Mori, Y. et al., 1982][Horinaka, J. et al., 1998][Antonsen, K.P. and Hoffman, A.S., 1992].

The sequence of events describing the protein rejecting capacity of PEO is described as follows. A protein approaches a surface bearing a PEO layer. The presence of the polymer layer gives rise to several effects that contribute to reduced adsorption [Leckband, D. et al., 1999]. First, the favourable free energy change when the protein adsorbs to the underlying substrate is countered by the steric repulsion caused by the compression of the grafted polymer chains as the protein approaches. Second, the protein must overcome a potential energy barrier to penetrate the polymer layer and reach the underlying surface. This impeded approach caused by the polymer chains also increases the effective viscosity and therefore significantly lowers the rate of transport to the surface compared to simple diffusion. The compression of the polyether chains against the surface by the approaching protein leads to an unfavourable negative entropy change due to the mobility constraints placed on the polymer chains. In addition, compression forces the release of water from the hydrated PEO chains, thus increasing the entropy of the system. However, this is accompanied by an increase in the local concentration of monomer units creating an osmotic driving force that draws water molecules back into the coils of the polyether chains. The net result is that the approach of a protein causes an increase in the overall free energy and therefore adsorption does not occur. This mechanism is referred to as steric repulsion [Gombotz, W.R. et al., 1992].

The proponents of this theory have argued that short chain PEO should be less effective in making a surface protein resistant due to the reduced ability of short chains to trap (and release) water, and to the reduced mobility of short chains and therefore smaller excluded volume [Mori, Y. et al., 1982][Antonsen, K.P. and Hoffman, A.S., 1992]. In addition, it is claimed that short PEO chains may not be able to mask the surface effectively from approaching proteins; i.e. the proteins may be able to "sense" the surface through the thin PEO layer [Bergstrom, K. et al., 1992]. However, results from recent studies suggest that the main requirement is high surface coverage by an ethylene oxide "film" or by very short oligomers of ethylene oxide [Lopez, G.P. et al., 1992; Palegrosdemange, C. et al., 1991; Prime, K.L. and Whitesides, G.M., 1993; Wu, Y.J. et al., 2000]. The water molecules associated with the ethylene oxide oligomers are tightly bound and it is postulated that the layer of hydrated oligomers prevents proteins from interacting with the underlying surface. However, there is evidence that even these oligomers must have a specific conformation to acquire protein rejecting characteristics (see below) [Harder, P. et al., 1998]. Regardless of the actual mechanism, the most important variables appear to be grafting density and chain length.

2.3.3 Factors Influencing Protein Repellency

Despite the large volume of experimental work in this area, only a handful of studies offer insight on the properties that PEO-modified surfaces should have to promote protein repellency effectively.

2.3.3.1 PEO Molecular Weight

Tan et al. adsorbed various Pluronics® (triblock copolymers with end blocks of PEO and a centre block or PPO) to polystyrene particles and found that fibrinogen adsorption decreased rapidly with increasing PEO block length up to ~75 ethylene oxide (EO) units (MW 3300); adsorption continued to decrease as the length of the PEO blocks increased, but at a much slower rate [Tan, J.S. et al., 1993]. Amiji and Park examined fibrinogen adsorption to Pluronics®-coated dimethyldichlorosilane (DDS)-treated glass and low density polyethylene (LDPE). They found similar reductions in fibrinogen adsorption on surfaces coated with triblock copolymers in which the PEO block length ranged from 19 to 129 EO units (MW between 800 and 5700) as long as the PPO block was long enough to ensure the polymers were tightly anchored to the surface. When copolymers with shorter PPO blocks were used, fibrinogen adsorption decreased as the length of the PEO blocks increased. The authors concluded that tight surface binding of the PPO anchors was more important than PEO chain length [Amiji, M. and Park, K., 1992].

In another study, several Pluronics® copolymers were covalently grafted by γ-irradiation to trichlorovinylsilane-treated glass tubes. This method made the preparation of a wide variety of stable films possible. The PPO and PEO blocks ranged in length from 16 to 67 and from 2 to 128 repeat units, respectively. Significant decreases in fibrinogen and lysozyme adsorption were observed on copolymers with PEO blocks as short as 3 EO units. The authors concluded that the length of the PEO blocks in the copolymer had only

a weak effect in reducing protein adsorption to the treated glass tubes [McPherson, T. et al., 1998][Mcpherson, T.B. et al., 1995].

In a series of papers, Bergström reported grafting PEO (MW 250-19000) to aminated polystyrene. They found that fibrinogen adsorption decreased sharply with increasing PEO molecular weight to a value of 1500 before levelling off [Bergstrom, K. et al., 1992][Bergstrom, K. et al., 1994]. Gombotz used RF glow discharge methods to deposit allyl amine and allyl alcohol films on polyethylene terephthalate (PET). The introduced amino and hydroxyl groups were then activated with cyanuric chloride and reacted with PEO (MW 200-20000). It was found that fibrinogen and albumin adsorption decreased sharply with increasing PEO molecular weight up to ~1000-2000 and then levelled off. It was suggested that the optimal PEO molecular weight is in the region of 2000-3500 [Gombotz, W.R. et al., 1991][Gombotz, W.R. et al., 1989]. Llanos and Sefton found little difference in the reduction of BSA adsorption to polyvinyl alcohol (PVA) grafted with PEO of MW 2000 or 5000 [Llanos, G.R. and Sefton, M.V., 1993]. Desai and Hubbell grafted PEO to PET and also used a surface-physical-interpenetrating-network (SPIN) method to entrap PEO (MW 5000-100000) in PET. Based on fibrinogen and albumin protein adsorption experiments, they concluded that the optimum MW to prevent protein adsorption was near 18,500 where protein adsorption was reduced by 80%. The other MWs showed decreases of only 5-25% [Desai, N.P. and Hubbell, J.A., 1991].

Prime and Whitesides chemisorbed alkanethiols terminated with oligo(ethylene oxide) chains on gold surfaces. The self-assembled monolayers (SAMs) generated by this method were used to give high density layers of short (1 to 17 repeat units) oligoethylene

oxide moieties. It was found that even one ethylene oxide unit significantly reduced protein adsorption, provided the surface density was sufficiently high. Surfaces prepared with chains having 2 repeat units of ethylene oxide completely inhibited protein adsorption of four different proteins, within detectable limits. In addition, when longer oligo(ethylene oxide) chains were used, lower surface densities were sufficient to inhibit protein adsorption; that is, the longer chains were more effective in reducing protein adsorption. Finally, the presence of terminal methoxy groups did not prevent inhibition of protein adsorption and the behaviour of MeO-terminated PEO was not much different than the hydroxy-terminated analogues [Prime, K.L. and Whitesides, G.M., 1993].

Lee and Laibinis prepared self assembled monolayers (SAM) on silicon wafers with a thin oxide layer by adsorbing oligo(ethylene oxide)-terminated alkanetrichlorosilanes [Lee, S.-W. and Laibinis, P.E., 1998]. The performance of the SAMs on the silica substrate was slightly inferior to similarly prepared SAMs on gold surfaces. The silicon-based SAMs had up to four ethylene oxide repeat units and were able to inhibit nearly completely the adsorption of four proteins and significantly reduce the adsorption of a fifth, fibrinogen. As the number of ethylene oxide units in the SAMs increased, the adsorbed protein layer thickness decreased .

2.3.3.2 Graft Density

McPherson's studies also examined the effect of PEO graft density on protein adsorption to glass tubes covalently grafted with Pluronics®. The grafting density was determined by radiolabeling the different block copolymers with ^{125}I. Protein adsorption

was found to decrease as the copolymer density on the surface increased. Indeed, the authors stated that the grafting density was the most important parameter influencing protein adsorption. They concluded that the ability of PEO to prevent protein adsorption is a result of covering the surface with PEO segments, thereby blocking protein binding sites [McPherson, T. et al., 1998][McPherson, T. et al., 1995].

Prime and Whitesides' studies with chemisorbed alkanethiols clearly showed the importance of graft density in developing a protein resistant material. They found that provided the graft density was high enough, even alkanethiols with a single ethylene oxide unit could significantly reduce protein adsorption. The density required to inhibit adsorption completely (within detectable limits) decreased as the length of the ethylene oxide oligomer increased [Prime, K.L. and Whitesides, G.M., 1993].

Sofia also examined the effect of PEO graft density on protein adsorption [Sofia, S.J. and Merrill, E.W., 1998a][Sofia, S.J. et al., 1998b]. The substrates used were silicon wafers silanised with a triaminosilane. Tresylated PEO was then used to couple the polyether to the amino groups on the wafers. Grafting density was calculated from the thickness of the dry PEO layer as determined by ellipsometry. Adsorption of cytochrome-c, albumin and fibronectin was reduced below the detectable limits of XPS and ellipsometry for a graft density of 100 ng/cm^2. For a given PEO-grafted substrate, the decrease in adsorption of all proteins to the minimal value occurred at similar graft densities. However, at a given graft density, adsorption was generally correlated to the size of the protein; adsorbed layers were thicker for the larger proteins than the smaller ones.

The authors proposed a model based on the spatial distribution of the PEO chains on the surface. Three regimes were identified with PEO chains arranged in a 2D lattice. The first includes arrangements with no overlap, where the distance between the chains is greater than twice the radius of gyration (R_G). The second regime occurs at the point of overlap of the PEO chains where the distance between the chains is exactly $2 \times R_G$. The third regime described arrangements where the PEO chains overlap, and where the distance between the chains is less than $2 \times R_G$. Within this regime, the surface becomes completely covered when the distance between the PEO chains is $1.6 \times R_G$.

The maximum graft density reached using the different chain lengths of PEO corresponded roughly to a distance between the chains equal to R_G; in other words where extensive overlap exists and the chains begin extending from the surface [Carignano, M.A. and Szleifer, I., 1995]. Therefore, this study suggests that the graft density required to inhibit protein adsorption depends on the chain length of the PEO grafts.

2.3.3.3 Temperature

Temperature has a significant impact on the behaviour of PEO in solution. In aqueous solutions, PEO has a closed miscibility loop; that is, there are lower and upper critical temperatures at which it comes out of solution. There are several different models that attempt to explain the temperature-dependent behaviour of PEO in water.

Goldstein has proposed that water adjacent to PEO molecules exists in two states: bonded and non-bonded [Goldstein, R.E., 1984]. Although the bonded state is

energetically favoured, the number of non-bonded molecules increases with temperature due to entropy. As a result, the solubility of PEO decreases as temperature increases.

According to Kjellander, the hydration of PEO is essentially hydrophobic (i.e. similar to the hydration of hydrocarbons) but modified by hydrogen bonding between water and ether groups [Kjellander, R., 1982]. PEO molecules fit into and actually strengthen the normal, imperfect hydrogen bonding network that exists in water. The dehydration of PEO molecules disrupts the hydration shell and results in decreased water structure. This results in large increases in both enthalpy (ΔH) and entropy (ΔS). In the expression for free energy (ΔG), the corresponding terms almost cancel at room temperature:

$$\Delta G = \Delta H - T\Delta S - T\Delta S_{id} \tag{2.5}$$

where T is the temperature and ΔS_{id} is the ideal entropy of mixing. The entropy of mixing is small compared to the other two terms at room temperature. However, as temperature increases, the sign of the free energy of demixing changes from positive (unfavourable) to negative (favourable), thus explaining the presence of the lower critical solution temperature.

Karlstrom's model considers the conformation of the PEO chains to explain the temperature-dependent behaviour [Karlström, G., 1985]. The most energetically favourable conformation of the ethylene oxide groups in the PEO chain has a large dipole moment. However, with an increase in temperature, other less polar conformations

become important for entropic reasons. As a result, the interaction between PEO and water is less favourable at higher temperatures.

Although the particulars vary, the effect of these theories is essentially the same: as temperature increases, the interactions between ethylene oxide groups becomes more attractive (or less repulsive).

Experiments with lysine-terminated PEO adsorbed to mica revealed a more compact layer structure at higher temperatures, due to a reduction of the amount of water associated with the layer. This leads to a decrease in the range of the steric repulsion force [Claesson, P.M., 1993].

As measured by ellipsometry and quantified using XPS data, protein adsorption from diluted plasma on surfaces coated with PEO has been shown to increase with temperature [Gölander, C.G. et al., 1992].

Other experiments have shown that higher graft densities of PEO can be achieved at higher temperatures because of the decrease in PEO molecular dimensions at these temperatures [Emoto, K. et al., 1997][Malmsten, M. et al., 1998].

2.3.3.4 Other factors

A study using EO-based SAMs [Harder, P. et al., 1998] showed that the conformations adopted by short oligo(ethylene oxide) moieties at high surface density appear to determine the protein rejecting ability of the layers. The helical configuration was found to be protein resistant whereas the "all-trans", or stretched zigzag, conformation was not. The orientation of the terminal methyl group in these SAMs was

the same in both helical and "all-trans" configurations, suggesting that the surface energy might not be the only important factor. The authors speculated that tightly bound water associated with the helical conformation and the ethylene oxide repeat units themselves form an interphase that prevents proteins from interacting with the surface. The "all-trans" configuration on the other hand appears to be unable to form a stable solvation layer and this results in a limitation of its protein rejecting capabilities.

3.0 OBJECTIVES

From the above discussion on PEO-grafted surfaces in relation to protein adsorption, it is clear that although considerable experimental data have been reported suggesting that PEO renders a surface protein repellent, there is insufficient knowledge to be able to describe unequivocally the mechanism of this effect, or to predict reliably the effect of PEO surface properties on adsorption. In addition, the impact of protein properties and the influence of environmental factors on adsorption to PEO-modified surfaces have not received much attention.

Given these points, the primary objective of this project is to investigate systematically the adsorption of proteins on surfaces to which PEO chains have been covalently grafted. This includes determining the impact of the length and grafting density of the PEO chains, the role of protein size and charge, and the influence of environmental factors such as temperature on the protein resistance of the modified surfaces. Polyurethanes have been selected as the substrate materials since their properties permit a wide array of potential applications, and there is considerable experience with these materials in our laboratory.

To accomplish this objective, a series of surface-modified polyurethanes, in which the chain length of the PEO chains is variable, was synthesised. The surface properties of these modified polymers was examined and compared to the unmodified polymers using water contact angles, XPS and AFM. Statistical analysis was used to identify correlations

between the factors listed above and protein adsorption.

This research may bring insight and understanding to questions of how grafted PEO chains promote protein resistance, and may also provide answers to unresolved issues such as the optimum PEO chain length and the impact of grafting density. In addition, a comprehensive examination of the protein adsorption behaviour of many different proteins to a range of PEO modified surfaces will provide data that could prove invaluable in the design of devices for biomedical or industrial applications where protein "fouling" presents a severe limitation.

4.0 EXPERIMENTAL METHODS

4.1 Materials

The chemicals and materials used in this research are listed in Table 4.1. Also included are the suppliers and their locations.

Table 4.1: Materials and suppliers.

Material	Supplier
Solvents	
Chloroform	Caledon, Georgetown, ON
DMF	Caledon, Georgetown, ON
DMSO	Aldrich, Milwaukee, WI
MDI	Aldrich, Milwaukee, WI
Methanol	Caledon, Georgetown, ON
Toluene	Caledon, Georgetown, ON
PUU synthesis and surface modification	
Calcium hydride	Fisher Scientific, Fair Lawn, NJ
MDA	Aldrich, Milwaukee, WI
Methoxy-poly(ethylene glycol)amine	Shearwater Polymers, Huntsville, AB
Poly(ethylene glycol) methyl ether	Aldrich, Milwaukee, WI
Poly(tetramethylene glycol)	QO Chemicals, West Lafayette IN
Protein Adsorption	
α-Lactalbumin (Type I)	Sigma, St.-Louis, MO
Concanavalin A (Type IV)	Sigma, St.-Louis, MO
Ferritin (Type I)	Sigma, St.-Louis, MO
HSA	Behring Diagnostics, Westwood, MA
Human Fibrinogen	Calbiochem, La Jolla, CA
Hydrochloric Acid	BDH, Toronto, ON
Lysozyme (Type I)	Sigma, St.-Louis, MO
Myoglobin (From Horse Skeletal Muscle)	Sigma, St.-Louis, MO
Phosphotungstic Acid	Sigma, St.-Louis, MO
Ribonuclease A (Type III-A)	Sigma, St.-Louis, MO
Sodium Chloride	Caledon, Georgetown, ON
Sodium Iodide ($Na^{125}I$)	ICN, Irvine, CA
Tris	Bioshop, Burlington, ON

Table 4.1: Materials and Suppliers (continued).

SDS-PAGE and Immunoblots	
Acrylamide	Gibco BRL Life Technologies, Gaithersberg MD
Ammonium persulfate	Gibco BRL Life Technologies, Gaithersberg MD
Bromophenol Blue	Sigma, St.-Louis, MO
Disodium hydrogen orthophosphate (Na_2HPO_4)	BDH, Toronto, ON
Glycerol	BDH, Toronto, ON
Glycine	Bioshop, Burlington, ON
Immobilon® membranes	Millipore, Bedford, MA
Magnesium chloride ($MgCl_2$)	BDH, Toronto, ON
N,N'-Methylenebisacrylamide	Gibco BRL Life Technologies, Gaithersberg MD
Prestained SDS-PAGE MW Standards, Low Range	Bio-Rad, Hercules, CA
Protogold	British Biocell International, Cardiff, UK
Pyronin Y	Bio-Rad, Hercules, CA
SDS	Bioshop, Burlington, ON
SDS-PAGE MW Standards, Low Range	Bio-Rad, Hercules, CA
Sodium dihydrogen orthophosphate ($NaH_2PO_4 \cdot H_2O$)	BDH, Toronto, ON
TEMED	Bioshop, Burlington, ON
Tween 20	Bio-Rad, Hercules, CA
VIM Instant Skim Milk	Ault Food Ltd., Toronto, ON

4.2 Polyurethaneurea Synthesis

The polyurethaneurea (PUU) used as the substrate material on which to graft PEO was synthesised in the usual two step method [Santerre, J.P., 1990]. The first step, the prepolymer reaction, involves the reaction of a hydroxyl-terminated polyether with a diisocyanate. In the second step, the chain extension, the prepolymer reacts with a di-functional (diol or diamine) chain extender to form the desired polymer. Previous work had shown that the polyurethane based on PTMO as the polyether, MDI as the

diisocyanate and MDA as the chain extender, gave solid films having suitable mechanical properties [Skarja, G.A., 1994]. This polymer was adopted as the standard substrate material in the present work.

4.2.1 Purification of reagents

Some of the reagents had to be further purified prior to use. The diisocyanate was vacuum distilled to remove multimeric impurities. Approximately 500 g of MDI and several boiling chips were introduced to a 1000 mL round bottom flask. The flask was attached to a vacuum distillation apparatus, consisting of a heating mantle, a condenser wrapped with a heating tape, several collection round bottom flasks and a thermometer. The molten MDI was slowly heated until completely melted. A vacuum was then applied to the system and the MDI was heated to the boiling point (between 170-180°C, depending on the pressure). The heating tape around the condenser was necessary to prevent premature solidification of the MDI prior to reaching the collection vessels. The first 20 mL of collected distillate was discarded. Once the distillation was complete, the product was stored in polyethylene bottles at –20°C until use.

The PTMO was treated to remove excess water that could interfere with the PUU synthesis. Initially, the dehydration of the polyether was performed in a vacuum oven at 60°C for at least 24 h. Later, a more efficient procedure was used. The PTMO was placed in a round bottom flask with a stir bar and heated at 60°C under vacuum with vigorous stirring for 3-4 hours. The water evaporation was readily observed as bubble formation in the molten polyether. These bubbles had disappeared by the end of the treatment.

4.2.2 Prepolymer Reaction

The molar ratios MDI:PTMO:MDA used for the synthesis were 2:1:1. In the first step, 0.16 mol MDI dissolved in 360 mL anhydrous DMSO was heated to 90°C in a 2 L reaction kettle equipped with a condenser, an electric stirrer, an addition funnel and a dry nitrogen stream. A solution of 0.08 mol PTMO in 450 mL DMSO was added drop-wise over the course of 30 min and the reaction was allowed to proceed an additional hour. The prepolymer reaction is illustrated in Figure 4.1.

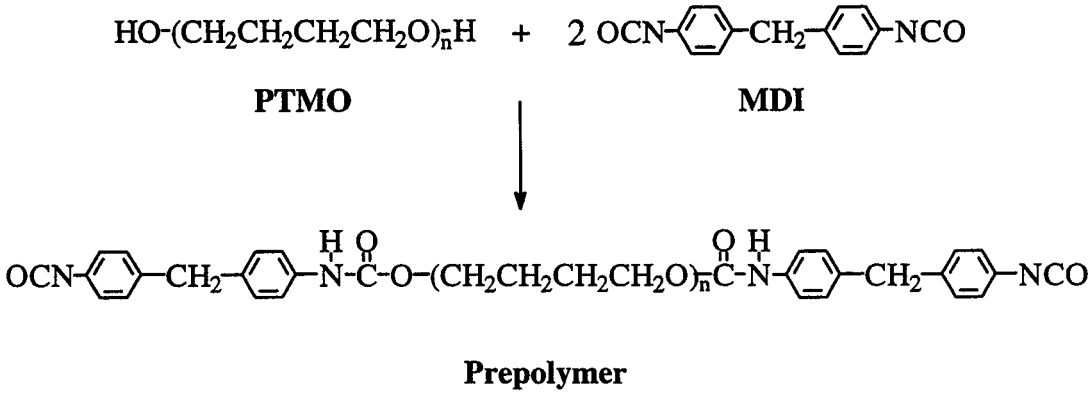

Prepolymer

Figure 4.1: Polyurethaneurea prepolymer reaction.

4.2.3 Chain Extension Reaction

The prepolymer solution was then cooled to 70°C. The second step in the PUU synthesis was initiated by adding a solution of 0.08 mol MDA in 160 mL DMSO drop-wise to the prepolymer solution over the course of 30 min. The reaction was allowed to proceed for another hour. The chain extension reaction is illustrated in Figure 4.2. Essentially, MDA links the prepolymer molecules to form long polymeric chains with the theoretical repeat structure given in Figure 4.2.

4.2.4 Purification and Processing

The resulting polymer solution was precipitated in distilled water, vacuum filtered, washed in several changes of water, and dried for at least 48 h in a convection oven at 50°C. The PUU was then dissolved in DMF at a concentration of 5% (w/v), vacuum filtered, reprecipitated in water, washed in several changes of water and dried in a convection oven as before.

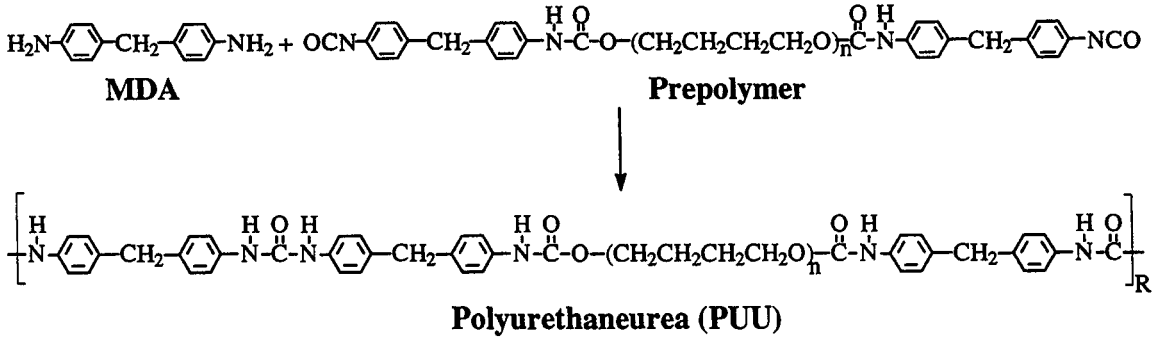

Figure 4.2: Polyurethaneurea chain extension reaction.

4.2.5 Film Casting

Thin films of PUU were cast from a 5% (w/v) solution in DMF in either 14.8 cm diameter glass Petri dishes or a 22.5 cm square casting apparatus. Once the dishes or casting apparatus had been levelled in the convection oven, the polymer solution was poured into the vessels (Petri dish, 100 mL; casting apparatus, 400 mL, see on page 89). The vessels were covered lightly to keep dust away from the polymer solution and slow the rate of evaporation. This was found to improve the surface smoothness of the films. The casting was performed at 50°C and was normally complete after 48 h.

Polymer disks (d = 6.8 mm), used in protein adsorption experiments, and squares (≈ 1 cm^2), used for surface characterisation, were cut from the PUU films. The polymer disks and squares were placed in a Soxhlet extractor, and extracted with toluene for approximately 18 h to remove soluble impurities. This treatment was followed by a brief rinse in ethanol and drying under vacuum at 50°C for 24 h.

4.3 Polyurethane Surface Modification

A two step surface modification reaction, based on previously published protocols, was used to graft PEO to the PUU substrate [Han, D.K. et al., 1989][Freij-Larsson, C. and Wesslén, B., 1993]. In the first step, isocyanate groups were introduced into the PUU surface by reaction with MDI. The isocyanate group is believed to react with surface urea or urethane groups, forming biuret and allophanate functional groups, respectively. If only one isocyanate group of MDI reacts, the other one is left free and can then react with PEO, thus attaching the polyether covalently to the PUU surface. Two forms of PEO, hydroxyl- and amine-terminated monomethoxy-polyethylene oxide (MeO-PEO-OH, MeO-PEO-NH_2), were grafted to the PUU. The molecular weights of the PEO varied between 165 and 5000 MW (PEO chain length 3 to 113, see Table 7.1 on page 134).

4.3.1 Purification of reagents

As with the polyurethane synthesis, the reagents in the grafting reaction were made as anhydrous as possible to minimise the side reaction between MDI and water that forms methylene dianiline (MDA). Any MDA in the reaction could compete with PEO

for available isocyanates on the polyurethane surface. Therefore, calcium hydride was added to the solvent, toluene, to scavenge trace amounts of water. Approximately 0.5 g of calcium hydride was added to 4 L of toluene at least 12 h prior to the reaction.

The PEO used in the grafting reaction was also treated to remove as much water as possible. Heating at 60°C under vacuum in a round bottom flask with vigorous stirring for 3-4 hours was found to be effective.

4.3.2 Surface Grafting Reactions

The grafting reactions were carried out in a 500 mL reaction kettle equipped with a condenser and a thermometer. The reaction conditions detailed in this section were used unless stated otherwise. For reactions with MeO-PEO-OH, 200 mL of a 2% (w/v) MDI solution in toluene with 0.3 mL stannous 2-ethyl-hexanoate was heated to 60°C under a stream of nitrogen. Approximately 300 polymer disks and 10 squares were added to the stirred solution. After 1 h , the polymer surfaces were rinsed twice with toluene and 200 mL of 7.5% (w/v) MeO-PEO-OH in toluene with 0.3 mL stannous 2-ethyl hexanoate was added. The reaction was allowed to proceed for 24 h at 60°C. The surfaces prepared using this protocol are given the following nomenclature: PUU-OPEOX, where X represents the molecular weight of the MeO-PEO-OH graft: e.g. PUU-OPEO550, has 550 MW PEO grafts and PUU-OPEO2K has 2000 MW grafts.

For reactions with MeO-PEO-NH_2, 200 mL of a 2% (w/v) MDI and 2% (w/v) triethylamine solution in toluene was heated to 60°C under a stream of nitrogen. Approximately 300 polymer disks and 10 squares were added to the stirred solution.

After 1 h , the polymer surfaces were rinsed twice with toluene and 200 mL of 1% (w/v) MeO-PEO-NH_2 in toluene was added. The reaction was allowed to proceed for 24 h at 60°. The surfaces prepared using this protocol are given the following nomenclature: PUU-NPEOX, where X represents the molecular weight of the MeO-PEO-NH_2 graft: e.g. PUU-NPEO550, has 550 MW PEO grafts and PUU-NPEO2K has 2000 MW grafts. The reactions involved in grafting PEO to the PUU substrate are illustrated in Figure 4.3.

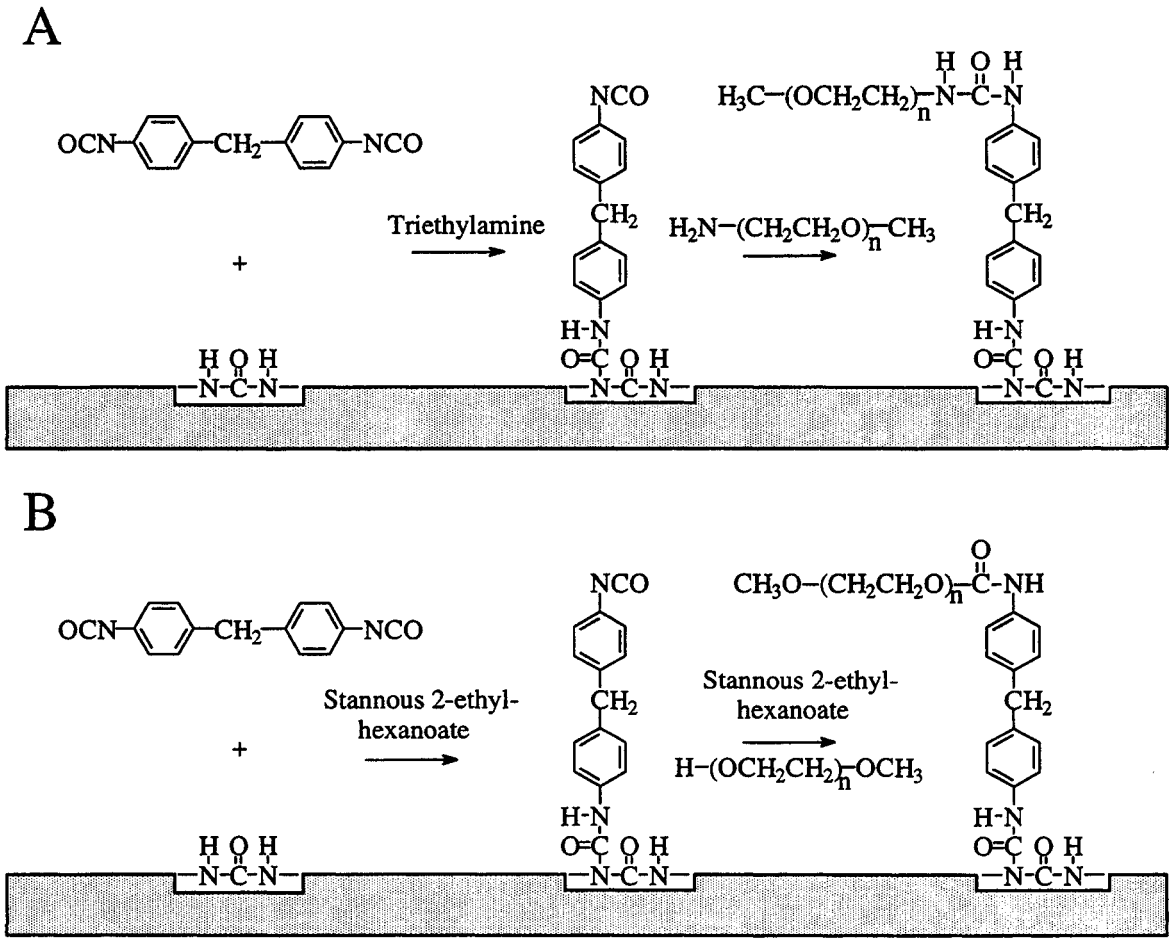

Figure 4.3: Two step reaction to graft PEO to the PUU. (A) Reaction sequence for grafting using amino-PEO. (B) Reaction sequence using hydroxy-PEO.

4.3.3 Purification and Processing

The polymer samples were removed from the reaction vessel and extracted in toluene for 18 h (Soxhlet extractor) to remove unbound PEO. This treatment was followed by a brief rinse in ethanol. The polymer disks were then placed on cheesecloth and dried under vacuum at 60°C for 24 h.

4.4 Surface Characterisation

4.4.1 Water Contact Angle Measurements

The relative hydrophilicity of the PUU and PEO-grafted PUU surfaces was probed by measuring water contact angles using a Ramé-Hart NRL C.A. goniometer (Mountain Lakes, NJ). Polymer samples were rinsed in methanol immediately prior to measurement. Advancing and receding contact angles were measured using the sessile drop method. The advancing contact angle was measured by placing a 10 μL drop of water on the polymer surface using a syringe. After allowing the drop to equilibrate, the angle between the polymer surface and the tangent to the contact line of the drop was measured, as illustrated in Figure 4.4 (a). To measure the receding water contact angle, the syringe was used to remove water from the drop until the contact line just began to retract. The drop was allowed to equilibrate once more and the angle measured.

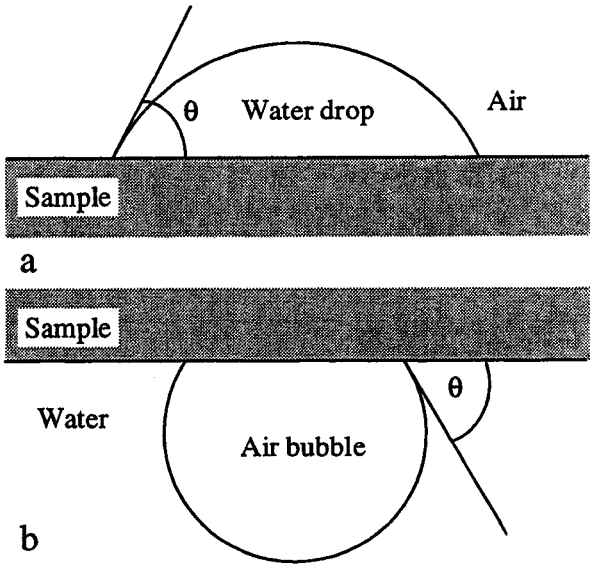

Figure 4.4: (a) Sessile drop and (b) captive bubble measurements of water contact angle θ.

The samples were also tested under more biologically relevant conditions, i.e. in an aqueous environment. These measurements were performed in an environmental chamber filled with water. Captive air bubbles were used to probe polymer samples that had been incubated in water for 24 h at room temperature as illustrated in Figure 4.4 (b). Samples were fixed to the testing stage using double-sided tape and immersed in water. Air bubbles were placed on the sample using a U-shaped needle affixed to a dispensing syringe.

4.4.2 X-Ray Photoelectron Spectroscopy (XPS)

This technique is used to obtain chemical composition and structural information on the surface of a test material. The surface is irradiated with an X-ray beam, causing an emission of photoelectrons from the sample. The energy of the emitted photoelectrons

identifies the elements from which they originated. The intensity of emission is used to determine the prevalence of different elements in the sample.

The mean free path of an electron in matter is limited to approximately 100 Å [Andrade, J.D., 1985b]; therefore, the probing depth of XPS is also limited to this value, making the method highly surface sensitive. It can be made even more surface sensitive by changing the take-off angle between the sample and the detector. Figure 4.5 illustrates how the take-off angle influences the effective probing depth. A depth profile of the composition of the sample can be obtained by scanning at different take-off angles.

XPS was performed in the Centre for Biomaterials at the University of Toronto using a Leybold Max 200 X-ray photoelectron spectrometer with a magnesium anode non-monochromatic source. The sampling spot was a 2×4 mm ellipse. Survey scans (0-1000 eV) were performed to identify constitutive elements. Low resolution scans of the peaks associated with these elements provided their atomic concentrations. High resolution C_{1s} scans were recorded to determine the contribution of different functional groups containing carbon atoms. These scans were measured with takeoff angles of 90° and 20°. Samples were rinsed in methanol and dried under vacuum for 24 h prior to measurement. Immediately prior to measurement, samples were rinsed with 1,1,2-trichlorotrifluoroethane to remove contaminants.

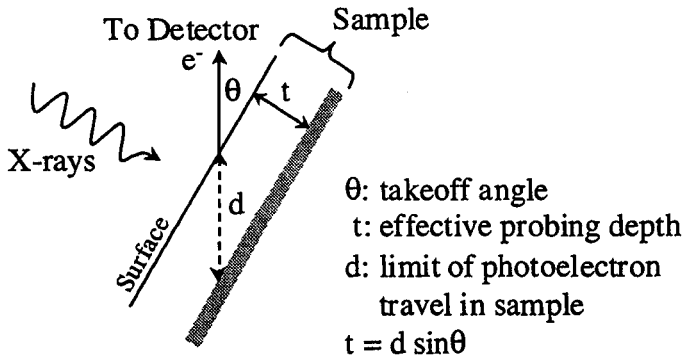

Figure 4.5: Relationship between the effective probing depth and takeoff angle in XPS. Adapted from [Andrade, J.D., 1985b].

4.4.3 Graft Density Measurements

The grafting density of PEO on the PUU substrate was measured by radiolabeling. Radioiodinated Bolton-Hunter reagent (iodinated 3-(4-hydroxyphenyl) propionic acid N-hydroxysuccinimide) was used to label diamino-PEO. This reaction is illustrated in Figure 4.6.

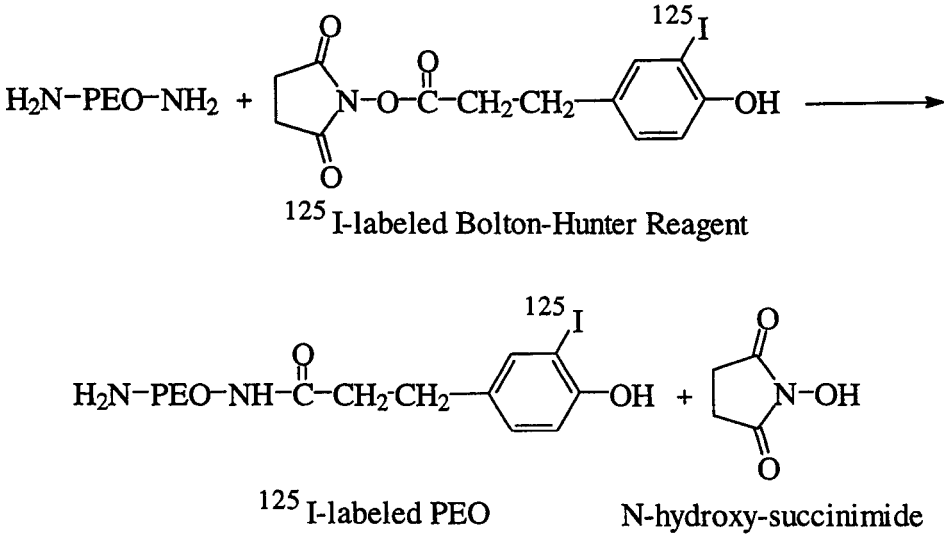

Figure 4.6: Radioiodination of diamino-PEO with ^{125}I-Bolton-Hunter reagent.

The first step in the labelling reaction consisted of drying 1.5 g diamino-PEO (either 2000 or 3400 MW) in a 50 mL round-bottom flask at 50°C and under vacuum for 6 h. The PEO was then dissolved in 20 mL anhydrous toluene and 3.5×10^{-5} μmol ^{125}I-Bolton-Hunter reagent was added to the stirred mixture. After 36 h at room temperature, the PEO was precipitated in 200 mL isopropyl ether, filtered, washed with fresh isopropyl ether and dried under vacuum for approximately 18 h. The precipitate was then redissolved in 10 mL dichloromethane and reprecipitated in 100 mL isopropyl ether. The precipitate was again filtered, washed and dried under vacuum for 48 h.

The grafting density measurement reaction is essentially a scaled-down version of the grafting reaction described in Section 4.3.2. In the first step, 10 PUU disks (6.8 mm diameter) were reacted with 10 mL 2% (w/v) MDI and 2% (w/v) triethylamine in anhydrous toluene for 1 h at 60°C. The reaction medium was then removed and the PUU disks were rinsed three times with 10 mL anhydrous toluene. In a second 50 mL round-bottom flask, 10 mL 1% (w/v) ^{125}I-PEO in anhydrous toluene was prepared. Four 100 μL aliquots of this solution were collected to determine the radioactivity of the PEO solution for use in subsequent calculations. The PUU disks were then transferred to this solution and allowed to react for 24 h at 50°C. The PUU disks were then rinsed briefly with anhydrous toluene before being placed in a Soxhlet extractor with toluene for 20 h. The disks were then placed in counting vials and the radioactivity measured with a gamma counter.

4.4.4 Atomic Force Microscopy (AFM)

Images of the PUU and PEO-grafted PUUs were obtained using atomic force microscopy. The atomic force microscope senses the interatomic forces between a tip on a cantilever spring and the sample surface. As the cantilever tip scans the surface, the deflections of the cantilever spring in response to proximal atoms can be translated into a topographic image of the surface.

The images were obtained with a Nanoscope III MultiMode scanning probe microscope (Digital Instruments, Santa Barbara, CA) equipped with an E scanning head operated in tapping mode. The samples were imaged in air using 125 mm single beam silicon nitride cantilevers (Digital Instruments). The AFM tips were exposed to UV radiation prior to use to remove organic contaminants.

4.5 Protein Adsorption

4.5.1 Proteins Investigated

The proteins investigated in this research are listed in Table 4.2. The molecular weight and isoelectric points are also included.

4.5.2 Protein Adsorption from Buffer

The protein to be used for a particular experiment was labelled with $Na^{125}I$ using Iodo-Gen® (Pierce Chemical Co, Rockford IL). Briefly, 10 μg of reagent was deposited in a glass vial by evaporation from a chloroform solution. A typical reaction involved adding 200-500 μg protein dissolved in TBS, pH 7.4 and 0.5 mCi of $Na^{125}I$ per vial. Multiple vials were usually required. The contents of the vials were stirred for 15 min at

room temperature, and then injected into a Slide-A-Lyzer® Dialysis Cassette (0.5-3.0 mL capacity, 10000 MW cut-off, Pierce). The labelled protein solutions were dialysed against TBS for approximately 18 h with three buffer changes in order to remove unbound ^{125}I.

Table 4.2: Proteins and associated properties.

Protein	Molecular weight (Da)	Isoelectric point
α-lactalbumin[b] (Bovine milk)	14200	4.3
Myoglobin[c] (Horse skeletal muscle)	17500	7.2
RNAse[b] (Bovine pancreas)	13600	9.4
Lysozyme[b] (Chicken egg white)	14600	11.1
Serum albumin[c] (Human)	66000	4.7
Concanavalin A[a] (Jack Bean)	120000	5.0
Fibrinogen[c] (Human)	340000	4.3
Ferritin[a] (Horse spleen)	440000	4.3

(a) [Righetti, P.G. and Caravaggio, T., 1976], (b) [Arai, T. and Norde, W., 1990], (c) [Herde, K. et al., 1977]

Protein solutions (2% labelled) ranging from 0.001 to 5 mg/mL in TBS were prepared. The adsorption experiments were performed in Falcon® 96-well Microtest III tissue culture plates (Becton Dickinson Co, Franklin Lakes, NJ), each well containing 250 μL labelled protein solution. Polymer disks (6.8 mm diameter) equilibrated in TBS at 4°C for 18 h, were placed upright in the wells so that both sides were exposed equally to the solution. Following a 3 h adsorption at room temperature, the samples were rinsed three times for 15 min in 250 μL TBS buffer. The samples were placed in counting vials and the radioactivity determined using a γ-counter. Typically, experiments with PUU-OPEO surfaces involved running 6 samples types (control and 5 PEO graft MW) in triplicate at 5 protein concentrations. For PUU-NPEO experiments, 4 sample types (control and 3 different PEO graft MWs) were run in triplicate at 6 protein concentrations.

4.5.3 Protein Adsorption from Plasma

In these experiments, human fibrinogen was labelled as described in Section 4.5.2. Platelet poor plasma (PPP) was prepared as follows. Whole blood was collected from 15 healthy donors by clean venipuncture and added to 3.8% sodium citrate (w/v) in a 9:1 ratio (volume blood:volume citrate). The citrated blood was centrifuged at 4°C and 3000 g for 20 min, after which the PPP supernatant was removed, pooled, aliquoted and stored at -70°C until use. The concentration of fibrinogen in the PPP was determined by Clinical Hematology at the McMaster University Medical Centre. Plasma solutions were prepared by diluting PPP with TBS buffer to concentrations ranging from 0.1-50 % (v/v) of the original plasma. The solutions contained fibrinogen of which 2% (w/w) was labelled with ^{125}I. The protein adsorption protocol using these solutions was the same as described in Section 4.5.2 for adsorption from buffer.

PUU samples used for SDS-PAGE and immunoblot analysis were incubated in 100% PPP using the same protocol as described in Section 4.5.2. Eight polymer disks per sample type were then incubated in 150 μL of 2% (w/v) SDS solution for 12-18 h. This treatment elutes the proteins from the PUU surface for subsequent analysis described as below.

4.6 SDS-Polyacrylamide Gel Electrophoresis (SDS-PAGE) and Immunoblotting

The identity of proteins adsorbed on the PUU and PEO-grafted PUU from plasma were determined using SDS-PAGE and immunoblotting. SDS-PAGE is used to separate proteins or protein fragments according to size. Upon staining with a colloidal gold

preparation, the resolved mixture appears on the membrane as a series of bands, each corresponding to either whole proteins, complexes, protein subunits or protein fragments.

The identity of these bands was determined by immunoblotting. The protein bands in the gel were transferred to an Immobilon® polyvinylidene fluoride (PVDF) membrane by electrophoresis. The membrane was cut into strips that were then probed with primary antibodies directed specifically against the proteins of interest. A series of secondary antibodies, conjugated to alkaline phosphatase and directed against the primary antibodies, were used to probe the membrane again. A chromogenic substrate, susceptible to cleavage by alkaline phosphatase, was used to identify the proteins of interest via colour generation. Detailed protocols on SDS-PAGE and immunoblotting are provided in Appendix A.

5.0 MATERIALS PREPARATION

5.1 Base Polyurethane-urea Synthesis

A polyurethane-urea (PUU) was chosen as the base substrate for PEO grafting for several reasons. Polyurethanes are used in the biomedical and biotechnology industries due to their excellent mechanical properties and relatively good biocompatibility [Lamba, N.M.K. et al., 1998; Lelah, M.D. and Cooper, S.L., 1986]. In addition, a considerable amount of previous work in our group has involved the study and characterisation of polyurethanes and polyurethaneureas [Skarja, G.A., 1994][Santerre, J.P., 1990].

The reagents selected for the polyurethane-urea synthesis were PTMO (MW 650), MDI and MDA. These were chosen for a number of reasons. Three molecular weights of PTMO were available for PUU synthesis: 650, 980 and 2000. The 2000 MW polyether was ill-suited for PUU synthesis due to its low solubility in the reaction solvent, DMSO [Skarja, G.A., 1994]. Early syntheses had also shown that the polymer films cast from PUU synthesised with 650 MW PTMO had better properties; i.e. smoother appearance and more transparent. Finally, PUUs prepared with the shorter polyether should theoretically provide more grafting sites for a given area of polymer surface. According to Figure 4.2 on page 40, the theoretical repeat unit of the PUU substrate has four potential grafting sites: two urea and two urethane groups. Since the molecular weight of the repeat unit using the 650 MW PTMO is lower than that of the 980 MW analogue, PUUs prepared with the former will have more grafting sites on a mass basis.

MDI was selected since it is one of the least toxic of the common diisocyanates and had been used extensively in previous work [Skarja, G.A., 1994][Santerre, J.P., 1990]. MDA is less reactive than aliphatic diamino chain extenders, such as ethylene diamine, but still reactive enough to be used without a catalyst in PUU synthesis. This lower reactivity made the PUU synthesis easier to control and more likely to reach completion. Additionally, MDA is convenient to use since it does not require any additional preparation prior to use.

5.1.1 Reaction Yield

The synthesis of the base PUU was performed several times during the course of experimentation. The yield was determined after the final precipitation and drying of the PUU and is expressed as a percentage of the expected theoretical yield by mass. Table 5.1 contains a summary of reaction yields for all PUU syntheses.

Because of the many steps involved in the purification of the polymer prior to final dissolution in DMF for film casting purposes, there was some variability in the yield of the reaction. Much of the material loss during processing occurs in the initial precipitation of the polymer solution in water. Although most of the polymer precipitates as a large solid mass, some of it forms as a very fine powder. Collection of these particulates required a lengthy filtration process for recovery of small quantities of polymer and was not deemed worthwhile or necessary to perform. Hence some of the observed variability in yield may be due to variations in the amount of this uncollected polymer.

Table 5.1: Reaction yields of the PUU substrate.

Reaction	Yield (%)
1	79.7
2	84.8
3	89.9
4	92.3
5	92.5
6	81.6
Average ± S.D.	86.9 ±5.7

5.1.2 Molecular Weight

The molecular weight of the base PUU was determined using gel permeation chromatography (GPC). The molecular weight is determined by comparing the elution times of the base polymer and a series of polystyrene standards. A typical GPC chromatogram is shown in Figure 5.1.

Peak A corresponds to the polymer. Peaks B, C and D, are attributed to LiBr, water and air, respectively [Sun, X., 1998]. Table 5.2 summarises the molecular weights of several batches of base PUU. The breadth of the polymer peak is expected due to the step growth polymerisation mechanism. Theory predicts a polydispersity of 2.0 for this type of mechanism [Flory, P.J., 1953]. The calculated average polydispersity is quite close to this value. Deviations are due to fractionation during precipitation and other work-up operations.

The molecular weights for the different batches of PUU were nearly identical to those found in previous work, where an average MW of 59,900 was determined [Skarja, G.A., 1994]. Although there was some variability from batch to batch, it was not excessive. In addition, there is some degree of subjectivity when interpreting the chromatograms due to the background noise present in each scan. This subjectivity arises when assigning the start and end points of the polymer peak. However, since the calculated polydispersity values for the polymers are all relatively near the expected value, the analysis may be considered valid.

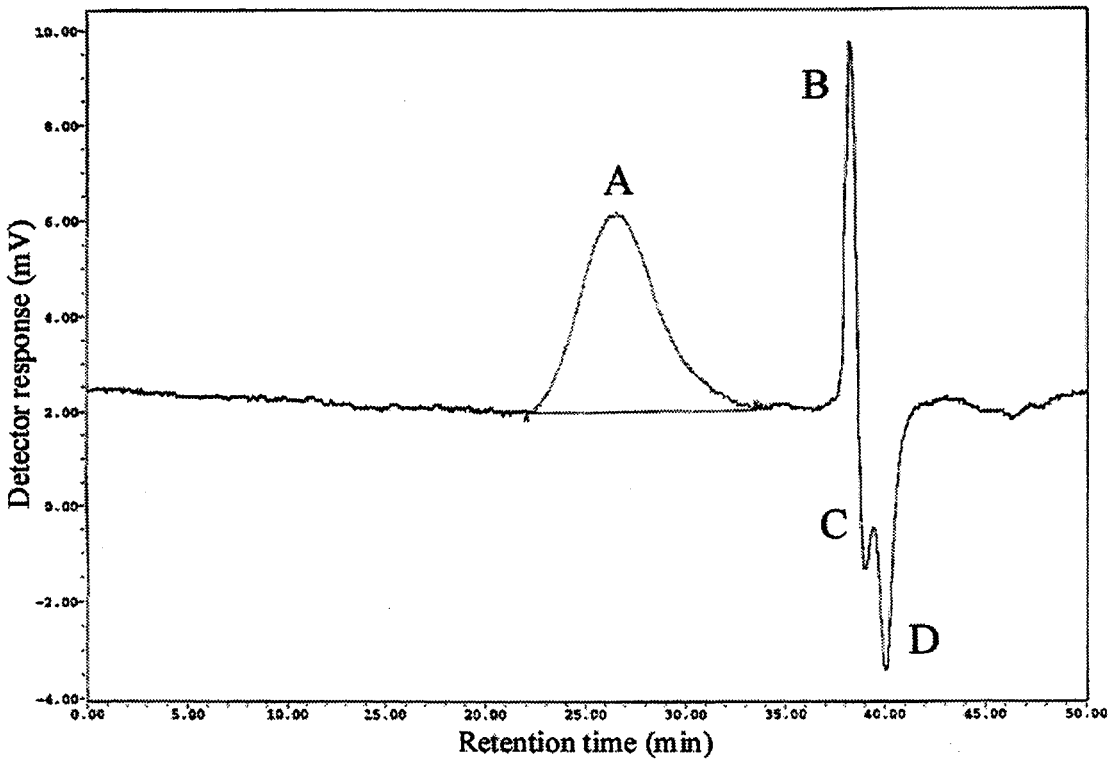

Figure 5.1: GPC chromatogram for the base PUU.

Table 5.2: Number average molecular weight of base PUU.

Reaction	Polystyrene equivalent molecular weight (M_n)	Polydispersity
4	61400	2.10
5	57100	1.82
6	60900	2.38
Average ± S.D.	59800±2400	2.10±0.28

5.1.3 Film Casting

The PUU syntheses used DMSO as the reaction solvent; however, DMF was used when casting thin PUU films. The increased volatility of DMF compared to DMSO decreased the time required for casting.

Initially, polymer films were cast on the covers and bottoms of glass Petri dishes. However, these glass surfaces were not flat which caused problems in obtaining films of uniform thickness due to the difficulty in levelling the dishes properly. Variations in film thickness caused variations in the surface area of the polymer disks used in protein adsorption experiments. It was therefore important to have as little variation in polymer film thickness as possible.

Table 5.3 shows the relationship between disk thickness and total surface area due to the edge contribution. Although edge effects are small, it was nonetheless important to minimise the variation and to ensure that the polymer disks were less than about 0.035 cm thick so that the area contributed by the edges was less than 5% of the total area.

Therefore a casting apparatus was designed to facilitate casting and obtain polymer films of more uniform thickness.

Table 5.3: Increase in total surface area of 6.8 mm diameter disk when edge contributions are included.

Disk thickness (cm)	Disk surface area (cm)	Area increase (%)
0.00	0.726	0.0
0.01	0.737	1.5
0.02	0.748	2.9
0.03	0.758	4.4
0.04	0.769	5.9
0.05	0.780	7.4

Figure 5.2 illustrates this apparatus. The casting apparatus uses a sheet of plate glass as the base, providing a uniformly smooth and flat surface. The casting area is sealed with a grooved casting sleeve, fitted with a butyl rubber gasket. A series of eight clamps apply pressure to the casting sleeve, thereby preventing leakage. The entire apparatus can be levelled using three levelling feet in a tripod arrangement. By using this apparatus, two significant improvements were realised. First, the size of the polymer film obtained was such that upwards of 1000 polymer disks (6.8 mm diameter) could be obtained from a single sheet; therefore many experiments could be performed with disks from the same sheet. Second, the plate glass that served as the bottom of the casting apparatus greatly improved the smoothness and uniformity of the PUU films. Although the variability of polymer film thickness was not completely eliminated using this

apparatus, it was much reduced. Generally, the thickness of the disks used in protein adsorption experiments varied between 0.015 and 0.025 cm.

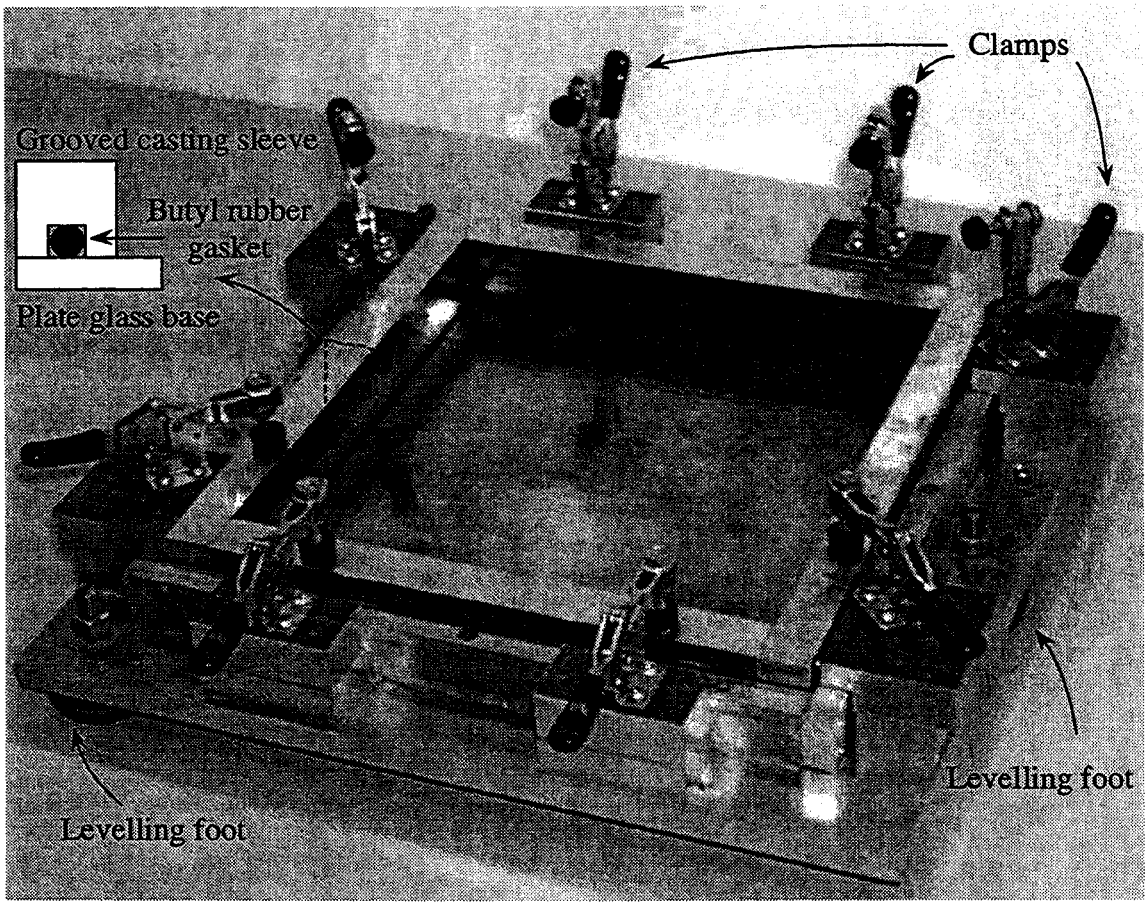

Figure 5.2: Casting apparatus.

5.1.4 Qualitative Observations

The PUU films obtained from casting were pale yellow in colour, translucent, flexible and had good mechanical strength. Prolonged exposure to air caused the film colour to deepen to a darker yellow-orange and the film to become slightly stiffer. Keeping the PUU samples in sealed polyethylene bags delayed the onset of this

phenomenon significantly. It seems likely that oxidation and/or photooxidation of the polymer is responsible for the colour change and loss of elasticity.

5.2 Polyurethane Surface Modification

The surface modification reaction used to graft PEO to the PUU substrate was adapted from two previously published protocols [Han, D.K. et al., 1989][Freij-Larsson, C. and Wesslén, B., 1993]. In both these studies, the relatively flexible diisocyanate HMDI was used to graft PEO to the polymer substrate. The rationale for the selection of the various reagents used in the grafting reaction in the present work is as follows.

To reduce the possibility that both isocyanate groups would react with the polymer substrate, the more bulky and less flexible diisocyanate MDI was used. The probability that both MDI isocyanate groups could react with the polymer should be lower than for a flexible diisocyanate such as HMDI. This is important to ensure that as many pendant free isocyanate groups as possible are available for the second step of the grafting reaction.

Monomethoxy-PEO, with only one reactive hydroxyl (or amino) group, was chosen for grafting to the PUU substrate. Formation of loop structures where both ends of the PEO chain are grafted to the polymer surface was thus avoided.

Finally, stannous octoate was initially used for catalysis because it was the more potent of the two catalysts used in the previous work. Tin alkyl compounds are catalysts for the reaction between isocyanate groups and urea/urethane groups [Lelah, M.D. and Cooper, S.L., 1986]. The proposed mechanism for this reaction, illustrated in Figure 5.3,

is based on the catalysed reaction between an isocyanate and primary amine [Saunders, J.H., 1969]. The isocyanate and urethane groups coordinate with the tin atom of the catalyst, thereby facilitating the reaction between the two reagents by bringing them into close proximity in a favourable orientation.

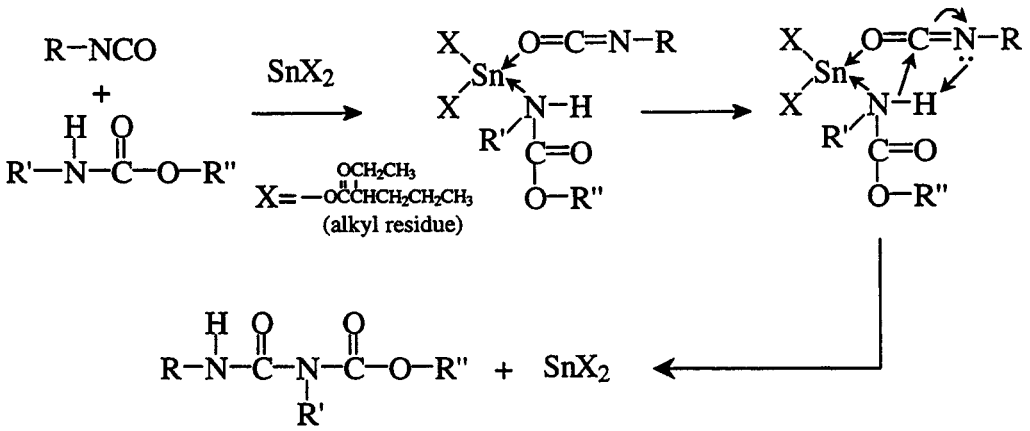

Figure 5.3: Proposed mechanism for stannous octoate catalysis of a reaction between an isocyanate and urethane to form an allophanate group.

The optimal protocol for the PEO grafting reaction was developed during the course of experimentation. At first, grafting was performed using relatively large (5 cm × 5 cm) pieces of polymer film. This approach was somewhat problematic for a number of reasons. First, only one piece of polymer film could be processed at a time. If several pieces of polymer film were introduced into the reaction vessel, they tended to aggregate thus restricting access of the adhering surfaces to the reaction medium. As well, since a stir bar was used to agitate the reaction solution, the surface of the polymer film in contact with the stir bar tended to become etched and scratched due to the motion of the stir bar. Finally, once the reaction was completed, disks were sectioned from the polymer

film for protein adsorption experiments. The edges of these disks, however, were not exposed to the modification reaction and were therefore the same as the base PUU.

To alleviate all these problems, the disks of 6.8 mm in diameter were sectioned from the substrate PUU films prior to the reaction. In this manner, large quantities of disks could be processed simultaneously. Also, because of their small size and greater freedom of movement, the disks were not etched or scratched by the stir bar during the reaction. In addition, the complete surface of the polymer disks, including the edges, was equally exposed to the surface modification reaction.

The grafting reaction was used to prepare PEO-grafted PUU surfaces with grafts of 165, 350, 750, 2000 and 5000 MW monomethoxy PEO. One interesting development was observed during the surface modification reaction. In the first step of the reaction when the PUU disks reacted with MDI, the solution invariably became cloudy following the addition of the catalyst, due to the formation of a white precipitate. The precipitate was probably produced by trace water present in the reaction medium. The isocyanate groups could react with water and form amino groups which could then rapidly react with MDI forming a polyurethane which likely precipitates out of solution when the chains become large enough. Even when the most stringent procedures were used to remove water from the solvents and reagents and to prevent water from entering the system, this effect could not be eliminated. However, the precipitate did not appear to prevent the successful grafting of PEO to the PUU surfaces.

5.2.1 Optimisation of Grafting Conditions

One of the first series of experiments was designed to identify factors that influence the grafting reaction. The goal was to optimise the reaction conditions to obtain the highest possible levels of surface grafting. Unfortunately, a method for measuring grafting density directly was not available at the time these experiments were performed. Only indirect indicators of surface grafting levels were used in this analysis. These optimisation experiments were performed exclusively with the monomethoxyhydroxy-PEO reagent.

A simple 2-level factorial design investigating temperature, reagent concentrations and reaction times was performed. Since five effects were investigated, a full 2^5 design would have required 32 separate runs to complete. However, the required information can be obtained by performing only a fraction of the full number of runs [Box, G.E.P. et al., 1978]. This is because high order interactions tend to be small and information on these is unnecessary. In a 2^{5-2}_{III} fractional design, none of the primary effects (temperature, [PEO], [MDI] and reaction times) are confounded with one another. However, since the design is resolution III, the primary effects are confounded with second order and higher interaction effects. The effects of temperature, PEO and MDI concentrations, MDI (t_{MDI}) and PEO (t_{PEO}) reaction times are identified as **1**, **2**, **3**, **4**, and **5**, respectively. The defining relation for the design is:

$$\mathbf{I = 124 = 135 = 2345}$$

where I has the following properties: any effect multiplied by I is unchanged and any effect multiplied by itself gives I. For example:

$$\mathbf{I24 = 24}$$

$$\mathbf{2424 = 2244 = II = I}$$

Therefore, if we multiply the defining relation by effect **1**, we obtain:

$$\mathbf{1I = 1124 = 1135 = 12345}$$

which simplifies to:

$$\mathbf{1 = I24 = I35 = 12345}$$

and finally:

$$\mathbf{1 = 24 = 35 = 12345}$$

This results in the following confounding patterns where all possible effects and interactions are accounted for:

$$\mathbf{1 = 24 = 35 = 12345}$$
$$\mathbf{2 = 14 = 345 = 1235}$$
$$\mathbf{3 = 15 = 245 = 1234}$$
$$\mathbf{4 = 12 = 235 = 1345}$$
$$\mathbf{5 = 13 = 234 = 1245}$$
$$\mathbf{23 = 45 = 125 = 134}$$
$$\mathbf{25 = 34 = 123 = 145}$$

This means, for example, that effect **1** will be confounded with the two-factor interaction effects **24** and **35** as well as the fifth order interaction effect **12345**. That is, the effect of temperature will be confounded with the second order interactions PEO concentration-t_{PEO} and MDI concentration-t_{MDI} as well as a fifth order interaction effect. The likelihood that high order interaction effects are significant is relatively remote and may be ignored [Box, G.E.P. et al., 1978]. This is analogous to dropping terms in a Taylor series expansion. Therefore, third and higher order interaction terms are not

considered here. If, however, a primary effect is judged to be significant, additional runs might be required to resolve the primary effect from second order interaction effect(s).

The model for fitting the responses is therefore:

$$y = b_0 + b_1x_1 + b_2x_2 + b_3x_3 + b_4x_4 + b_5x_5 + b_6x_2x_3 + b_7x_2x_5 \qquad (5.1)$$

where b_0 to b_7 are parameters, x_1 to x_5 are the five primary effects listed above, and x_2x_3, x_2x_5 are confounded two-factor interactions. The last two terms are the two-factor interaction terms confounded only with other two-factor interactions. This equation can be written in matrix form:

$$\mathbf{y} = \mathbf{Xb} \qquad (5.2)$$

where $\mathbf{y}$ is an 8×1 vector of measured responses, $\mathbf{X}$ is an 8×7 matrix of variables, representing the reaction conditions of each experimental run, and b is the 7×1 vector of parameters. The variables in $\mathbf{X}$ are coded so that the high level of a variable is 1 and the low level is -1. The vector of parameters can then easily be calculated using the following equation:

$$\mathbf{b} = \left[\mathbf{X}^T\mathbf{X}\right]^{-1}\mathbf{X}^T\mathbf{y} \qquad (5.3)$$

Once the values of the parameters for a particular response are known, they can be plotted to identify any significant effects. The residuals are also plotted as a verification procedure.

Table 5.4 lists the different reaction conditions used in the factorial design to optimise the grafting reaction. The choice of the levels for the different reaction variables was partly influenced by the two papers originally describing the method [Han, D.K. et

al., 1989][Freij-Larsson, C. and Wesslén, B., 1993]. Their studies used temperatures of either 40 or 50°C, and reaction times between 1 and 24 h for the MDI and PEO reactions respectively.

Table 5.4: Experimental conditions for the 2^{5-2}_{III} factorial design.

Run	Temperature (°C)	PEO concentration (%w/v)	MDI concentration (%w/v)	MDI reaction time (h)	PEO reaction time (h)
1	40	2	0.5	3	48
2	40	2	2.0	3	24
3	40	5	0.5	1	48
4	40	5	2.0	1	24
5	60	2	0.5	1	24
6	60	2	2.0	1	48
7	60	5	0.5	3	24
8	60	5	2.0	3	48

Several responses were used to gauge the effect of the variables on the grafting reaction. The first responses examined were the most readily measurable, i.e. water contact angles. By measuring the advancing and receding contact angles, a qualitative assessment of the hydrophilicity of each experimental surface was obtained. The most hydrophilic surfaces, exhibiting low water contact angles, are expected to have the highest levels of surface-bound PEO and therefore represent the best reaction conditions. The water contact angle measurements for the various runs are listed in Table 5.5.

The normal probability plot of the parameters for advancing contact angles is shown in Figure 5.4. If the advancing contact angle data were the result of random

variation about a fixed mean, and changes in the levels of the different variables did not have an effect on the grafting reaction, then the parameters obtained would plot as a straight line on a normal probability plot [Box, G.E.P. et al., 1978]. However, as can be seen in Figure 5.4, four parameters are not easily explained as chance occurrences. Although the parameters represent primary effects confounded with two-factor interaction effects, only the impact of the primary effects will be examined initially. A further discussion on the relevance of the second order interactions will be given later in this section.

Table 5.5: Water contact angle measurements for the 2_{III}^{5-2} factorial design (Average ± S.D., n=16).

Run	Advancing water contact angle (°)	Receding water contact angle (°)
1	64.6±2.7	42.5±5.6
2	69.5±3.0	45.9±5.8
3	61.0±3.4	36.4±4.1
4	65.6±5.8	38.2±7.0
5	63.7±3.6	41.6±8.5
6	64.9±2.6	42.0±5.9
7	65.0±5.8	40.4±6.2
8	60.8±5.2	33.8±5.2

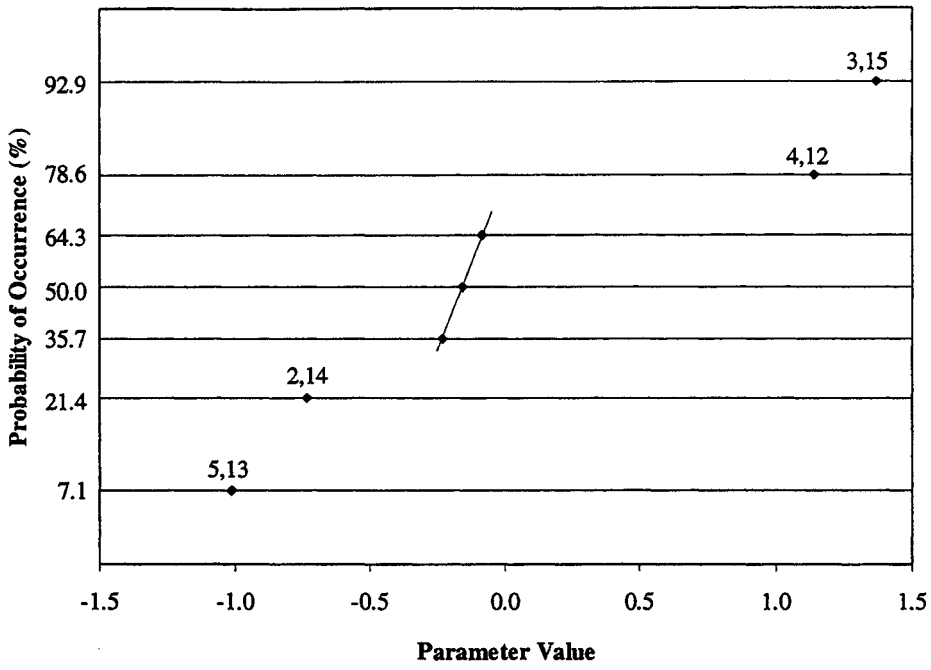

Figure 5.4: Normal probability plot of parameters influencing the grafting reaction using advancing water contact angles as the response.

The parameters indicate that lower contact angles are obtained when the lower levels of MDI concentration and t_{MDI}, and higher levels of PEO concentration and t_{PEO}, were used during the grafting reaction. Normally, plotting the residuals would serve as a check of the model resulting from the identification of significant variables. However, this verification is only valuable if the number of significant variables is fairly small compared to the total number of variables [Box, G.E.P. et al., 1978]. Since four of the seven variables were identified as significant, plotting the residuals would not yield any additional information. Analysis of other responses was compared to these results to assess their validity.

In the case of the receding contact angles, none of the parameters appears to be significant, as illustrated by Figure 5.5.

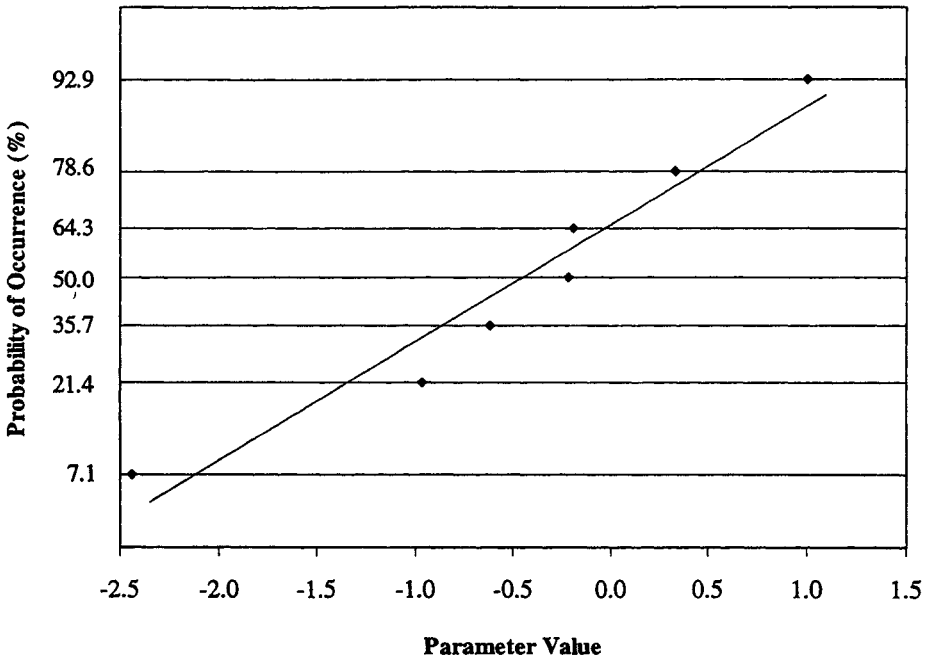

Figure 5.5: Normal probability plot of parameters influencing the grafting reaction using receding water contact angles as the response.

The use of the residuals to check the validity of the identified effects can be used in this instance since none of the seven parameters was deemed significant. If all the effects can be attributed to random noise, then the residuals will form a roughly straight line. An examination of the residuals in Figure 5.6 confirms that the variations from the different runs appear to be the result of chance occurrences. This may be due in part to the large variance in the receding contact angle measurements, illustrated by the large standard deviations in Table 5.5. As a result, the analysis was unable to resolve significant parameters from the random noise of the experiment.

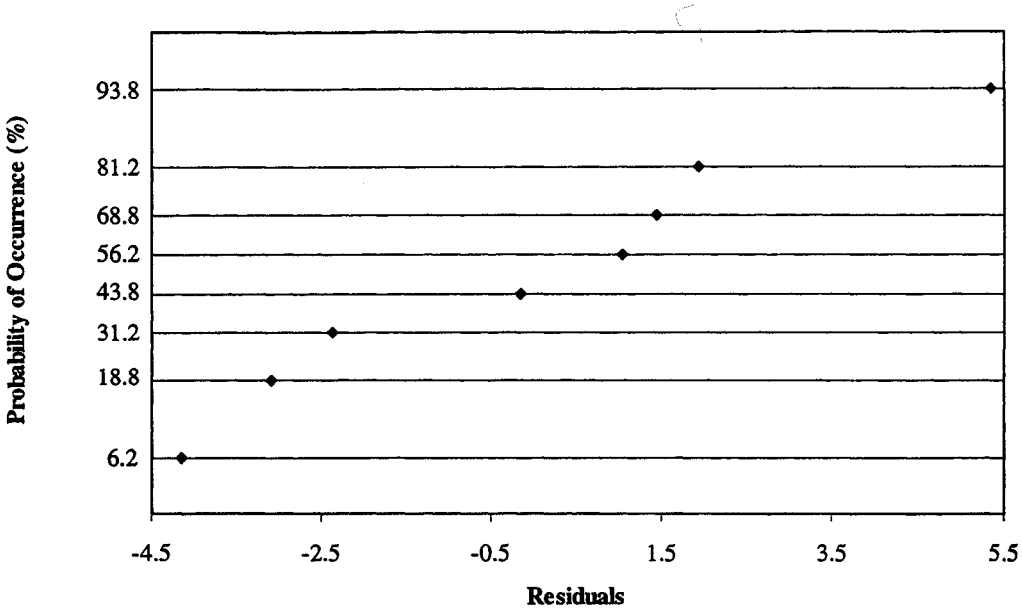

Figure 5.6: Normal probability plot of the residuals from advancing water contact angle response.

Another approach used to optimise the grafting reaction was to examine the changes in the surface chemical composition following the reaction, using XPS data. Table 5.6 lists XPS data for all experimental conditions. The listed atomic ratios, O_{1s}/N_{1s} and C_{1s}/O_{1s}, are used to assess the content of PEO on the surface following the grafting reaction. The O_{1s}/N_{1s} ratio is used to detect increases in oxygen content relative to the PUU substrate. The increase in oxygen due to PEO grafting on the surface is normalised to the nitrogen content of the PUU which should be constant from sample to sample. Therefore a higher value of this ratio would indicate higher quantities of PEO on the surface. The second ratio, C_{1s}/O_{1s}, takes advantage of the low carbon to oxygen ratio in PEO compared to the PUU. The ratio should therefore decrease when PEO is grafted to the PUU surface. Lower values of this ratio would imply higher levels of grafting.

Table 5.6: XPS elemental ratios for the factorial design (n=1).

Run	O_{1s}/N_{1s}	C_{1s}/O_{1s}
1	4.7	3.7
2	3.5	4.3
3	4.5	4.4
4	4.1	4.4
5	4.2	3.6
6	4.8	5.2
7	5.3	3.2
8	5.5	4.0

Figure 5.7 illustrates the normal probability plot of the parameters associated with the O_{1s}/N_{1s} ratio response. Once again, all the parameters seem to result from chance occurrences. The linearity of the residuals in Figure 5.8 confirms that all parameters can plausibly be explained as random occurrences.

Figure 5.9 shows the normal probability plot of the parameters for the C_{1s}/O_{1s} response. In this case, effects **3** and **5** are shown to be significant; these effects represent the MDI concentration and the reaction time of the second step of the grafting reaction, respectively. Since lower values of the C_{1s}/O_{1s} ratio indicate higher levels of surface bound PEO, and since both parameters are positive, this means that lower levels of both these effects will promote higher levels of surface grafting. Therefore the lower concentration of MDI during the first step and the lower reaction time in the second (PEO) step are more favourable. The residuals plotted in Figure 5.10 confirm that the other parameters do not appear to influence the grafting reaction.

Finally, the ultimate test of the effectiveness of the grafting reaction is to determine how these various effects impact on the ability of the surfaces to prevent or reduce protein adsorption. Therefore, each test surface was exposed to 2% (w/v) ^{125}I-labeled fibrinogen solutions in TBS for 3 h at room temperature. Each surface was tested in triplicate at each protein concentration. After the radioactivity on each surface was counted, the protein adsorption levels were determined using the following formula.

$$\text{Adsorbed protein} = \frac{\text{Net surface count} \cdot \text{Concentration of protein solution}}{\text{Protein solution count} \cdot \text{Surface area of sample}} \qquad (5.4)$$

The net surface count is the difference between the surface count and the background count. The adsorbed protein values were averaged at each concentration. The isotherms are plotted in Figure 5.11 and Figure 5.12. For clarity, only a few isotherms have error bars to show representative error associated with these measurements. Also the curves through the data points serve only to highlight the different isotherms and do not represent any theoretical model. This is true for all protein adsorption data presented unless noted otherwise.

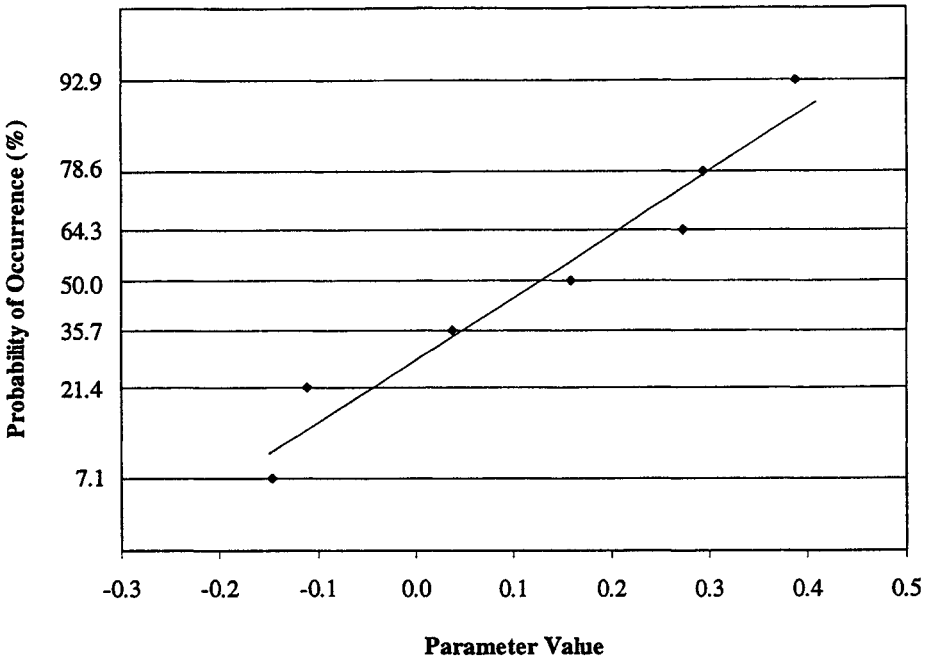

Figure 5.7: Normal probability plot of parameters influencing the grafting reaction using the ratio O_{1s}/N_{1s} as the response.

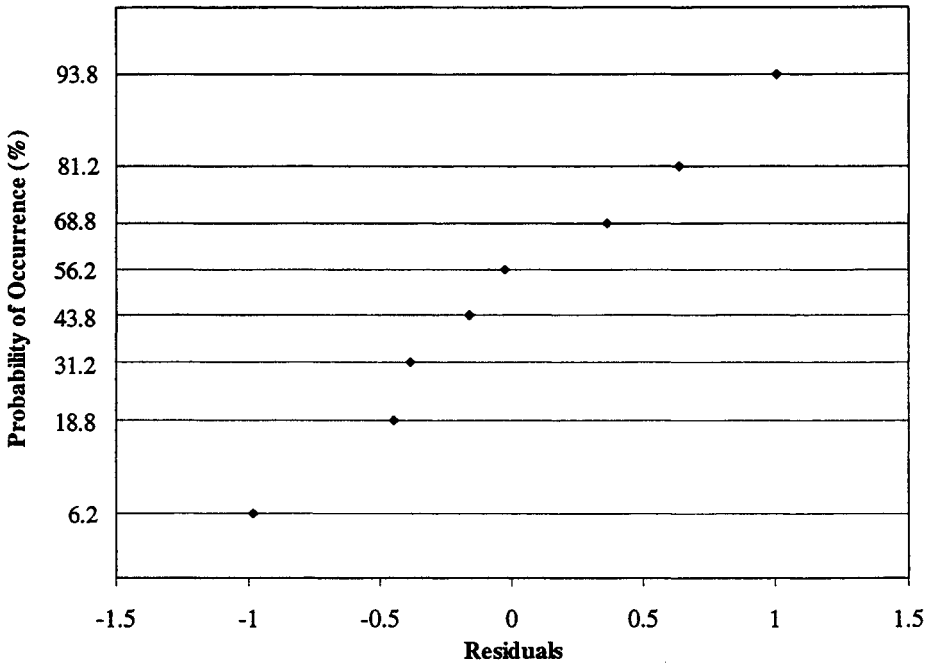

Figure 5.8: Normal probability plot of the residuals of the O_{1s}/N_{1s} response.

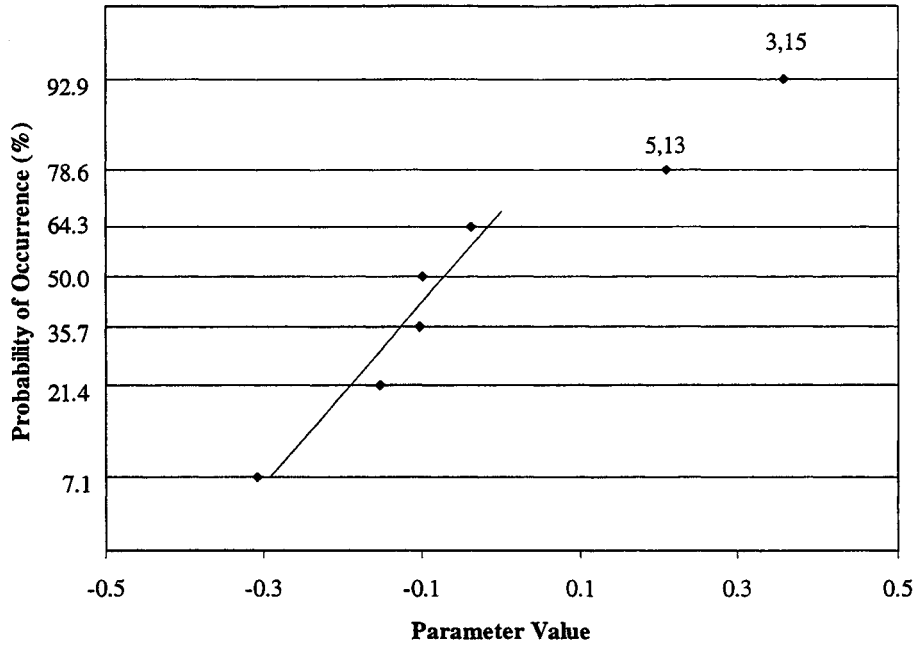

Figure 5.9: Normal probability plot of parameters influencing the grafting reaction using the ratio C_{1s}/O_{1s} as the response.

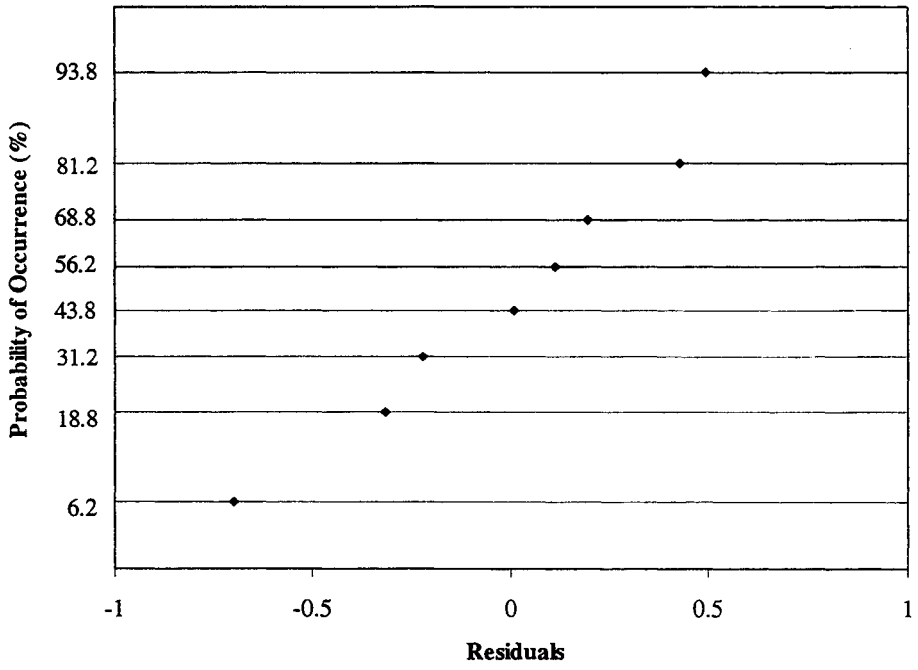

Figure 5.10: Normal probability plot of the residuals of the C_{1s}/O_{1s} response.

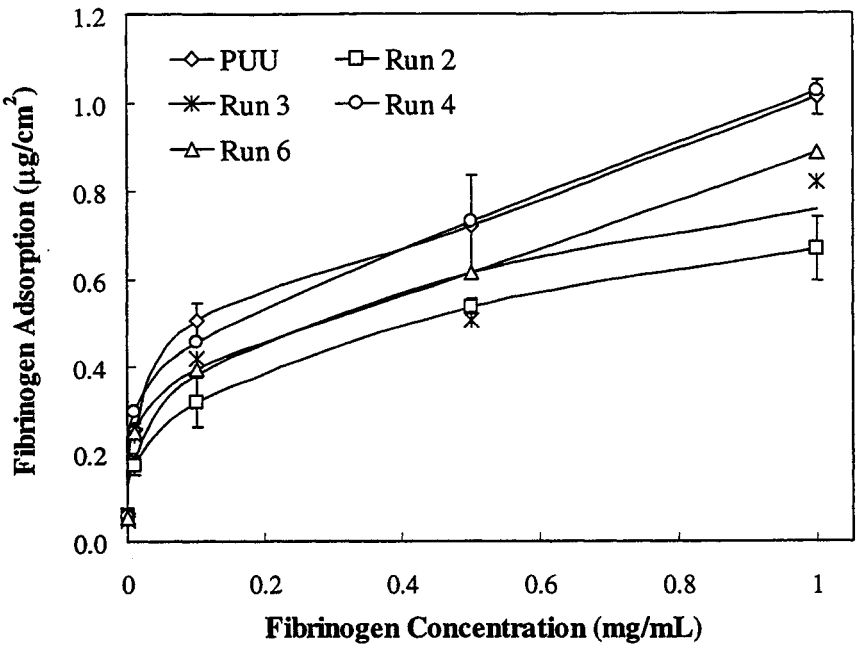

Figure 5.11: Fibrinogen adsorption on test surfaces (from TBS buffer at 22°C for 3 h, average ± S.D., n=3). Refer to Table 5.4 on page 89 for reaction conditions used to prepare the surfaces for each run.

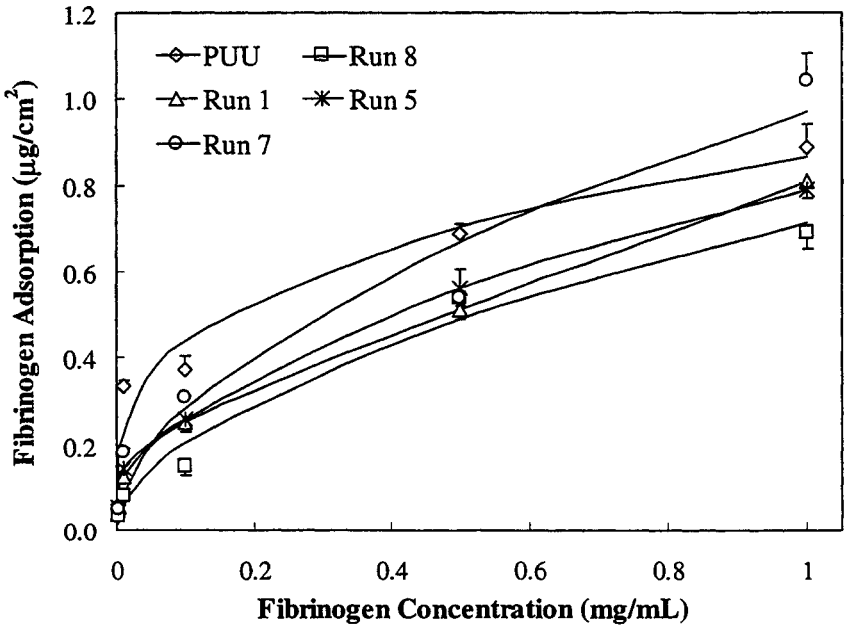

Figure 5.12: Fibrinogen adsorption on test surfaces (from TBS buffer at 22°C for 3 h, average ± S.D., n=3). Refer to Table 5.4 on page 89 for reaction conditions used to prepare the surfaces for each run.

Since the adsorptions could not all be performed simultaneously, two sets of test surfaces were randomly selected to be processed in separate experiments. Nearly all the test surfaces demonstrate lowered protein adsorption compared to the PUU control.

The difficulty for purposes of using the factorial design is to represent each isotherm as a single value. Since there is some variability in the response of the PUU control surface, normalisation was used to enable a more direct comparison of the two sets of data.

The following procedure was used to obtain the normalised adsorption parameter. First, the adsorption level on each sample for every concentration was normalised by dividing by the adsorption level on the control PUU at the same concentration. This gives the adsorption level as a fraction of the adsorption on the control PUU. Finally these fractions are averaged for each surface to give a single value that represents the protein adsorption response. While other indicators, such as the initial slope of the isotherms or the plateau values could also have been used in the analysis, these are only representative of a portion of the adsorption data. The normalised adsorption parameter, on the other hand represents the whole data set. Table 5.7 lists these values for the various runs in the factorial design. The values obtained reflect the patterns of the isotherms quite well. Only one run, 4, with a response of 101.2%, seems no different from the control. Figure 5.11 confirms that this is indeed the case.

Table 5.7: Normalised adsorption for the factorial design (Average ± S.D., n=15). Refer to on page 89 for reaction conditions used to prepare the surfaces for each run.

Run	Normalised adsorption (%)
1	72.1±22.2
2	74.7±17.0
3	82.0±12.1
4	101.2±14.0
5	74.5±20.2
6	87.6±10.0
7	82.9±21.6
8	56.0±22.4

Figure 5.13 illustrates the normal probability plot of the parameters for the protein adsorption response. Since all fall on a roughly straight line, all the parameters in the model can be plausibly explained as chance occurrences; that is, they do not impact the model significantly. The linearity of the residuals in Figure 5.14 confirms this conclusion.

Therefore, following the analysis of five separate responses in an attempt to optimise the reaction conditions of the grafting reaction, the following conclusions can be drawn. In three of the five responses, none of the examined variables could satisfactorily explain the variations observed and these were ultimately attributed to random experimental error. More telling is the fact that three completely different types of responses were used: water contact angle, elemental composition and protein adsorption. This seems to suggest that the inherent variability of the grafting reaction is quite large or that the magnitude of the difference between levels for each variable was not large

enough to result in measurable differences in surface properties above normal fluctuations. For the advancing water contact angle and the C_{1s}/O_{1s} ratio, of the four different parameters identified as being significant, only two were shared by both responses and of those, only one gave a consistent result. Since so few primary effects were identified as being significant, it is unlikely that any two-factor interactions would be significant, therefore only the primary effects are considered.

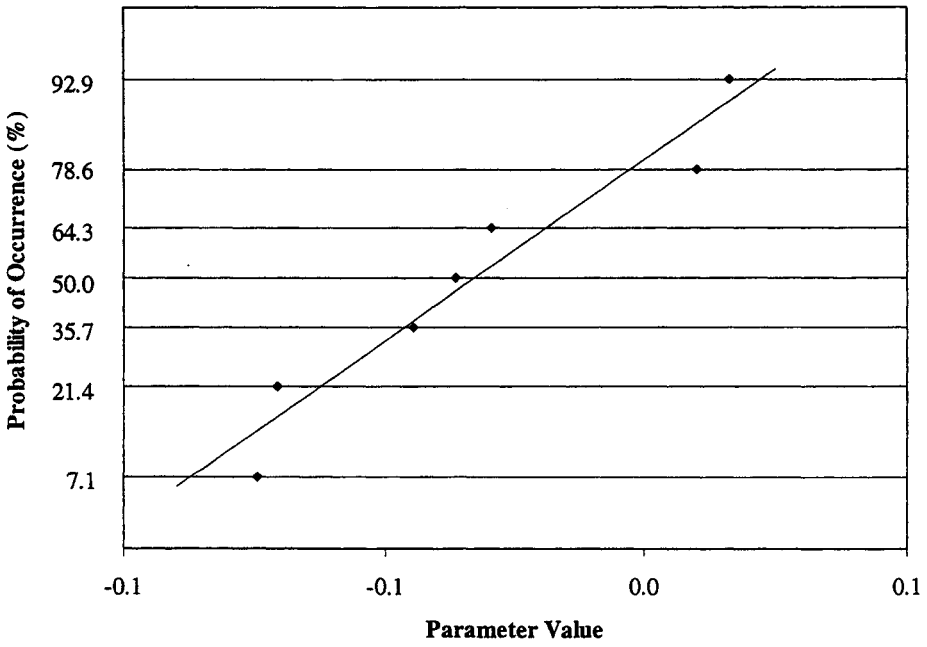

Figure 5.13: Normal probability plot of parameters influencing the grafting reaction using protein adsorption as the response.

The only consistent effect is **3**, MDI concentration. Two responses, advancing contact angle and C_{1s}/O_{1s}, suggested that the lower level of MDI concentration would promote higher levels of surface grafting. Parameters identified in only one response as impacting graft levels are **2** and **4**, PEO concentration and t_{MDI}, respectively. In this instance, the higher level of PEO concentration and lower level of t_{MDI} were determined

to be favourable. Two responses gave contradictory information regarding the impact of parameter **5**, t_{PEO}. Given these results, only variable **3**, MDI concentration, which was found significant in two measured responses can be credibly viewed as having an impact on the grafting reaction; the others are uncorroborated or contradictory. It is also possible that the range selected for the high and low levels of some parameters in this analysis was not large enough to impact the grafting reaction beyond normal experimental fluctuations.

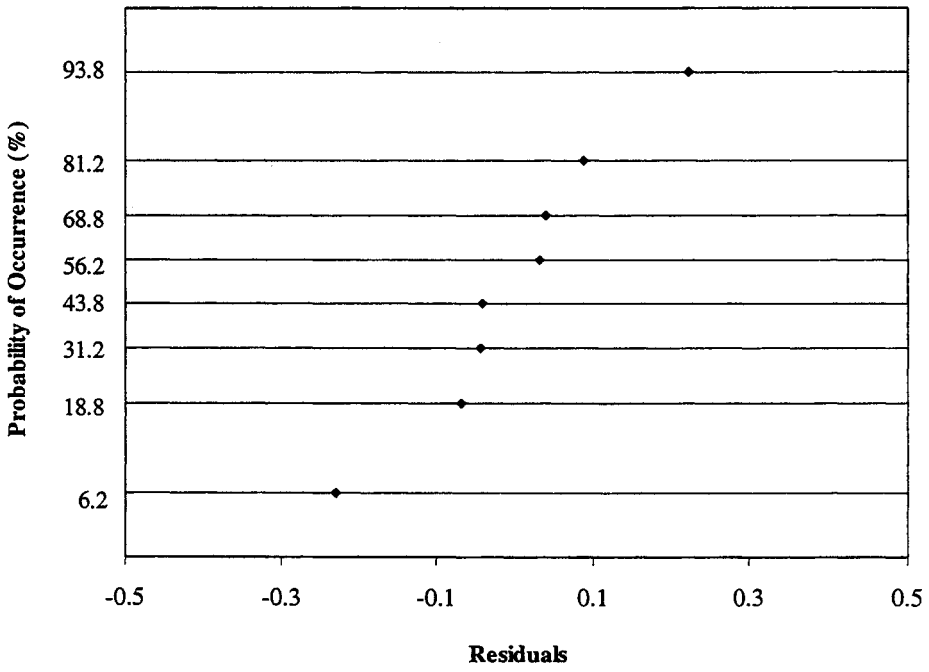

Figure 5.14: Normal probability plot of the residuals of the protein adsorption response.

Given the information obtained from this analysis, no further attempt was made to determine optimal grafting conditions. The responses available did not appear to be sensitive enough to identify the parameters that would promote the highest degree of grafting on the surface. Ideally, the graft density on the surface would be the best response with which to assess the effects of the parameters. Unfortunately, such data were

available only late in the project and it was not feasible at that time to revisit the optimisation issue.

Since the result of the optimisation study only suggested the lower level of MDI concentration as favouring the grafting reaction, other parameters were altered slightly for the sake of experimental convenience. For example, reaction times for both steps were increased slightly to ensure enough time for the reactions to occur. The conditions selected for the grafting reactions with the monomethoxy-PEO reagents are listed in Table 5.8. The tin catalyst was used in both steps. These conditions were maintained for the first two batches of grafted polymers.

Table 5.8: Conditions for grafting reactions with monomethoxy-PEO reagent.

Surfaces	[MDI] (%w/v)	t_{MDI} (h)	[PEO] (%w/v)	t_{PEO} (h)
Batch 1, 2	2	6	5	60
Batch 3	2	24	7.5	24

Problems with temperature control made it quite difficult to maintain a constant temperature during the lengthy second step of the reaction. After dealing with this problem for the first two batches, steps were taken to improve the situation. Therefore the PEO reaction time was reduced to 24 h and the PEO concentration was increased to 7.5% to compensate. Also, the time for the first step was increased to 24 h to better synchronise the operations with respect to the workday. As will be seen later, fluctuations in the properties of all obtained surfaces were such that these small changes in reaction conditions were inconsequential.

5.2.2 Impact of More Reactive PEO Derivatives

The conditions listed in Table 5.8 were the basis for all experiments in which monomethoxyhydroxy-PEO was used as the grafting reagent. Over time, XPS revealed a persistent low-level tin signal on the surface of the PEO-grafted PUUs. This implied that some of the tin catalyst, stannous octoate, was present on the PEO-grafted PUUs. Since stannous octoate has detergent properties, its presence on the surfaces could alter their properties vis-à-vis protein adsorption. Therefore it was desirable to remove this tin contaminant. Various types of cleaning regimens using several solvents were unsuccessful in completely removing the tin surfactant.

The only solution to this problem was to eliminate stannous octoate from the reaction protocol. Therefore another catalyst, triethylamine, was selected to replace stannous octoate in the grafting reaction. The proposed mechanism for the catalytic effect of tertiary amines on the isocyanate-urethane (or urea) reaction is illustrated in Figure 5.15. This mechanism is an extension of the triethylamine catalysed reaction between isocyanate and amines [Lelah, M.D. and Cooper, S.L., 1986].

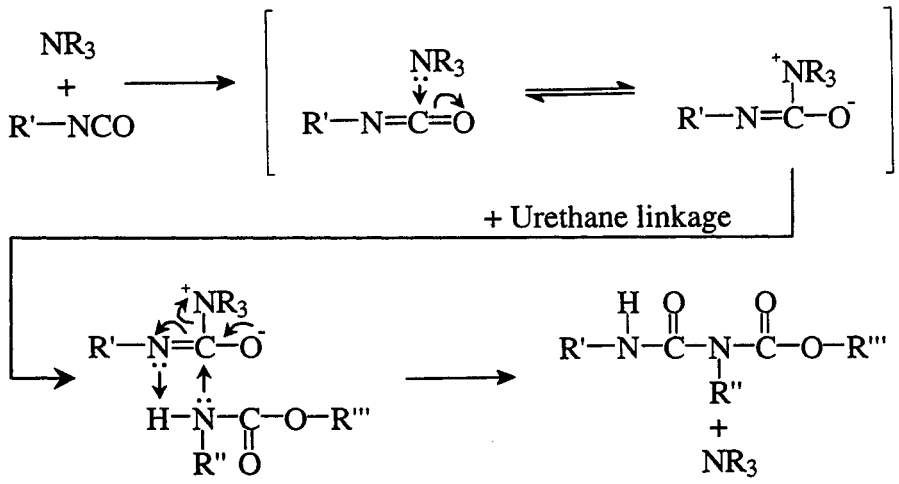

Figure 5.15: Proposed mechanism for tertiary amine catalysis of the reaction between an isocyanate and a urethane to form an allophanate group.

The first step is the reversible formation of a reactive intermediate between the tertiary amine and the isocyanate. When this intermediate comes into proximity with a urethane or urea group, a rapid rearrangement to an allophanate or biuret group, respectively, results. Triethylamine also catalyses the reaction of isocyanates with water [Lelah, M.D. and Cooper, S.L., 1986]; therefore its use was limited to the first step of the grafting reaction. To compensate for the absence of catalyst in the second step, monomethoxyamino-PEOs were used in place of monomethoxy-hydroxy-PEOs because of their anticipated higher reactivity.

Following the preliminary reactions, the reaction conditions were modified slightly since the amino-PEO reagents were much more expensive than monomethoxyhydroxy-PEOs. Therefore lower concentrations of PEO were used. However, as will be seen in subsequent sections, the grafting reaction with the amino-

PEOs was much more successful than with hydroxy-PEOs. As well, only PEOs of molecular weight 550, 2000 and 5000 were used.

Initially, the effect of changing the catalyst was examined. The grafting reaction was performed using triethylamine with three different types of PEO: dihydroxy-PEO, monomethoxyhydroxy-PEO and monomethoxyamino-PEO. For the hydroxy-PEOs, both steps were catalysed with 2% w/v triethylamine (first step with 2% w/v MDI for 24 h at 60°C, second step with 7.5% w/v PEO for 24 h at 60°C). The reaction conditions for the amino-PEO were identical to those for the hydroxy-PEOs except that only the first step was catalysed with 2% w/v triethylamine. Water contact angle data for these surfaces are shown in Figure 5.16.

According to these data, there is little difference in hydrophilicity between the surfaces prepared with the hydroxy-PEO reagents (MeO-PEO-OH and HO-PEO-OH). Both the advancing and receding water contact angles of these surfaces are very similar. The water contact angles measured in an aqueous environment using a captive air bubble are also quite similar. The methoxy group does not seem to have a large effect on the hydrophilicity of the surface. However, the surface prepared with the amino-PEO reagent displays significantly lower water contact angles for all three measurements. This implies increased hydrophilicity possibly due to higher concentrations of surface-bound PEO.

A protein adsorption experiment with myoglobin in TBS buffer was also performed using these surfaces to test their protein repellent properties. Figure 5.17 shows the isotherms obtained at room temperature.

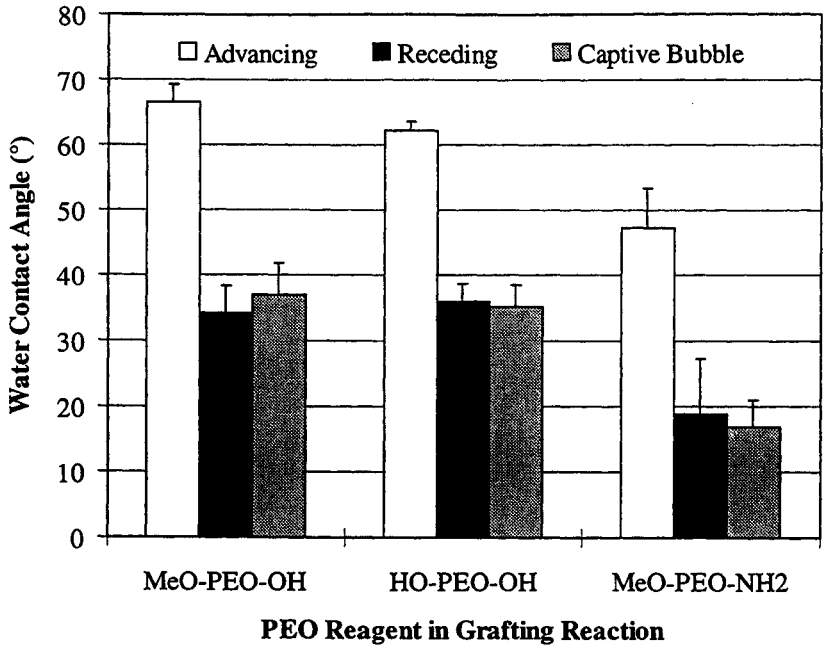

Figure 5.16: Water contact angles of test surfaces. (±S.D, n ≥ 12).

The advantage of using the more reactive PEO reagent is quite apparent from the protein adsorption data. The surface prepared with the monomethoxyamino-PEO reagent reduces the adsorption of myoglobin to a greater extent than either of the other PEO reagents. As well, the surface prepared with dihydroxy reagent shows lower adsorption than the surface prepared with the monomethoxy-PEO. This could be due either to the effect of –OH versus –OMe end groups on the PEO grafts, or to the fact that a higher graft density was achieved with the di-hydroxy PEO. The large difference in adsorption properties is somewhat surprising given the similarity of the water contact angle measurements on the two hydroxy PEO surfaces. This shows the extreme sensitivity of protein adsorption to surface properties. The result that the surface prepared with monomethoxyhydroxy-PEO adsorbed as much or more than the control PUU was

unexpected. Given this result, it appears that only the first step of the grafting reaction occurred, causing the resulting surface to adsorb slightly more protein than the control. The reasons for this behaviour are discussed in Section 7.1. In support of the previous observation, a subsequent experiment with a monomethoxyhydroxy-PEO-grafted surface showed lower adsorption than the control PUU (see text and Figure 5.19 below).

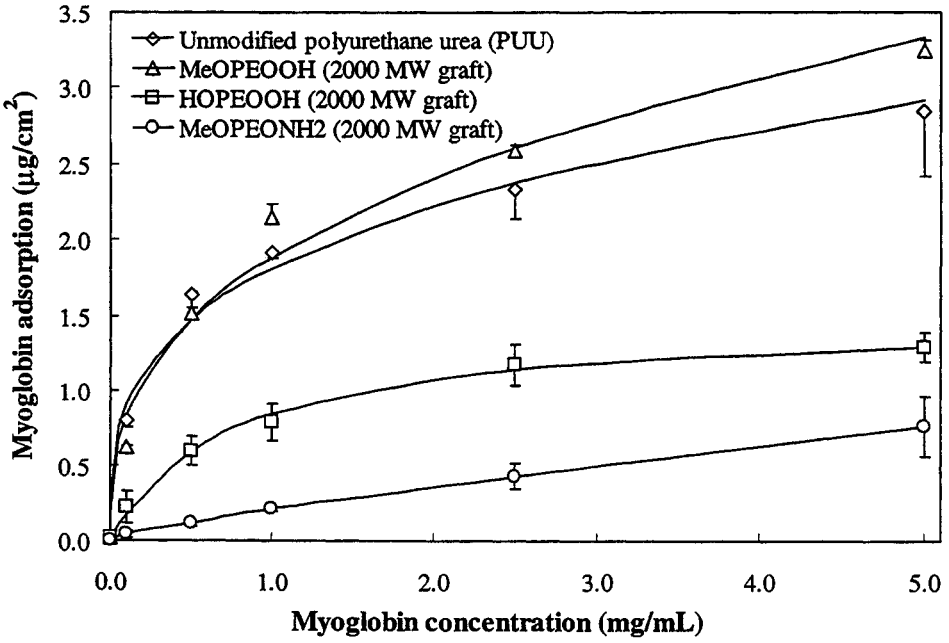

Figure 5.17: Adsorption of myoglobin on test surfaces (from TBS buffer for 3 h at 22°C, ±S.D., n = 3).

An additional experiment was performed to assess the importance of some of the reaction parameters. The detailed factorial design study done for the hydroxy terminated PEO was however not repeated. Four 2000 MW PEO-grafted surfaces were prepared. The details of the experimental conditions are listed in Table 5.9.

In these experiments the reactions were catalysed with 2% w/v triethylamine in the first step only, with the exception of the reaction using MeO-PEO-OH where both

steps were catalysed with 2% w/v triethylamine. The issue of reaction time for the MDI-urethane (urea) reaction step was re-examined. Also, a control experiment with PEO concentrations at the high levels of the previous protocol compared to the much reduced levels of the new protocol was required.

Table 5.9: Conditions for additional examination of reaction conditions for the grafting protocol using amino-PEO reagents.

Experiment	MDI concentration (%w/v)	t_{MDI} (h)	PEO concentration (%w/v)	t_{PEO} (h)	PEO Reagent
1	2	1	7.5	24	MeOPEOOH
2	2	24	7.5	24	$MeOPEONH_2$
3	2	1	1	24	$MeOPEONH_2$
4	2	24	1	24	$MeOPEONH_2$

Water contact angles were measured on each of the product surfaces and the data are summarised in Figure 5.18. The advancing and receding water contact angles are significantly lower on surfaces prepared with the MeO-PEO-NH_2 reagent (2-4) compared to surfaces prepared with the MeO-PEO-OH (1). Usually, the underwater water contact angle measurement using the captive bubble technique gives values quite similar to the receding water contact angle measurement by the sessile drop technique. This is not the case for experiment 1, suggesting that incubation in water causes surface rearrangements to expose more PEO to the surface thereby increasing hydrophilicity. If the PEO graft density is higher on the surfaces from experiments 2-4 as hypothesised, such rearrangements may not have as large an impact on the hydrophilicity of the surfaces.

Although the surface from experiment 1, prepared with MeO-PEO-OH, has a similar captive bubble water contact angle to the surface from experiment 3, prepared with MeO-PEO-NH_2, the protein adsorption behaviour is much different (see below).

Surfaces from experiments 2 and 4, which differ only in the concentration of the amino-PEO reagent during the grafting reaction show very similar water contact angles. This suggests that similar surface hydrophilicity and therefore similar content of surface-bound-PEO is achieved with either the low or high concentration of the PEO reagent. The water contact angles of the surface from experiment 3, with the shorter MDI reaction time, were all slightly higher than those of surfaces from experiments 2 and 4, suggesting less effective grafting reactions.

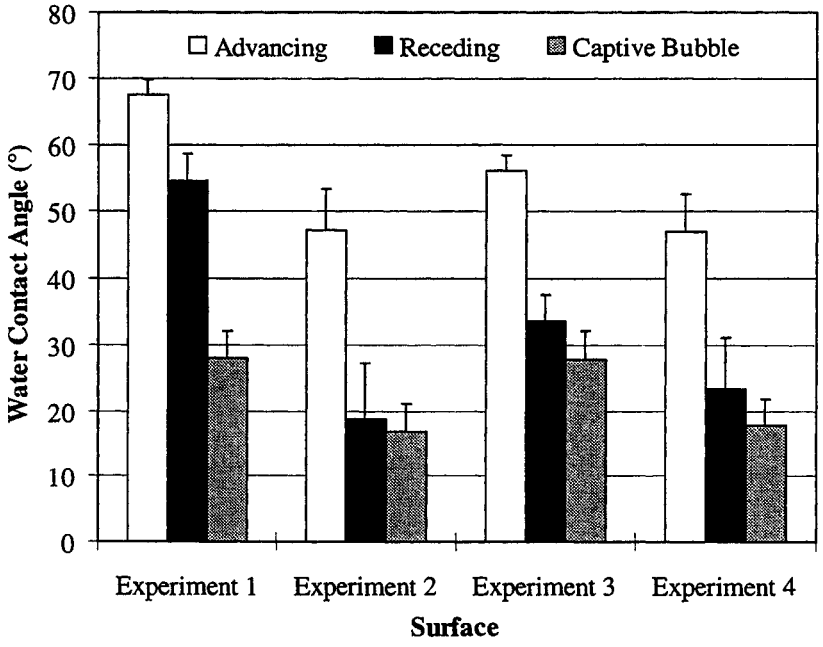

Figure 5.18: Water contact angles of surfaces prepared under reaction conditions outlined in Table 5.9 (±S.D., n ≥ 12).

A protein adsorption experiment with myoglobin was also performed on the four test surfaces and the unmodified PUU control surface. The isotherms are shown in .

All the PEO-grafted surfaces show significant reduction in adsorption compared to the control PUU. The improved protein repellent properties of the grafted surfaces prepared using the amino-PEO reagent (experiments 2-4) is clearly illustrated by the much lower level of myoglobin adsorption compared to experiment 1.

According to the isotherms in Figure 5.19, the adsorption behaviour of surfaces from experiments 3 and 4 are nearly identical even though the reaction time of the first step differed. Therefore, although slightly less hydrophilic than surface 4, surface 3 has nearly identical protein adsorption behaviour. This confirms that the MDI reaction time between 1 and 24 h does not impact on the protein adsorption properties of the grafted polymer and that the choice of the shorter reaction time is warranted. Finally, in comparing the isotherms of surfaces 2 and 4, it is clear that higher amino-PEO concentration leads to grafted polymers that are more protein repellent. However, the cost of the monomethoxyamino-PEO reagent discouraged continuing experiments at this concentration of PEO. Therefore, given that the protein repellent effect at the lower PEO concentration was similar, this level was used for subsequent experimentation with amino-PEO-based surfaces.

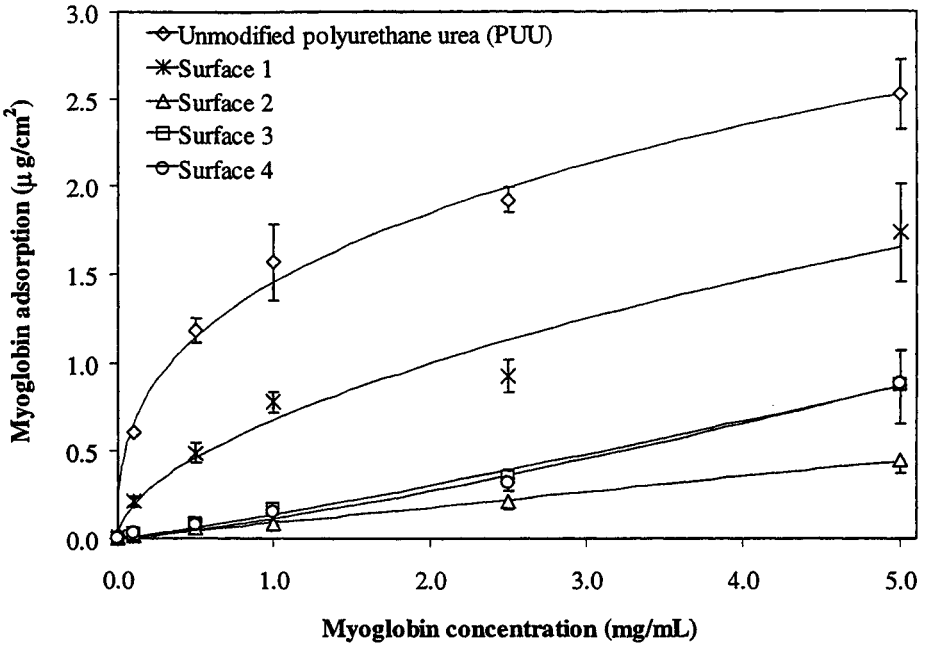

Figure 5.19: Adsorption of myoglobin on test surfaces (from TBS buffer for 3 h at 22°C, ±S.D., n = 3). See Table 5.9on page 89 for experimental conditions for each surface.

6.0 MATERIALS CHARACTERISATION

The previous chapter explained in detail how the reaction conditions for the PEO-grafting reaction were selected. Once prepared, the surface properties of the experimental surfaces were determined using several techniques including water contact angle measurements, X-ray photoelectron spectroscopy (XPS) and atomic force microscopy (AFM). By comparing the properties of the different experimental surfaces, valuable information about the PEO-grafted PUU system was obtained. Labelling with a fluorine-containing molecule was also used to gain information about grafting density. In the late stages of the project, a direct method based on radiolabeling was used to measure graft density.

6.1 Water Contact Angle Measurements

Water contact angle measurement is a simple method to assess in a qualitative manner the surface properties of materials. Water is the logical choice as test liquid since all subsequent protein adsorption experiments were performed in aqueous solutions. Also, materials used in a biomedical or biotechnological setting are expected to be in contact with aqueous environments.

6.1.1 Substrate PUU

The properties of the substrate PUU were determined in order to have suitable reference data when examining the effects of surface grafting. Several batches of the substrate PUU were synthesised during the course of experimentation. GPC data (Section

5.1.2) showed a high degree of similarity in the molecular weight distribution of the polymers from the different batches. Given this result, the properties of the polymer solids were expected to be similar as well. Figure 6.1 shows water contact angle data for the PUU substrate. The advancing and receding contact angles were measured using the sessile drop technique. Contact angles were also measured on surfaces incubated in water using a captive air bubble. The average advancing and receding contact angles on surfaces from all three batches are indeed quite similar. The contact angle measured by captive air bubble in water is almost identical to the receding contact angle for the first PUU batch. This suggests that the latter measurement is a good indicator of the properties of the surface in an aqueous environment.

When the data were pooled, the advancing water contact angle was 69.7° ± 1.8° and the receding contact angle is 58.1° ± 4.1°. These values are similar to those previously obtained by Skarja: 78.9° ± 2.0° and 58.4° ± 2.9° [Skarja, G.A., 1994]. The difference may be due to the more rigorous cleaning protocol employed in the current studies, which included a lengthy extraction in toluene. This treatment may have removed more hydrophobic contaminants from the surface region, resulting in slightly lower contact angles.

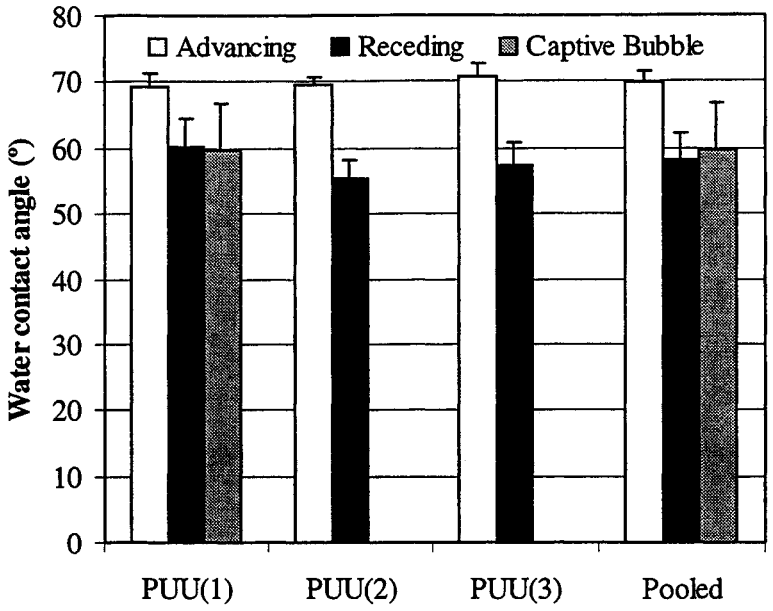

Figure 6.1: Water contact angle data on different batches of the substrate PUU. (Average ± S.D., n ≥12).

The difference between the advancing and receding contact angles is referred to as hysteresis and has been attributed to many phenomena [Marmur, A., 1998]. One explanation attributes the effect to surface group rearrangement due to interactions with water. It has been shown that chemical groups present at a polymer surface are influenced by the local environment [Marmur, A., 1998]. Therefore when this environment changes from hydrophobic air to hydrophilic water, chemical groups near the interface will rearrange in order to minimise the surface free energy. Other explanations for the hysteresis effect include heterogeneous distribution of surface chemical groups, surface roughness and polymer swelling due to water uptake.

The hysteresis in the case of the substrate PUU is relatively small; less than 12°. This implies that contributions from any of the above mentioned causes are small. A

water uptake study on the polymer substrate showed that over a 20 day incubation period in water, the average polymer mass increase was only 2.3%. This level was reached within a day of incubation and remained constant thereafter. Therefore, since the substrate PUU does not absorb much water when exposed to an aqueous environment, any hysteresis caused by this effect is likely small. This is not surprising given the chemical composition of the polymer. Both the diisocyanate, MDI, and the chain extender, MDA, contain large hydrophobic phenyl groups. As well, the soft segment, PTMO, is not strongly hydrophilic.

6.1.2 CH_3O-PEO-OH grafted PUU surfaces

The water contact angles on the PUU surfaces prepared using monomethoxyhydroxy-PEOs (PUU-OPEO) are summarised in Figure 6.2 to Figure 6.6. Samples from all three batches of each grafted polymer type were tested. As mentioned in Section 5.2.1, the first two batches were prepared using identical reaction conditions, whereas the third batch was prepared using a slightly modified reaction protocol. Therefore comparing the values of the first two batches provides some information on the variability inherent in the grafting reaction. The advancing water contact angles for the first two batches of each type of PEO-grafted surface were very similar. This was not so for the receding water contact angle measurements. In the case of the surfaces prepared with the 165, 2000 and 5000 MW monomethoxyhydroxy-PEOs, the difference between the first and second batches is significant. The reason for these differences is unclear since the surfaces prepared with the 350 and 750 MW monomethoxyhydroxy-PEOs have

very similar receding water contact angles for the first two batches. As well, most of the contact angle data determined by captive bubble were once again quite similar to the receding contact angle measurements. Therefore, the receding water contact angle appears to provide information on the properties of the PEO-grafted surfaces in an aqueous environment.

The water contact angle data for the third batch, both advancing and receding, are either very similar to or fall between those of the first two batches. This supports the previously stated conclusion that as far as water contact angles are concerned, the changes to the reaction protocol made no difference.

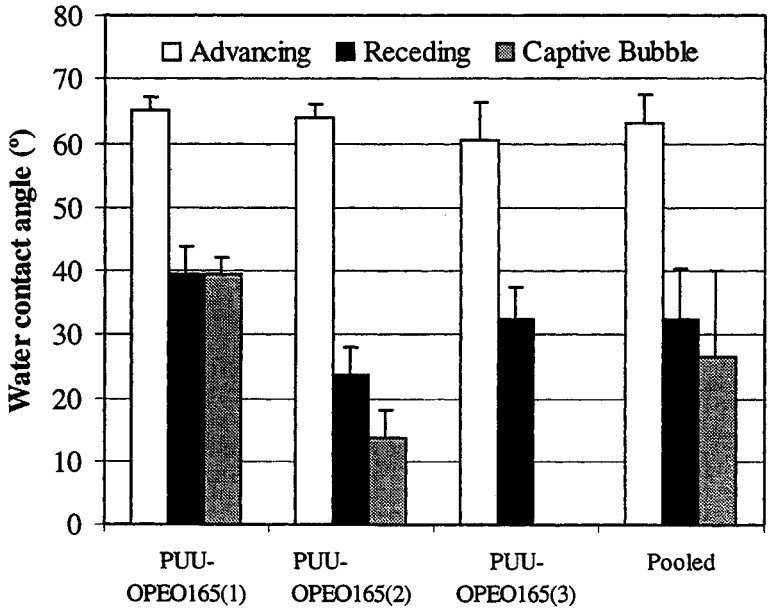

Figure 6.2: Water contact angle measurements on different batches of PUU-OPEO165. (Average ± S.D., n ≥12).

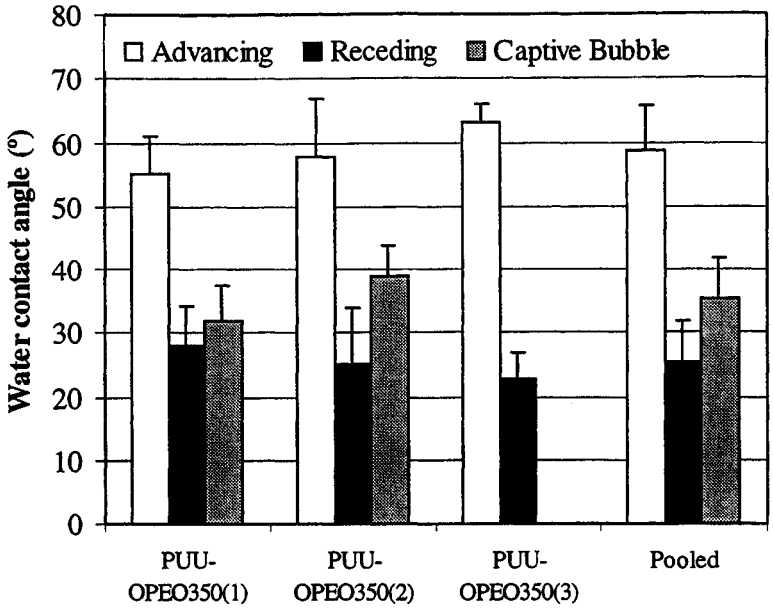

Figure 6.3: Water contact angle measurements on different batches of PUU-OPEO350. (Average ± S.D., n ≥10).

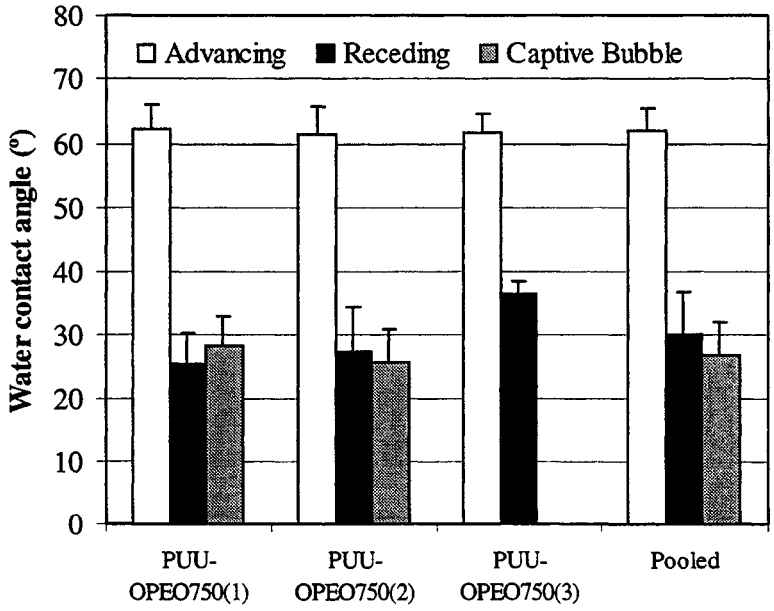

Figure 6.4: Water contact angle measurements on different batches of PUU-OPEO750. (Average ± S.D., n ≥10).

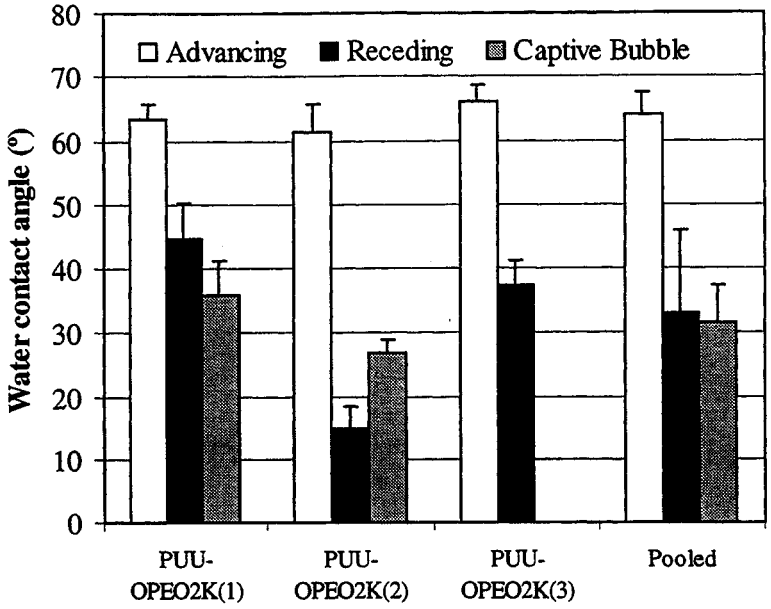

Figure 6.5: Water contact angle measurements on different batches of PUU-OPEO2K. (Average ± S.D., n ≥12).

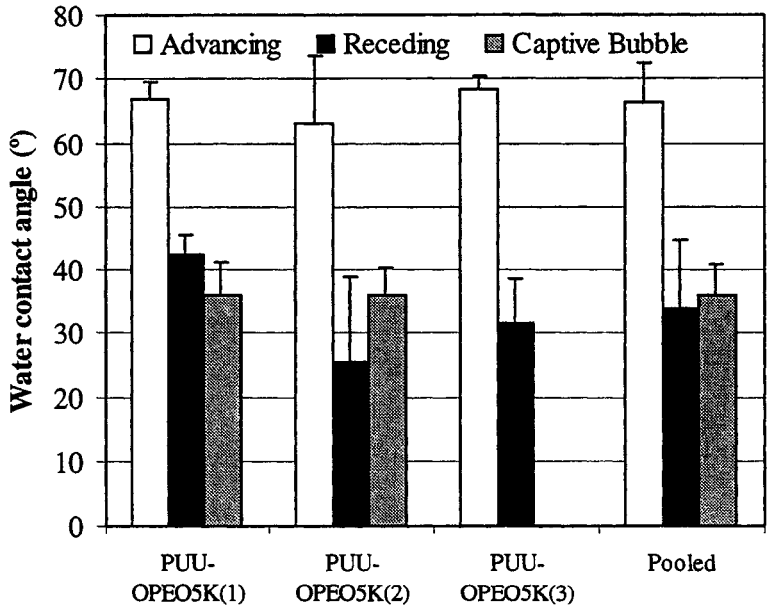

Figure 6.6: Water contact angle measurements on different batches of PUU-OPEO5K. (Average ± S.D., n ≥10).

The data for all the experimental surfaces were pooled and are plotted together in Figure 6.7 to facilitate comparison. The average advancing water contact angles are all significantly lower on the PEO-grafted surfaces than on the PUU substrate, as expected. However the magnitude of the decrease is relatively small: generally less than 10°. Also, although some advancing contact angles on the PEO-grafted surfacs are significantly different from one another, there is no clear trend with respect to the molecular weight of the PEO grafts. Direct comparison of data from surfaces with PEO grafts of different molecular weights is also complicated by the lack of information about the PEO graft density on the surfaces.

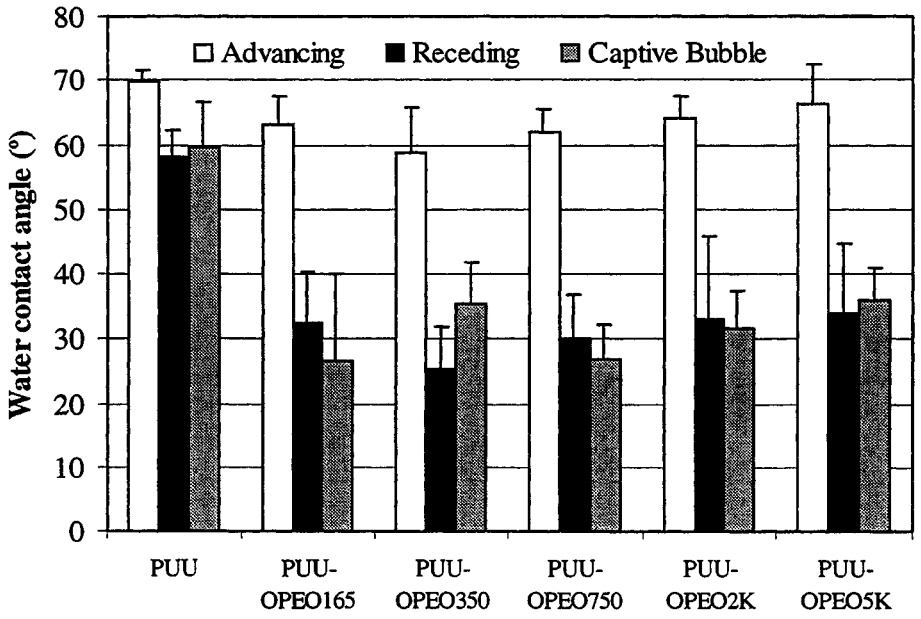

Figure 6.7: Pooled water contact angle measurements on the substrate PUU and PUU-OPEO surfaces. (Average ± S.D., n ≥32).

The average receding water contact angles on the PEO-grafted surfacs are also not significantly different from one another except for PUU-OPEO350 which is significantly

lower than the others. Again, there is no trend relating to PEO MW dependence. However, all are much lower than the average value measured on the substrate PUU. The water contact angles measured by captive bubble are in most cases quite similar to the receding contact angles and also show no dependence on the molecular weight of the PEO grafts. From these data, it appears that the PEO-grafted surfaces are more hydrophilic than the control PUU. This implies significant levels of PEO grafts on all the experimental surfaces. The presence of the PEO grafts also increases contact angle hysteresis (difference between the advancing and receding contact angles). This may be due to increased chemical heterogeneity following the grafting reaction or possibly to changes in the surface roughness.

6.1.3 CH_3O-PEO-NH_2 grafted PUU surfaces

The water contact angles on PUU surfaces prepared using monomethoxyamino-PEOs (PUU-NPEO) are summarised in Figure 6.8 to Figure 6.10. In this instance, all batches were prepared using identical reaction conditions. Therefore, the variability in the data between different batches provides an indication of the variability inherent in the grafting reactions. Both the advancing and receding water contact angles of the various batches for a particular surface type were similar. The reproducibility of the surface properties was better for the PUU-NPEO than for the PUU-OPEO surfaces. Captive bubble measurements were not taken on these surfaces since previous data had shown that receding water contact angles measured by sessile drop gave similar values.

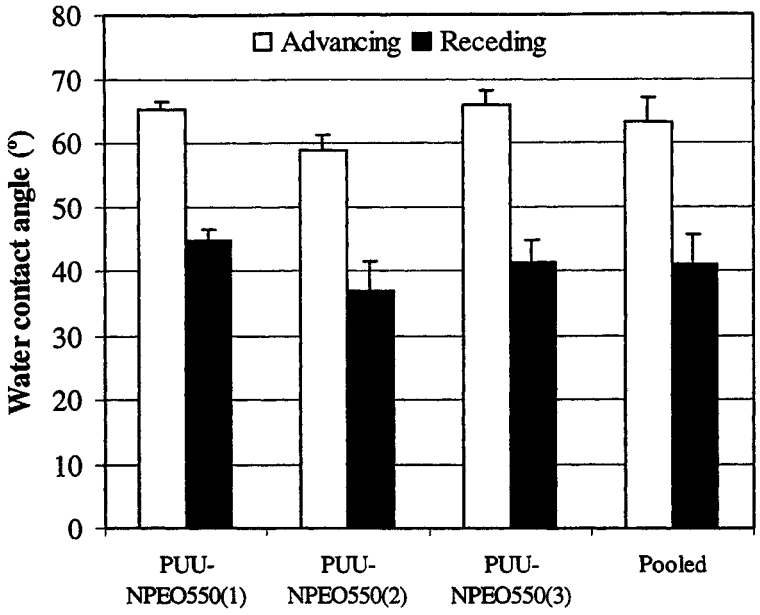

Figure 6.8: Water contact angle measurements on different batches of PUU-NPEO550. (Average ± S.D., n ≥12).

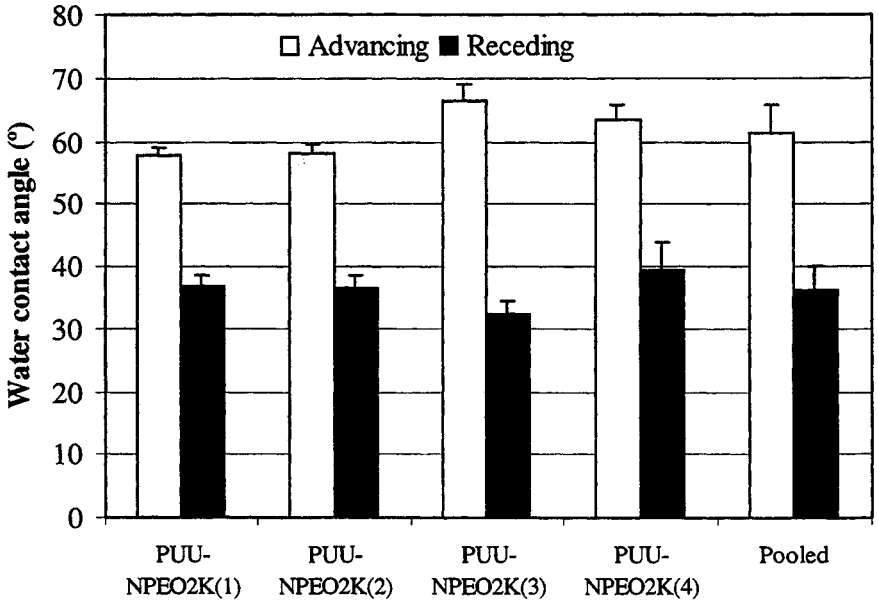

Figure 6.9: Water contact angle measurements on different batches of PUU-NPEO2K. (Average ± S.D., n ≥12).

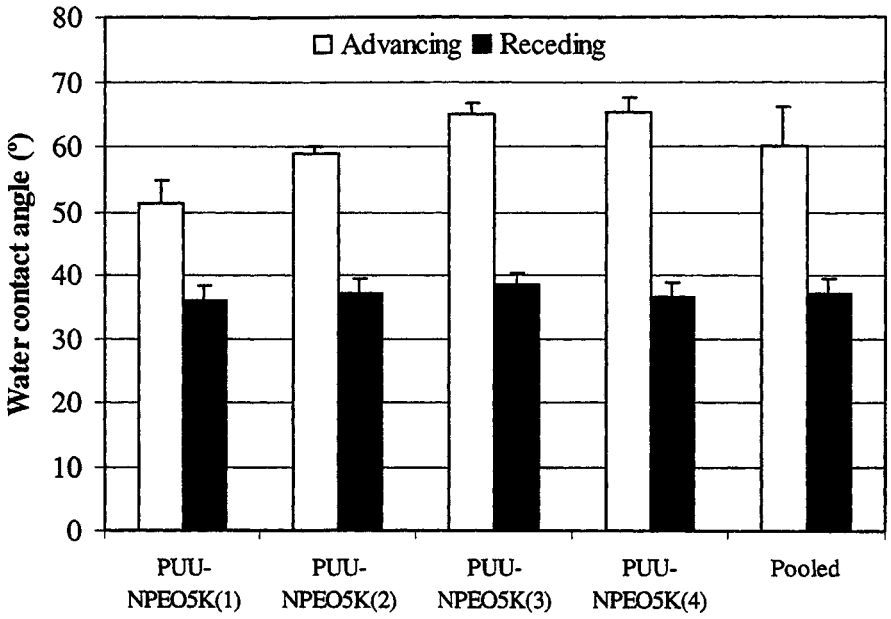

Figure 6.10: Water contact angle measurements on different batches of PUU-NPEO5K. (Average ± S.D., n ≥12).

The pooled data are plotted together in Figure 6.11. As expected, both advancing and receding water contact angles of the grafted surfaces are significantly lower than those of the PUU substrate. Also, the values for PUU-NPEO550 are significantly higher than for either PUU-NPEO2K or PUU-NPEO5K. However, contact angles on the latter two surfaces are not significantly different from each other.

The same trends were observed for the receding contact angles. The contact angles on the PEO-grafted surfaces were all significantly lower than on the substrate PUU. Also the receding contact angles on PUU-NPEO2K and PUU-NPEO5K were significantly lower than on PUU-NPEO550 but not significantly different from each other. The PUU-NPEO surfaces show a reduction in water contact angle with increasing PEO molecular weight. The effect appears to level off at graft values of 2000 MW and

higher, however. This suggests that 2000 MW may be the threshold value for achieving desirable surface properties.

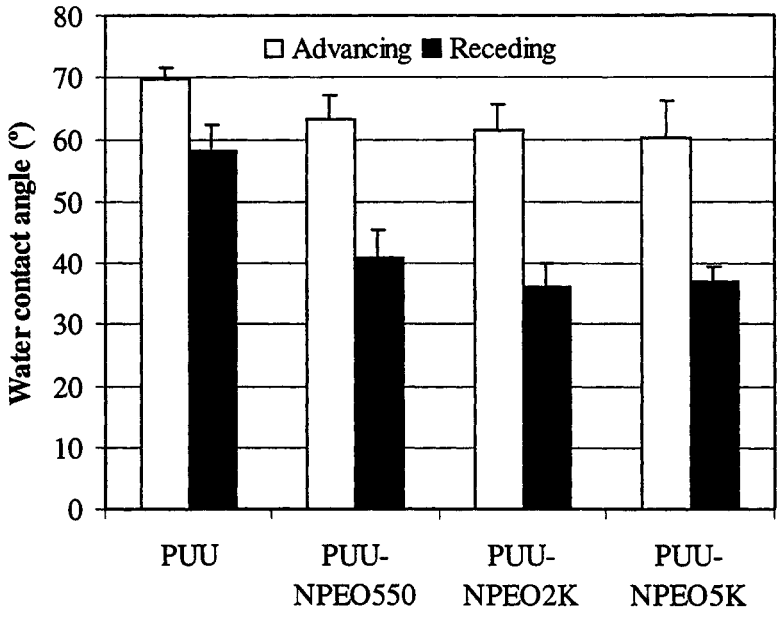

Figure 6.11: Pooled water contact angle measurements on the substrate PUU and PUU-NPEO surfaces. (Average ± S.D., n ≥36).

Finally, the water contact angles for similar PEO-grafted surfaces prepared with different PEO reagents (-OH and $-NH_2$ terminated) are compared in Figure 6.12. It is important to note that this comparison is done without knowledge of the actual PEO graft density on any of the surfaces. The advancing contact angles on both PUU-NPEOs are significantly lower than on their PUU-OPEO counterparts ($p < 0.05$), although the difference is less than 10°. There is no significant difference in the receding contact angles, although the average values on the PUU-NPEOs are slightly higher than on the PUU-OPEOs. Therefore, it appears that the type of PEO reagent does not have much impact on surface properties, at least using water contact angle as the criterion.

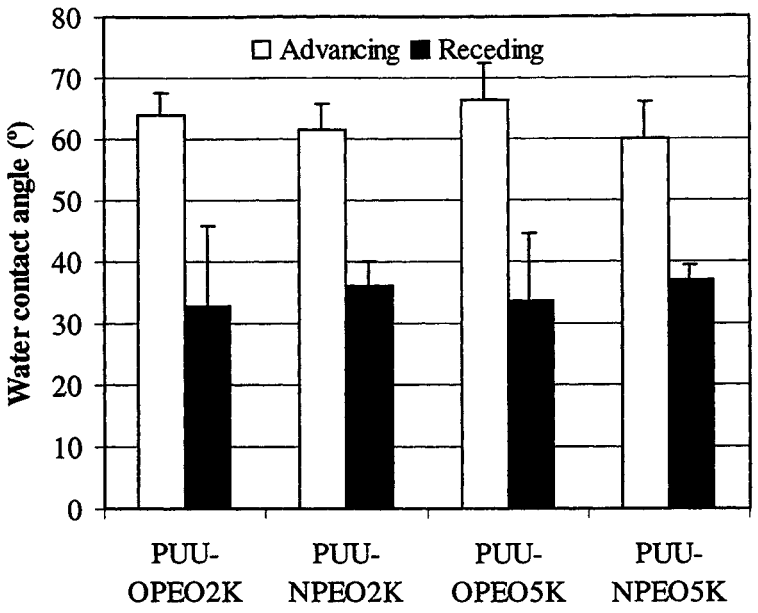

Figure 6.12: Comparison of water contact angle measurements on surfaces prepared with different PEO reagents (Average ± S.D., n ≥40).

6.2 X-Ray Photoelectron Spectroscopy

XPS is used to determine the chemical elemental composition of a sample surface. The probing depth is limited to approximately the outermost ~100 Å, the average electron mean free path through matter [Andrade, J.D., 1985b]. Since the chemical grafting used in this project is limited to the surface, XPS is an appropriate method to monitor the grafting reaction by following changes in chemical composition.

6.2.1 Substrate PUU

In order to have a suitable basis for comparing the changes in chemical composition following the grafting reaction with PEO, the substrate PUU was analysed with XPS. A typical survey scan of the PUU substrate is illustrated in Figure 6.13.

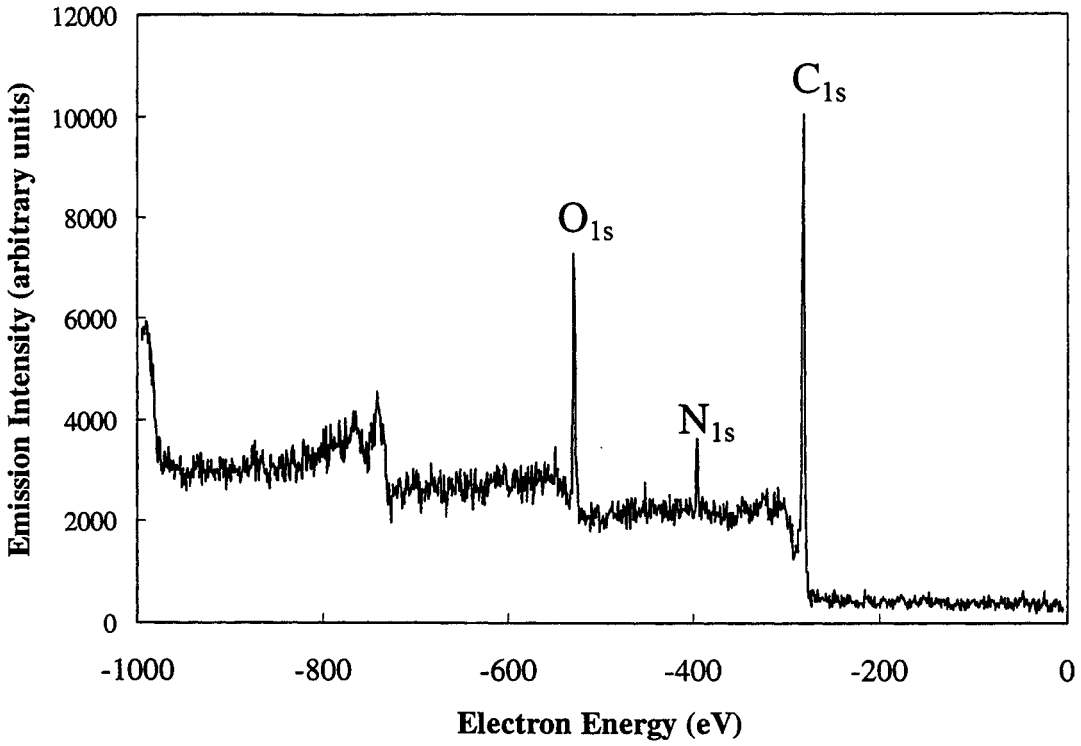

Figure 6.13: Survey scan of the substrate PUU at a 90° take-off angle.

The significant elemental peaks are identified as: carbon (C_{1s}) at 285 eV, nitrogen (N_{1s}) at 402 eV and oxygen (O_{1s}) at 532 eV. Following the survey scan, low resolution scans were performed on all detected elemental peaks. The areas beneath these peaks were then used to determine the elemental composition of the surface region.

High resolution scans were also performed on the C_{1s} peak to obtain information about the types of chemical groups with which carbon atoms present at the surface are associated. Curve fitting was used to assign sub-peaks to the various chemical groups that make up the C_{1s} signal. The fitting was performed with a MATLAB® analysis package called ESCA Tools, obtained from the Centre for Biomaterials at the University of Toronto. The fitting procedure consists of inputting peaks at appropriate energy levels,

based on the chemical groups expected to be found at the surface of the sample. The program then finds the best fit given this input data. An example of a high resolution C_{1s} scan is shown in Figure 6.14.

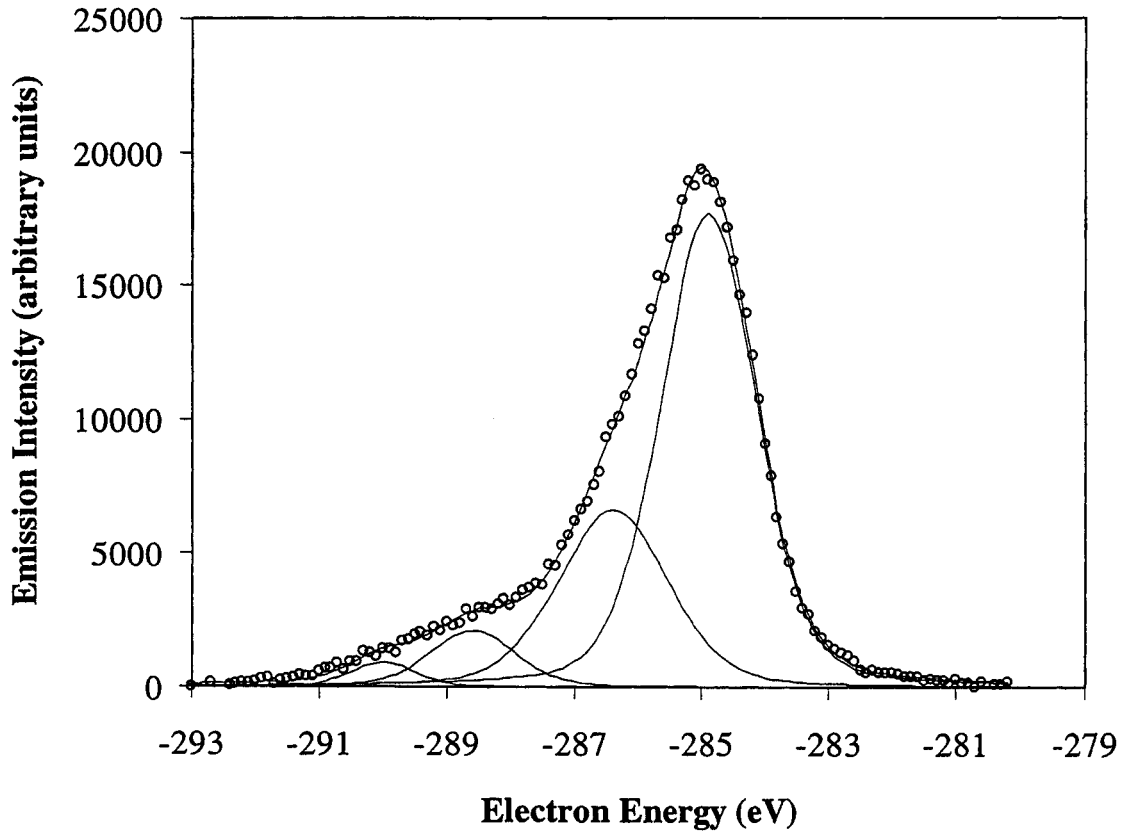

Figure 6.14: High resolution C_{1s} scan of the substrate PUU at a 20° take-off angle.

The circles represent the experimental data and the curve through the circles shows the overall fit. The fitted sub-peaks from right to left represent the signal from hydrocarbon carbons (C-C) at 285 eV, ether carbons (C-O) at 286.5 eV, carbons in urea groups at about 288.8 eV and carbons in urethane groups at about 289.5 eV [Beamson, G. and Briggs, D., 1992].

The XPS data for the PUU substrate are summarised in Table 6.1 and Table 6.2. The elemental chemical composition of the outermost ~34 Å, for a 20° take-off angle and 100 Å for a 90° take-off angle (assuming an average electron mean free path of ~100 Å and using trigonometric relationships), are listed along with the theoretical composition of the PUU substrate repeat unit for the stoichiometry used in its synthesis.

Table 6.1: Low resolution XPS data for PUU substrate (Avg. ± S.D., n=3).

Polymer	Elemental chemical composition (atom %)			
	O	N	C	Si
PUU (20°)	17.1 ± 0.4	3.3 ± 0.4	78.6 ± 0.9	1.0 ± 1.5
PUU (90°)	16.7 ± 1.5	4.6 ± 0.5	78.3 ± 1.3	0.4 ± 0.6
PUU (Theo)	14.1	6.1	79.8	0.0

Table 6.2: High resolution C_{1s} data for PUU substrate (Avg. ± S.D., n=3).

Polymer	Fraction of C_{1s} signal (%)			
	C-C	C-O	Urea	Urethane
PUU (20°)	63.0 ± 4.8	33.9 ± 5.0	1.5 ± 0.4	1.7 ± 0.5
PUU (90°)	61.1 ± 13.5	33.2 ± 12.7	3.0 ± 1.0	2.7 ± 1.2
PUU (Theo)	64.7	30.1	2.6	2.6

The values at 90° may be considered to give an estimate of the bulk composition of the sample. These values are reasonably close to the calculated theoretical values. Discrepancies could be due to differences between the actual structure of the PUU substrate and the theoretical structure based on stoichiometry. When examining the data at 20°, an enrichment in oxygen and a depletion of nitrogen at the surface is observed

relative to 90°. There are two possible explanations for this. First, it is possible that significant surface contamination is present. The presence of a significant silicon signal implies surface contamination, probably by some form of silicone. This would explain the higher oxygen values and lower nitrogen values at both sampling depths relative to the expected composition, since silicone would contribute to the silicon and oxygen content but not to the nitrogen content. Another possibility is surface enrichment of soft segment domains in the vacuum environment. Since PTMO is composed of approximately 25% oxygen, surface enrichment of the soft segment would increase the surface concentration of oxygen and decrease the concentration of nitrogen relative to the theoretical composition, as is observed in Table 6.1. The results of the high resolution C_{1s} scans, summarised in Table 6.2, support this hypothesis. The data at 90° are quite similar to the theoretical values. As well, the urea and urethane components of the C_{1s} signal are smaller near the surface. Since these chemical groups are associated with the hard segment, this would imply surface enrichment of the soft segment. However the ether signal was only very slightly increased near the surface; a larger increase would be expected if there was significant surface enrichment. It is possible that both surface contamination and soft segment surface enrichment contribute to the observed results.

6.2.2 CH_3O-PEO-OH grafted PUU surfaces

The chemical composition of the substrate PUU is expected to change following the grafting reaction and introduction of PEO. However, the chemical composition of the PEO grafts varies depending on molecular weight. Figure 6.15 shows the chemical

structure of the PEO grafts on the PUU-OPEO surfaces. The overall composition of the graft depends on the value of n: the shorter the graft, the larger the contribution of the MDI linker and vice versa. As the graft density on a surface increases, the surface composition is expected to approach the theoretical composition of the PEO grafts. A summary of the data for the PUU-OPEO surfaces along with the theoretical graft compositions are listed in Table 6.3.

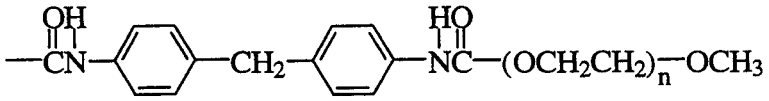

Figure 6.15: Chemical structure of PEO grafts on PUU-OPEO surfaces.

The difference between the graft composition and that of the PEO repeat unit, 33.3% oxygen and 66.7% carbon, is most noticeable at lower molecular weights where the chemical contribution of the MDI linker is proportionally much greater due to the small number of repeat units. At higher PEO molecular weights, the composition is closer to the theoretical composition of the PEO repeat unit.

In the case of PUU-OPEO165, by comparing the theoretical composition of the PUU substrate and the graft, increases in oxygen and nitrogen content and the O/N ratio were expected along with a decrease in the carbon content and the C/O ratio. This was found to be true for all data on this surface except the O/N ratio, suggesting the successful grafting of 165 MW PEO on the PUU substrate. Comparing the 20° and 90° data from the PUU substrate shows oxygen enrichment and nitrogen depletion at the surface compared to the bulk. Similar trends were also noted for PUU-OPEO165.

Table 6.3: Low resolution XPS data for the PUU-OPEO surfaces (Avg. ± S.D., n=2 or 3).

Surface	Elemental chemical composition (atom %)					Elemental ratios	
	O	N	C	Si	Sn	O/N	C/O
PUU (20°)	17.1±0.4	3.3±0.4	78.6±0.9	1.0±1.5	--	5.2±0.5	4.6±0.1
PUU (90°)	16.7±1.5	4.6±0.5	78.3±1.3	0.4±0.6	--	3.6±0.1	4.7±0.5
PUU (Theo)	14.1	6.1	79.8	--	--	2.3	5.7
PUU-OPEO165 (20°)	18.6±0.3	4.6±1.0	74.4±2.3	1.7±1.8	0.7±0.3	4.1±1.0	4.0±0.1
PUU-OPEO165 (90°)	18.0±0.4	6.6±0.9	73.9±2.1	0.8±0.7	0.8±0.0	2.8±0.3	4.1±0.2
PEO165 graft (Theo)	20.0	6.7	73.3	--	--	3.0	3.6
PUU-OPEO2K (20°)	20.9±0.9	3.9±0.8	72.9±3.7	1.9±2.2	0.6±0.4	5.4±0.9	3.5±0.3
PUU-OPEO2K (90°)	20.6±3.3	5.6±0.6	72.9±4.4	0.6±0.7	0.5±0.2	3.7±0.2	3.6±0.8
PEO2K graft (Theo)	30.7	1.3	68.0	--	--	23.7	2.2
PUU-OPEO5K (20°)	19.7±0.9	5.0±0.1	71.4±1.3	3.5±0.1	0.5±0.3	4.0±0.2	3.6±0.2
PUU-OPEO5K (90°)	20.2±2.9	6.6±0.3	71.5±4.4	1.4±1.1	0.4±0.1	3.0±0.3	3.6±0.7
PEO5K graft (Theo)	32.2	0.6	67.2	--	--	59.2	2.1

Expected changes in composition were also noted for the PUU-OPEO2K and PUU-OPEO5K surfaces with the exception of nitrogen content and the O/N ratio. In the case of nitrogen content, there is an increase rather than a decrease relative to the substrate PUU. This higher level of nitrogen may be due to the presence of water in the first step of the reaction. Water can react the isocyanate groups of MDI in solution to form MDA, as shown in Figure 6.16(a).

The amine groups of MDA can then react with isocyanate groups on the surface before the introduction of PEO, as shown in Figure 6.16(b). With both MDI and MDA

present in the reaction solution, this reaction could be repeated multiple times before a PEO molecule is grafted to the surface, if at all. This reaction would also result in increased levels of nitrogen on the surface.

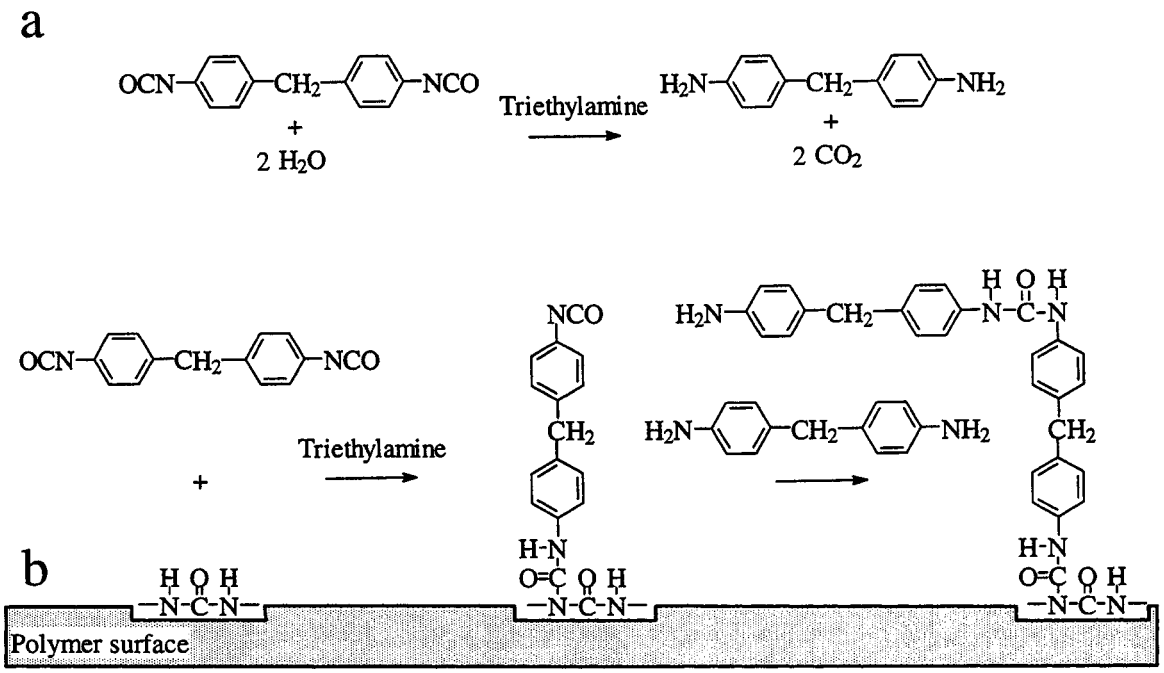

Figure 6.16: (a) Triethylamine catalysed reaction between MDI and water forming MDA. (b) Possible side reaction with MDA during the first step of the grafting reaction.

By examining the level of oxygen and the C/O ratio, it appears that in relative terms, the amount of PEO on the experimental surfaces is: PUU-OPEO2K ≈ PEO-OPEO5K > PUU-OPEO165. High oxygen content and a low C/O ratio implies high PEO content on the surface.

The high resolution C_{1s} data, summarised in Table 6.4, support the observations made for the elemental composition. The theoretical values are again based on the graft structure shown in Figure 6.15. The trends expected by comparing the theoretical values

of the PUU substrate with the values of the 165 MW graft are in fact observed, i.e. an increase in the fraction of ether, urea and urethane signals, and a decrease in the hydrocarbon signal.

The PUU-OPEO2K and PUU-OPEO5K surfaces follow the expected trends for the hydrocarbon and ether fractions of the C_{1s} signal. However both show increases in the urea and urethane signals when a decrease was expected. This may be partially explained by the possible effect of water on the length of the tether between the surface and the PEO graft. If the tether consists of several MDI molecules instead of one, this would result in a stronger urea signal and a weaker urethane signal. Another factor to consider is that these values are obtained by curve fitting. The C1s electrons emitted from urea and urethane groups have very similar energy levels. Furthermore, few of these electrons are detected since urea and urethane groups are not found in abundance at the polymer surface. Therefore, the error in fitting these small peaks, with very similar emission energy levels, is proportionately larger than with the larger peaks. This may explain some of the observed discrepancies.

6.2.3 CH_3O-PEO-NH_2 grafted PUU surfaces

The elemental compositions and ratios for the PUU-NPEOs are summarised in Table 6.5. The listed theoretical compositions are based on the graft structure shown in Figure 6.17.

Table 6.4: High resolution C_{1s} data for the PUU-OPEO surfaces (Avg. ± S.D., n=2 or 3).

Surface	Fraction of C_{1s} signal (%)			
	C-C	C-O	Urea	Urethane
PUU (20°)	63.0±4.8	33.9±5.0	1.5±0.4	1.7±0.5
PUU (90°)	61.1±13.5	33.2±12.7	3.0±1.0	2.7±1.2
PUU (Theo)	64.7	30.1	2.6	2.6
PUU-OPEO165 (20°)	51.9±3.6	39.4±8.9	6.1±5.4	2.5±0.1
PUU-OPEO165 (90°)	56.5±7.4	34.9±12.0	3.7±0.9	5.0±3.7
PEO165 Graft (Theo)	50.0	40.9	4.5	4.5
PUU-OPEO2K (20°)	46.5±4.0	44.5±2.4	4.4±1.7	4.7±4.7
PUU-OPEO2K (90°)	47.2±0.4	44.7±2.1	4.5±1.6	3.6±0.9
PEO2K Graft (Theo)	10.4	87.7	0.9	0.9
PUU-OPEO5K (20°)	50.7±0.1	39.1±4.3	5.2±1.1	5.0±3.2
PUU-OPEO5K (90°)	44.4±9.5	43.5±6.5	5.8±2.4	6.3±0.6
PEO5K Graft (Theo)	4.6	94.6	0.4	0.4

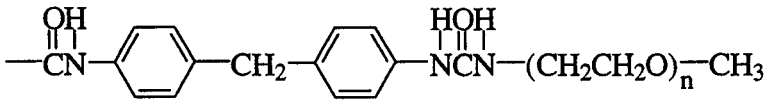

Figure 6.17: Chemical structure of PEO grafts on PUU-NPEO surfaces.

The changes in elemental compositions and ratios following the grafting reactions generally follow the trends predicted by comparing the theoretical composition of the PUU substrate with the theoretical composition of the grafts. Expected increases of oxygen were noted at both sampling depths for all these surfaces. The elemental ratios

also behave as expected, i.e. the O/N ratios increase and the C/O ratios decrease for all surfaces.

Table 6.5: Low resolution XPS data for the PUU-NPEO surfaces (Avg. ± S.D., n = 3).

Surface	Elemental chemical composition (atom %)				Elemental ratios	
	O	N	C	Si	O/N	C/O
PUU (20°)	17.1±0.4	3.3±0.4	78.6±0.9	1.0±1.5	5.2±0.5	4.6±0.1
PUU (90°)	16.7±1.5	4.6±0.5	78.3±1.3	0.4±0.6	3.6±0.1	4.7±0.5
PUU (Theo)	14.1	6.1	79.8	--	2.3	5.7
PUU-NPEO550 (20°)	19.4±1.0	3.1±0.6	76.2±2.8	1.2±1.9	6.4±0.9	3.9±0.3
PUU-NPEO550 (90°)	18.9±0.5	5.1±0.4	75.5±0.7	0.5±0.8	3.7±0.2	4.0±0.1
PEO550 Graft (Theo)	24.5	5.3	70.2	--	4.6	2.9
PUU-NPEO2K (20°)	22.3±1.1	3.6±0.9	70.2±1.0	3.9±0.9	6.4±1.3	3.2±0.2
PUU-NPEO2K (90°)	22.9±0.6	5.2±0.5	70.4±0.8	1.5±0.3	4.5±0.4	3.1±0.1
PEO2K Graft (Theo)	30.1	1.9	68.0	--	15.6	2.3
PUU-NPEO5K (20°)	21.9±2.8	3.1±1.1	72.1±3.7	2.0±1.4	8.3±4.8	3.3±0.5
PUU-NPEO5K (90°)	22.2±4.2	5.2±0.4	71.7±4.5	0.9±0.8	4.2±0.6	3.3±0.8
PEO5K Graft (Theo)	31.9	0.8	67.2	--	38.5	2.1

The level of nitrogen measured at the surface, however, does not follow the expected trend. The nitrogen content should decrease in all the experimental surfaces following the grafting reaction. The data in Table 6.5 show either little change or slight increases in nitrogen content compared to the values of the PUU substrate. As mentioned in Section 6.2.2, the reason for the higher levels of nitrogen may be due to multiple MDI molecules linking the PEO graft to the PUU substrate as a result of trace amounts of water reacting with isocyanate groups. From the oxygen levels and the C/O ratio, the

density of PEO on the PUU-NPEO surfaces can be ranked as follows: PUU-NPEO2K ≈ PUU-NPEO5K > PUU-NPEO550. This ranking reflects the quantity of "ethylene oxide" groups on the surface irrespective of the molecular weight of the PEO graft.

The high resolution C_{1s} data, summarised in Table 6.6, generally support the conclusions based on the elemental composition data. The experimental surfaces all exhibit the expected increase in the ether contribution. The expected trends for the urea and urethane fractions are generally followed for the PUU-NPEO550, with an increase in the urea fraction and a decrease in the urethane fraction. For PUU-NPEO2K and PUU-NPEO5K, decreases in both urea and urethane fractions were expected. However, slight increases for both are noted for each of these two surfaces. The reason for this may again be that multiple MDI moieties link the PEO graft to the PUU surface as a result of water being present in the initial step of the grafting reaction. This would only explain higher than expected levels of urea groups at the polymer surface. The error associated with curve fitting these small peaks with very similar emission energy signatures may also explain the higher than expected levels of the urea and urethane groups.

Table 6.7 compares the XPS measurements on experimental surfaces having similar molecular weight PEO grafts but prepared with either OPEO or NPEO reagents.

The PUU-NPEO surfaces appear to have higher levels of PEO grafting given the higher levels of oxygen, higher O/N ratios and lower C/O ratios for both PEO molecular weights and both sampling depths. Although most of these differences are not statistically significant due to the small sample size, the fact that all these indicators point to higher PEO levels on the PUU-NPEOs provides some measure of confidence for this

conclusion. It is unlikely that all the values would point in the same direction if the PEO levels on both types of surfaces were the same.

Table 6.6: High resolution C_{1s} data for the PUU-NPEO surfaces (Avg. ± S.D., n = 3).

Surface	Fraction of C_{1s} signal (%)			
	C-C	C-O	Urea	Urethane
PUU (20°)	63.0±4.8	33.9±5.0	1.5±0.4	1.7±0.5
PUU (90°)	61.1±13.5	33.2±12.7	3.0±1.0	2.7±1.2
PUU (Theo)	64.7	30.1	2.6	2.6
PUU-NPEO550 (20°)	52.4±1.9	44.4±2.8	1.9±0.9	1.2±0.2
PUU-NPEO550 (90°)	52.5±3.9	43.4±4.5	2.0±0.4	2.1±1.0
PEO550 Graft (Theo)	27.8	67.1	5.1	--
PUU-NPEO2K (20°)	49.5±2.5	43.7±4.0	4.3±3.8	2.7±1.0
PUU-NPEO2K (90°)	43.6±2.8	48.5±2.3	4.0±1.9	3.9±1.8
PEO2K Graft (Theo)	10.4	87.7	1.8	--
PUU-NPEO5K (20°)	47.6±14.9	47.0±14.6	2.2±1.9	3.2±3.2
PUU-NPEO5K (90°)	47.1±6.5	46.7±5.7	2.7±2.0	3.6±2.8
PEO5K Graft (Theo)	4.6	94.6	0.8	--

Table 6.7: Comparison of low resolution XPS data for the PUU-OPEO and PUU-NPEO surfaces (Avg. ± S.D., n = 2 or 3).

Surface	Elemental chemical composition (atom %)					Elemental ratios	
	O	N	C	Si	Sn	O/N	C/O
PUU-OPEO2K (20°)	20.9±0.9	3.9±0.8	72.9±3.7	1.9±2.2	0.6±0.4	5.4±0.9	3.5±0.3
PUU-NPEO2K (20°)	22.3±1.1	3.6±0.9	70.2±1.0	3.9±0.9	--	6.4±1.3	3.2±0.2
PUU-OPEO2K (90°)	20.6±3.3	5.6±0.6	72.9±4.4	0.6±0.7	0.5±0.2	3.7±0.2	3.6±0.8
PUU-NPEO2K (90°)	22.9±0.6	5.2±0.5	70.4±0.8	1.5±0.3	--	4.5±0.4	3.1±0.1
PUU-OPEO5K (20°)	19.7±0.9	5.0±0.1	71.4±1.3	3.5±0.1	0.5±0.3	4.0±0.2	3.6±0.2
PUU-NPEO5K (20°)	21.9±2.8	3.1±1.1	72.1±3.7	2.0±1.4	--	8.3±4.8	3.3±0.5
PUU-OPEO5K (90°)	20.2±2.9	6.6±0.3	71.5±4.4	1.4±1.1	0.4±0.1	3.0±0.3	3.6±0.7
PUU-NPEO5K (90°)	22.2±4.2	5.2±0.4	71.7±4.5	0.9±0.8	--	4.2±0.6	3.3±0.8

Table 6.8 compares the high resolution C_{1s} measurements on similar PUU-OPEO and PUU-NPEO surfaces. Only the ether contribution to the C_{1s} signal provides insight regarding graft density in this instance. Generally the ether fraction of the C_{1s} signal was higher in the PUU-NPEO surfaces. This supports the conclusions from the elemental composition data, that higher levels of grafted PEO were achieved on the PUU-NPEO surfaces.

6.3 Grafting Density Determination

The contact angle and XPS methods give only indirect evidence as to the quantity of PEO on the surface. Both methods showed that PEO was successfully grafted to the base PUU. However, the former gives only qualitative information and the latter has the

disadvantage that the PEO grafts do not contain any chemical element that is not already present in the base PUU, thus making it difficult to quantify the level of PEO grafting.

Table 6.8: Comparison of high resolution C_{1s} data for the PUU-OPEO and PUU-NPEO surfaces (Avg. ± S.D., n = 2 or 3).

Surface	Fraction of C_{1s} signal (%)			
	C-C	C-O	Urea	Urethane
PUU-OPEO2K (20°)	46.5±4.0	44.5±2.4	4.4±1.7	4.7±4.7
PUU-NPEO2K (20°)	49.5±2.5	43.7±4.0	4.3±3.8	2.7±1.0
PUU-OPEO2K (90°)	47.2±0.4	44.7±2.1	4.5±1.6	3.6±0.9
PUU-NPEO2K (90°)	43.6±2.8	48.5±2.3	4.0±1.9	3.9±1.8
PUU-OPEO5K (20°)	50.7±0.1	39.1±4.3	5.2±1.1	5.0±3.2
PUU-NPEO5K (20°)	47.6±14.9	47.0±14.6	2.2±1.9	3.2±3.2
PUU-OPEO5K (90°)	44.4±9.5	43.5±6.5	5.8±2.4	6.3±0.6
PUU-NPEO5K (90°)	47.1±6.5	46.7±5.7	2.7±2.0	3.6±2.8

In an attempt to quantify more precisely the levels of grafting on the PEO-modified surfaces, 2-fluorophenylethylamine was used as a "surrogate" for MeO-PEO-NH_2. It was believed that this would allow evaluation of the grafting reaction by fluorine analysis. The reaction conditions were the same as for the MeO-PEO-NH_2 grafting reactions except that PEO was replaced by 2-fluorophenylethylamine. Following the reaction and standard workup, XPS was performed on these fluorinated surfaces (designated PUU-FPEA). Low resolution XPS data are listed in Table 6.9.

Table 6.9: Low resolution XPS data for the fluorinated PUU-FPEA surfaces (Avg. ± S.D., n = 2 or 3).

Surface	Elemental chemical composition (atom %)				
	O	N	C	Si	F
PUU (20°)	17.1±0.4	3.3±0.4	78.6±0.9	1.0±1.5	--
PUU (90°)	16.7±1.5	4.6±0.5	78.3±1.3	0.4±0.6	--
PUU (Theo)	14.1	6.1	79.8	--	--
PUU-FPEA (20°)	20.6±1.8	2.8±0.1	70.4±0.5	2.1±1.1	4.3±0.4
PUU-FPEA (90°)	23.9±3.4	4.1±0.4	67.5±4.9	1.0±0.4	3.6±1.6
FPEA Graft (Theo)	6.9	10.3	79.3	--	3.4

The grafting reaction was apparently successful given the quantity of fluorine detected. However based on the theoretical composition of the grafts, the measured fluorine content was higher than expected. This may be due to the limited precision associated with peak integration to determine composition. The fluorine peaks were relatively small and the baseline was somewhat noisy; this makes determination of the integration start and end points somewhat subjective and may explain the high values. The other elements, however, do not follow the expected trends. From the theoretical composition of the PUU and the graft, the changes expected on grafting are a decrease in oxygen content, an increase in nitrogen content and little change in carbon content. Instead, an increase in oxygen content, a slight decrease in nitrogen content and a large decrease in carbon content were observed. The expected composition trends would be the same even considering the possibility of water converting MDI to MDA during the first step of the grafting reaction and being introduced in greater quantities to the surface (i.e. a

multimeric "MDI" linker between the surface and the PEO graft). The reasons for these unexpected composition results, especially the high oxygen values are unknown.

The high resolution C1s scans in Table 6.10, also confirmed successful grafting by the presence of C-F carbons in the grafted surface. The hydrocarbon, C-O and urea content followed the trends predicted by the listed theoretical compositions. However the urethane content increases sharply, contrary to expectations. It is important to note that these results are derived from peak fitting which is somewhat subjective, and this may explain deviations from expected values.

Table 6.10: High resolution C_{1s} data for the fluorinated PUU-FPEA surfaces (Avg. ± S.D., n = 2 or 3).

Surface	Fraction of C_{1s} signal (%)				
	C-C	C-O	Urea	Urethane	C-F
PUU (20°)	63.0±4.8	33.9±5.0	1.5±0.4	1.7±0.5	--
PUU (90°)	61.1±13.5	33.2±12.7	3.0±1.0	2.7±1.2	--
PUU (Theo)	64.7	30.1	2.6	2.6	--
PUU-FPEA (20°)	63.3±11.0	23.5±6.6	4.3±3.1	6.3±0.1	2.7±1.3
PUU-FPEA (90°)	63.5±0.8	25.8±5.4	4.3±2.6	5.0±0.8	1.5±1.1
FPEA Graft (Theo)	73.9	13.0	8.7	--	4.3

These results demonstrate conclusively that the grafting reaction was appropriate for chemically linking an amine-terminated molecule to the polymer substrate. It is therefore likely that monomethoxyamino-PEOs were grafted to the PUU in a similar fashion. However, these data cannot be used to estimate the grafting density on the surfaces. This would require knowledge of the arrangement of the polymer molecules

near the surface (XPS probing depth), as well as precise information on the chemical structure of the PUU (not all polymer chains are of identical length or composition). Furthermore, since the probing depth is relatively shallow, any surface enrichment/depletion effects will be important, making the composition at the surface different from the bulk, and making the determination of the surface composition extremely difficult. Finally, since the PEO grafts contain the same chemical elements as the PUU substrate, it is difficult to differentiate PUU from PEO.

One solution to this problem is to label the PEO with a radioactive tracer. This was accomplished by using diamino-PEO and ^{125}I-Bolton-Hunter reagent. The chemical reaction between these two molecules is shown in Figure 4.6 (page 47). A very small amount of radioiodinated Bolton-Hunter reagent ($<4.0\times10^{-3}$ mol %) was used in the labelling reaction so as to minimise the number of diamino-PEO molecules with both end groups tagged; such molecules would not be grafted to the PUU and would introduce error in the determination of grafting density. The reaction was allowed to proceed for an extended period (36 h) to ensure as complete a reaction as possible and reduce the possibility of trace quantities of unreacted Bolton-Hunter reagent being present in the radioiodinated PEO. The results of several grafting experiments with 3400 MW PEO are shown in Figure 6.18.

The average grafting density was estimated as 0.89 ± 0.21 μmol/cm^2. The reproducibility of the measurement is reasonable although the fluctuations within experiments are somewhat elevated.

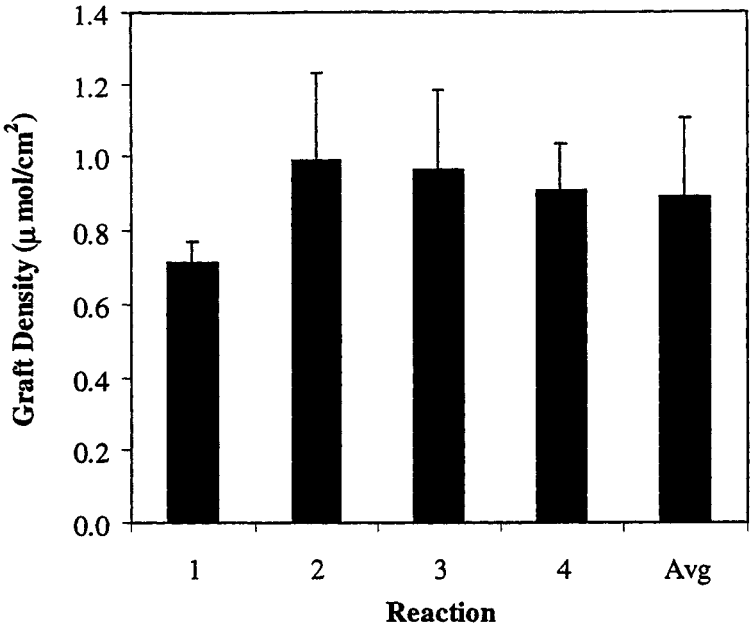

Figure 6.18: Grafting density measurements with 3400 MW PEO labelled with ^{125}I-Bolton-Hunter reagent (n≥10, ± S.D.). In the first step, 10 PUU disks (6.8 mm diameter) were reacted with 10 mL 2% (w/v) MDI and 2% (w/v) triethylamine in anhydrous toluene for 1 h at 60°C. The reaction medium was then removed and the PUU disks were rinsed three times with 10 mL anhydrous toluene. In a second 50 mL round-bottom flask, the PUU disks reacted with 10 mL 1% (w/v) ^{125}I-PEO in anhydrous toluene for 24 h at 50°C.

The effect of PEO concentration on grafting density was also briefly examined as shown in Figure 6.19. An approximately linear increase in grafting density with increasing PEO solution concentration was observed, suggesting that to maximise the grafting density, as high a concentration of PEO as possible should be used. Presumably a concentration exists at which this effect would reach a plateau, but this concentration was not within the experimental range examined.

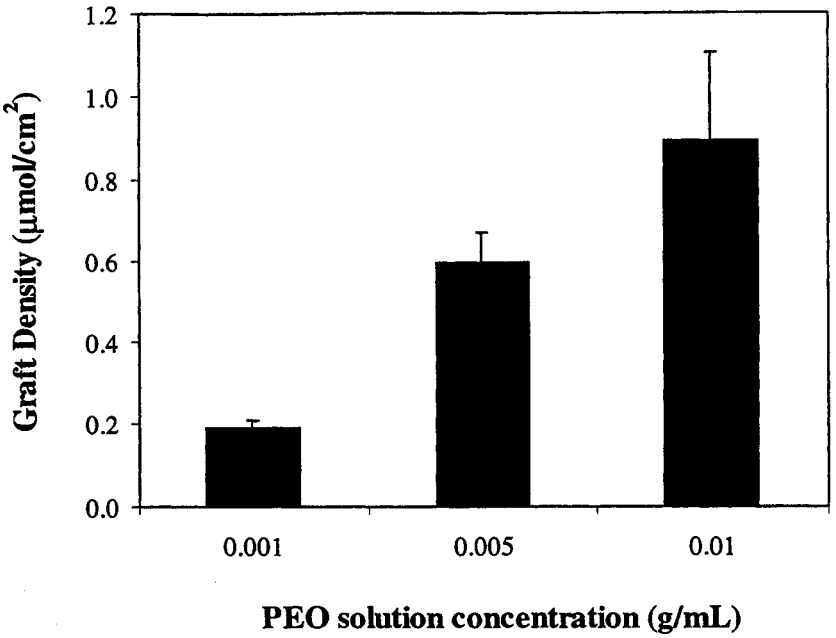

Figure 6.19: Effect of PEO (3400 MW) solution concentration on graft density (n≥15, ±SD).

As part of the grafting density determination, a control experiment was performed where the MDI reaction step was omitted. However, much higher levels of radioactivity than expected were detected, implying high levels of PEO incorporation even though no chemical grafting should have occurred. At a ^{125}I-PEO concentration of 0.01 g/mL, the apparent "grafting" density of the control was 0.32±0.06 μmol/cm^2 (±S.D., n=5). The same experiment using low density polyethylene instead of PUU, gave a "grafting" density of 0.006±0.001 μmol/cm^2 (n=5, ± S.D.), i.e. there was essentially no detectable PEO on the surface.

A somewhat more rigorous control experiment was also performed in which the PUU substrate was reacted with MDI, then incubated in aqueous triethylamine to convert any isocyanate groups on the surface to amines. Following this treatment, the surfaces

were incubated with radiolabeled PEO. This control is probably more appropriate since in the actual reaction, the PEO is incubated with a PUU containing grafted MDI. In this case, the PUU surface presumably had amino groups at the free end of the MDI graft, thus more closely resembling the substrate for the PEO reaction than just the bare polymer surface. The grafting density in this experiment was nearly identical to that in the first control, i.e. 0.34±0.05 μmol/cm^2 (n=10, ±S.D.). It was concluded that the first control protocol was, after all, adequate.

Based on these results, it appeared that some property specific to the PUU substrate resulted in unexpectedly high radioactivity levels in the absence of reactive groups to chemically graft the PEO to the surface. One possibility is that traces of unreacted Bolton-Hunter reagent were present in the radiolabeled PEO preparation and reacted directly with the PUU substrate. Another experiment confirmed that the Bolton-Hunter reagent could react directly with the PUU substrate, resulting in high levels of radioactivity, even following the usual workup protocols. Hence part of the radioactivity detected on the PUU surfaces could be attributed to traces of Bolton-Hunter reagent present in the ^{125}I-PEO.

Another possibility is that PEO chains became entangled in the PUU substrate as a result of swelling in the reaction solvent, toluene, during the grafting reaction. The behaviour of the polymer substrate in toluene was therefore examined. Figure 6.20 shows the increase in mass of the PUU substrate following incubation in toluene for different time intervals. It appears that the polymer substrate becomes saturated with toluene within 24 h with a mass increase of approximately 40%. Given this level of swelling, it is

not unreasonable to conclude that some PEO might be entrapped in the swollen polymer during the 24 h exposure to the radiolabeled PEO solution. The procedure to remove unbound PEO might not completely remove these entrapped PEO molecules, leading to the high level of radioactivity detected in the control experiment.

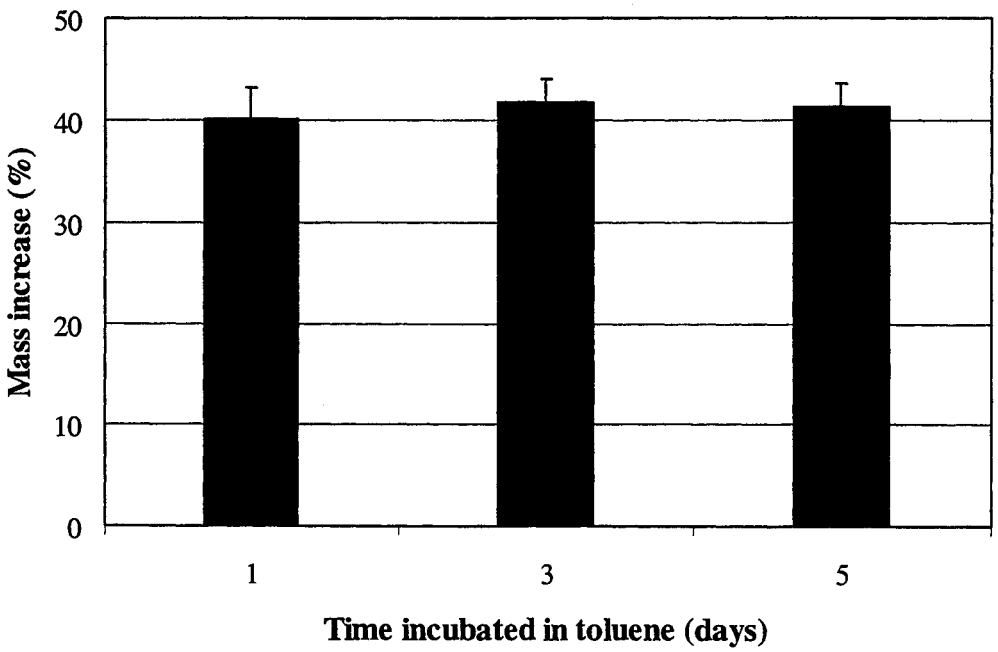

Figure 6.20: Toluene uptake by the PUU substrate following incubation at 22°C (±S.D., n=5).

Finally, a potential source of radioactivity could arise from free iodide in the radioiodinated PEO solution. If iodide could complex to the PUU substrate in some manner, it would contribute to the elevated levels of radioactivity detected in the control experiments. Therefore, an experiment where the PUU substrate was exposed to a solution of $Na^{125}I$ was performed. Samples were incubated in solutions of $Na^{125}I$ in TBS buffer for three hours at 22°C. The level of radioactivity in these solutions was approximately 65-fold greater than background levels. Following three 15 min rinses in

TBS buffer, the radioactivity of the PUU surfaces was measured. The average measured radioactivity was only 5.1% higher than background levels. Therefore free iodide does not appear to be a cause of the elevated radioactivity levels in the control experiments.

The average level of grafting using the 3400 MW PEO, assuming none of the radioactivity associated with the negative control originates from entangled PEO is therefore approximately (0.89-0.34) $\mu mol/cm^2 = 0.55\ \mu mol/cm^2$.

To put this value into perspective, an estimate of a probable upper limit is required. For example, the helical conformation of PEO has a cross-section of 21.3 $Å^2$ [If Harder, P. et al., 1998], an idealised surface consisting of grafted PEO exclusively in this helical conformation in a close-packed, non-overlapping configuration were prepared, the theoretical maximum grafting density would be 0.78 $nmol/cm^2$. The experimental value of grafting density does not seem credible in comparison, as it is nearly three orders of magnitude greater than the theoretical maximum. There are a few possible explanations for this discrepancy. If the radiolabeled PEO were to react preferentially over unlabeled PEO, the graft density estimate would be inflated. As well, if the swelling of the polymer surface in the reaction solvent were to create a porous surface, the effective surface area would be much higher than for the corresponding flat surface; this would allow much more PEO to react with the surface and inflate the graft density measurement.

6.4 Atomic Force Microscopy

AFM scans were performed to examine the surface morphology of the PUU substrate before and after the PEO grafting reaction. Figure 6.21 shows a 5μm × 5μm

scan of the PUU substrate. The colour scheme represents the roughness of the substrate where dark areas are low and bright areas are high. The substrate appears relatively rough. From estimates using the AFM software the distance between the lowest and highest point (z-range) was 171.9 nm; the roughness was 9.54 nm and the increase in surface area compared to a flat surface was 2.3%.

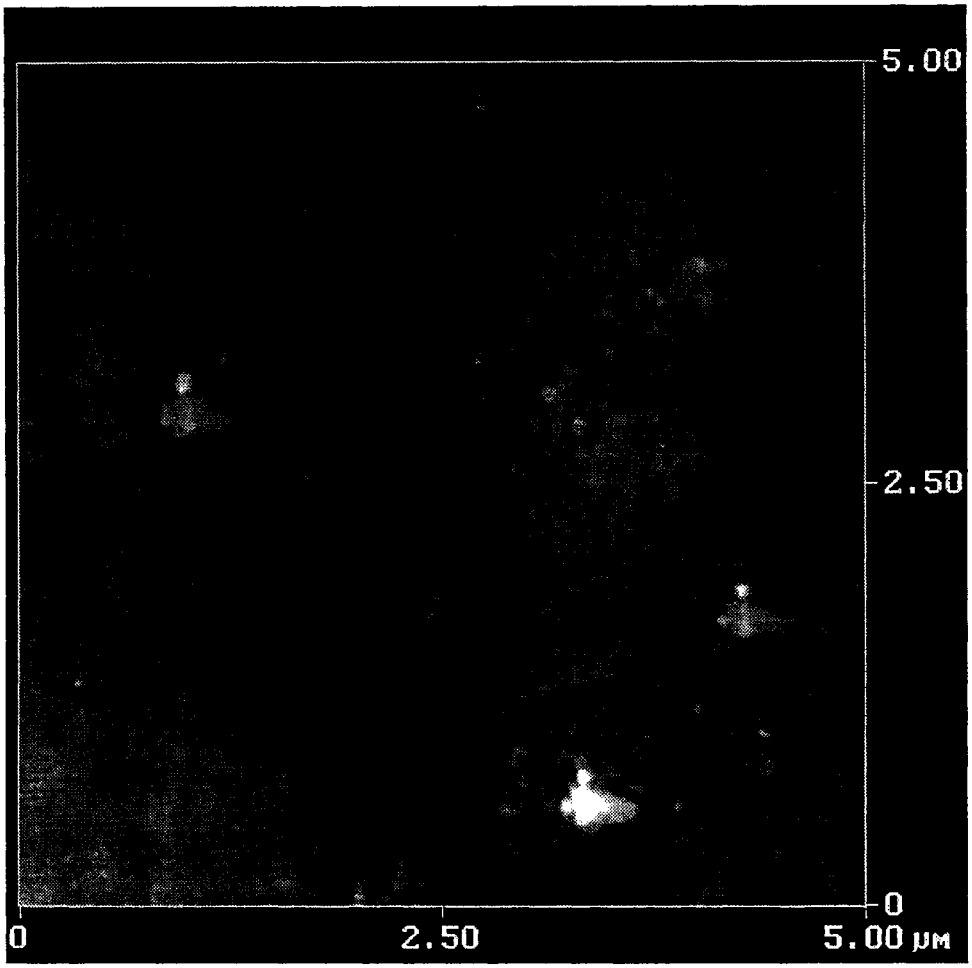

Figure 6.21: AFM image of the substrate polyurethane urea (5µm × 5µm scan).

Figure 6.22 shows a 0.5µm × 0.5µm scan of the PUU substrate. The surface features are more apparent at this increased magnification. Much of the surface appears to

be covered by discrete globular domains. The z-range in this image was 24.2 nm, the roughness was 3.98 nm, and the increase in surface area compared to a flat surface was 3.48%. Again, these values describe a relatively rough surface.

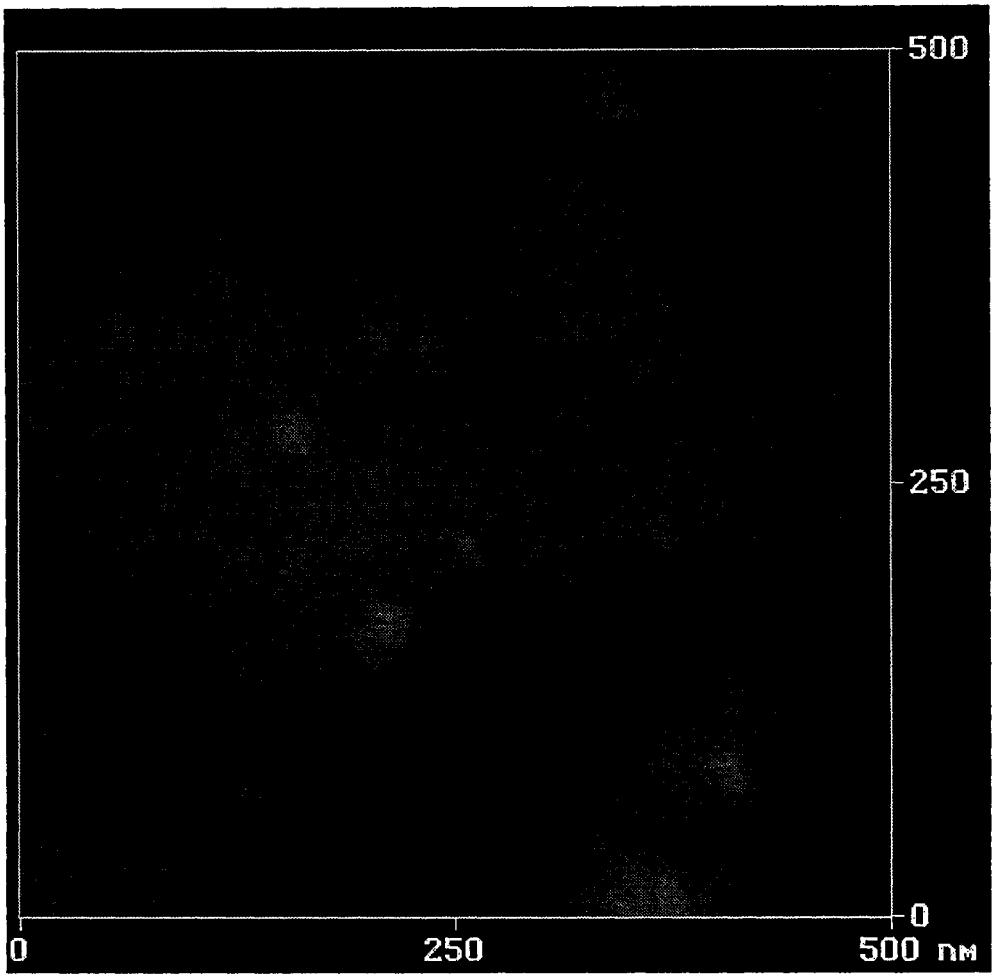

Figure 6.22: AFM image of the substrate polyurethane-urea (0.5μm × 0.5μm scan).

Figure 6.23 shows a 5μm × 5μm scan of PUU-NPEO2K. Compared to the image of the PUU substrate, the surface morphology is more "grainy"; i.e. there are globular domains of many different sizes from small to large. The z-range of this image was 82.0

nm, the roughness 7.89 nm, and the increase in surface area was 3.14%. It appears that the grafting reaction decreases the roughness and increases the total surface area slightly.

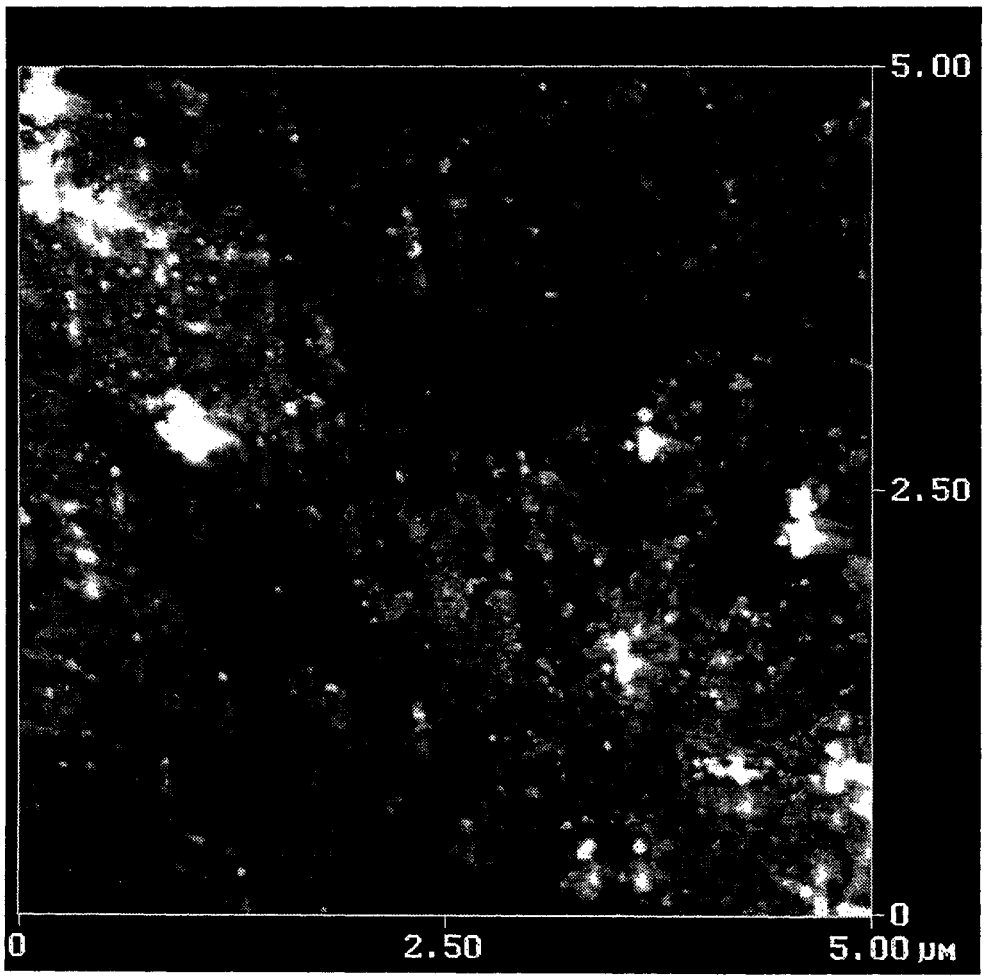

Figure 6.23: AFM image of PUU-NPEO2K (5µm × 5µm scan).

Figure 6.24 shows a 0.5µm × 0.5µm scan of PUU-NPEO2K. At this magnification, the varying sizes of the surface globular clusters is evident. The z-range of this image was 36.5 nm, the roughness 3.73 nm, and the increase in surface area was 3.35%. Although there is evidence of some morphological differences before and after the grafting reaction, on the whole, the changes are fairly small.

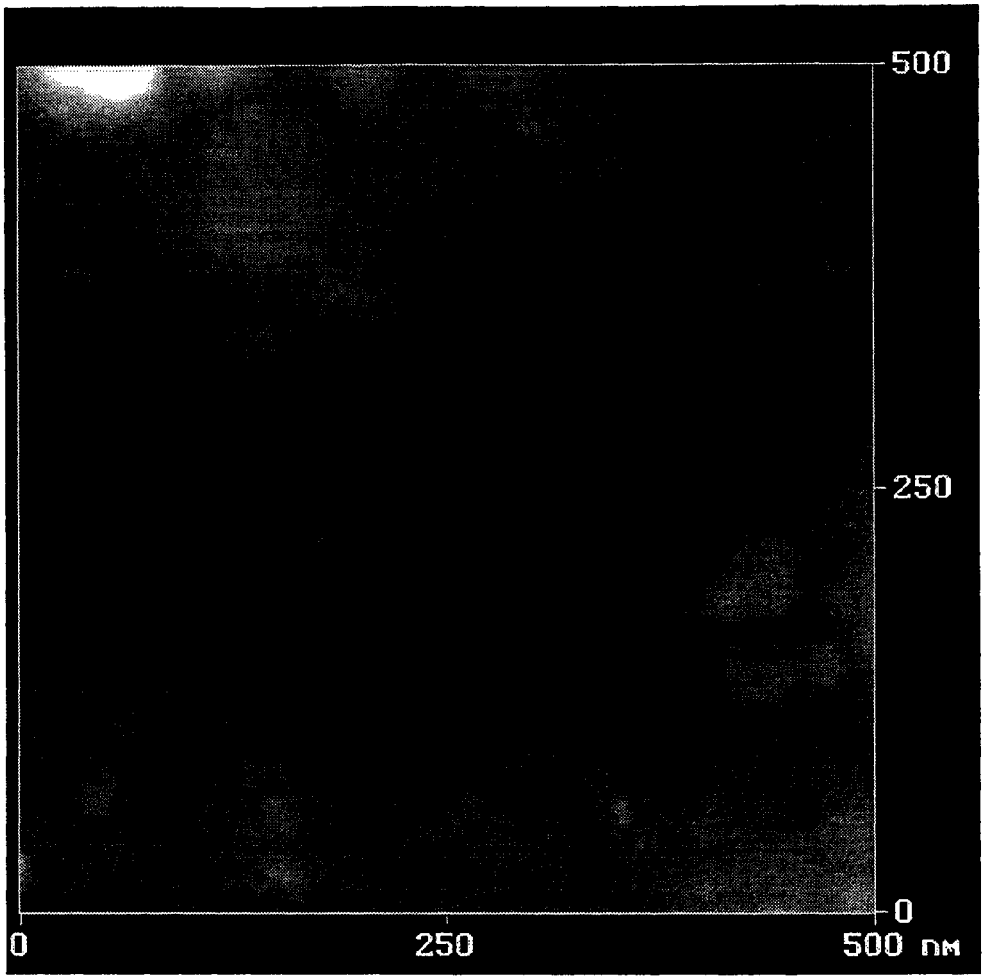

Figure 6.24: AFM image of PUU-NPEO2K (0.5μm × 0.5μm scan).

7.0 PROTEIN ADSORPTION STUDIES

Although the surface characterisation of the control PUU and PEO-grafted surfaces provides valuable information, the main interest is to determine to what extent these surfaces are able to reduce or prevent protein adsorption, and to identify and investigate properties that may have an impact on how effective the PEO grafts are in reducing protein adsorption.

7.1 Single Protein Adsorption from Buffer

For the majority of the investigations of the protein adsorption properties of the PEO-grafted surfaces, single protein adsorption from buffer was used. This simple system enables the comparison of adsorption behaviour of proteins having a range of properties. We were interested particularly in protein size and isoelectric point. The resistance of a PEO-grafted surface to adsorption is expected to be protein size dependent. Smaller proteins may be expected to access the underlying substrate more easily for a given graft density and chain length. The isoelectric point of a protein determines its overall charge at a given pH. This property is of interest for two reasons. First, it has been shown that PEO can form complexes with cations thus acquiring a positive charge [Zhivkova, I.V. et al., 1998]; this could have an impact on protein adsorption behaviour. Secondly, electrokinetic studies have shown that a grafted PEO layer can "mask" surface charges [Emoto, K. et al., 1997]. Although the present work does not employ an adsorption experiment with a convective component, this property of PEO may have an impact on

adsorption behaviour. Depending on the protein, the uncharged PUU surface could acquire charge during the adsorption process and the PEO grafts might have an effect under those circumstances. A series of eight proteins was used in these investigations and their sizes (nm^3) and isoelectric points (pI) are listed in Table 7.15 on page 200 and in Table 4.2 on page 50, respectively.

Variability in the measured protein levels on the various control and PEO-grafted surfaces was often encountered during the course of this work. These fluctuations were attributed to batch-to-batch differences in the surfaces or to the experiment itself. Figure 7.1 shows the concanavalin A adsorption isotherms for two independent experiments using the control PUU and PUU-NPEO2K surfaces. The isotherms were determined by measuring the radioactivity on a given surface and calculating the adsorbed protein using equation 7.1.

$$\text{Adsorbed protein} = \frac{\text{Net surface count} \cdot \text{Concentration of protein solution}}{\text{Protein solution count} \cdot \text{Surface area of sample}} \qquad (7.1)$$

The net surface count is the difference between the surface count and the background count. Each point represents the average protein adsorption from three measurements at a given protein concentration. Also, the isotherms throughout this section and elsewhere are used as a visual aid only and do not imply any model. Both the control and PEO-grafted surfaces were from the same batch in this instance. Although the replicate isotherms were similar at low protein concentration, more significant deviations were noted at the higher concentrations. Some potential sources of error that could contribute to these fluctuations are as follows. First is the inability to measure protein

concentration directly. Protein concentrations are determined by measuring absorbance at 280 nm and interpolation on a calibration curve. As well, the protein solution usually needs to be diluted prior to the measurement in order to fall in the linear portion of the calibration curve. Second, serial dilution is used to prepare the protein solutions. Since this requires many transfers to accomplish, there are many opportunities for error to be introduced. Therefore even in a repeat experiment where conditions are as close as possible to the initial experiment, the inherent variability can be high.

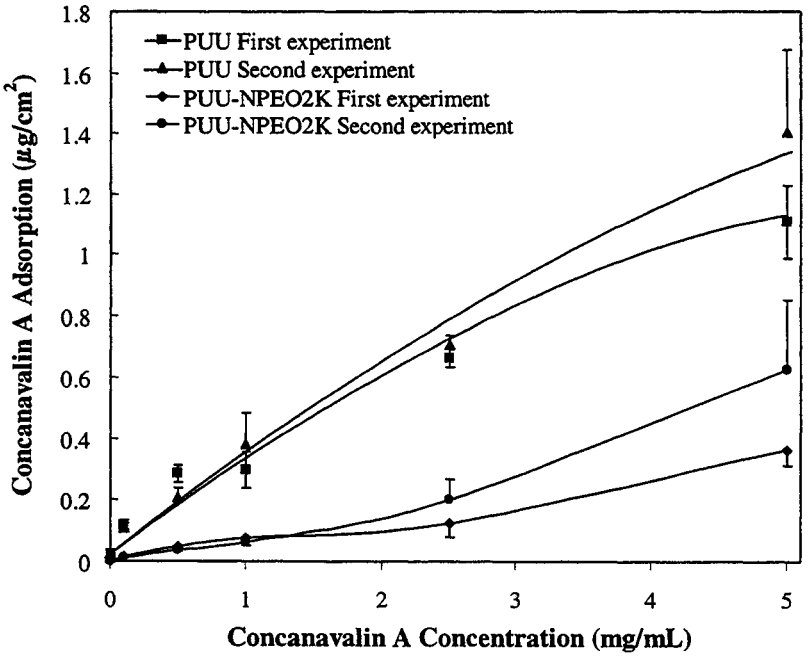

Figure 7.1: Concanavalin A adsorption on PUU and PUU-NPEO2K from TBS buffer at 22°C for 3h (±S.D., n=3).

Also, during the course of experimentation, several batches of the control PUU and different PEO-grafted surfaces were prepared. Some of the variability can therefore also be attributed to batch-to-batch variations in the properties of the resulting PUU and PEO-grafted surfaces, although care was taken to replicate experimental conditions as

closely as possible for the different batches. Figure 7.2 shows the α-lactalbumin adsorption isotherms for different batches of the PUU-OPEO2K surfaces. The substrate PUUs were all from the same batch; the labels refer to the grafted surface it was tested against. Again, the adsorption levels are reasonably close to one another but variability occurs even on the control PUU, more significantly at the higher concentrations. In addition, this protein was chosen because three independent experiments were performed as opposed to the more usual two. There are other systems where the differences between batches is greater (see below).

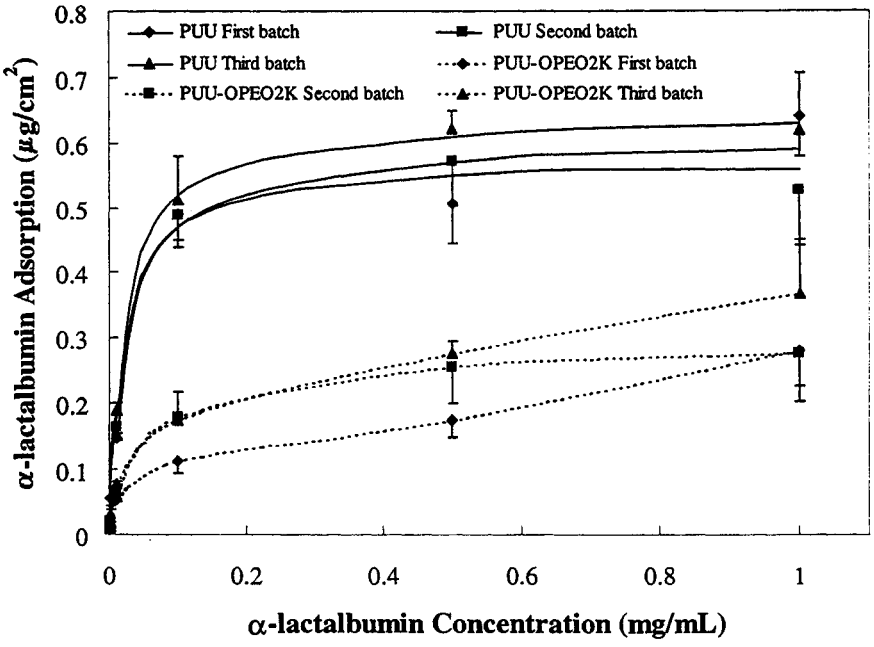

Figure 7.2: α-lactalbumin adsorption on PUU and three different batches of PUU-NPEO2K from TBS buffer at 22°C for 3h (±S.D., n=3).

An adsorption experiment was also performed on the surface resulting from only the first part of the PEO-grafting reaction; that is, the PUU substrate that has reacted with MDI but not with the PEO graft. Evaluation of this surface is important because patches

of this type may remain following the grafting reaction; knowing how this type of surface behaves with respect to protein adsorption is therefore relevant. Figure 7.3 shows a fibrinogen adsorption experiment with the PUU-MDI surface compared to the control. The PUU-MDI surface adsorbs as much as or more than the control PUU at all concentrations. Therefore, bare patches of this type of surface would not contribute to reducing protein adsorption on PEO-grafted surfaces.

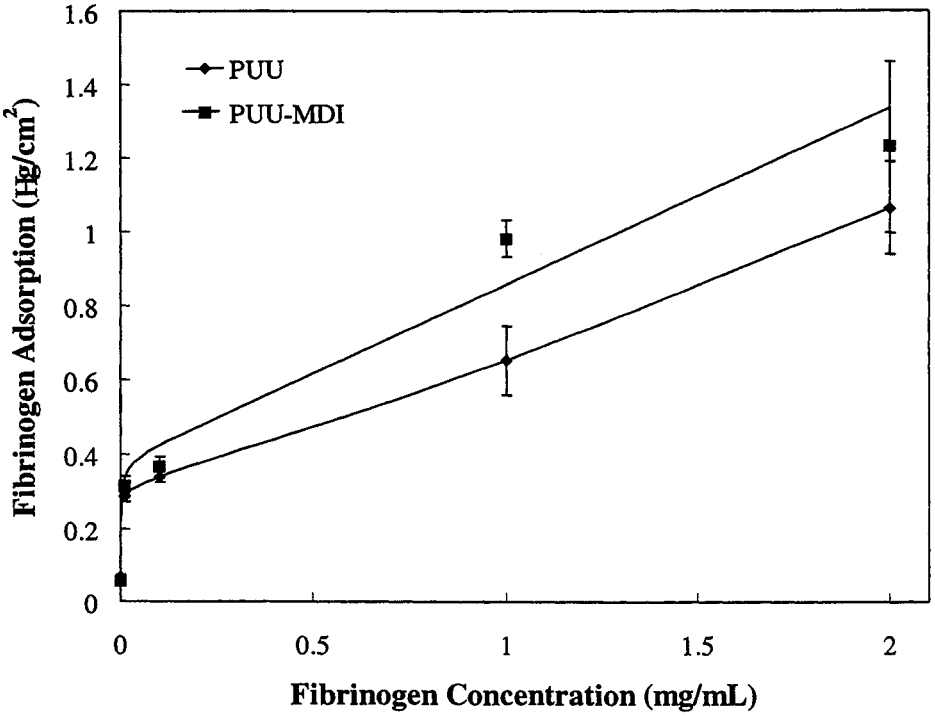

Figure 7.3: Fibrinogen adsorption on PUU and PUU-MDI from TBS buffer at 22°C for 3h (±S.D., n=3).

7.1.1 Effect of PEO Chain Length

The main property of PEO examined in this work (other than a brief consideration of grafting density in Section 6.3) was the length of the PEO grafts, characterised by the number of ethylene oxide repeat units or molecular weight.

The data reported in this section are used to examine the effect of the PEO graft molecular weight on the protein adsorption properties of the experimental surfaces. In addition, the same data are used in later sections to investigate the effects of the properties of the proteins themselves on the protein rejecting character of the experimental surfaces.

7.1.1.1 PUU-OPEO Surfaces

The initial investigations examining the PEO-grafted surfaces were conducted using the PUU-OPEO surfaces (i.e. where hydroxy-terminated PEO was used in the grafting reactions). A range of monomethoxyhydroxy-PEO (MeO-PEO-OH) reagents varying widely in molecular weight were used to prepare these surfaces. Table 7.1 lists the average length in ethylene oxide repeat units of the various PEO reagents used to prepare the PUU-OPEO surfaces (and later, the NPEO surfaces).

Table 7.1: Length in ethylene oxide repeat units of PEO reagents.

PEO MW	Average chain length (ethylene oxide repeat units)
165	3
350	7
550	12
750	16
2000	45
5000	113

A series of eight proteins was used to probe the protein repelling properties of the experimental surfaces. These proteins varied in size and isoelectric point (see Table 4.2

on page 50 and Table 7.15 on page 200). Data on the effect of PEO molecular weight are presented first. The adsorption data for all eight proteins are presented in this section.

α-lactalbumin

α-lactalbumin is a 14.2 kDa protein with dimensions of approximately 37×32×25 Å [Norde, W. and Haynes, C.A., 1995] and an isoelectric point of 4.3. Based on these molecular dimensions, a rough estimate of the expected monolayer coverage value would be in the range of 0.2-0.3 $\mu g/cm^2$. This calculation likely underestimates the monolayer coverage since the protein is viewed as a rigid ideal geometric shape. The protein would be able to achieve a greater surface coverage due to its actual shape and at least some degree of deformability. Figure 7.4 to Figure 7.6 show the adsorption isotherms of α-lactalbumin on three different batches of experimental surfaces. The adsorption on the native PUU reaches a plateau at about 0.6 $\mu g/cm^2$; this is above monolayer coverage according to the above estimate, but is reasonable for the reasons stated.

These data show batch-to-batch and/or experiment-to-experiment variation for both control PUU and PEO-grafted surfaces. In the first and third experiments, PUU-OPEO2K showed the lowest overall adsorption whereas in the second, PUU-OPEO5K had the lowest adsorption. PUU-OPEO165 adsorbed more protein at all concentrations than the control PUU in two of the three batches. Also, in the second experiment, PUU-OPEO2K showed higher α–lactalbumin adsorption than both PUU-OPEO5K and PUU-OPEO750. In general however, protein adsorption on the experimental surfaces is seen to decrease with increasing molecular weight of the grafted PEO.

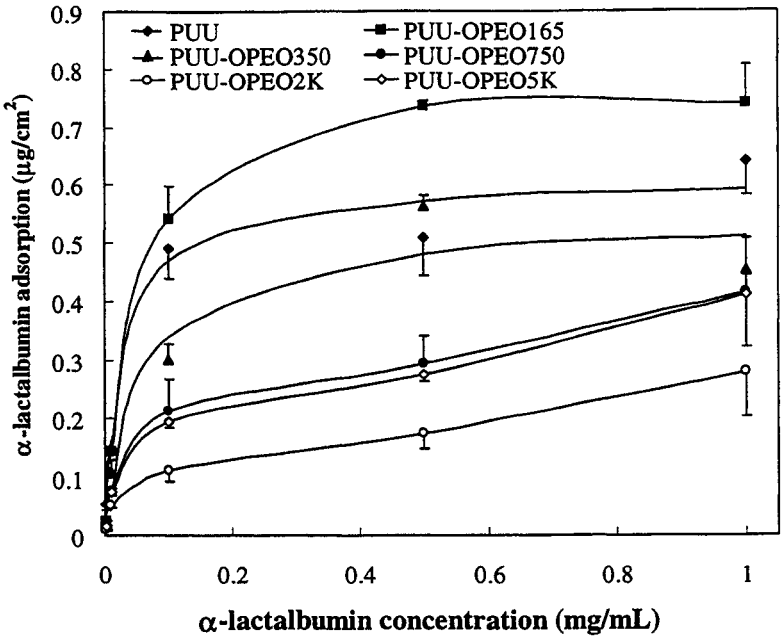

Figure 7.4: α-lactalbumin adsorption on PUU and PUU-OPEOs (first batch) from TBS buffer at 22°C for 3h, ±S.D., n=3.

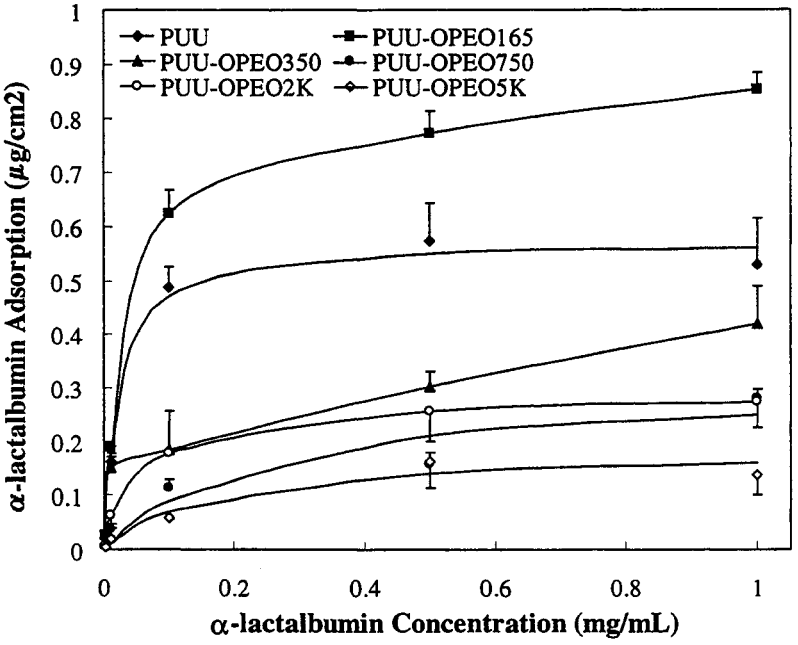

Figure 7.5: α-lactalbumin adsorption on PUU and PUU-OPEOs (second batch) from TBS buffer at 22°C for 3h, ±S.D., n=3.

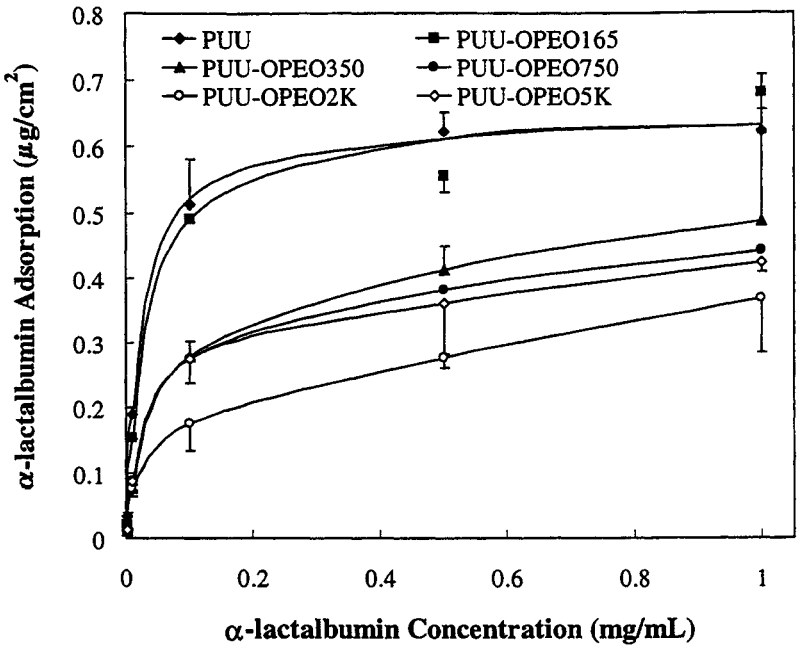

Figure 7.6: α-lactalbumin adsorption on PUU and PUU-OPEOs (third batch) from TBS buffer at 22°C for 3h, ±S.D., n=3. Note: some error bars omitted for clarity.

The initial slope of the adsorption isotherm can be used to estimate the affinity of the protein for the test surface. The Langmuir isotherm describing gas adsorption to metals [Hunter, R.J., 1993] has an equilibrium constant given by:

$$K = k_a / k_d \tag{7.2}$$

where k_a is the adsorption rate coefficient
k_d is the desorption rate coefficient

Therefore, the higher the value of K, the more affinity the gas has for the metal surface. The Langmuir isotherm is given by:

$$\theta = \frac{Kp_a}{1 + Kp_a} \tag{7.3}$$

where θ is the fractional surface coverage

K is the equilibrium constant
p_a is the pressure of gas a.

If the pressure is very low ($Kp_a << 1$), the expression reduces to:

$$\theta = Kp_a \tag{7.4}$$

Therefore, in a low pressure regime, the slope of the isotherm gives the equilibrium constant. By analogy, at very low protein concentrations, the slope of the isotherm for a given protein can be interpreted as giving information about the affinity of a protein for a given surface. It is important to note however, that many of the underlying assumptions of the Langmuir isotherm are not met in protein adsorption, especially the fact that protein adsorption is generally non-reversible (see Section 2.2.3 on page 12).

The initial slopes of the isotherms in Figure 7.4 to Figure 7.6 were determined using the data at the lowest protein concentration, i.e. 0.001 mg/mL. The average value of the 3 repeated measurements are reported. Upon examination of the data in Table 7.2, the same trends emerge as were noted above. The affinity of α–lactalbumin for the surface decreases as the molecular weight of the PEO graft increases; the average values for the 2000 and 5000 MW surfaces were similar.

It seemed desirable to find a method to present these data in such a way that the effects of the variables emerge clearly. The response of interest is the reduction in protein adsorption compared to the control PUU. By examining the reduction (or increase) in protein adsorption compared to the control PUU, the variation in the absolute levels of adsorption from experiment to experiment is eliminated. The analysis method first used in Section 5.2.1 was therefore used to present the combined data in terms of adsorption

normalised to the control PUU. That is, at a given concentration, the adsorption level on the PEO-grafted surface is divided by the average adsorption level on the control PUU and expressed as a percentage.

Table 7.2: Initial slopes of the α-lactalbumin isotherms.

Surface	Initial Slope (mL/cm^2) (Average ± S.D., n=3)			Average Initial Slope (± 95% C.I.)
	Figure 7.4	Figure 7.5	Figure 7.6	
PUU	54.7±9.8	20.7±1.9	32.0±6.6	35.8±12.4
PUU-OPEO165	25.0±2.1	26.6±4.3	19.2±5.4	23.6±3.7
PUU-OPEO350	16.7±3.0	10.5±2.3	11.6±1.6	12.9±2.7
PUU-OPEO750	14.7±2.1	7.6±3.3	13.6±1.8	12.0±3.0
PUU-OPEO2K	10.9±1.1	7.1±0.7	11.7±1.7	9.9±1.8
PUU-OPEO5K	15.3±3.6	3.6±0.4	12.2±3.1	10.4±4.4

The data from Figure 7.4 to Figure 7.6 were thus normalised, pooled and plotted as shown in Figure 7.7. A logarithmic scale is used to show the response at low concentrations more clearly. This plot shows the variability in the pooled measurements. Figure 7.8 shows the same data as a three dimensional response surface to more clearly see the trends. In general, adsorption decreases with increasing molecular weight of PEO; sharply at first but more slowly on surfaces with longer PEO grafts. There is no significant difference in adsorption levels for PEO grafts of 750 MW and above. The reduction in protein adsorption reaches a limit at a molecular weight of about 2000 with a reduction ranging between 60-70%. PUU-OPEO350 and PUU-OPEO165 clearly adsorb more protein than the surfaces with longer PEO grafts. Moreover, at the higher concentration, PUU-OPEO165 adsorbs more protein than the control PUU. This may be

due to exposed patches of MDI-treated surface that was shown to adsorb more protein than the PUU control (Figure 7.3 on page 133). There also appears to be a slight increase in adsorption with increasing protein concentration on all surfaces. It is possible that at higher protein concentrations, the proteins may "overwhelm" the surface.

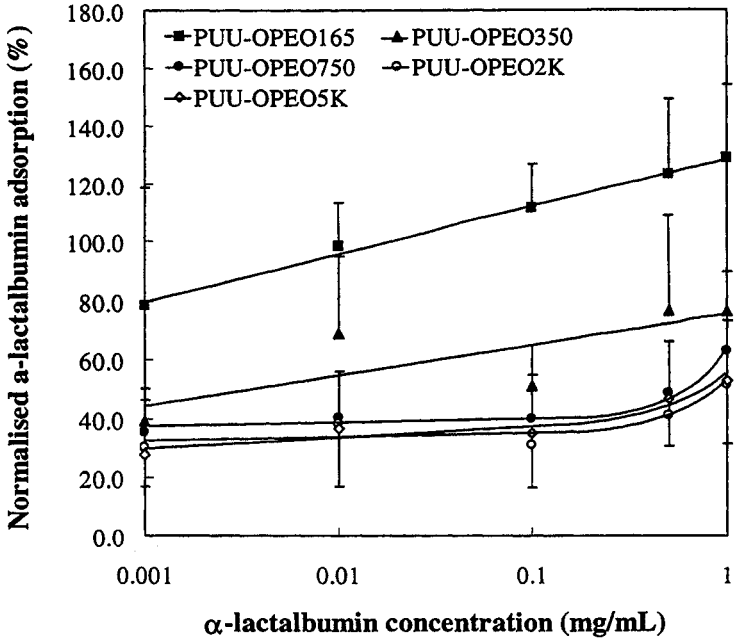

Figure 7.7: α-lactalbumin adsorption on PUU-OPEO surfaces, normalised to the PUU control (±S.D., n=9).

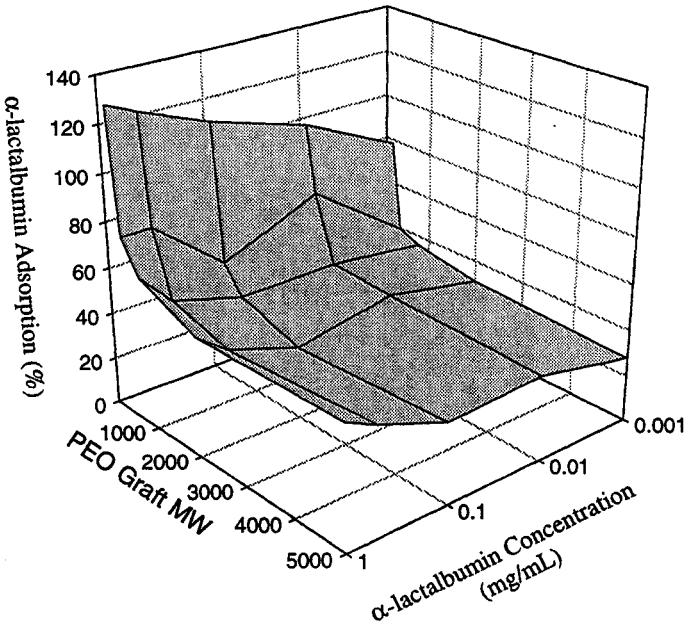

Figure 7.8: α-lactalbumin adsorption response surface showing the effects of PEO graft MW and α-lactalbumin concentration.

These results can be rationalised if it is assumed that the graft densities on the PEO-grafted surfaces are similar. In that instance, the higher the molecular weight of the PEO graft, the greater the coverage of PEO is expected to be. It appears that the shortest graft (3 EO repeat units) is unable to cover enough of the underlying surface and adsorption actually increases slightly compared to the control because of increased adsorption on the exposed MDI-treated PUU substrate.

Myoglobin

Myoglobin is a 17.5 kDa protein with dimensions of approximately 45×35×25 Å [Kendrew, J.C., 1963] and an isoelectric point of 7.2. The monolayer coverage based on these dimensions is 0.18-0.33 μg/cm^2. Figure 7.9 and Figure 7.10 show the adsorption isotherms for myoglobin for two batches of experimental surfaces. The adsorption levels on the control surface are again well above the monolayer coverage estimate. It is unclear whether this difference is due to underestimating the level of monolayer coverage for reasons mentioned above, or if there actually is greater than monolayer adsorption on these surfaces. Also, most of the isotherms do not appear to have reached the plateau region at the highest protein concentration.

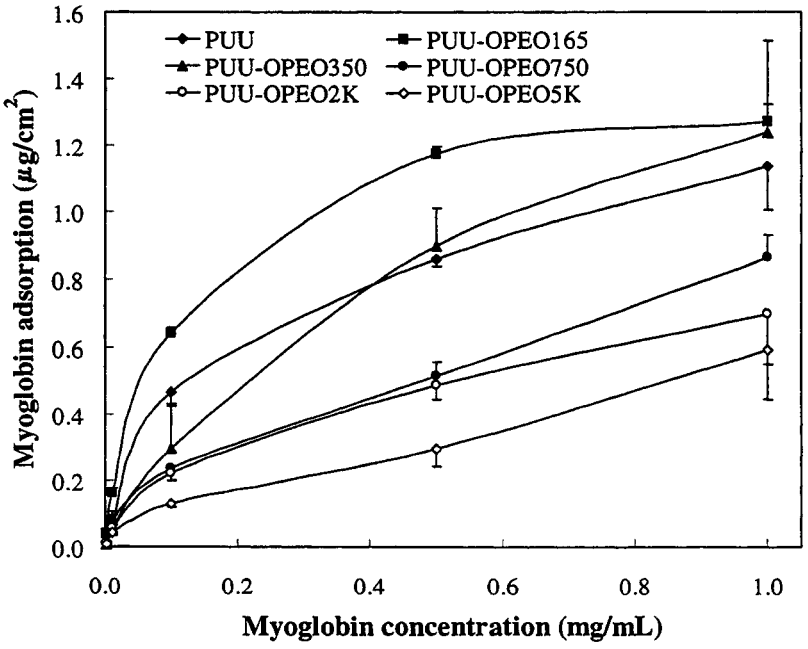

Figure 7.9: Myoglobin adsorption on PUU and PUU-OPEOs (first batch), from TBS buffer at 22°C for 3h, ±S.D., n=3.

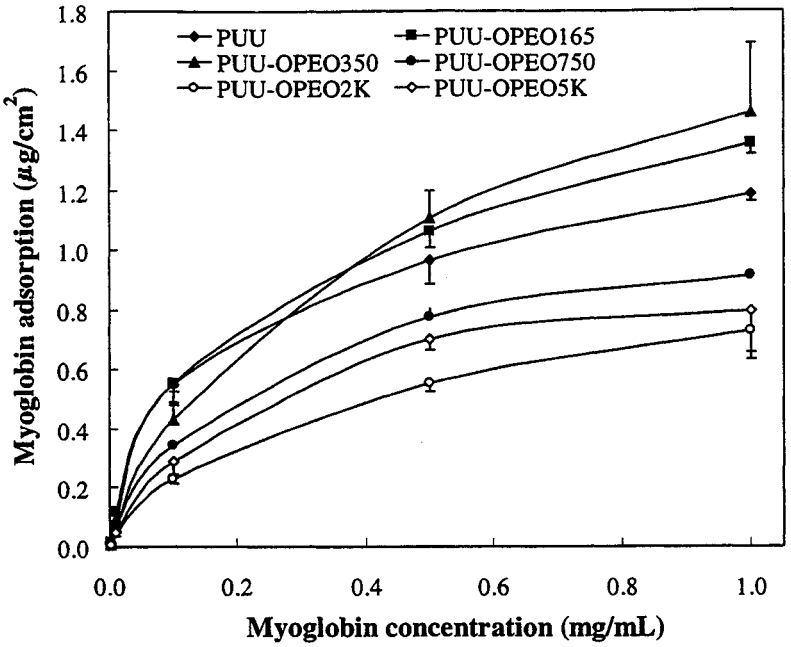

Figure 7.10: Myoglobin adsorption on PUU and PUU-OPEOs (second batch), from TBS buffer at 22°C for 3h, ±S.D., n=3.

Again PUU-OPEO165 generally adsorbs more than the control PUU, as does PUU-OPEO350 at the higher protein concentrations. In the first experiment, the lowest adsorption levels were on PUU-OPEO5K, whereas in the second experiment, PUU-OPEO2K showed the lowest adsorption levels. Both experiments generally follow the trend of lower protein adsorption with increasing PEO molecular weight.

An examination of the initial isotherm slopes in Table 7.3 confirms many of these observations. The affinity of myoglobin for PUU-OPEO165 is higher than for the control surface in both experiments. On all other PEO-grafted surfaces, the initial slopes of the isotherms were lower than the control surface and generally decreased as the length of the PEO graft increased. PUU-OPEO350 is a notable exception. The initial slope of this

isotherm was lower than the control surface but PUU-OPEO350 adsorbed more protein than the control surface in both experiments.

Table 7.3: Initial slopes from the myoglobin isotherms.

Surface	Initial Slope (mL/cm^2) (Average ± S.D., n=3)		Average Initial Slope (± 95% C.I.)
	Figure 7.9	Figure 7.10	
PUU	13.7±2.8	12.1±1.5	12.9±2.3
PUU-OPEO165	37.3±2.6	16.5±2.3	26.9±12.1
PUU-OPEO350	6.7±0.2	9.5±0.7	8.1±1.7
PUU-OPEO750	11.7±2.3	11.4±1.6	11.5±2.0
PUU-OPEO2K	10.2±0.5	9.2±1.4	9.7±1.2
PUU-OPEO5K	5.7±0.2	7.7±1.8	6.7±1.6

The normalised myoglobin adsorption curves from the two experiments are plotted in Figure 7.11 and the associated adsorption response surface in Figure 7.12. There is no significant difference between PUU-OPEO2K and PUU-OPEO5K except at the lowest myoglobin concentration. In general these data confirm the trend of decreasing adsorption with increasing PEO molecular weight. The relatively low adsorption on PUU-OPEO350 at low protein concentration was not expected. There do not appear to be any clear trends with respect to protein concentration. There was also more variability associated with the surfaces having shorter PEO grafts, possibly due to larger areas without PEO coverage on these surfaces. Finally, the largest reductions in adsorption levels compared to the control PUU were of the order of 40-45%.

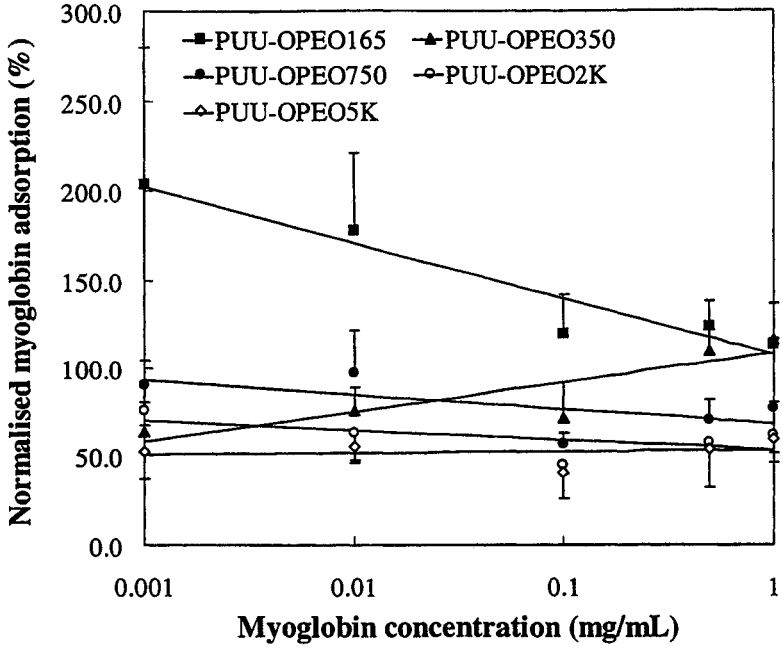

Figure 7.11: Normalised myoglobin adsorption on PUU-OPEO surfaces (±S.D., n=6).

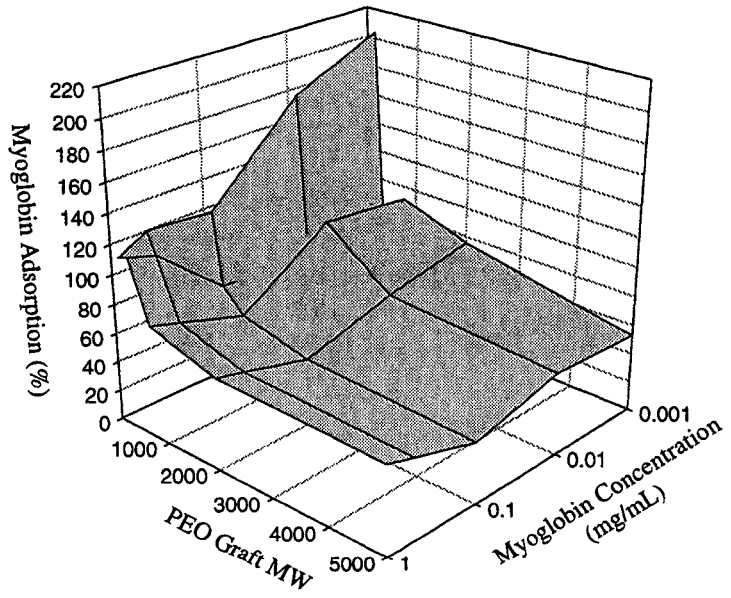

Figure 7.12: Myoglobin adsorption response surface showing the effects of PEO graft MW and myoglobin concentration.

Ribonuclease A (RNAse)

Ribonuclease A is a 13.6 kDa protein with dimensions of approximately 38×38×22 Å [Kartha, G. et al., 1967] and an isoelectric point of 9.4. The monolayer coverage based on these dimensions is 0.16-0.27 $\mu g/cm^2$. The isotherms from two experiments with RNAse are shown in Figure 7.13 and Figure 7.14. In this instance, the adsorption on the control PUU surface at the highest protein concentration seems to fall within the range of monolayer coverage, although the isotherms do not appear to have reached a plateau. However, adsorption on some of the PEO-grafted surfaces exceeds the predicted range, possibly suggesting multilayer adsorption.

The adsorption data from the first experiment show high levels of adsorption for PUU-OPEO165, PUU-OPEO350 and PUU-OPEO750. The lowest levels of adsorption are generally on PUU-OPEO5K. The isotherms from the second experiment were similar to those observed for α–lactalbumin and myoglobin. PUU-OPEO2K generally adsorbed the least and PUU-OPEO 350 adsorbed the most. The difference in response for the surfaces with the shortest PEO grafts, i.e. PUU-OPEO165 and PUU-OPEO350 is significant. The reason for this is unclear since such large differences were not observed in other experiments using the same batches of PEO-grafted surfaces (α-lactalbumin, myoglobin, and lysozyme below).

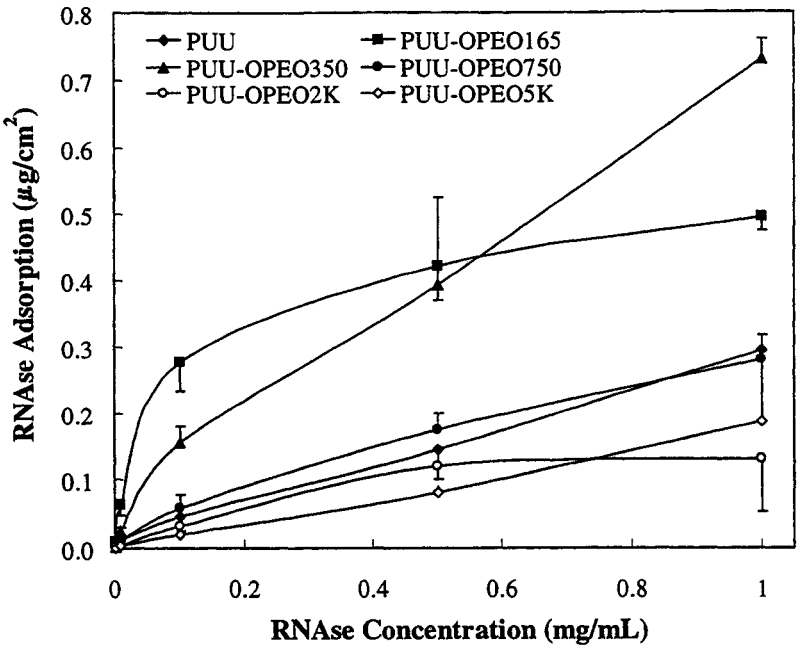

Figure 7.13: RNAse adsorption on PUU and PUU-OPEOs (first batch) from TBS buffer at 22°C for 3h, ±S.D., n=3.

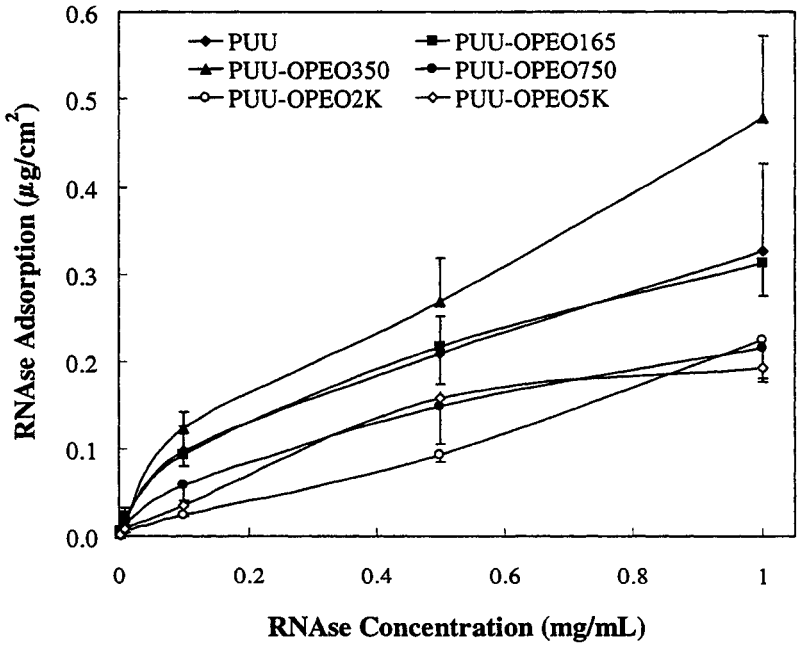

Figure 7.14: RNAse adsorption on PUU and PUU-OPEOs (second batch) from TBS buffer at 22°C for 3h, ±S.D., n=3.

An examination of the initial slopes in Table 7.4 generally supports the discussion above. In both experiments, the affinity of the protein for the surface decreases as the length of the PEO graft increases. In addition only PUU-OPEO165 in the first experiment has a higher initial slope than the control surface even though several surfaces in either experiment adsorb as much or more than the control surface. Unlike myoglobin, this behaviour is not limited to adsorption at high protein concentration. The reason for the high level of adsorption on the surfaces with the shorter PEO-grafts may again be the result of areas of surface not grafted with PEO but modified with the diisocyanate.

Table 7.4: Initial slopes from the RNAse isotherms.

Surface	Initial Slope (mL/cm^2) (Average ± S.D., n=3)		Average Initial Slope (± 95% C.I.)
	Figure 7.13	Figure 7.14	
PUU	5.0±2.2	7.5±2.1	6.3±2.4
PUU-OPEO165	8.1±1.3	5.5±1.5	6.8±2.0
PUU-OPEO350	2.4±1.0	2.7±0.4	2.5±0.7
PUU-OPEO750	2.2±1.3	2.7±0.7	2.4±1.0
PUU-OPEO2K	0.9±0.2	1.5±0.3	1.2±0.4
PUU-OPEO5K	0.5±0.1	1.4±0.3	1.0±0.6

The normalised RNAse adsorption curves from the two experiments are summarised in Figure 7.15 and the adsorption response surface is shown in Figure 7.16. The adsorption levels on PUU-OPEO2K and PUU-OPEO5K are not significantly different from each other. PUU-OPEO750 adsorbed significantly higher levels of RNAse than the latter two surfaces, however. Again there is much more variability for the

surfaces with the short PEO grafts. The adsorption response surface shows the general trend of lower levels of protein adsorption with increasing PEO-graft length. There does not appear to be a concentration effect, but the high variability of adsorption levels on PUU-OPEO165 and PUU-OPEO350 makes it difficult comment on any trends. The reduction in protein adsorption appears reach an upper limit for the 2000MW PEO grafts. For these surfaces, RNAse adsorption was reduced by about 55% compared to the control.

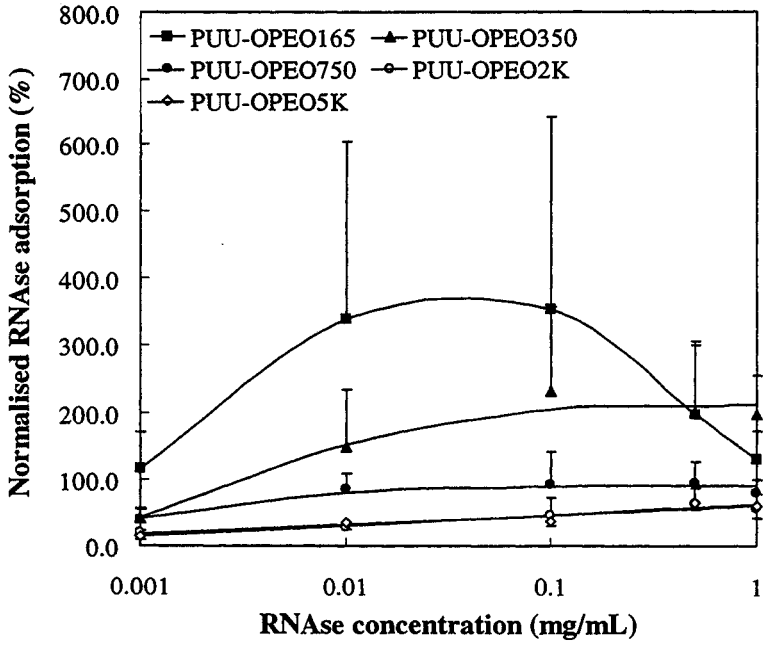

Figure 7.15: Normalised RNAse adsorption on PUU-OPEO surfaces (±S.D., n=6).

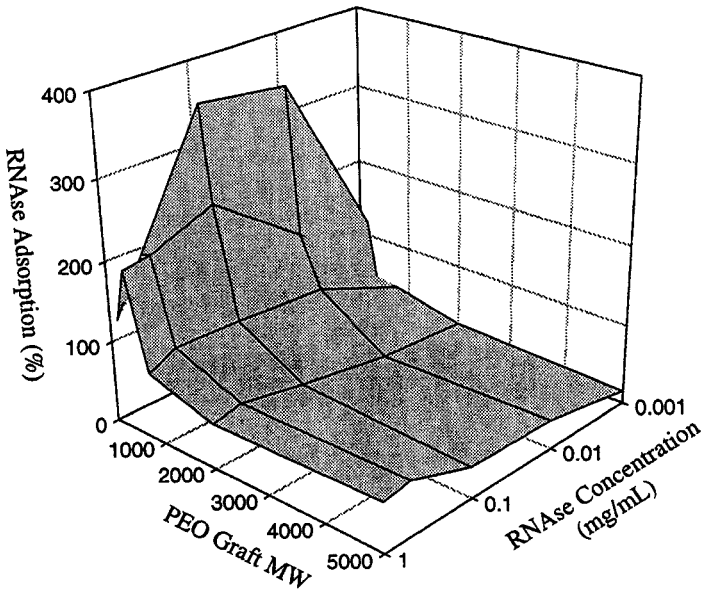

Figure 7.16 : RNAse adsorption response surface showing the effects of PEO graft MW and RNAse concentration.

Lysozyme

Lysozyme is a 14.6 kDa protein with dimensions of approximately 46×30×20 Å [Norde, W. and Haynes, C.A., 1995] and an isoelectric point of 11.1. The monolayer coverage based on these dimensions is 0.18-0.27 μg/cm^2. The adsorption isotherms for lysozyme from two separate experiments are shown in Figure 7.17 and Figure 7.18. The adsorption levels on the control PUU surface reach a maximum value of about 0.5-0.6 μg/cm^2. The possible reasons for the difference between the calculated monolayer coverage and the adsorption levels found on the control surface were discussed previously.

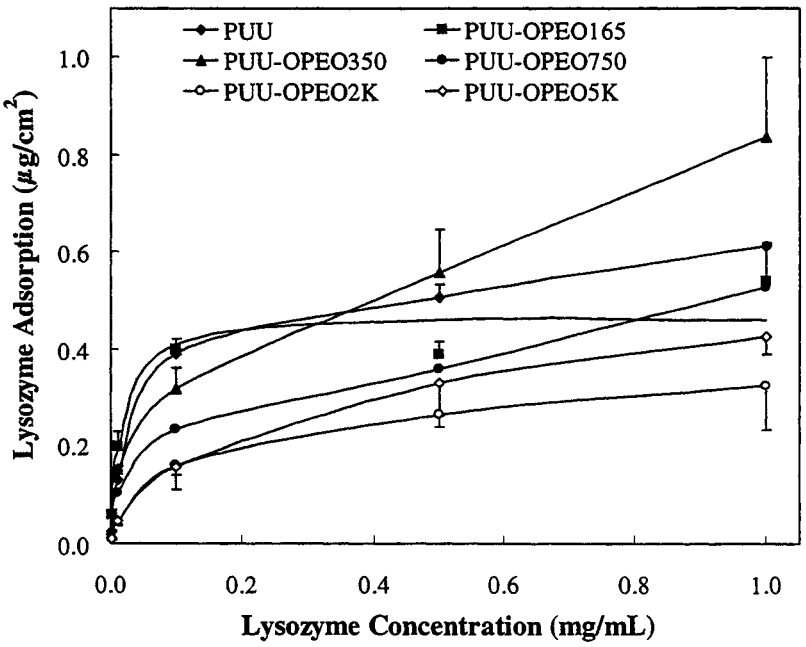

Figure 7.17: Lysozyme adsorption on PUU and PUU-OPEOs (first batch) from TBS buffer at 22°C for 3h, ±S.D., n=3. Note: Some error bars omitted to improve clarity.

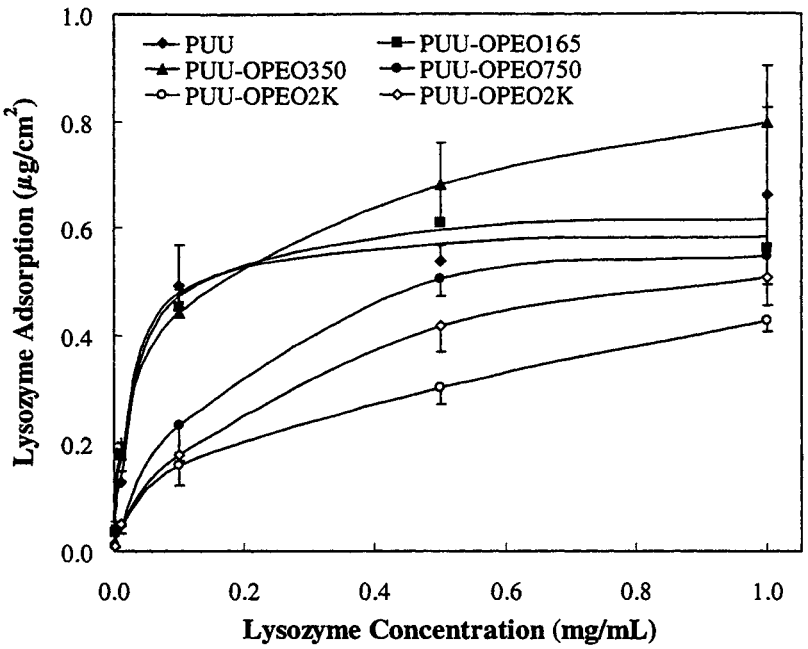

Figure 7.18: Lysozyme adsorption on PUU and PUU-OPEOs (second batch) from TBS buffer at 22°C for 3h, ±S.D., n=3.

The trends are similar to those for the proteins discussed previously. In this instance, both PUU-OPEO165 and PUU-OPEO350 adsorbed, in general, close to the same as, or somewhat more than, the control PUU depending on the protein concentration. These two surfaces again displayed much greater experimental variability than the others. The adsorption levels also generally decreased with increasing PEO molecular weight. PUU-OPEO2K showed the lowest levels of lysozyme adsorption in both experiments.

The affinity of the protein for PUU-OPEO165 and PUU-OPEO350, as estimated by the initial slopes of the isotherms (Table 7.5), was higher than for the control surface in both experiments. This reflects the adsorption levels on these PEO-grafted surfaces which are generally close to or above the adsorption levels on the control surface. The

initial slopes of the isotherms for the other PEO-grafted surfaces were all lower than that of the control PUU surface and decreased with increasing PEO graft length.

Table 7.5: Initial slopes from the lysozyme isotherms.

Surface	Initial Slope (mL/cm^2) (Average ± S.D., n=3)		Average Initial Slope (± 95% C.I.)
	Figure 7.17	Figure 7.18	
PUU	24.2±2.5	39.1±16.2	31.7±13.9
PUU-OPEO165	57.6±2.2	35.9±11.3	46.8±14.6
PUU-OPEO350	62.2±5.7	42.5±4.8	52.4±12.4
PUU-OPEO750	18.0±6.8	10.5±1.3	14.3±6.3
PUU-OPEO2K	9.9±1.1	8.6±2.1	9.3±1.7
PUU-OPEO5K	9.2±1.4	8.1±2.5	8.6±2.0

The normalised lysozyme adsorption curves from these experiments are shown in Figure 7.19 and the adsorption response surface in Figure 7.20. The responses for PUU-OPEO2K and PUU-OPEO5K are significantly different only at the highest protein concentrations. The adsorption levels on PUU-OPEO750 are significantly higher than on PUU-OPEO2K except at the lowest lysozyme concentration. Generally, however, the adsorption levels decreased with increasing PEO graft length and there does seem to be a slight increase in adsorption levels with increasing protein concentration on the surfaces with the longest PEO-grafts; perhaps this indicates that the surfaces are "overwhelmed" with protein at these higher concentrations. The largest reduction in lysozyme adsorption was approximately 50-55% compared to the control PUU.

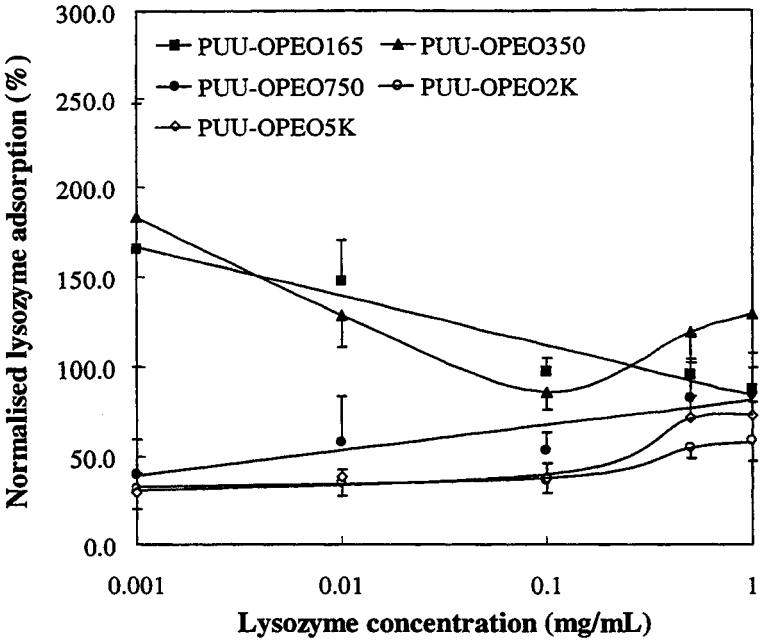

Figure 7.19: Normalised lysozyme adsorption on PUU-OPEO surfaces (±S.D., n=6).

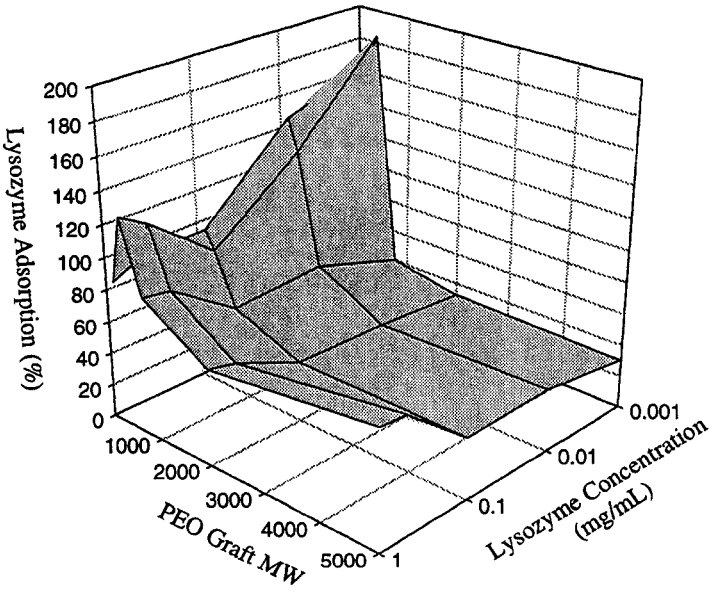

Figure 7.20: Lysozyme adsorption response surface showing the effects of PEO graft MW and lysozyme concentration.

Human Serum Albumin (HSA)

HSA is a 66 kDa protein with dimensions of approximately 140×44×44 Å [He, X.M. and Carter, D.C., 1992] and an isoelectric point of 4.7. The monolayer coverage based on these dimensions is 0.18-0.57 $\mu g/cm^2$. Isotherms for two separate batches of experimental surfaces are shown in Figure 7.21 and Figure 7.22. As was the case with lysozyme, the control PUU surface does adsorb albumin in the range of monolayer coverage. However, the indication from the shape of the isotherms is that higher adsorption levels would be observed at higher protein concentrations.

Trends similar to those noted for the other proteins examined are also present in the HSA isotherms. In the first experiment, most of the surfaces behave as previously seen except for PUU-OPEO5K, which unexpectedly adsorbed the most protein of any of the surfaces at the highest HSA concentration. In the second experiment, both PUU-OPEO165 and PUU-OPEO350 showed adsorption levels higher than the control PUU at high protein concentrations. PUU-OPEO2K showed the lowest adsorption levels in both experiments.

The affinities of this protein for the PEO-grafted surfaces (from the initial slope of the isotherms, listed in Table 7.6) were all less than the control surface with the exception of PUU-OPEO165 in the first experiment. There was also a decrease in affinity with increasing length of the PEO grafts. PUU-OPEO2K had the lowest protein affinity, on average, supporting the observations discussed above.

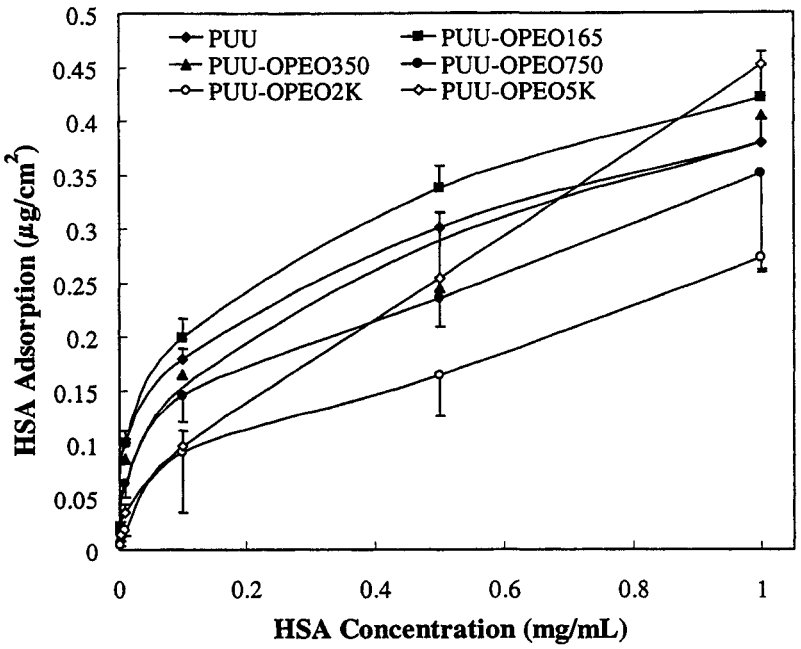

Figure 7.21: HSA adsorption on PUU and PUU-OPEOs (first batch) from TBS buffer at 22°C for 3h, ±S.D., n=3. Note: Some error bars omitted to improve clarity.

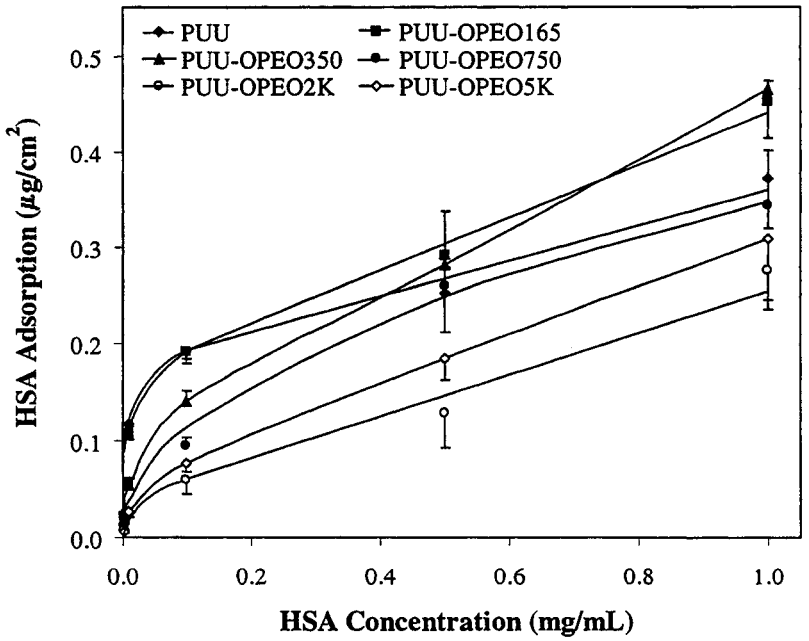

Figure 7.22: HSA adsorption on PUU and PUU-OPEOs (second batch) from TBS buffer at 22°C for 3h, ±S.D., n=3.

The normalised HSA adsorption curves for these experiments are shown in Figure 7.23 and the adsorption response surface in Figure 7.24. The adsorption levels on PUU-OPEO2K are lower than on any of the other surfaces. The adsorption levels on PUU-OPEO750 and PUU-OPEO5K are generally not significantly different from each other. The response surface clearly shows the decrease in adsorption as the length of the PEO grafts on the experimental surfaces increases. There also appears to be a trend of increasing protein adsorption with increasing protein concentration. The PEO grafts appear to be less effective at repelling proteins at high protein concentrations. The lowest levels of adsorption were on PUU-OPEO2K, with an average reduction of nearly 60% compared to the control PUU.

Table 7.6: Initial slopes from the HSA isotherms.

Surface	Initial Slope (mL/cm^2) (Average ± S.D., n=3)		Average Initial Slope (± 95% C.I.)
	Figure 7.21	Figure 7.22	
PUU	18.0±3.5	25.2±3.2	21.6±5.2
PUU-OPEO165	21.7±4.3	22.5±4.7	22.1±4.3
PUU-OPEO350	11.9±1.9	12.3±1.2	12.1±1.5
PUU-OPEO750	16.8±4.8	12.6±2.3	14.7±4.3
PUU-OPEO2K	4.4±1.1	6.9±2.0	5.7±2.1
PUU-OPEO5K	14.3±3.6	5.7±0.6	10.0±5.5

Experiments using similar surfaces were conducted by Wesslén et al. [Wesslén, B. et al., 1994]. PEOs of 1500 and 20000 MW were grafted to a commercial polyurethane, Pellethane®, using the diisocyanate, HMDI. Following a 1 h incubation in 5

mg/mL HSA in buffer at 37°C, neither of the two PEO-grafted surfaces reduced protein adsorption from levels detected on the control polymer. However, no rinsing steps were performed prior to determining the radioactivity of the samples. The adsorption level on the control was approximately 10.7 $\mu g/cm^2$, i.e. an order of magnitude greater than determined in the present experiments.

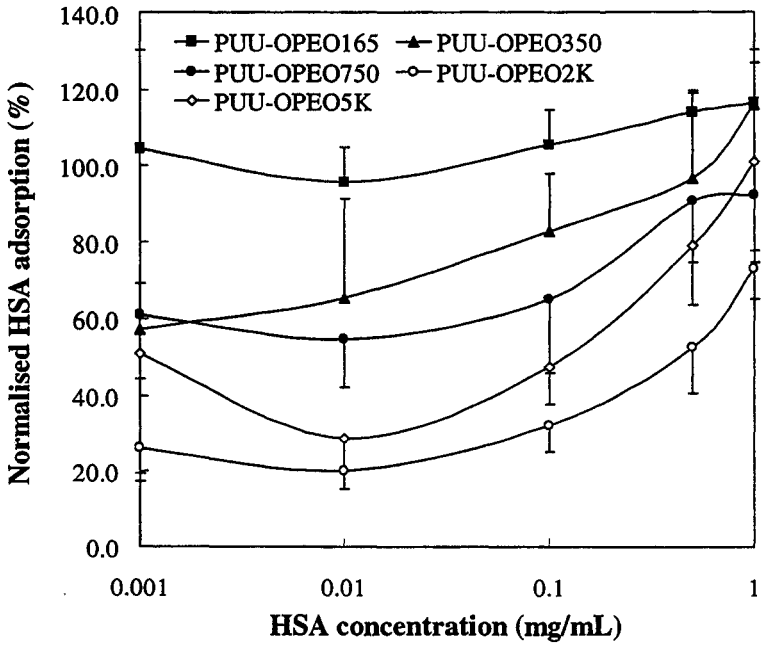

Figure 7.23: Normalised HSA adsorption on PUU-OPEO surfaces (±S.D., n=6).

Han et al. also prepared a polyurethane surface (Pellethane®) grafted with 1000 MW PEO using HMDI as the grafting agent [Han, D.K. et al., 1996]. Following a 5 min incubation in bovine plasma, BSA adsorption on the control polymer reached 0.18 $\mu g/cm^2$, but only 0.12 $\mu g/cm^2$ on the PEO-grafted surface: i.e. a reduction of about 33%.

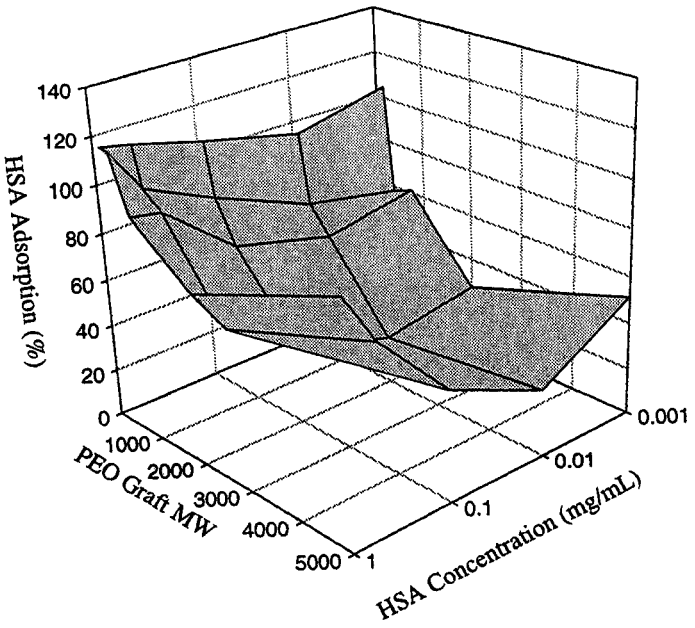

Figure 7.24: HSA adsorption response surface showing the effects of PEO graft MW and HSA concentration.

Concanavalin A

Concanavalin A is a 102 kDa tetrameric protein with dimensions of approximately 84×80×39 Å [Reeke, G.N. et al., 1975] and an isoelectric point of 5.0. The monolayer coverage based on these dimensions is 0.26-0.54 $\mu g/cm^2$. Each 25.5 kDa subunit is 42×40×39 Å in size and would give an expected monolayer coverage of 0.25-0.27 $\mu g/cm^2$. Above pH 6, concanavalin A is largely found in the tetrameric configuration; below this pH, dimers are found [Reeke, G.N. et al., 1975].

Adsorption isotherms for concanavalin A from two separate experiments are shown in Figure 7.25 and Figure 7.26. Again, adsorption on the control and some of the PEO-grafted surfaces exceed the estimate for monolayer coverage by nearly a factor of 2 in some cases. Another noticeable feature of these isotherms is that the overall reduction of protein adsorption on the PEO surfaces is generally less than for the proteins discussed previously. In the first experiment, PUU-OPEO165 and PUU-OPEO350 again adsorbed more protein than the control PUU. Some batch-to-batch variation is evident given that in the second experiment all the PEO surfaces adsorbed less protein than the control PUU. Moreover, PUU-OPEO165 displayed much lower adsorption levels relative to the control than previously seen for the other proteins. PUU-OPEO2K adsorbed the least concanavalin A in the first experiment whereas in the second experiment, PUU-OPEO2K and PUU-OPEO5K showed similar responses.

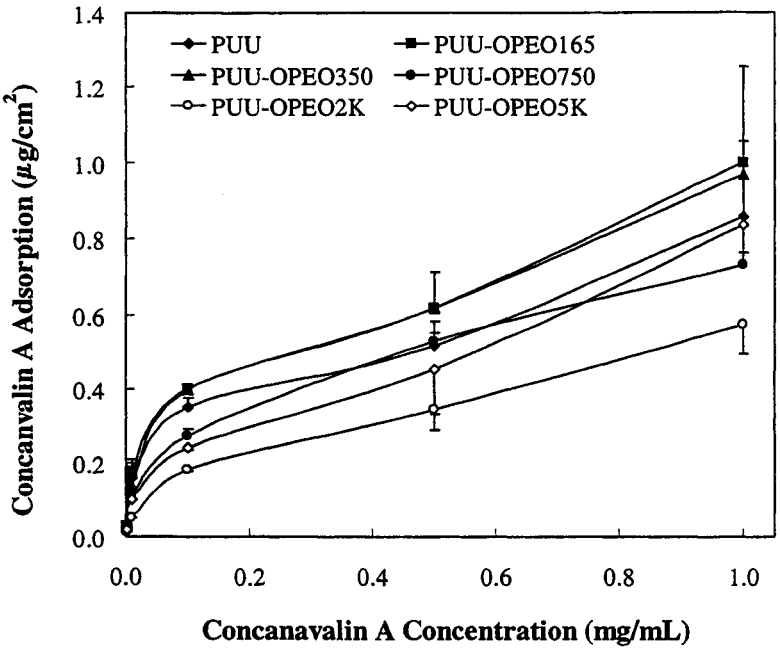

Figure 7.25: Concanavalin A adsorption on PUU and PUU-OPEOs (first batch) from TBS buffer at 22°C for 3h, ±S.D., n=3.

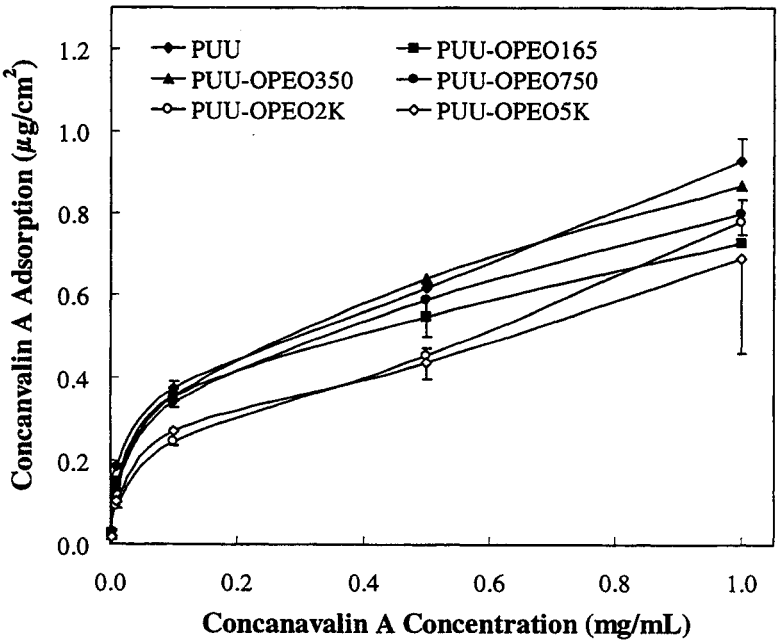

Figure 7.26: Concanavalin A adsorption on PUU and PUU-OPEOs (second batch) from TBS buffer at 22°C for 3h, ±S.D., n=3.

The initial slopes of the isotherms, given in Table 7.7, were all lower than for the PUU control, except for PUU-OPEO165 in the first experiment. However the reduction in affinity on the PEO-grafted surfaces was lower than previously observed for the other proteins, supporting the observation above that the reduction in protein adsorption was less than previously seen for other proteins. The trends were similar to those previously discussed; as the length of the PEO grafts increased, the affinity of the protein for the surface decreased. This protein had the lowest affinity for PUU-PEO2K.

Table 7.7: Initial slopes of the Concanavalin A isotherms.

Surface	Initial Slope (mL/cm^2) (Average ± S.D., n=3)		Average Initial Slope (± 95% C.I.)
	Figure 7.25	Figure 7.26	
PUU	26.6±1.1	31.7±3.0	29.1±3.6
PUU-OPEO165	28.8±6.2	25.1±1.9	26.9±4.8
PUU-OPEO350	21.2±0.8	22.4±0.9	21.9±1.2
PUU-OPEO750	17.9±1.6	20.1±0.9	19.3±1.7
PUU-OPEO2K	12.8±0.6	16.4±2.1	15.0±3.1
PUU-OPEO5K	18.8±4.2	17.3±0.9	17.7±3.0

The normalised concanavalin A adsorption curves from the two experiments are plotted in Figure 7.27 and the response surface in Figure 7.28. Although PUU-OPEO2K shows consistently lower adsorption than PUU-OPEO5K, these surfaces are generally not significantly different from each other at the different protein concentrations. PUU-OPEO750, however, generally adsorbed significantly more concanavalin A than the surfaces with the longest PEO grafts. The response surface shows the general decrease in

adsorption with increasing PEO graft molecular weight and also a slight trend of increasing adsorption with protein concentration. Again, PUU-OPEO2K showed the lowest protein adsorption levels, with a reduction of about 40% compared to the control PUU. This is a considerably lower reduction than for most of the other proteins so far reported.

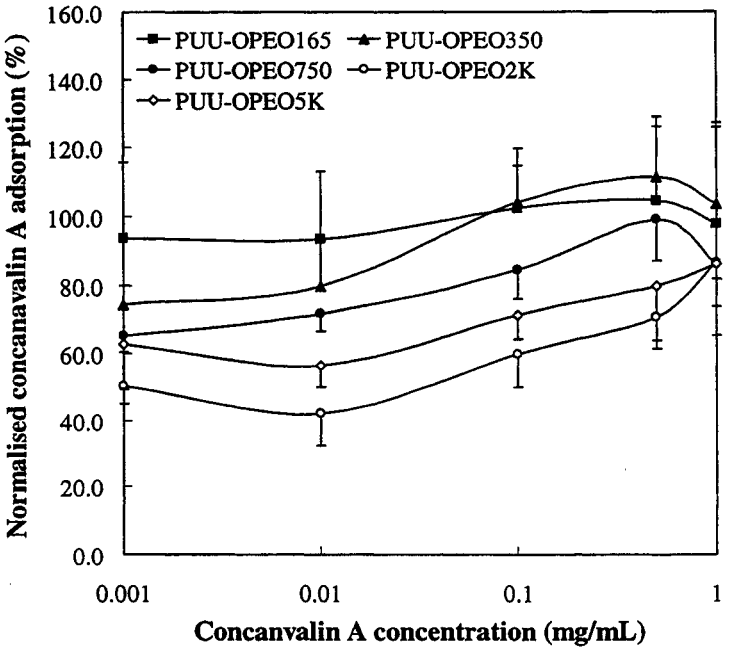

Figure 7.27: Normalised concanavalin A adsorption on PUU-OPEO surfaces (±S.D., n=6).

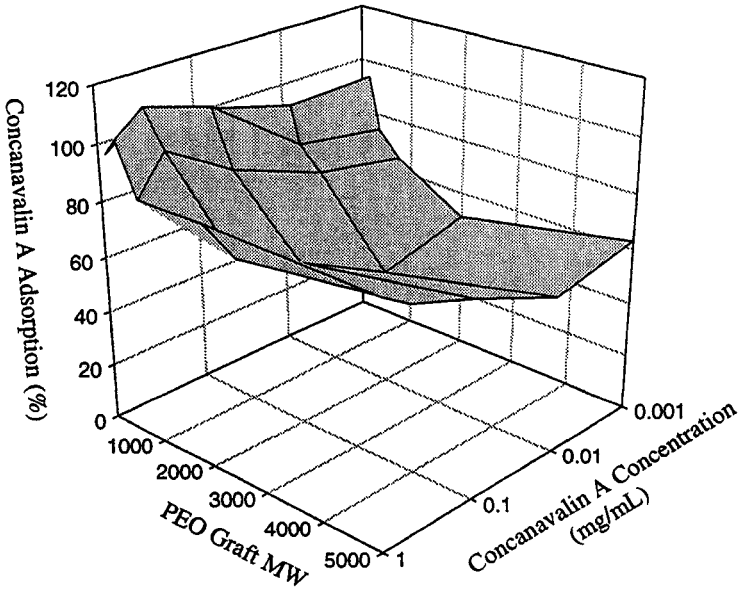

Figure 7.28 : Concanavalin A adsorption response surface showing the effects of PEO graft MW and Concanavalin A concentration.

Fibrinogen

Fibrinogen is a 340 kDa protein with dimensions of approximately 450×90×90 Å and has an isoelectric point of 4.3. The monolayer coverage based on these dimensions is 0.14-0.7 $\mu g/cm^2$. Figure 7.29 and Figure 7.30 show adsorption isotherms for fibrinogen for two different batches of the PUU-OPEO surfaces. As for some of the other proteins, the adsorption on the control and some PEO-grafted surface exceed the estimated monolayer coverage. The general trends in Figure 7.29 are similar to those previously noted: adsorption decreases with increasing molecular weight of PEO and reaches a minimum at a molecular weight of 2000. The trends in Figure 7.30 are a little less clear. Both PUU-OPEO165 and PUU-OPEO350 adsorb more than the control PUU and the surfaces with the longer PEO grafts adsorb less than the control. PUU-OPEO2K and PUU-OPEO5K show fairly similar responses and generally exhibit the lowest protein adsorption.

The affinity of fibrinogen for the surfaces, given by the initial slopes of the isotherms (Table 7.8), show that fibrinogen has a lower affinity for all the PEO-grafted surfaces than for the PUU control. Furthermore, in general the affinity decreases with increasing PEO graft length, reaching a minimum with the 2000MW and 5000MW grafts.

The normalised fibrinogen adsorption curves from the two experiments are shown in Figure 7.31 and the adsorption response surface in Figure 7.32. The large error bars indicate where significantly different responses were obtained for the two experiments. PUU-OPEO2K and PUU-OPEO5K are generally not significantly different from each other. PUU-OPEO750 generally adsorbed significantly more fibrinogen than the surfaces

with the longest PEO grafts. PUU-OPEO350 and PUU-OPEO165 were not significantly different from each other. The general trend of decreasing adsorption with increasing PEO graft length can be seen on the response surface. However, there does not appear to be a consistent trend with respect to protein concentration. The greatest reduction in fibrinogen adsorption achieved was approximately 40-45% compared to the control PUU.

Wesslén's study also examined fibrinogen adsorption on PEO-grafted polyurethanes [Wesslén, B. et al., 1994]. The adsorption level on the control surface was approximately 0.7 $\mu g/cm^2$ for incubation in a 0.035 mg/mL fibrinogen solution for 1 h at 37°C. A 1500 MW PEO-grafted polyurethane showed adsorption that was reduced by about 17% whereas the 20000 MW PEO-grafted polyurethane showed a reduction of 61% compared to the control surface. Han et al. measured bovine fibrinogen adsorption from diluted plasma (5 min) on polyurethanes grafted with PEO of MW 1000. The adsorption levels on the control polymer reached a plateau of 0.1 $\mu g/cm^2$ whereas only 0.04 $\mu g/cm^2$ adsorbed to the PEO-grafted surface for a reduction of 60%.

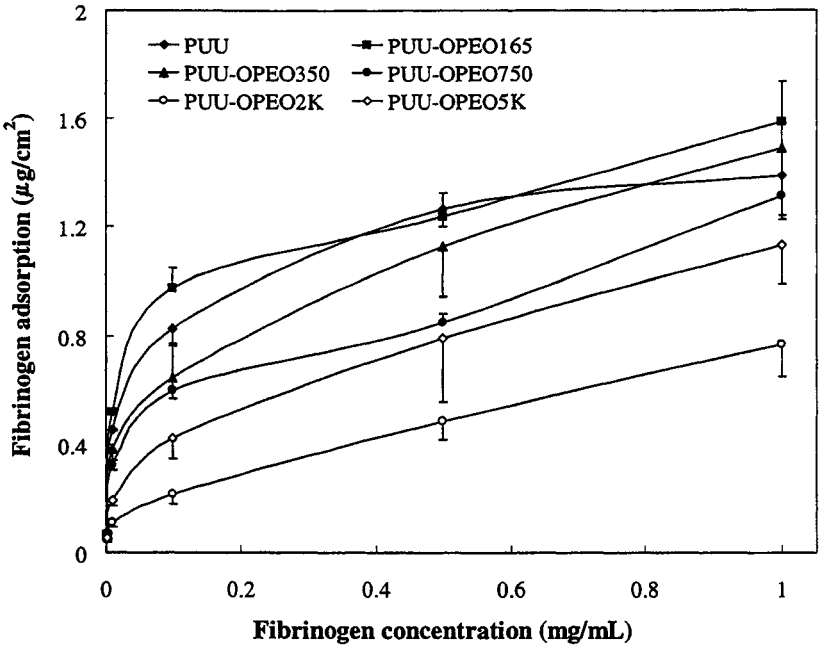

Figure 7.29: Fibrinogen adsorption on PUU and PUU-OPEOs (first batch) from TBS buffer at 22°C for 3h, ±S.D., n=3.

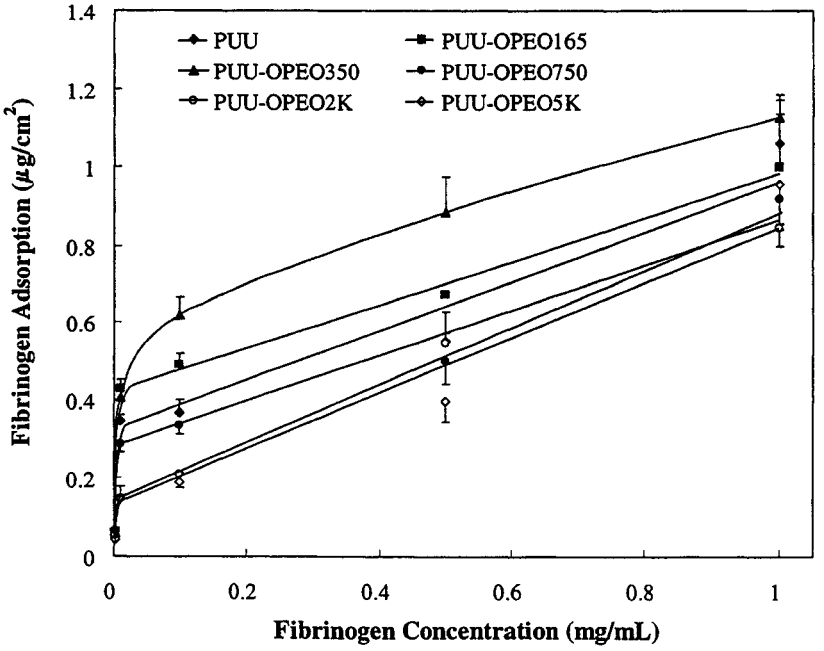

Figure 7.30: Fibrinogen adsorption on PUU and PUU-OPEOs (second batch) from TBS buffer at 22°C for 3h, ±S.D., n=3.

Table 7.8: Initial slopes from the fibrinogen isotherms.

Surface	Initial Slope (mL/cm^2) (Average ± S.D., n=3)		Average Initial Slope (± 95% C.I.)
	Figure 7.29	Figure 7.30	
PUU	76.6±9.3	67.3±5.4	72.0±8.9
PUU-OPEO165	68.1±4.8	60.7±0.9	64.4±5.4
PUU-OPEO350	62.9±5.9	59.2±2.1	61.0±4.6
PUU-OPEO750	68.1±3.9	60.5±3.8	64.3±5.7
PUU-OPEO2K	46.4±8.6	50.7±6.8	48.5±7.7
PUU-OPEO5K	55.4±7.5	42.9±2.9	49.1±8.9

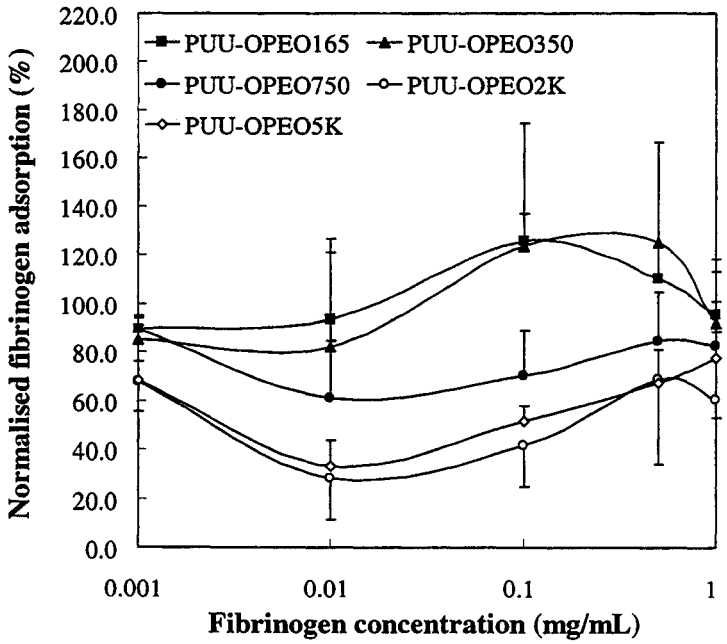

Figure 7.31: Normalised fibrinogen adsorption on PUU-OPEO surfaces (±S.D., n=6).

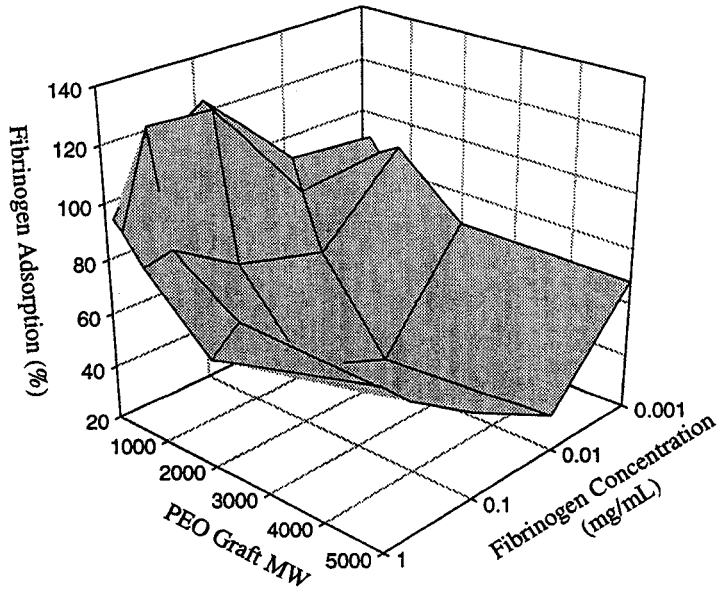

Figure 7.32: Fibrinogen adsorption response surface showing the effects of PEO graft MW and Fibrinogen concentration.

Ferritin

Ferritin is a 440 kDa spherical multimeric protein with an outer diameter of 125 Å and an isoelectric point of 4.3. The monolayer coverage based on these dimensions is approximately 0.54 $\mu g/cm^2$. The 24 subunits (18.5 kDa, 25×25×50 Å) form a hollow shell with an inside diameter of 80 Å, where up to 4500 Fe(III) atoms can be stored [Harrison, P.M. and Arosio, P., 1996]. The protein shell is stable at elevated temperatures (70°C) [Harrison, P.M. and Arosio, P., 1996] and wide ranges of pH (3-11) [Crichton, R.R., 1973]. The expected monolayer coverage based on the subunit size is 0.25-0.49 $\mu g/cm^2$.

The adsorption isotherms for ferritin for two separate experiments are illustrated in Figure 7.33 and Figure 7.34. The adsorption levels on the PUU control in the first experiment are very close to the predicted monolayer levels. However, in the second experiment, the response of the control PUU surface is very different; most of the PEO-grafted surfaces, however, give similar responses in the two experiments. The reason for the large difference in response for some of the surfaces, including the control, is not clear. The trends in the first experiment are similar to those found for the other proteins studied. PUU-OPEO165 adsorbed more than the control PUU. PUU-OPEO2K generally adsorbed the smallest amount of protein. In the second experiment, PUU-OPEO350 unexpectedly showed the lowest levels of adsorption. In addition, all the experimental surfaces in this batch adsorbed less than the control PUU.

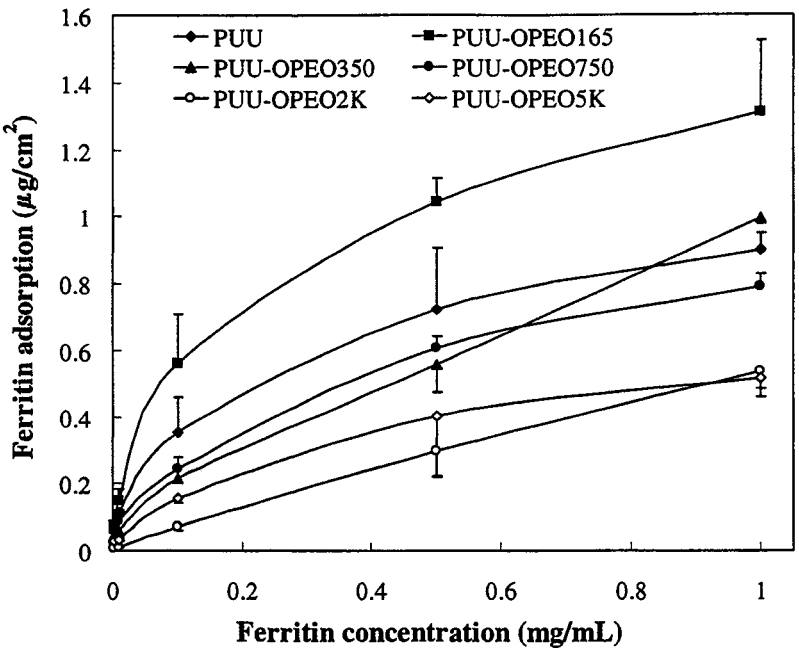

Figure 7.33: Ferritin adsorption on PUU and PUU-OPEOs (first batch) from TBS buffer at 22°C for 3h, ±S.D., n=3.

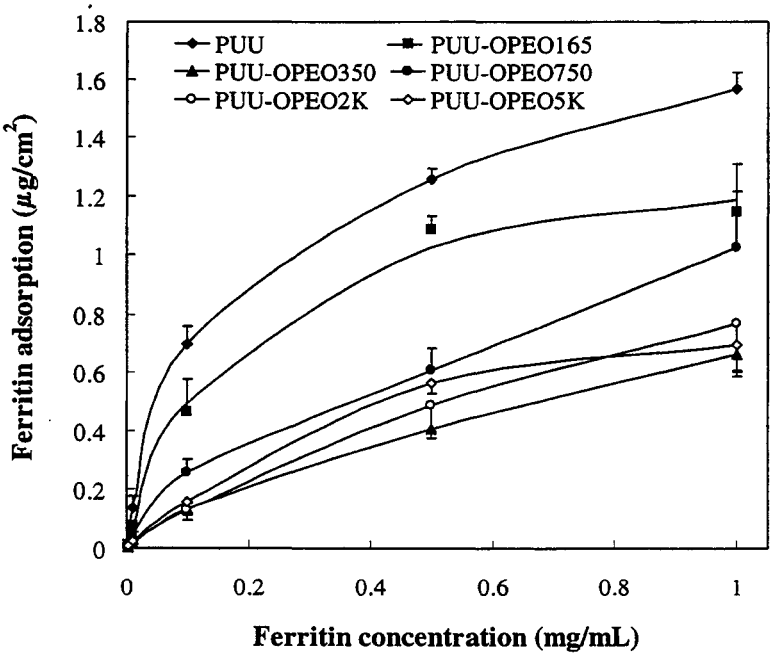

Figure 7.34: Ferritin adsorption on PUU and PUU-OPEOs (second batch) from TBS buffer at 22°C for 3h, ±S.D., n=3.

The affinities of the protein for the surfaces, given by the initial slopes of the isotherms (Table 7.9), were similar to those discussed for the other proteins. The affinity of ferritin for the PEO-grafted surfaces was lower than for the control in all cases except PUU-OPEO165 in the first experiment. Ferritin showed the lowest affinity for the PUU-OPEO2K surface.

Table 7.9: Initial slopes from the ferritin isotherms.

Surface	Initial Slope (mL/cm^2) (Average ± S.D., n=3)		Average Initial Slope (± 95% C.I.)
	Figure 7.33	Figure 7.34	
PUU	56.4±19.7	19.3±2.1	37.8±25.0
PUU-OPEO165	72.5±17.1	12.5±0.8	42.5±36.3
PUU-OPEO350	22.6±7.9	5.9±2.6	12.6±12.6
PUU-OPEO750	24.4±8.7	7.4±1.7	15.9±11.4
PUU-OPEO2K	7.1±3.5	5.6±2.3	6.3±2.9
PUU-OPEO5K	27.7±6.4	7.3±1.2	17.0±12.5

The normalised ferritin adsorption curves for the two experiments are shown in Figure 7.35 and the adsorption response surface in Figure 7.36. The difference in response for PUU-OPEO165 between the two experiments is reflected in these curves. In the first experiment, adsorption was well above that of the control PUU, whereas in the second experiment, adsorption on PUU-OPEO165 was slightly below the control PUU. The variation in response for PUU-OPEO350 was also large. Although it appears that the batch-to-batch variation for these two surfaces was particularly high, surfaces from these batches used with other proteins did not show such a large degree of variation.

Adsorption on PUU-OPEO2K was generally significantly lower than on PUU-OPEO5K. Somewhat unexpectedly, although adsorption levels on PUU-OPEO350 were generally higher than on PUU-OPEO2K and PUU-OPEO5K, the differences were not significant. PUU-OPEO750 generally adsorbed more protein than the two surfaces with the longest PEO grafts. The response surface clearly shows the trend of decreasing protein adsorption with increasing PEO graft length on the experimental surfaces. There does appear to be a slight trend of increasing adsorption with increasing protein concentration. The largest reduction in ferritin adsorption, compared to the control PUU, was approximately 70% on PUU-OPEO2K.

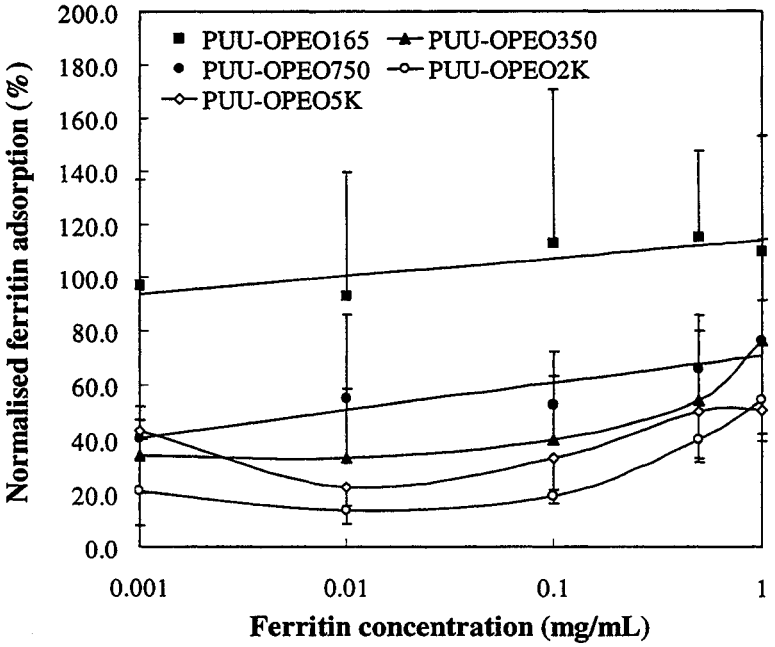

Figure 7.35: Normalised ferritin adsorption on PUU-OPEO surfaces (±S.D., n=6).

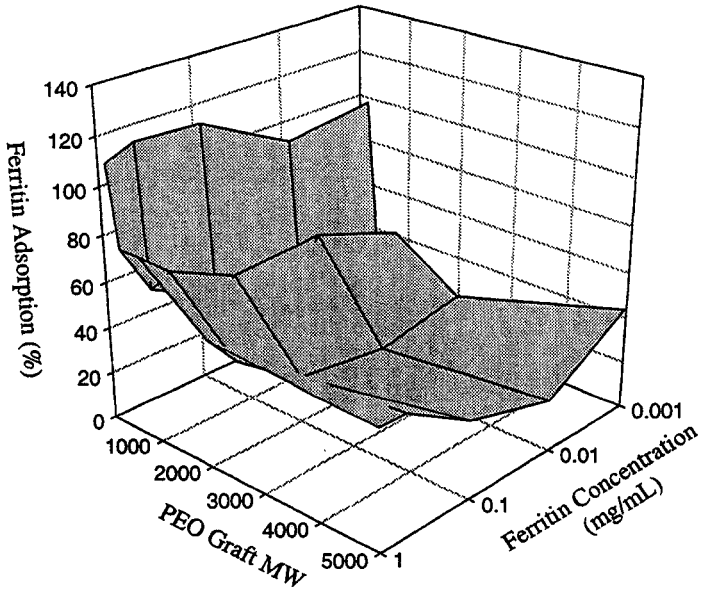

Figure 7.36: Ferritin adsorption response surface showing the effects of PEO graft MW and Ferritin concentration.

Summary

Upon examination of all the adsorption results for the different proteins on the PUU-OPEO surfaces, the following general conclusions can be made. As the length of the PEO grafts increased, the level of adsorption decreased on the PUU-OPEO surfaces. Adsorption was generally the lowest with 2000 MW grafts, although adsorption on surfaces with 5000 MW grafts was similar in most cases.

The PUU-OPEO surfaces with the shortest grafts (165 MW and 350 MW) frequently adsorbed more protein than the PUU control. It therefore appears that the PEO coverage on these surfaces is insufficient to reduce protein adsorption to any extent. The increased adsorption compared to the control PUU surface is likely due to surface patches where the base PUU has reacted with MDI but where PEO grafting has not occurred.

Control experiments with this type of surface showed increased protein adsorption relative to the control PUU (see Figure 7.3 on page 133).

It is possible that there may be an inherent limit to the graft density that can be achieved on the PUU surfaces used in the present work. Polyurethanes exhibit microphase separation whereby discrete domains of hard and soft segments are formed in the solid state. Since the grafting of PEO to the polymer substrate is believed to occur only via urethane and urea groups present in the hard segment, it is expected that ungrafted surface patches corresponding to soft segment domains, which do not contain these groups, will exist. On the other hand, the domains of hydrophilic character (i.e. the PEO grafted regions) should dominate the interface in contact with water if the surfaces are "mobile". Also, a larger effective coverage is expected for surfaces prepared with the longer PEO grafts compared to those prepare with shorter grafts at the same density. The observations above support this hypothesis.

In general the data on the PUU-OPEO surfaces support McPherson's theory that the ability of PEO layers to prevent protein adsorption originates from the effective coverage of the surface by PEO segments, thereby blocking adsorption sites [McPherson, T. et al., 1998]. The most important parameter, according to this theory, is the graft density of the PEO on the surface. Experiments by Prime and Whitesides [Prime, K.L. and Whitesides, G.M., 1993] support this theory. Using self-assembled monolayers (SAMs) on gold coated silicon wafers, protein adsorption could be eliminated (as measured by ellipsometry) by SAMs based on C_{11} alkane thiols having end-attached oligo(ethylene oxide), with chain lengths ranging from one to six EO units. Since very

high PEO densities were obtained using these SAMs, as little as two ethylene oxide repeat units could reduce protein adsorption below the detectable limit. This layer of PEO would therefore block all adsorption sites given the high graft density attainable on SAMs. In the case of these oligo-EO SAMs, protein repulsion is believed to be due to water binding and not steric repulsion.

The surface preparation methods used in this work (with phase separated polyurethanes as substrates) therefore do not appear to be well suited to prepare protein repellent surfaces using relatively short PEO grafts, presumably because the grafting density achieved does not result in adequate PEO coverage of the surface. To obtain significant protein rejecting properties, the PEO grafts needed to have a minimum molecular weight of approximately 750 MW (or 16 ethylene oxide repeat units), according the data. Protein rejection seems to be optimal with a PEO MW of 2000, since the reduction in adsorption levels appeared to be a maximum for this molecular weight.

7.1.1.2 PUU-NPEO surfaces

Since the experiments detailed in Section 5.2.2 showed that surfaces with improved protein repelling properties could be prepared using amino-terminated PEO, a series of protein adsorption experiments were performed to examine the behaviour of these surfaces in more detail.

Myoglobin

Adsorption isotherms for myoglobin (MW 17.5 kDa, IEP 7.2) on the PUU-NPEO surfaces are shown in Figure 7.37 and Figure 7.38. A significant difference is seen in the adsorption levels on the control PUU surface in the two experiments. Also the surface concentrations are substantially higher than the estimated monolayer values of 0.18-0.33 $\mu g/cm^2$. These adsorption levels are also higher than those found on the control PUU during experimentation with the PUU-OPEO surfaces. The reason for these differences is not clear but could be due to batch to batch variation since the control PUU used in the preparation of the PUU-NPEO surfaces was a different batch than that used to prepare the PUU-OPEO surfaces.

The trend in both experiments with respect to adsorption levels is PUU-NPEO550>PUU-NPEO5K>PUU-NPEO2K. The data for the PUU-NPEO5K surface showed greater scatter, probably due to batch-to-batch variation during the grafting reactions.

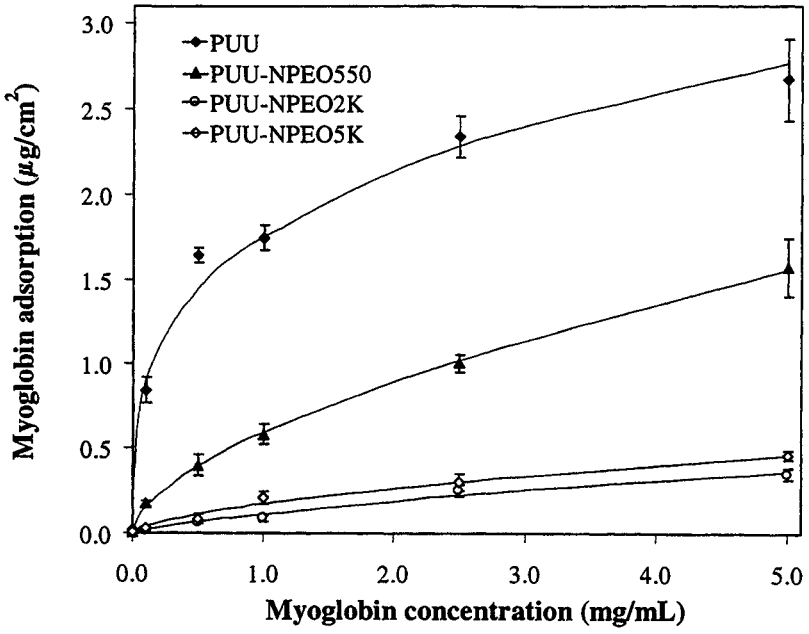

Figure 7.37: Myoglobin adsorption on PUU and PUU-NPEOs (first experiment) from TBS buffer at 22°C for 3h, ±S.D., n=3.

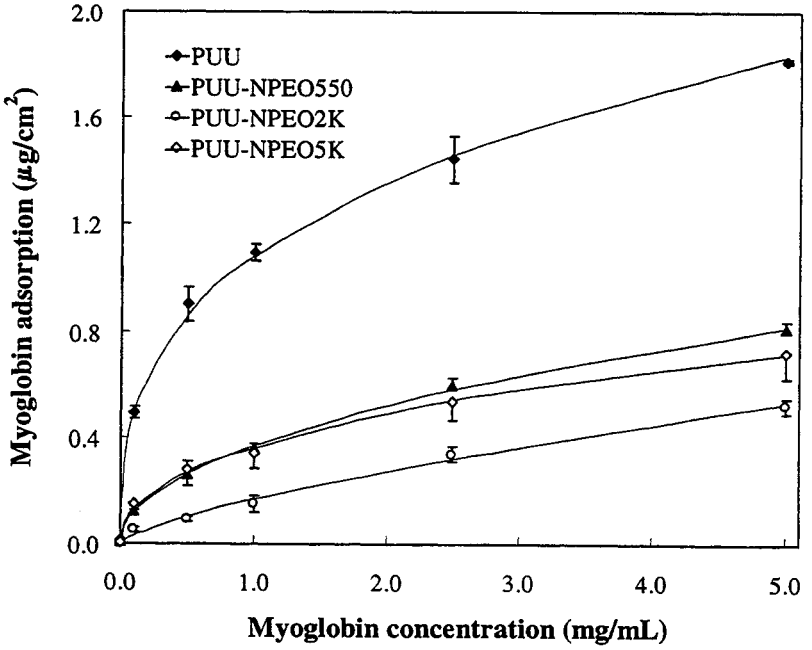

Figure 7.38: Myoglobin adsorption on PUU and PUU-NPEOs (second experiment) from TBS buffer at 22°C for 3h, ±S.D., n=3.

An examination of the initial slopes of the isotherms to estimate the adsorption affinities (Table 7.10) reveals that myoglobin has much lower affinity for all the PEO-grafted surface compared to the control PUU. Furthermore, the affinity reaches a minimum with PEO grafts of 2000 MW. This supports the observations above. As well, when comparing these data to those from experiments with the PUU-OPEO surfaces in Table 7.3 (page 144), the notably lower initial slopes on the PUU-NPEO surfaces suggest a lower affinity of myoglobin for these surfaces. The value for the control PUU is also similar for the two sets of experiments.

Table 7.10: Initial slopes from the myoglobin isotherms.

Surface	Initial Slope (mL/cm^2) (Average ± S.D., n=3)		Average Initial Slope (± 95% C.I.)
	Figure 7.37	Figure 7.38	
PUU	17.9±2.7	13.7±1.0	15.8±3.1
PUU-NPEO550	7.6±1.3	4.8±0.4	6.5±2.3
PUU-NPEO2K	1.2±0.4	1.8±1.0	1.5±0.8
PUU-NPEO5K	4.4±2.7	4.3±0.9	4.3±1.9

The normalised myoglobin adsorption curves from the two experiments are shown in Figure 7.39 and the adsorption response surface in Figure 7.40. Because of the large variability in the PUU-NPEO5K response, this surface is generally not significantly different from PUU-NPEO2K, even though the latter shows lower adsorption levels at all concentrations of myoglobin. PUU-NPEO550, however, generally showed significantly higher levels of adsorption than PUU-NPEO5K. The response surface clearly shows the

protein adsorption minimum on surfaces with the 2000MW PEO grafts. There also appears to be a trend of increasing adsorption with increasing protein concentration after an initial drop at very low concentrations. The maximum reduction in adsorption on the PUU-NPEO2K surface was over 90%, whereas on similar PUU-OPEO surfaces, the reduction was only 40-50% (see Figure 7.11 on page 145). Even PUU-NPEO550 performed better than the best PUU-OPEO surface, supporting previous characterisation data and preliminary protein adsorption results that indicated that amino-PEO reagents lead to surfaces having greater protein repellency. The improved performance of the surfaces prepared using amino-terminated PEOs is presumably due to the higher reactivity between the amino PEOs and surface isocyanate groups, resulting in higher PEO graft densities.

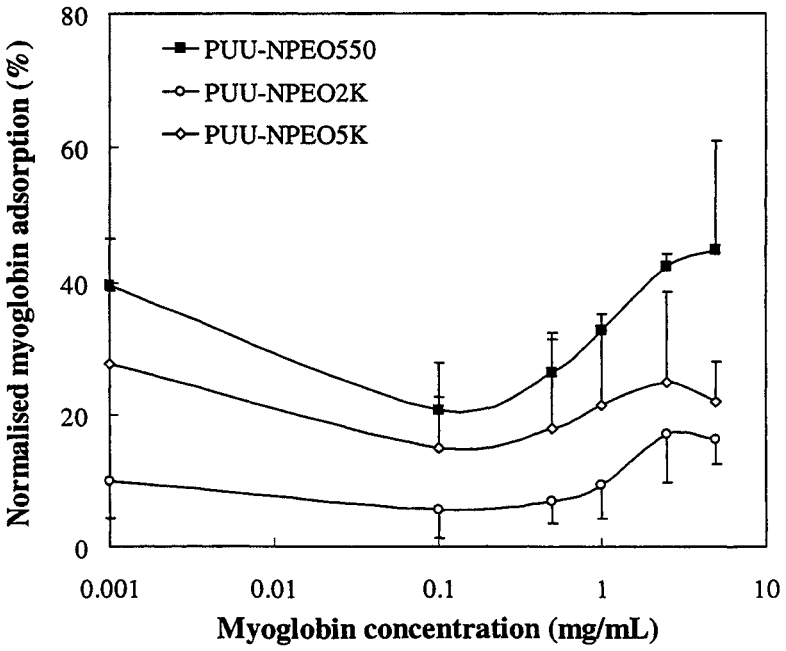

Figure 7.39: Normalised myoglobin adsorption on PUU-NPEO surfaces (±S.D., n=6).

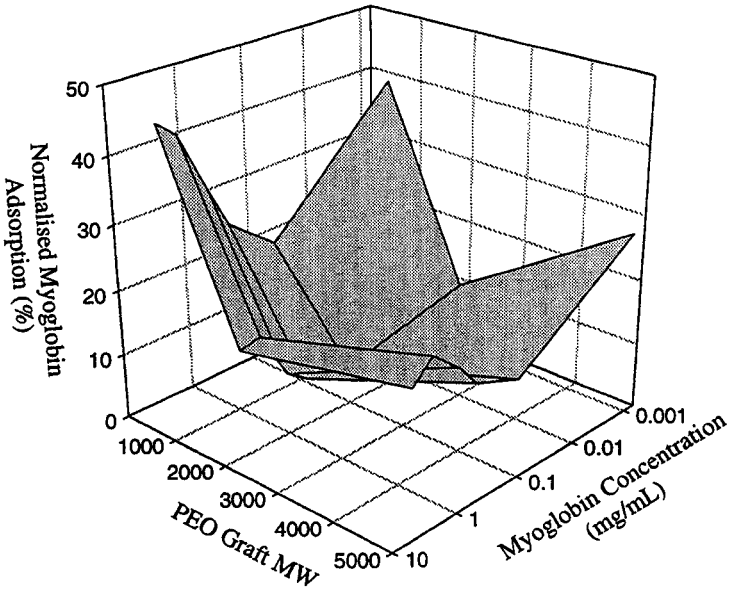

Figure 7.40: Myoglobin adsorption response surface showing the effects of PEO graft MW and myoglobin concentration.

Human Serum Albumin (HSA)

Adsorption isotherms for HSA (MW 66 kDa, IEP 4.7) for two separate experiments using PUU-NPEO surfaces are shown in Figure 7.41 and Figure 7.42. In both experiments, the adsorption levels on the control surface fall within the range of calculated monolayer coverage for albumin (0.18-0.57 $\mu g/cm^2$), although the responses are significantly different in the two experiments. The adsorption levels at a given protein concentration were similar for the controls in the PUU-OPEO and PUU-NPEO experiments (see Figure 7.21 and Figure 7.22 on page 156).

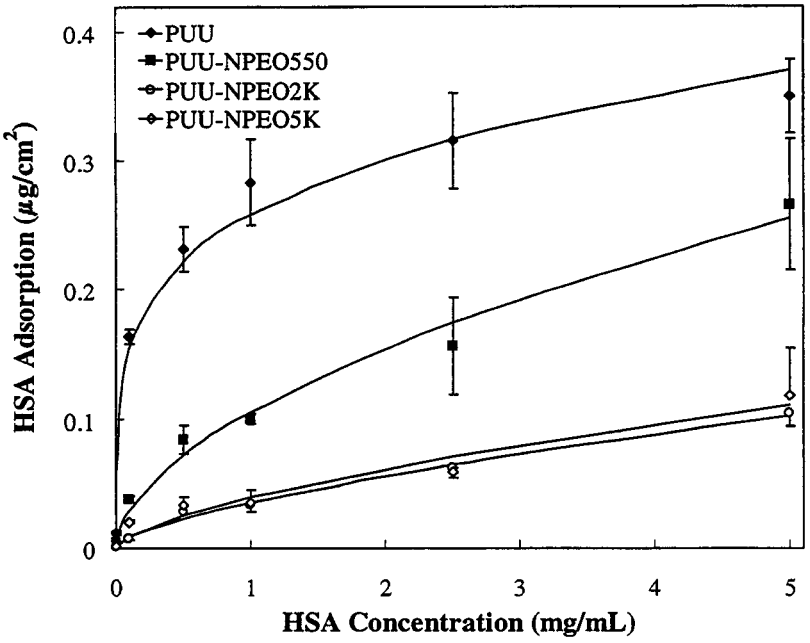

Figure 7.41: HSA adsorption on PUU and PUU-NPEOs (first experiment) from TBS buffer at 22°C for 3h, ±S.D., n=3.

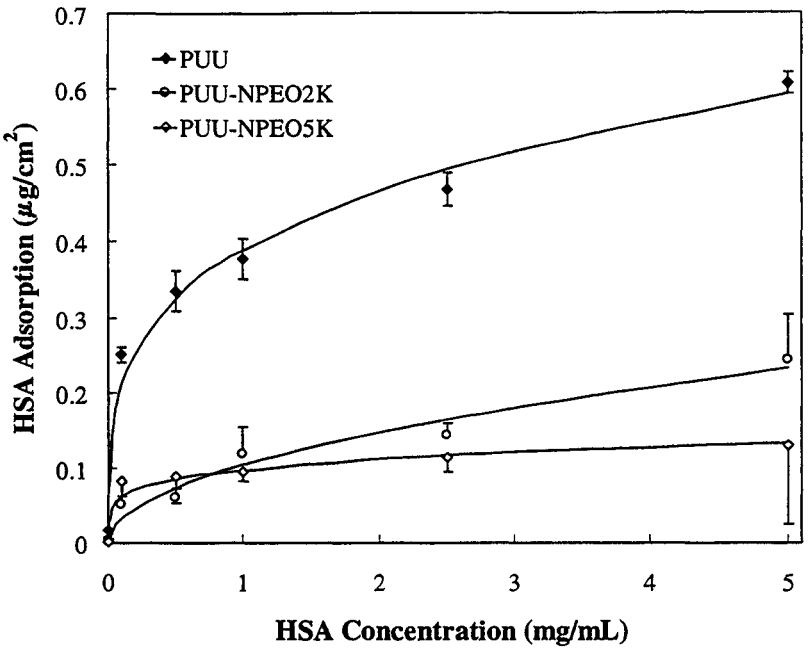

Figure 7.42: HSA adsorption on PUU and PUU-NPEOs (second experiment) from TBS buffer at 22°C for 3h, ±S.D., n=3.

The familiar pattern of increasing protein resistance with increasing molecular weight of PEO grafts is observed in Figure 7.41. The levels of adsorption on PUU-NPEO2K and PUU-NPEO5K are very similar in both experiments.

The initial slopes, listed in Table 7.11, show that the affinity of HSA for the PEO-grafted surfaces is much lower than for the control PUU. As observed previously, the affinities generally decrease with increasing PEO graft MW. The values were also lower than those of the PUU-OPEO surfaces (see Table 7.6 on page 157). The values for the control PUU were slightly different; probably due to surface property differences between batches of the base polyurethane substrate.

Table 7.11: Initial slopes from the HSA isotherms.

Surface	Initial Slope (mL/cm^2) (Average ± S.D., n=3)		Average Initial Slope (± 95% C.I.)
	Figure 7.41	Figure 7.42	
PUU	11.8±2.1	17.4±0.7	14.6±3.5
PUU-NPEO550	4.9±0.9	--	4.9±2.3
PUU-NPEO2K	1.1±0.2	3.6±1.9	2.3±1.9
PUU-NPEO5K	1.5±0.2	2.2±0.6	1.8±0.6

The normalised HSA adsorption curves from the two experiments are plotted in Figure 7.43 and the adsorption response surface in Figure 7.44. The HSA adsorption levels on PUU-NPEO2K and PUU-NPEO5K are not significantly different from each other. However, HSA adsorption on PUU-NPEO550 is generally significantly higher than on the other two PEO-grafted surfaces. The response surface shows the decrease in adsorption levels with increasing length of the PEO grafts. The effect appears to level off at 2000 MW. The PEO-grafted surfaces were less effective at higher protein concentrations, especially the surface with the shortest PEO grafts, PUU-NPEO550. The decrease in HSA adsorption compared to the control PUU reached 75-85% on the PUU-NPEO2K and PUU-NPEO5K surfaces, up to 1 mg/mL protein concentration, compared to about 30-80% on the PUU-OPEO2K in the same protein concentration range (see Figure 7.23 on page 158).

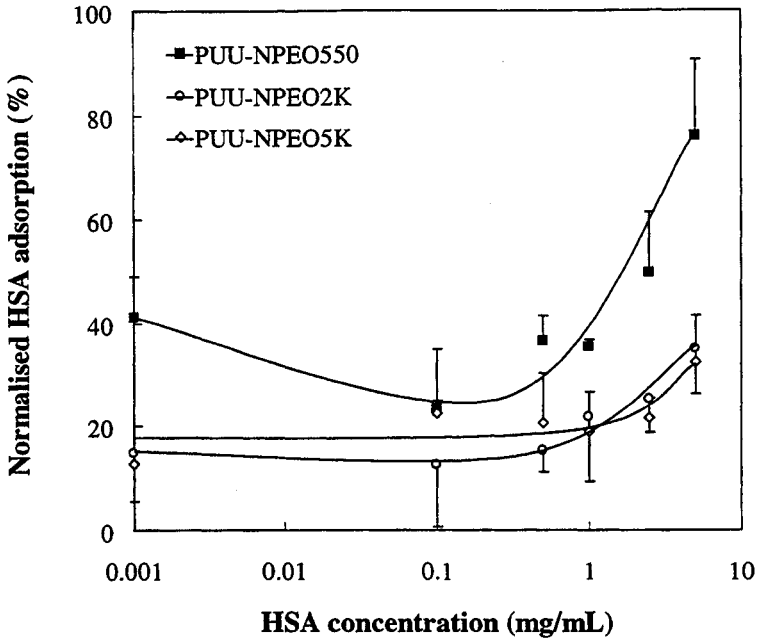

Figure 7.43: Normalised HSA adsorption on PUU-NPEO surfaces (±S.D., n=6 (n=3 for PUU-OPEO550)).

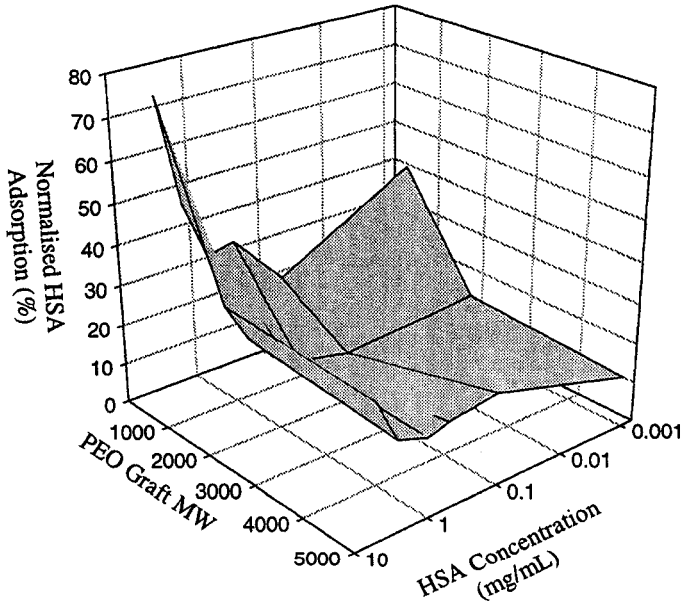

Figure 7.44: HSA adsorption response surface showing the effects of PEO graft MW and HSA concentration.

Concanavalin A

Figure 7.45 and Figure 7.46 show the isotherms for concanavalin A (MW 102 kDa, IEP 5.0) for two separate experiments. The levels of protein adsorption on the control PUU surfaces exceed the calculated monolayer coverage range of 0.26-0.54 $\mu g/cm^2$. Compared to the control PUU isotherms from the PUU-OPEO experiments, the protein levels are generally lower in these experiments, again possibly due to batch-to-batch variations in the base PUU and/or to experiment-to-experiment variability.

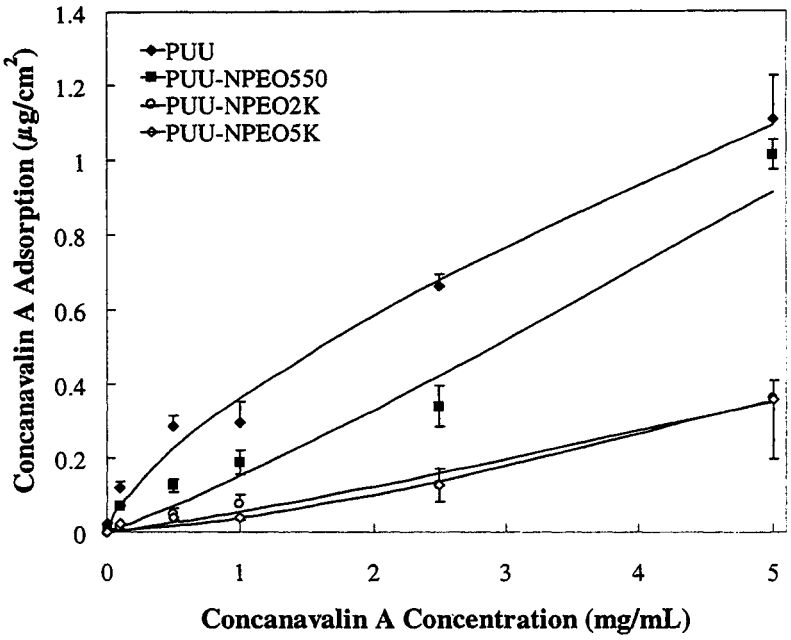

Figure 7.45: Concanavalin A adsorption on PUU and PUU-NPEOs (first experiment) from TBS buffer at 22°C for 3h, ±S.D., n=3.

The adsorption isotherms for the surfaces grafted with 2000 and 5000 MW PEO are in good agreement for both experiments. The data for the PUU-NPEO550 surface are similar at lower concentrations in the two experiments but are quite different from each other at the higher protein concentrations.

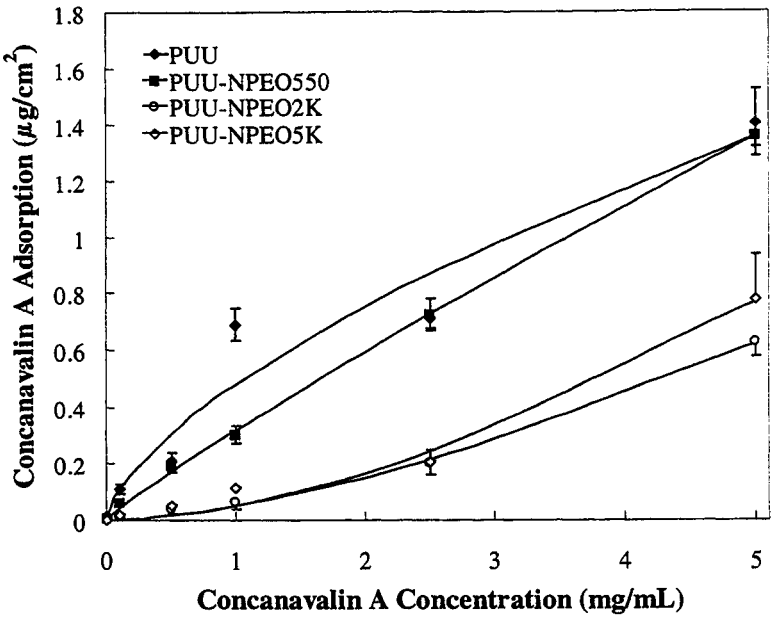

Figure 7.46: Concanavalin A adsorption on PUU and PUU-NPEOs (second experiment) from TBS buffer at 22°C for 3h, ±S.D., n=3.

The affinities of concanavalin A for the PEO-grafted surfaces, given by the initial slopes of the isotherms (Table 7.12), were lower than for the control surface in all cases. The affinity also generally decreased with increasing length of the PEO graft, reaching a minimum with a graft length of 2000 MW. The values for PUU-NPEO2K and PUU-NPEO5K were similar. The initial slopes for the PUU-NPEO surfaces are lower than those for the PUU-OPEO surfaces (see Table 7.7 on page 162). It is important to note that the average initial slope on the control PUU was significantly lower in experiments with PUU-NPEO surfaces, perhaps reflecting batch differences. However, even when taking this difference into account, the affinity of concanavalin A for the PUU-NPEO surfaces is lower than for the PUU-OPEO surfaces.

Table 7.12: Initial slopes from the concanavalin A isotherms.

Surface	Initial Slope (mL/cm^2) (Average ± S.D., n=3)		Average Initial Slope (± 95% C.I.)
	Figure 7.45	Figure 7.46	
PUU	22.5±4.3	11.9±1.0	17.2±6.8
PUU-NPEO550	8.5±2.2	3.6±0.7	6.0±3.2
PUU-NPEO2K	1.1±0.4	0.5±0.1	0.8±0.4
PUU-NPEO5K	1.5±0.2	1.1±0.5	1.3±0.4

The normalised concanavalin A adsorption curves for the two experiments are shown in Figure 7.47 and the adsorption response surface in Figure 7.48. As expected from the adsorption isotherms, there is generally no significant difference between the levels of adsorption on PUU-NPEO2K and PUU-NPEO5K. Only at the lowest concanavalin A concentration was the adsorption level on PUU-NPEO2K significantly lower. The adsorption levels on PUU-NPEO550 were significantly higher than on the other two grafted surfaces at all concanavalin A concentrations. The response surface clearly shows the decrease in protein adsorption with increasing PEO graft molecular weight. The effect appears to level off at 2000MW. Also clear is the increase in protein adsorption as the protein concentration increased. Compared to the unmodified PUU, PUU-NPEO2K and PUU-NPEO5K reduced protein adsorption by about 80-95% at protein concentrations up to 1 mg/mL. In contrast the PUU-OPEO surfaces reduced protein adsorption by about 20-60% in the same concentration range (see Figure 7.27, page 163).

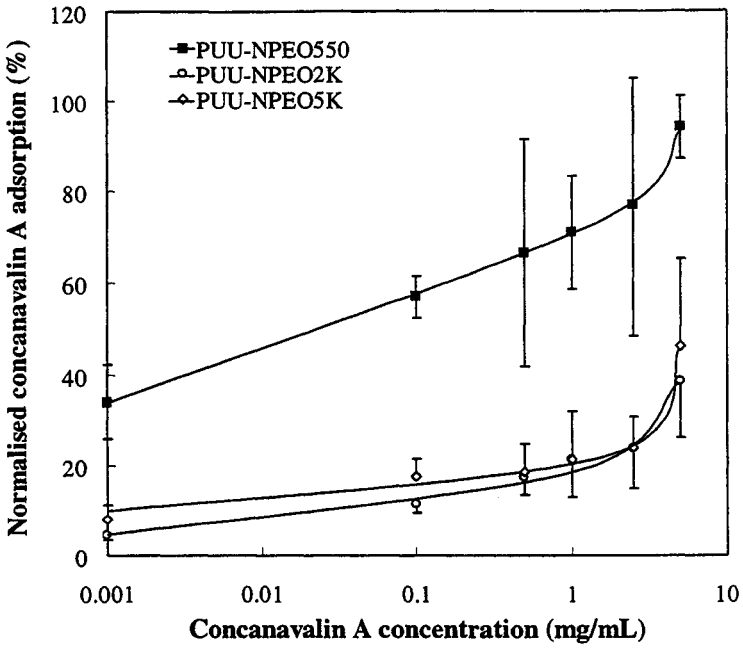

Figure 7.47: Normalised concanavalin A adsorption on PUU-NPEO surfaces (±S.D., n=6).

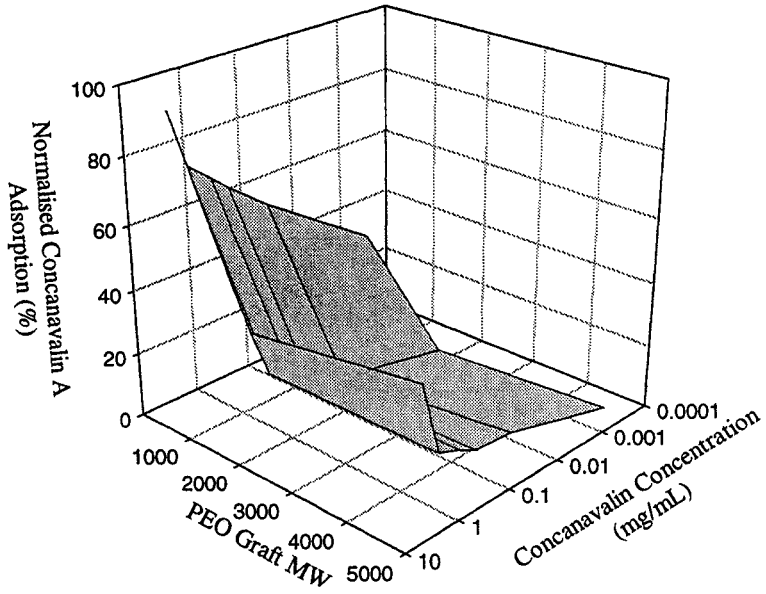

Figure 7.48: Concanavalin A adsorption response surface showing the effects of PEO graft MW and concanavalin A concentration.

Fibrinogen

Fibrinogen (MW 340 kDa, IEP 4.3) adsorption data for the PUU-NPEO surfaces are shown in Figure 7.49 and Figure 7.50. The levels of fibrinogen on all the surfaces appear to reach a plateau at the higher protein concentrations. The plateau levels are different on the control PUU surfaces; in the first experiment, the level is in agreement with the calculated monolayer coverage range (0.14-0.7 $\mu g/cm^2$) whereas in the second experiment, the recorded level exceeds this range.

All three PUU-NPEO surfaces in Figure 7.49 show very large reductions in protein adsorption compared to the PUU control. Adsorption levels on PUU-NPEO550 were much lower than observed for the other proteins examined. Figure 7.50 shows similar behaviour for both PUU-NPEO surfaces.

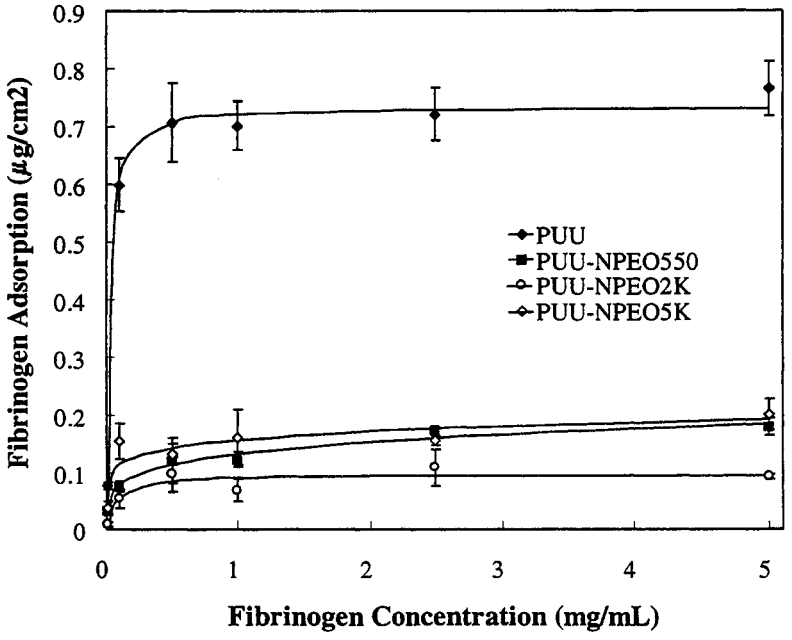

Figure 7.49: Fibrinogen adsorption on PUU and PUU-NPEOs (first experiment) from TBS buffer at 22°C for 3h, ±S.D., n=3.

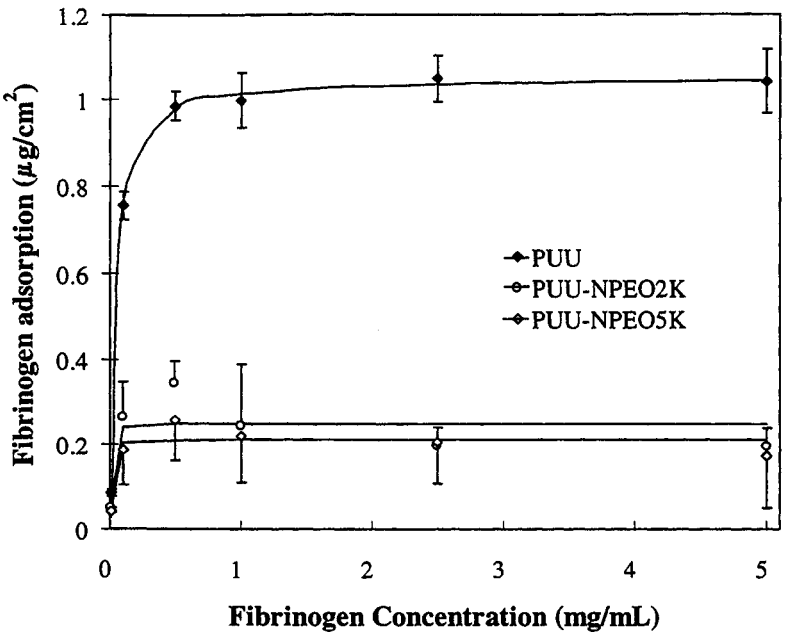

Figure 7.50: Fibrinogen adsorption on PUU and PUU-NPEOs (second experiment) from TBS buffer at 22°C for 3h, ±S.D., n=3.

The affinities of fibrinogen for the PEO-grafted surfaces, given by the initial slopes of the isotherms (Table 7.13), were lower than for the control surface in all cases. The magnitudes of the initial slopes on the control PUU were similar to those observed in the PUU-OPEO experiments (see Table 7.8, page 168). In this instance, the affinities were, on average, similar for all the PEO-grafted surfaces. Only the initial slope of the PUU-NPEO2K isotherm from the first experiment was significantly lower than the other surfaces.

The normalised fibrinogen adsorption curves from the two experiments are plotted in Figure 7.51 and the adsorption response surface in Figure 7.52. It is clear from these figures that none of the PEO-grafted surfaces is significantly different from any of the others. The response surface confirms these observations. Only the adsorption levels on

PUU-NPEO550 are lower than expected; in many of the cases discussed previously, the responses on PUU-NPEO2K and PUU-NPEO5K have been similar. Furthermore, there does not appear to be a strong protein concentration effect on adsorption. There is a relatively high level of adsorption compared to the control at the lowest protein concentration, but at all other concentrations, there is no consistent trend between protein concentration and adsorption level. The greatest reduction for the PUU-OPEO surfaces was approximately 30-70% (see Figure 7.32 on page 169). This compares to about 65-80% reduction for the PUU-NPEO surfaces

Table 7.13: Initial slopes from the fibrinogen isotherms.

Surface	Initial Slope (mL/cm^2) (Average ± S.D., n=3)		Average Initial Slope (± 95% C.I.)
	Figure 7.49	Figure 7.50	
PUU	76.7±6.1	85.7±8.8	81.2±8.8
PUU-NPEO550	31.9±3.9	--	31.9±9.6
PUU-NPEO2K	7.9±4.5	49.3±1.3	28.6±24.0
PUU-NPEO5K	38.1±13.0	41.6±3.0	39.9±9.1

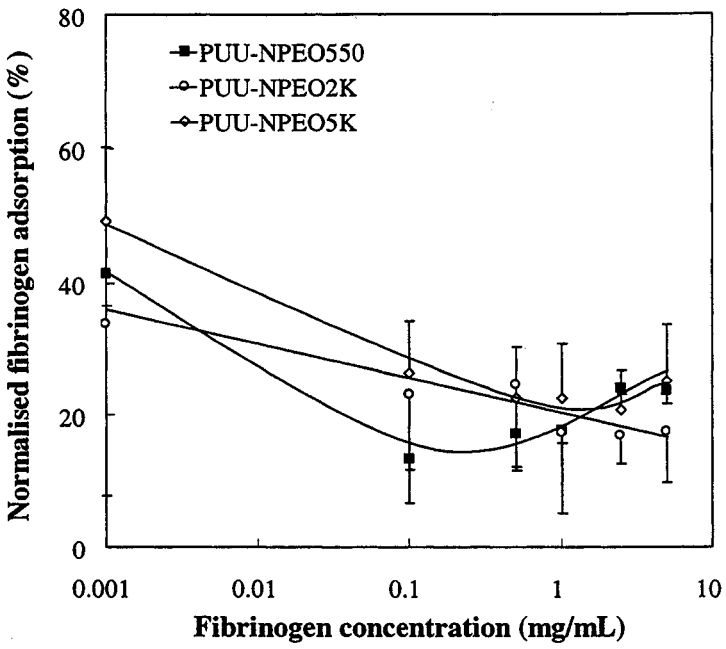

Figure 7.51: Normalised fibrinogen adsorption on PUU-NPEO surfaces (±S.D., n=6 (n=3 for PUU-NPEO550)).

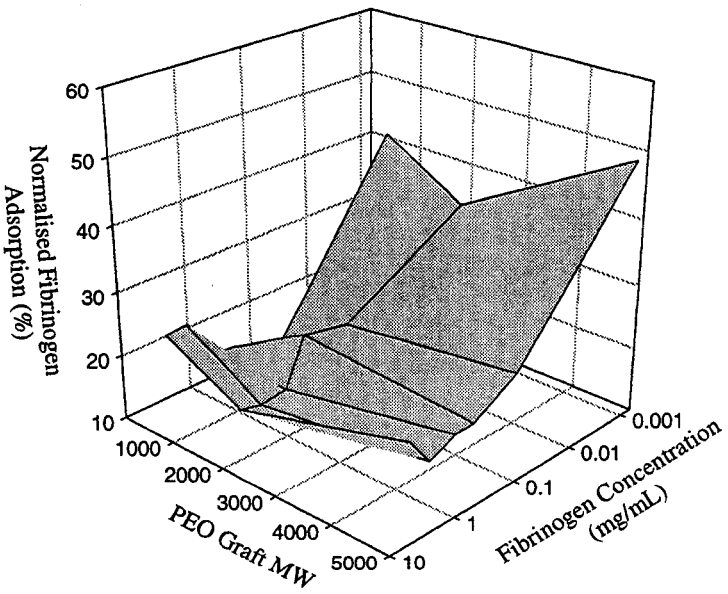

Figure 7.52: Fibrinogen adsorption response surface showing the effects of PEO graft MW and fibrinogen concentration.

Ferritin

Ferritin (MW 440 kDa, IEP 4.3) adsorption isotherms from three separate experiments are shown in Figure 7.53 to Figure 7.55. The levels of ferritin adsorbed to both the control PUU and PEO-grafted surfaces exceed the calculated monolayer coverage estimate of 0.54 mg/cm^2. The adsorption on the control surface is also significantly higher than the adsorption on the control surfaces in the PUU-OPEO experiments at comparable protein solution concentrations. Again, batch-to-batch variation and experiment-to-experiment variations are the likely reasons.

PUU-NPEO550 shows considerable variability from experiment to experiment, again probably due to different surface properties as a result of batch-to-batch variations in the grafting reaction. In the first experiment, PUU-NPEO2K and PUU-NPEO5K showed nearly identical adsorption levels. However in the other two experiments, PUU-NPEO2K adsorbed less ferritin than PUUNPEO5K.

The affinities of ferritin for the PEO-grafted surfaces, given by the initial slopes of the isotherms (Table 7.14), were lower than for the control surface in all cases. The magnitudes of the initial slopes in the first and third experiments were similar to the values obtained on the control PUU for the PUU-OPEO experiments (see Table 7.9, page 172). The value for the second experiment was much lower; however the variability associated with experiments using ferritin appears to be much higher than for the other proteins examined. The affinity also generally decreased with increasing length of the PEO graft, reaching a minimum at a graft length of 2000 MW. The values for PUU-NPEO2K and PUU-NPEO5K were similar in all three experiments.

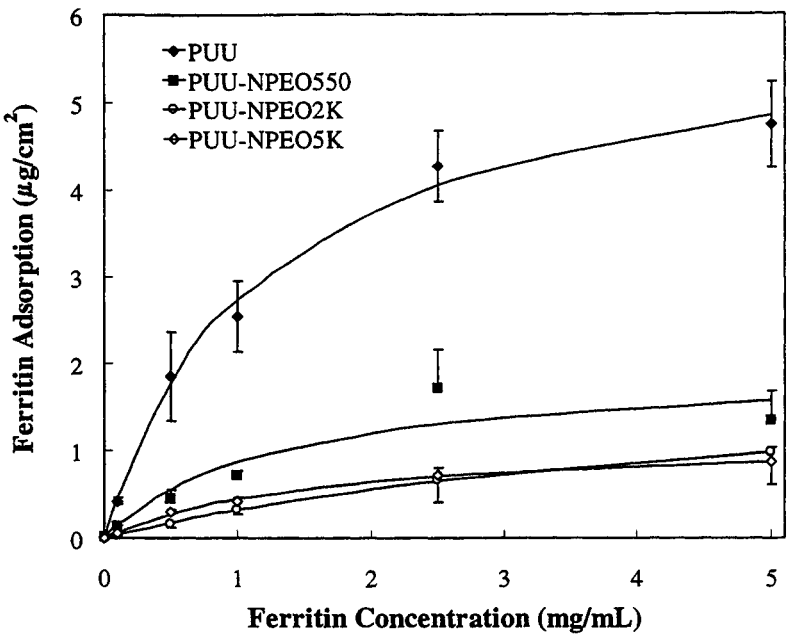

Figure 7.53: Ferritin adsorption on PUU and PUU-NPEOs (first experiment) from TBS buffer at 22°C for 3h, ±S.D., n=3.

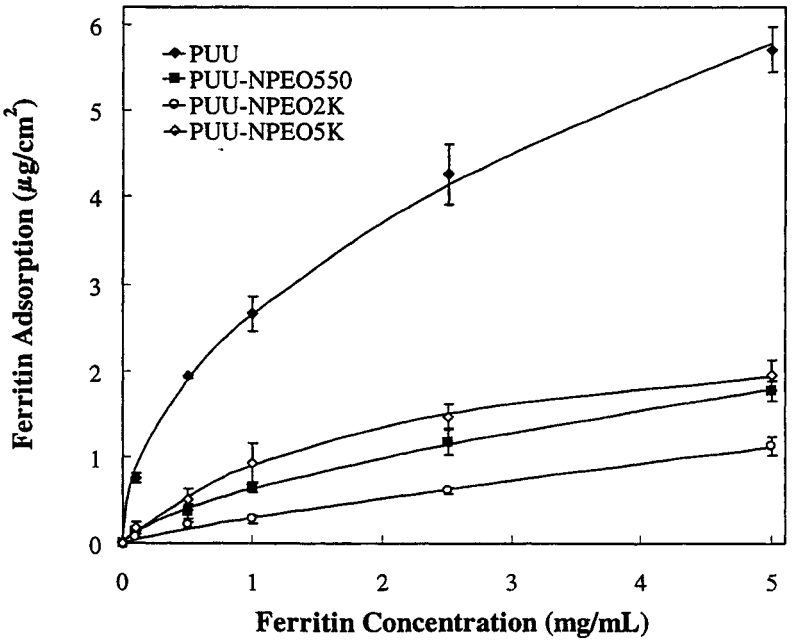

Figure 7.54: Ferritin adsorption on PUU and PUU-NPEOs (second experiment) from TBS buffer at 22°C for 3h, ±S.D., n=3.

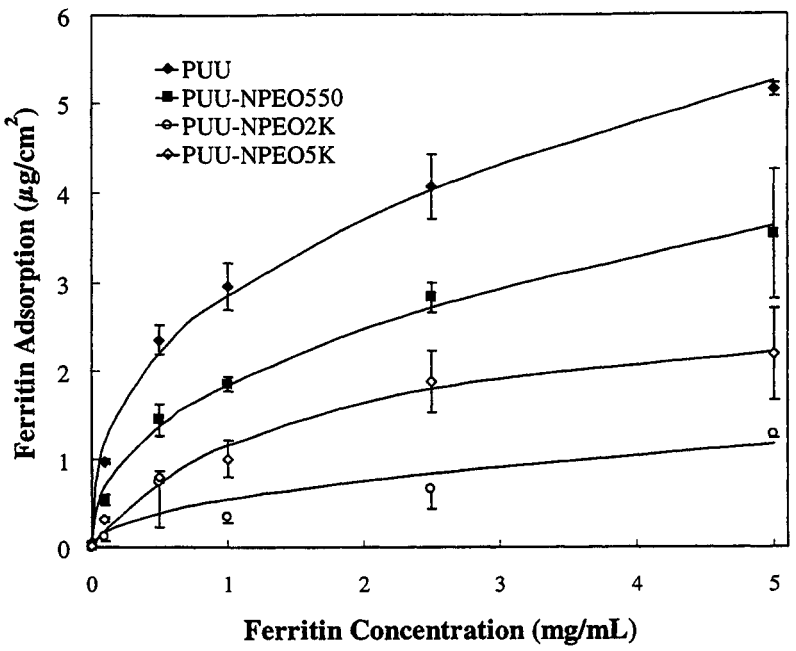

Figure 7.55: Ferritin adsorption on PUU and PUU-NPEOs (third experiment) from TBS buffer at 22°C for 3h, ±S.D., n=3.

Table 7.14: Initial slopes from the ferritin isotherms.

Surface	Initial Slope (mL/cm^2) (Average ± S.D., n=3)			Average Initial Slope (± 95% C.I.)
	Figure 7.53	Figure 7.54	Figure 7.55	
PUU	19.7±6.4	8.3±0.9	46.7±13.5	24.9±14.3
PUU-NPEO550	7.4±2.9	2.3±1.3	14.9±5.4	8.2±4.9
PUU-NPEO2K	2.5±0.8	0.9±1.6	4.2±4.4	2.6±2.5
PUU-NPEO5K	1.6±0.5	1.9±0.5	6.8±2.5	3.4±2.2

The normalised ferritin adsorption curves for the three experiments are shown in Figure 7.56 and the adsorption response surface in Figure 7.57. PUU-NPEO2K shows significantly lower adsorption than PUU-NPEO5K at most ferritin concentrations. The latter was generally lower, though not significantly so (high data scatter), than PUU-

NPEO550. The response surface shows the decrease in adsorption with increasing molecular weight, with an optimum for 2000 MW grafts. There also appears to be a slight trend of increasing adsorption levels with increasing protein concentration. PUU-NPEO2K reduced adsorption by 80-90% of the control levels. The largest reduction in ferritin adsorption for the PUU-OPEO surfaces was about 50-85% (see Figure 7.35, page 173).

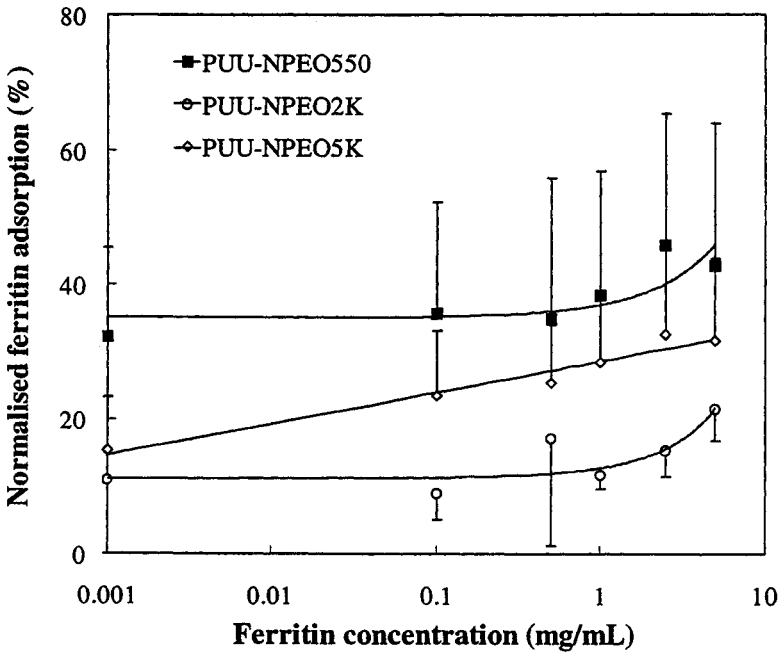

Figure 7.56: Normalised ferritin adsorption on PUU-NPEO surfaces (±S.D., n=9).

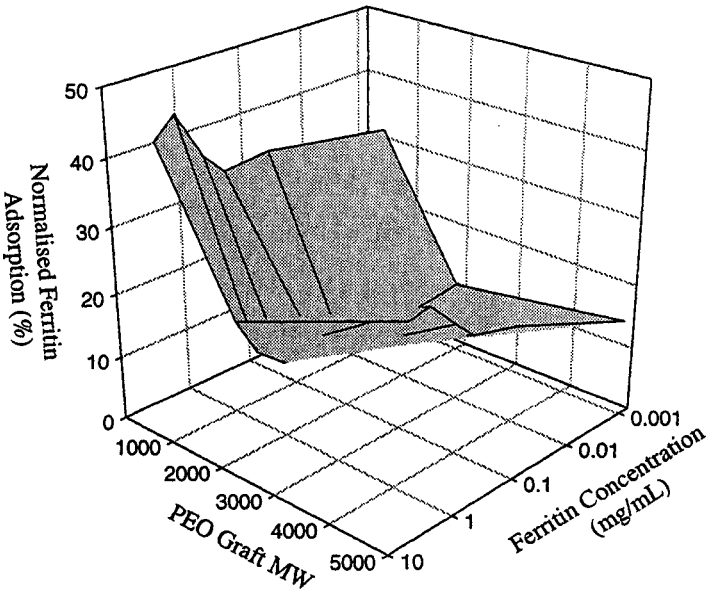

Figure 7.57: Ferritin adsorption response surface showing the effects of PEO graft MW and ferritin concentration.

Summary

As observed for the PUU-OPEO surfaces, protein adsorption on the PUU-NPEO surfaces decreased with increasing PEO graft MW. In all cases, the adsorption was the lowest on surfaces with 2000 MW grafts, although in many cases, surfaces with 5000 MW grafts showed similar responses.

The protein adsorption levels on all of the PUU-NPEO surfaces were consistently below those of the control surfaces. This is in contrast to the PUU-OPEO surfaces with short PEO grafts where adsorption was generally greater than on the controls. Furthermore, protein adsorption was lower on the PUU-NPEO surfaces compared to the corresponding PUU-OPEO surfaces. These observations provide strong evidence that higher PEO graft density was obtained on the PUU-NPEO surfaces compared to the

PUU-OPEO surfaces. The higher graft density would result in increased PEO surface coverage, thereby giving improved protein repelling properties.

Overall the data again show that the optimum graft length for this system is near 2000 MW. Increasing the graft length to 5000 MW either gave surfaces with similar or decreased protein repelling properties. This implies that at some value between these two molecular weights, the size of the polymer chain begins to interfere with the obtainable graft density. Increasing the PEO MW past this point might therefore lower the repelling property of the surface due to lower graft density.

7.1.2 Effect of Protein Size

The data presented in Sections 7.1.1.1 and 7.1.1.2 can also be used to investigate whether the size of the studied proteins has an influence on the ability of PEO-grafted surfaces to repel the proteins. The data must be interpreted cautiously, however. In the previous sections, the data contained in graphs or tables all originated from the same experiment using a specific protein. To examine the effect of protein size, data from different experiments must be used. This can be done by examining the effects of protein size and PEO MW at a given protein concentration. To estimate the size of the proteins, the approximate volume occupied by the proteins, based on their molecular dimensions was used. Table 7.15 lists these values. The volumes are estimated by simple multiplication of the three dimensions.

Table 7.15: Approximate volumes of proteins.

Protein	Molecular weight (kDa)	Dimensions (Å)	Volume (nm^3)
α-lactalbumin	14.2	37×32×25	29.6
Concanavalin A	102	84×80×39	262
HSA	66	140×44×44	271
Ferritin	440	125×125×125*	1953
Fibrinogen	340	450×90×90	3645

* represented as a cube rather than a sphere to better conform to how the volumes of the other proteins were calculated.
NB References for dimensions cited in text.

As can be seen, the sizes of the proteins are not in proportion to the molecular weights. It is important to note also that these dimensions represent the crystalline structure of the proteins; the dimensions in an aqueous medium may be different.

The response surfaces at the various protein concentrations were similar. For the PUU-OPEO surfaces, the response surface at the intermediate concentration of 0.1 mg/mL, shown in Figure 7.58, is a representative example. The response surfaces for the other concentrations are shown in Appendix B, on page 239. Some of the features of the response surface are seen more clearly in Figure 7.59. One feature that stands out is the difference between Concanavalin A and HSA. Although these two proteins are rather different in molecular weight, according to their crystalline dimensions they are similar in size (see Table 7.15). The difference in response for these proteins, highlighted in the blue dashed box in Figure 7.59, suggests that there may be factors other than size that influence adsorption. This is not surprising given the complexity of protein structure.

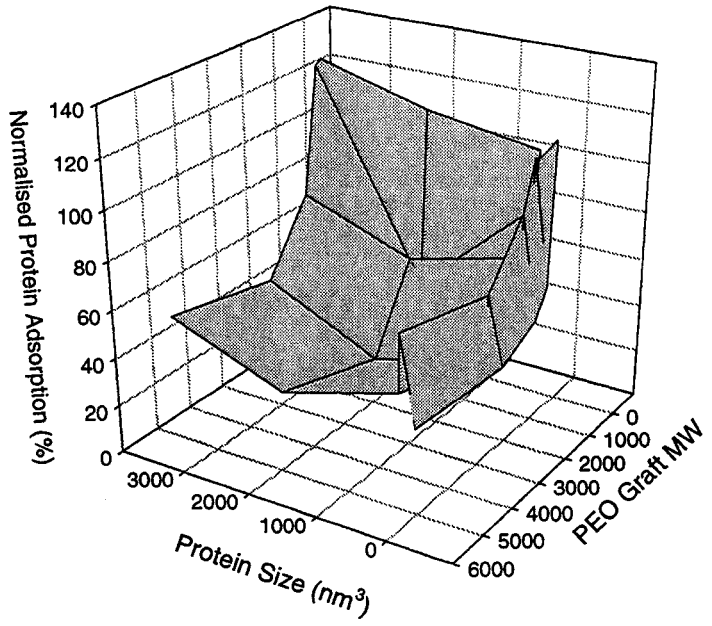

Figure 7.58: Protein adsorption response surface showing the effects of protein size and PEO graft MW on adsorption to PUU-OPEO surfaces at 0.1 mg/mL protein concentration.

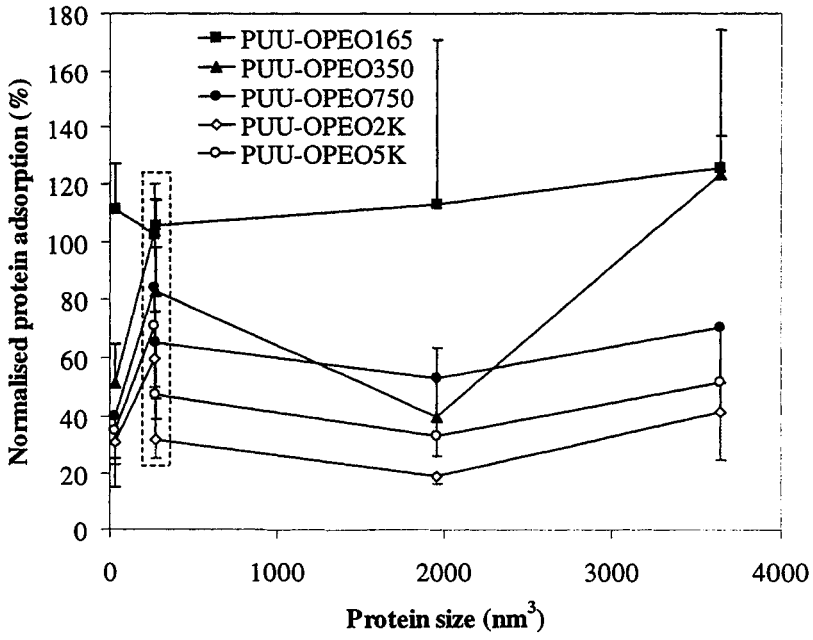

Figure 7.59: Protein adsorption as a function of protein size on the PUU-OPEO surfaces at 0.1 mg/mL protein concentration (±S.D., n=6 or 9).

Examining the response surface in Figure 7.58 as a whole, there does not appear to be a clear trend with respect to the protein size. The response surfaces at other protein concentrations support this observation (see Appendix B on page 239).

These results do not support Halperin's theoretical model that predicts different responses for small and large proteins. The model predicts two modes of adsorption: primary adsorption, close to the surface and secondary adsorption, at the periphery of the grafted PEO chains. Small proteins are expected to penetrate the PEO layer between the grafted chains whereas larger proteins would adsorb at the edge of the PEO layer through attractive van der Waals interactions between the protein and the surface. The model also predicts that regardless of the size of the protein, increases in PEO-graft density and/or layer thickness could eventually suppress adsorption.

However this model is based on the premise that the grafted PEO layer is in the brush regime; that is, that the distance between grafting points is less than R_F, causing the chains to extend from the surface. Therefore, one of the reasons that the predicted behaviour is not observed could be that the "brush" conformation is not present on the experimental surfaces.

The microphase structure of polyurethanes may give a surface distribution of PEO that precludes the formation of a brush structure. Polyurethanes generally have microdomains that are either rich in "hard" or "soft" segments, or an amorphous mixture of both. The chemical grafting of the PEO chains to the polyurethane presumably takes place in the semicrystalline, "hard" segment rich microdomains where the urethane and urea chemical groups are located. Microdomains rich in "soft" segment may therefore not

obtain a sufficient density of grafts to meet the criteria required for the theoretical predictions. It is also possible that the overall level of grafts is insufficient to satisfy the model criteria.

The analysis was repeated using the data for the PUU-NPEO surfaces which appear to have a higher graft density than the PUU-OPEO surfaces based on surface characterisation and protein adsorption data.

Again the response surfaces at the various protein concentrations were similar. The response surface at the intermediate protein concentration of 1.0 mg/mL for the PUU-NPEO surfaces was representative of the other concentrations and is shown in Figure 7.60. The response surfaces for the other concentrations can be found in Appendix B on page 239.

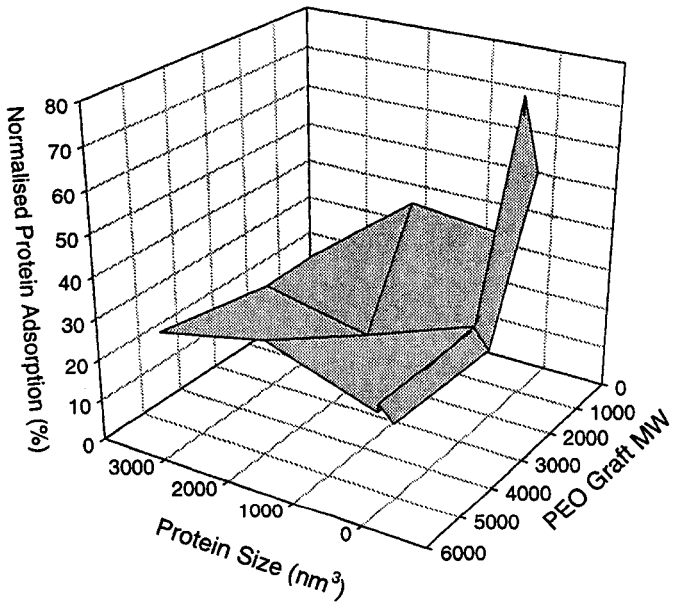

Figure 7.60: Protein adsorption response surface showing the effects of protein size and PEO graft MW on adsorption to PUU-NPEO surfaces at 1.0 mg/mL protein concentration.

On surfaces with the higher MW PEO grafts (2000 and 5000 MW), the response surface is fairly flat; i.e. the size of the protein does not have an impact on the ability of the PEO-grafted surfaces to prevent protein adsorption. However, surfaces with the 550 MW grafts seemed to be able to repel larger proteins more effectively. These general trends were observed at all concentrations except the most dilute, 0.001 mg/mL, where no consistent trends were observed.

It therefore appears that the PEO layer on PUU-NPEO550 is "porous" enough to allow smaller proteins access to the underlying substrate, but is able to repel larger proteins.

7.1.3 Effect of Protein Isoelectric Point

In addition to size, proteins have many other physical properties that distinguish one from another. One of these properties is the isoelectric point (IEP, or pI), defined as the pH at which the overall net charge on the protein is zero. It is important to note that this is a global property of the protein; individual positively and negatively charged domains are present even if the charge on the protein is neutral overall.

This property is of interest given that PEO has the ability to complex positive cations thereby becoming in essence, a polyelectrolyte [Zhivkova, I.V. et al., 1998]. If this behaviour of PEO does not occur in the present experimental system, then the overall charge of the protein should have no effect on the protein adsorption. However, in the event that PEO does indeed behave as a positive polyelectrolyte, the proteins with an IEP above the experimental solution pH 7.4, i.e. those which are positively charged at pH 7.4,

would be repelled by the PEO-grafted surfaces. In addition, negatively charged proteins may adsorb in higher quantity.

Another property of PEO-grafted surfaces, as shown by electrokinetic studies, is the ability to mask surface charges [Emoto, K. et al., 1997]. Although the experimental system used in the present work does not have a convective component this masking property of PEO may still be in evidence and may have an impact on adsorption behaviour. The underlying polyurethane substrate does not have any formal surface charge. However, the surface will acquire charge as proteins adsorb. In this instance, proteins with IEPs far from the solution pH will have larger overall charges than proteins with IEPs near the solution pH. As a result, the charge build-up on the surface will be greater for proteins with IEPs at the extremes. If the PEO grafts are able to mask some of the surface charge, there may be less difference in adsorption levels between proteins with high net charge and those with low net charge than would be expected were the surface charge not masked by the PEO layer. Without the masking effect, charged proteins may be repelled by the like-charged surface which results from the adsorption of a protein layer. This would result in lower adsorption levels for proteins with IEPs far from the solution pH since greater repulsion would be expected with more highly charged proteins. The molecular weights of the PEO grafts will also determine the thickness of the PEO layer and its ability to mask the underlying surface.

For these reasons, investigation of the influence of IEP on protein interactions with PEO-grafted surfaces is of interest and could shed additional light on the mechanism of protein repulsion by PEO. The data presented in Section 7.1.1.1 are used to examine

the effect of IEP on adsorption to these surfaces. Again, for this analysis, data from different experiments were combined to observed the effect of IEP and PEO-graft MW on normalised protein adsorption at different concentrations. Although included in the analysis, the data for RNAse adsorption should be viewed with caution due to the extreme values obtained (and the very large associated error) compared to all other adsorption experiments in this work.

Table 7.16 lists the properties of the proteins used. It is important to note that the sizes of the four proteins are similar. This was done purposely to remove the effect of protein size in this series of experiments.

Table 7.16: Properties of proteins used in IEP investigations.

Protein	Molecular weight (kDa)	Dimensions (Å)	Volume (nm^3)	Isoelectric Point
α-lactalbumin	14.2	37×32×25	29.6	4.3
Myoglobin	17.5	45×35×25	39.4	7.2
RNAse	13.6	38×38×22	31.8	9.4
Lysozyme	14.6	46×30×20	27.6	11.1

Figure 7.61 shows the effect of IEP and PEO graft MW on adsorption at 0.01 mg/mL protein concentration and generally represents the behaviour at other concentrations as shown in Appendix B, page 239. Also included in Appendix B are line plots showing the error associated with the measurements.

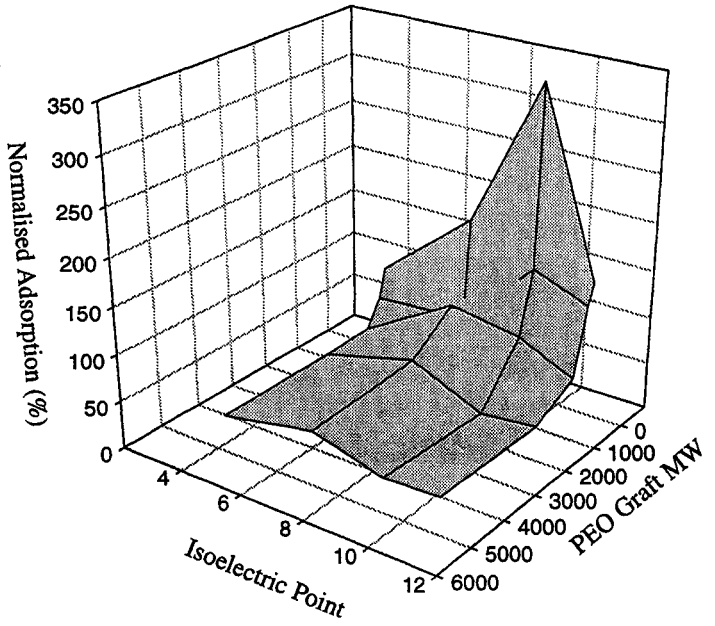

Figure 7.61: Protein adsorption response surface showing the effects of protein isoelectric point and PEO graft MW on PUU-OPEO surfaces at 0.01 mg/mL protein concentration.

Generally, the differences in adsorption levels for the various proteins on PEO-grafted surfaces with the longer PEO grafts (750, 2000 and 5000 MW) were small and the profiles generally flat indicating little or no effect of the protein IEP. However, for the surfaces with short PEO grafts, the differences were relatively large, although the proteins with the extreme IEPs, α-lactalbumin (4.3) and lysozyme (11.1) were generally adsorbed less than those of intermediate IEP, myoglobin (7.2) and RNAse (9.4). Myoglobin was expected to show the highest adsorption (if there were differences) because of its lower net charge at pH 7.4. However, RNAse frequently showed the highest level of adsorption and often by a very large margin. Furthermore, the error associated with the RNAse measurements was also large. The difference in adsorption levels between RNAse and the

other proteins, as well as the large associated error, make these data suspect. There is no obvious reason why RNAse would adsorb in such large quantities to PUU-OPEO165 and PUU-OPEO350.

Adsorption to the surfaces with short PEO grafts may be explained if it is assumed that the thickness of the PEO layer on these surfaces is insufficient to "mask" the surface charges (presumably associated with adsorbed protein). This would explain the lower adsorption levels for proteins with significant charge under the adsorption conditions (α-lactalbumin, lysozyme). As the protein layer forms, the surface acquires charge. The insufficiently thick PEO layer is unable to mask this charge effectively and therefore proteins would be repelled.

On the other hand, the relatively flat profiles on surfaces with longer PEO grafts supports the hypothesis that longer grafts form thicker PEO layers, better able to "mask" the surface charge on the underlying substrate, thereby lessening the effect of the charge on the protein.

The data also indicate that PEO does not behave as a positively charged polyelectrolyte in these experiments. On the surfaces with the highest density of PEO segments (2000, 5000 MW grafts), the adsorption profiles are relatively flat with respect to IEP; i.e. there is no dependence of adsorption on the IEP. If PEO behaved as a positive polyelectrolyte, a decrease in adsorption of positively charged proteins relative to neutral or negatively charged proteins would be expected due to electrostatic repulsion.

7.1.4 Effect of Temperature

Temperature is another variable that may be able to provide insight into the mechanism of protein repulsion by PEO-grafted surfaces. The currently most widely accepted mechanism for repulsion of proteins where the PEO is of relatively long chain length and the graft density is relatively low is the steric repulsion mechanism. This mechanism relies partly on the notion of the rapid motion of flexible PEO chains, and thus it follows that temperature, which will influence the motions of the PEO grafts, should have an impact on protein repulsion. The aqueous solution behaviour of PEO as a function of temperature must also be considered. It is known that the solubility decreases as temperature increases in a certain temperature range (including the range studied here) [Saeki, S. et al., 1976]. The effect is due to the loss of bound water at higher temperature, causing the chains to interact with each other more strongly. This reduced solubility results in more compact PEO chains that may not provide as much "coverage" due to a larger degree of exposed underlying substrate and possibly reduced chain compressibility. Under these conditions the protein repulsion effect would be expected to diminish.

The effects of temperature were investigated by performing protein adsorption experiments at three temperatures: 4, 20 and 37°C. The limited range examined is due to constraints on the system. Using temperatures lower than 4°C would risk localised ice formation that could cause protein denaturation and/or precipitation. An upper limit on temperature is imposed by the potential for protein denaturation at elevated temperatures.

Figure 7.62 shows the adsorption isotherms for myoglobin to the control polyurethane surface at three different temperatures. Although generally not significantly

different from each other, especially at the lower concentrations, the overall impression is that adsorption increases as temperature increases suggesting that myoglobin adsorption is an endothermic process.

If temperature has little influence on the effectiveness of the PEO grafts in repelling proteins, we expect little or no change in the *normalised* adsorption (i.e. relative to the control polyurethane) as a function of temperature, although the absolute levels of adsorption may change according to basic thermodynamic considerations (i.e. depending on whether the adsorption process is endothermic or exothermic). In other words, the *relative* decrease in protein adsorption due to the PEO grafts should be the same at different temperatures if temperature has no influence on repulsion.

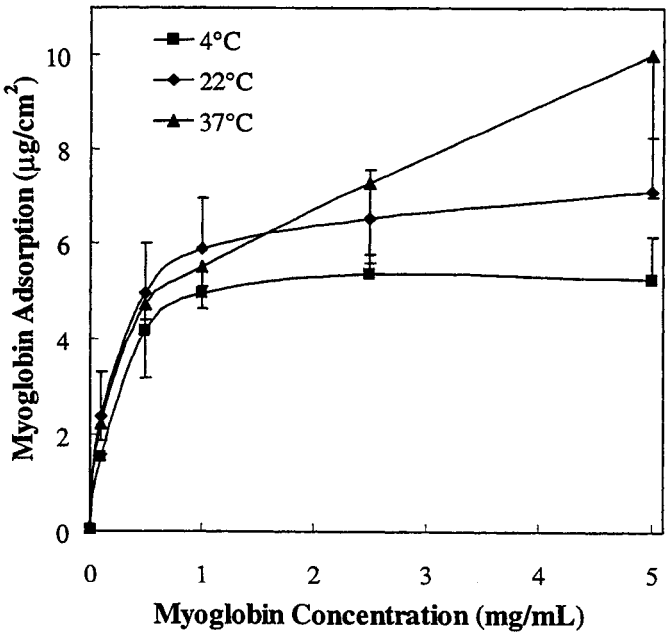

Figure 7.62: Myoglobin adsorption on the PUU control surface at 4, 22 and 37°C, from TBS buffer for 3h, ±S.D., n≥3.

Figure 7.63 shows the normalised adsorption isotherms for PUU-NPEO550 at the three selected temperatures. There is no clear dependence of adsorption on temperature. The very high level of adsorption at the lowest concentration is likely due to the error associated with low radioactivity counts near background levels. For PUU-NPEO2K (Figure 7.64) and PUU-NPEO5K (Figure 7.65), on the other hand, there does appear to be a temperature effect, with adsorption decreasing as temperature increases.

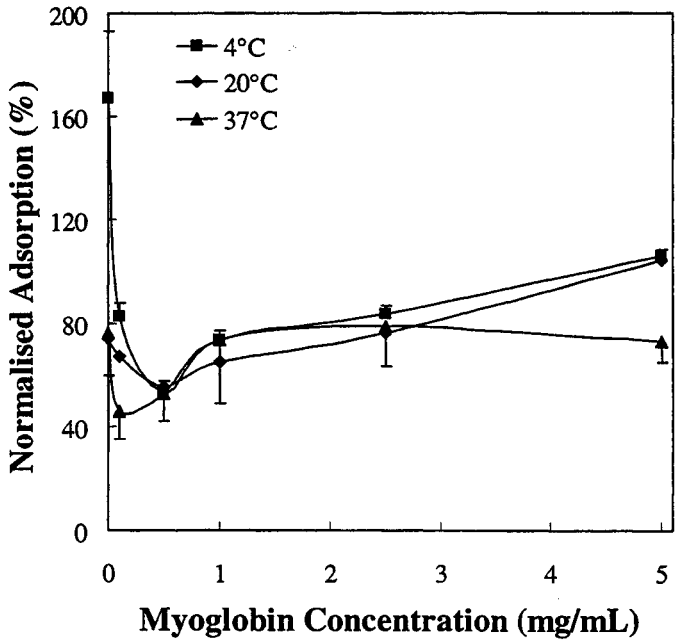

Figure 7.63: Normalised adsorption of myoglobin on PUU-NPEO550 at 4, 20 and 37°C, (TBS buffer, pH 7.4, 3 h).

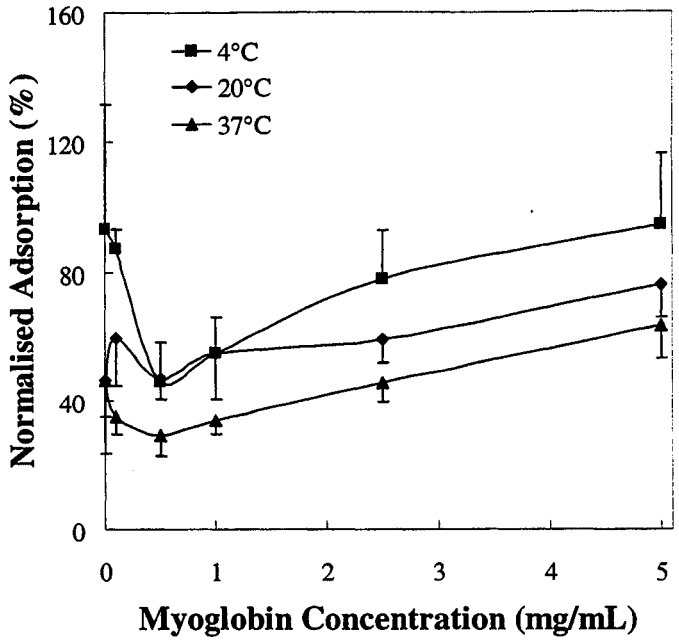

Figure 7.64: Normalised adsorption of myoglobin on PUU-NPEO2K at 4, 20 and 37°C (TBS buffer, pH 7.4, 3 h).

It does not seem likely that these temperature effects could be due to reduced coverage caused by chain compaction. Other effects may be in play. Simple thermodynamic considerations may be enlightening. Adsorption to the control PUU (which can be assumed to be responsible for any adsorption seen on the PEO surfaces as well) appears to be endothermic ($\Delta H > 0$). This means that the driving force for adsorption is entropic. Entropy is gained by dehydration of the surface and the protein due to adsorption. Conformational change may also contribute. When PEO grafts are present, compression of the PEO chains as the protein approaches the surface represents a loss of entropy. Since the data for myoglobin on the grafted surfaces show decreasing adsorption with increasing temperature, the chain compression effects appear to be more important at

higher temperature, and are sufficient to reverse the temperature dependence of adsorption to the PUU.

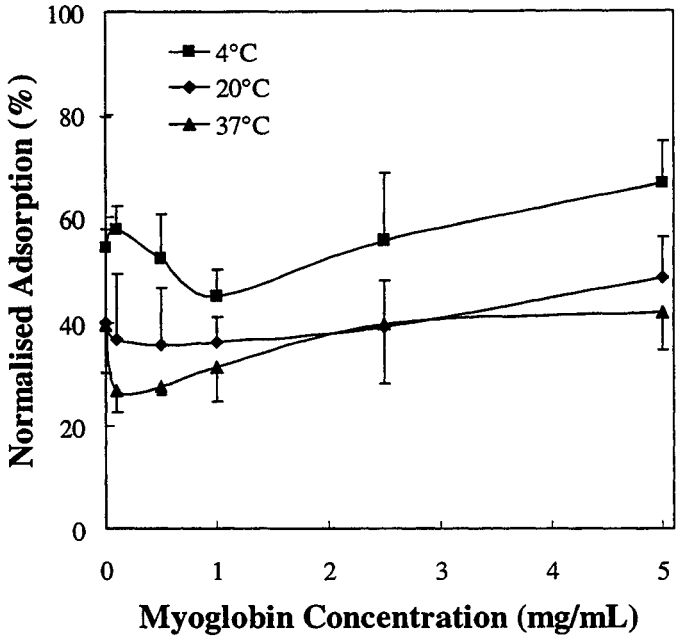

Figure 7.65: Normalised adsorption of myoglobin on PUU-NPEO5K at 4, 20 and 37°C (in TBS buffer pH 7.4 for 3 h).

Figure 7.66 shows the adsorption isotherms for ferritin on the control PUU at the three selected temperatures. Adsorption appears to be independent of temperature over the range examined, suggesting that for this protein the process is effectively thermoneutral. This is in contrast to myoglobin which showed increasing adsorption with increasing temperature.

Figure 7.67 shows the normalised ferritin adsorption isotherms for PUU-NPEO550 at the three selected temperatures. Again ferritin behaves quite differently from myoglobin. Adsorption at 37°C is significantly greater than at the lower temperatures for all concentrations, and adsorption at 4 and 20°C are essentially identical. Similar trends

are seen for PUU-NPEO2K (Figure 7.68). For PUU-NPEO5K (Figure 7.69) it is concluded that adsorption is independent of temperature, although the data scatter is high.

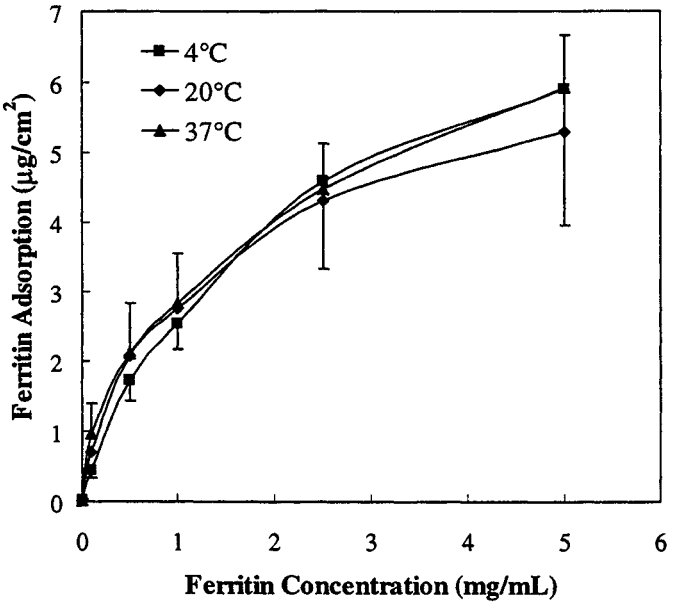

Figure 7.66: Ferritin adsorption on the PUU control surface at 4, 22 and 37°C, from TBS buffer for 3h, ±S.D., n≥6.

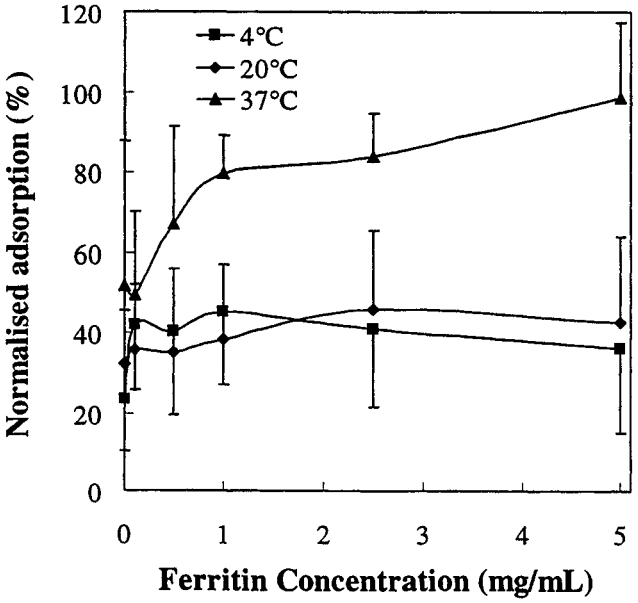

Figure 7.67: Normalised adsorption of ferritin on PUU-NPEO550 at 4, 20 and 37°C (in TBS buffer pH 7.4 for 3 h).

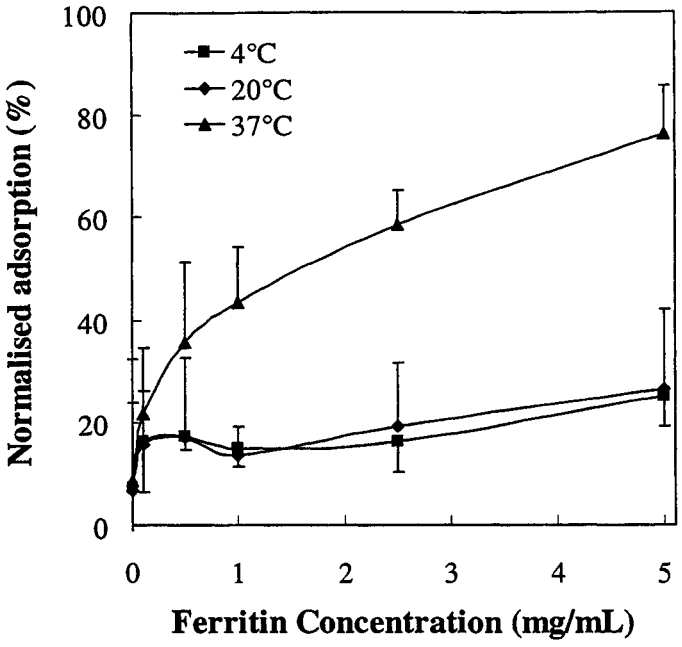

Figure 7.68: Normalised adsorption of ferritin on PUU-NPEO2K at 4, 20 and 37°C (in TBS buffer pH 7.4 for 3 h).

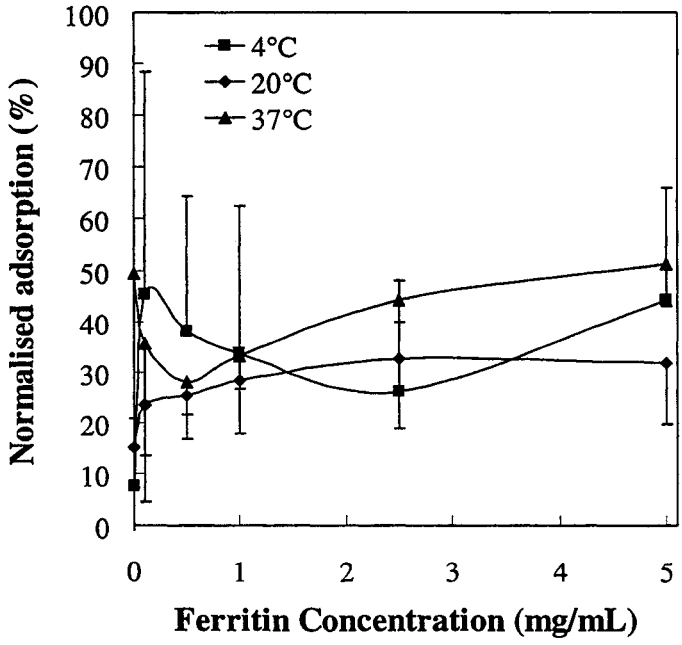

Figure 7.69: Normalised adsorption of ferritin on PUU-NPEO5K at 4, 20 and 37°C (in TBS buffer pH 7.4 for 3 h).

The trends observed with ferritin may be interpreted along the lines indicated previously for myoglobin. First, in relation to the solution properties of PEO, as the solubility of PEO decreases, the dimensions of the PEO chains will be reduced, thus decreasing the effective PEO coverage for a given graft density. Reduction of surface coverage would lead to increased adsorption. However, an increase in adsorption is only observed for PUU-NPEO550 and NPEO2K and only between 20 and 37°C. This suggests that the reduction in surface coverage from 4 to 20°C is not sufficient to observe an effect beyond normal experimental error. However, between 20 and 37°C, the reduction in surface coverage is sufficient to observe an increase in adsorption for the surfaces with shorter PEO grafts (550 and 2000 MW) but not for the surfaces with the longest grafts. Under the assumption that the graft density of PEO is approximately the same for all grafted surfaces, the PEO surface coverage on PUU-NPEO5K should be greater than on either PUU-NPEO550 or PUU-NPEO2K. Therefore, it appears that the reduction in surface coverage for PUU-NPEO5K at 37°C is not sufficient to increase adsorption significantly.

With regard to thermodynamics, the lack of a temperature effect on the isotherms for the control PUU (Figure 7.66) suggests that entropy drives the adsorption. For the grafted surfaces, the two opposing phenomena are the entropy gain from dehydration and conformational change, and the entropy loss from PEO chain compression. Also as the temperature increases, the contribution of the entropy to the free energy change will increase. The data for PUU-NPEO550 and PUU-NPEO2K suggest that the difference

between these two effects is increased at higher temperatures, i.e. the entropy gained by adsorption is greater than that lost by the compression of the PEO chains. However, for 5000 MW PEO grafts, the entropy penalty for compression of the longer chains is greater and therefore the increase in adsorption does not occur.

It appears that the behaviour of PEO-grafted surfaces with respect to temperature cannot be adequately explained in terms of the solution properties of PEO alone. The properties of the proteins themselves also have a significant impact on the resulting behaviour of the system. Therefore, no generalisation is possible regarding the effect of temperature since the properties of the proteins themselves appear to be important in determining the final response.

7.2 Adsorption from Multi Protein Systems

To be effective in practical applications, protein repelling surfaces must be able to function in real biological fluids containing many proteins at high total concentration. For materials that may be used in blood contacting applications or other biological systems, blood plasma provides an ideal, readily available multiple protein environment. It contains several hundred different protein species with a variety of chemical, physical and biological properties.

7.2.1 Fibrinogen Adsorption from Plasma

Fibrinogen is a suitable protein for investigation since it is involved in the blood coagulation cascade and is present in plasma at relatively high concentration. Reducing the levels at which fibrinogen adsorbs to a biomaterial may prevent or delay clot

formation. Furthermore, other thrombotic events triggered by blood-material contact, such as platelet activation, are known to be mediated by fibrinogen adsorption.

In the experiments reported here, the PEO-grafted surfaces were exposed to human pooled normal plasma (PNP) diluted with TBS buffer. Radioiodinated fibrinogen was added to the plasma to enable monitoring of the adsorption of this specific protein.

Figure 7.70 shows plasma fibrinogen adsorption "isotherms" for the surfaces prepared using amino-terminated PEO. Given that the data were pooled from two independent experiments with the same batch of surfaces, reproducibility is good. Overall, the adsorption of fibrinogen is quite low. The adsorption isotherm on the unmodified PUU displays a very prominent Vroman peak [Vroman, L. and Adams, A.L., 1969]. The presence of this peak indicates that other proteins, with higher affinity for the surface, are displacing initially adsorbed fibrinogen from the surface at higher plasma concentrations.

The PEO-grafted surfaces all show a significant reduction in fibrinogen adsorption compared to the control PUU. It seems likely that adsorption of other plasma proteins would be reduced as well. The "isotherms" for the PEO-grafted surfaces also display Vroman peaks though much less prominently than the control PUU surface. Since less protein adsorbs to the PEO-grafted surfaces, less prominent Vroman effects are to be expected. The levels of fibrinogen on the three PEO-grafted surfaces are fairly similar, although PUU-NPEO2K shows significantly lower adsorption than the others at all but the highest plasma concentration.

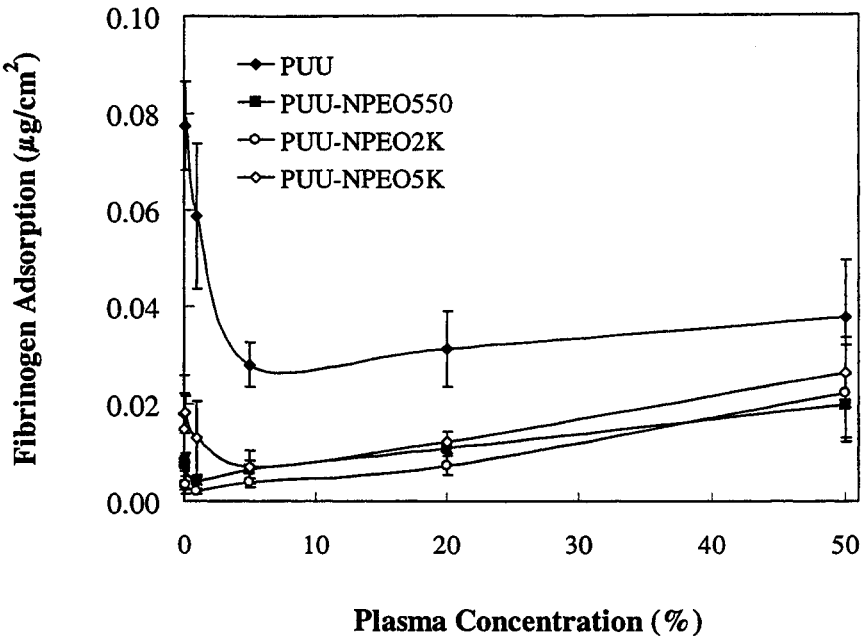

Figure 7.70: Fibrinogen adsorption from pooled normal plasma (diluted with TBS buffer) on PUU and PEO grafted surfaces. 3 h, 22°C (±S.D., n=6).

7.2.2 Adsorption from Plasma Evaluated by Gels and Western Blots of Eluted Proteins

To achieve a more comprehensive picture of the effect of PEO on adsorption from plasma, SDS-PAGE and immunoblots were performed on proteins eluted from the surfaces following exposure to plasma. Since the PUU-NPEO2K surfaces generally showed the best protein rejecting properties, they were selected for these experiments.

An adsorption experiment was performed using radiolabeled fibrinogen in plasma as described previously. Following adsorption, the surfaces were incubated in 200 μL 2% SDS for approximately 18 h. The surfaces and eluates were then separated and the radioactivity determined. The data revealed that only 25-55% of the fibrinogen adsorbed to the control PUU and 25-70% of the fibrinogen adsorbed to the PEO-grafted surfaces

could be eluted, depending on the plasma concentration. Generally, the higher the plasma concentration, the greater the fraction of adsorbed fibrinogen that was elutable. Other proteins probably exhibit this behaviour as well, although the fraction of elutable protein may differ.

Immunoblots were performed on protein eluates from the base PUU and PUU-NPEO2K. The blots were probed with antibodies directed against 22 different plasma proteins and are shown in Figure 7.71 and Figure 7.72. Many different plasma proteins are present in the eluates from both surfaces. Prekallikrein, fibrinogen, C3, albumin, IgG, β-lipoprotein, vitronectin, factor H and apolipoprotein AI are noted in particular. Additionally, a very faint response for factor B was detected on the PUU-NPEO2K blot. The blot data suggest that the same proteins are present on both the control and PEO-grafted surfaces. The PEO grafts therefore do not appear to repel proteins selectively; only the quantity of proteins adsorbing to the surface appears to be influenced. Since the protein patterns on the control PUU and PEO-grafted surfaces are similar, it appears that protein rejection by this type of surface is not selective for one species over another. This result is in accord with data from the experiments that examined the impact of protein size and IEP (in the case of the longer PEO-grafted surfaces) on the protein rejecting ability of the PEO-grafted surfaces.

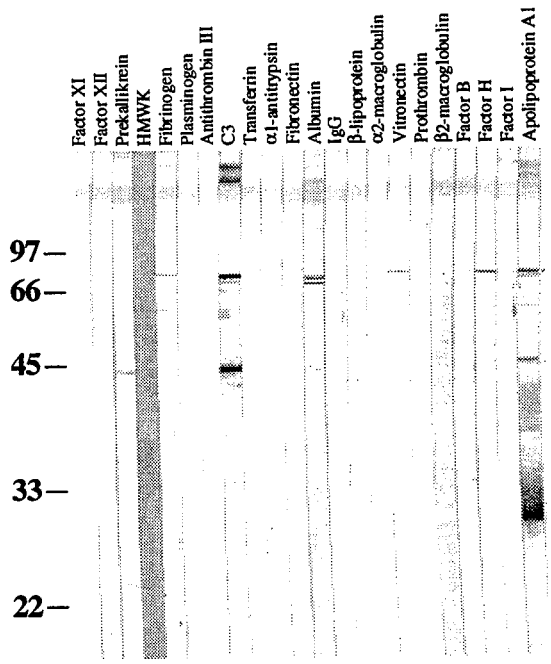

Figure 7.71: Immunoblot of plasma proteins eluted from the PUU base polymer exposed to 100% PNP for 3 h at 22°C.

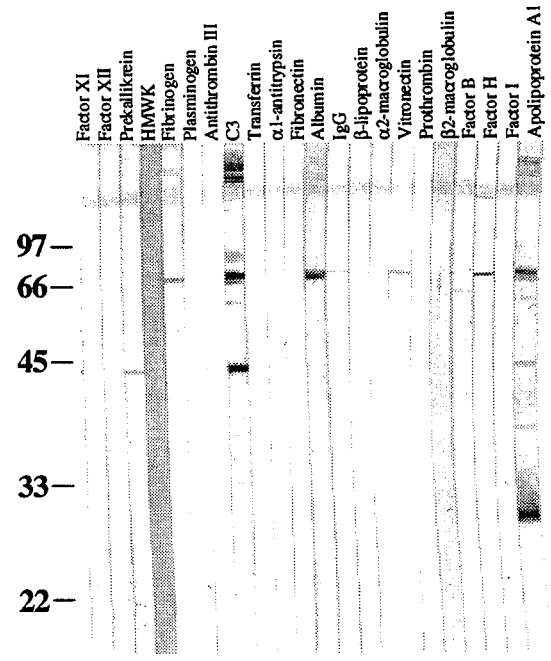

Figure 7.72: Immunoblot of plasma proteins eluted from PUU-NPEO2K exposed to 100% PNP for 3h at 22°C.

8.0 SUMMARY, CONCLUSIONS AND RECOMMENDATIONS

A polyurethane-urea for use as a substrate for the grafting of polyethylene oxide was synthesised and characterised. A PEO grafting reaction protocol was developed from existing procedures in the literature. Surfaces with grafted methoxyhydroxy-PEO (165, 350, 750, 2000 and 5000 MW) or methoxyamino-PEO (550, 2000 and 5000 MW) were prepared and characterised by water contact angle, XPS and AFM. The data clearly showed that grafting had occurred and that the levels of grafting were higher when using the more reactive methoxyamino-PEOs in the grafting reaction.

A method to measure the graft density directly on the surfaces was developed. However, due to some unresolved problems, only qualitative information on the graft density was obtained. The levels of grafting determined were several orders of magnitude higher than the theoretical maximum calculated on the basis of a close packed layer of helical PEO.

Protein adsorption experiments were performed to identify factors that influence the effectiveness of the PEO grafts in preventing adsorption. These experiments were performed with single protein solutions in buffer, using radiolabeled proteins. The results showed that protein adsorption levels decreased as the length of the PEO grafts increased, reaching an optimum at approximately 2000 MW. As well, surfaces prepared with the methoxyamino-PEOs consistently showed lower adsorption levels than surfaces prepared with methoxyhydroxy-PEOs of the same molecular weight.

The effects of the properties of the proteins themselves were also examined. Experiments to examine the effect of protein size on the protein-rejecting capabilities of the grafted-PEO surfaces generally showed that size was not of great significance. Previous theoretical studies that predicted a dependence of rejection on size of the protein were based on systems where the PEO was in the "brush" regime. The fact that no size effect was seen in the present work implies that the grafted-PEO surfaces were in the "mushroom" regime and did not have sufficiently high graft density to discriminate among proteins of different size.

It was also shown that protein isoelectric point does not affect the ability of the PEO-surfaces to repel protein when long PEO grafts are used. This implies that as proteins adsorb to the surface, the PEO layer masks the accumulating charge on the surface. However, for smaller PEO grafts, proteins with large net charge adsorbed less than proteins with low charge, presumably due to electrostatic repulsion from proteins already adsorbed to the surface.

Experiments to examine the effect of temperature on protein repulsion showed that the data could not be explained solely based on the solution properties of PEO. The effects were different for proteins of different size. It is thus difficult to generalise the effects of temperature and each protein probably has its own unique characteristics in this regard.

Adsorption experiments from plasma showed that, as observed in the single protein experiments, the overall levels of adsorption were greatly reduced on the PEO-grafted surfaces. It was also shown that the PEO-grafted surfaces and the controls adsorb

the same proteins in roughly the same proportions, suggesting that these PEO surfaces do not discriminate among the different proteins with regard to inhibition of adsorption. Rather, inhibition is the same regardless of protein size and other properties.

Recommendations

The use of a polyurethane-urea may not have been the best choice for this study. The large number of experiments performed required the synthesis of several batches of the base PUU. This is a source of variability because no two batches will be exactly the same. Therefore for this type of investigation, where information about factors influencing the response of a system is to be gathered, the use of a model surface might prove to be a better choice. For example, gold-coated silicone wafers could be used and surfaces prepared by chemisorption of thiol terminated PEOs . There would certainly be less variation in surface properties. Another advantage with this type of surface is that higher levels of graft density could be achieved, at least in principle, since thiol binding sites are present at ~5Å spacing on these surfaces. In this way, comparing the experimental results with the theoretical models would be easier since most of the models are based on PEO in the "brush" regime.

Another important problem yet to be resolved is to obtain accurate graft density data. Most theoretical studies have shown that graft density is the single most important factor in determining the protein-rejecting efficiency of a PEO surface. It is therefore imperative that future studies overcome the problems encountered in this work. Again the use of a model substrate such as gold on silicon may prove useful.

The innate complexity of proteins made it difficult to rationalise the results from the experimental design, based mainly on varying size and isoelectric point. The different proteins may be too different in other properties not considered here to make the simple categorisations with respect to size and IEP able to yield useful information. A possible solution would be to focus on one protein and use site-directed mutagenesis to make protein mutants and examine the impact of controlled property changes on adsorption behaviour. Changes could be small and controlled compared to using a series of different proteins as in the present work.

It would also be of interest to expand the multi-protein studies by investigating the competitive adsorption of two or more proteins using radiolabeling methods. Such studies would potentially give more reliable insights into the effects of protein properties on repulsion by surface localised PEO.

9.0 REFERENCES

Adamson, A. W., "Physical Chemistry of Surfaces," Wiley-Intersciences, New York, 1990.

Amiji, M., Park, K., "Prevention of Protein Adsorption and Platelet-Adhesion on Surfaces by Peo PPO Peo Triblock Copolymers," *Biomaterials,* **13**, 682-692 (1992).

Andrade, J. D., "Principles of Protein Adsorption," in *Surface and Interfacial Aspects of Biomedical Polymers*, J. D. Andrade (ed), Plenum Press, New York, 1985a, pp. 1-80.

Andrade, J. D., "X-ray Photoelectron Spectroscopy (XPS)," in *Surface Chemistry and Physics*, J. D. Andrade (ed), Plenum Press, New York, 1985b, pp. 105-196.

Antonsen, K. P., Hoffman, A. S., "Water Structure of PEG Solutions by Differential scanning calorimetry measurments," in *Poly(Ethylene Glycol) Chemistry: Biotechnical and Biomedical Applications*, J. M. Harris (ed), Plenum Press, New York, 1992, pp. 15-28.

Arai, T., Norde, W., "The Behavior of Some Model Proteins at Solid Liquid Interfaces .1. Adsorption from Single Protein Solutions," *Colloids Surfaces,* **51**, 1-15 (1990).

Beamson, G., Briggs, D., "High Resolution XPS of Organic Polymers: The Scienta ESCA300 Database," John Wiley & Sons, Chichester, 1992.

Bergstrom, K., Holmberg, K., Safranj, A., Hoffman, A. S., Edgell, M. J., Kozlowski, A., Hovanes, B. A., Harris, J. M., "Reduction of Fibrinogen Adsorption on Peg-Coated Polystyrene Surfaces," *J. Biomed. Mater. Res.,* **26**, 779-790 (1992).

Bergstrom, K., Osterberg, E., Holmberg, K., Hoffman, A. S., Schuman, T. P., Kozlowski, A., Harris, J. M., "Effects of Branching and Molecular-Weight of Surface-Bound Poly(Ethylene Oxide) on Protein Rejection," *J. Biomater. Sci. Polym. Ed.,* **6**, 123-132 (1994).

Box, G. E. P., Hunter, W. G., Hunter, J. S., "Statistics for Experimenters: An Introduction to Design, Data Analysis, and Model Building," John Wiley & Sons, New York, 1978.

Brash, J. L., "The Fate of Fibrinogen Following Adsorption at the Blood-Biomaterial Interface," *Ann. NY. Acad. Sci.,* **516**, 206 (1987).

Brash, J. L., Horbett, T. A., "Proteins at Interfaces: An Overview," in *Proteins at Interfaces II: Fundamentals and Applications*, T. A. Horbett, J. L. Brash (eds), American Chemical Society, Washington, DC, 1995, pp. 1-23.

Brash, J. L., Tenhove, P., "Effect of Plasma Dilution on Adsorption of Fibrinogen to Solid- Surfaces," *Thromb. Haemost.*, **51**, 326-330 (1984).

Brinkman, E., Poot, A., Beugeling, T., Vanderdoes, L., Bantjes, A., "Surface Modification of Copolyether-Urethane Catheters with Poly(Ethylene Oxide)," *Int. J. Artif. Organs,* **12** , 390-394 (1989).

Brinkman, E., Poot, A., Vanderdoes, L., Bantjes, A., "Platelet Deposition Studies on Copolyether Urethanes Modified with Poly (Ethylene-Oxide)," *Biomaterials,* **11**, 200-205 (1990).

Carignano, M. A., Szleifer, I., "On the Structure and Pressure of Tethered Polymer Layers in Good Solvent," *Macromolecules,* **28**, 3197-3204 (1995).

Claesson, P. M., "Poly(ethylene oxide) Surface Coatings: Relations Between Intermolecular Forces, Layer Structure and Protein Repellency," *Colloids Surfaces A: Physicochem. Eng. Aspects,* **77**, 109-118 (1993).

Coleman, D. L., Andrade, J. D., Gregonis, D. E., "Blood-Materials Interactions - The Minimum Interfacial Free- Energy and the Optimum Polar Apolar Ratio Hypotheses," *J. Biomed. Mater. Res.*, **16**, 381-398 (1982).

Crichton, R. R., "The Biochemistry of Ferritin," *British Journal of Haematology,* **24**, 677-680 (1973).

De Gennes, P. G., "Scaling Concepts in Polymer Physics," Conrnell University Press, Ithaca, NY, 1979.

De Gennes, P. G., "Polymers at an Interface; A Simplified View," *Adv. Colloid Interface Sci.*, **27** , 189-209 (1987).

Desai, N. P., Hubbell, J. A., "Solution Technique to Incorporate Polyethylene Oxide and Other Water-Soluble Polymers into Surfaces of Polymeric Biomaterials," *Biomaterials,* **12**, 144-153 (1991).

Du, Y.J., "PEO and PEO-Heparin Modified Surfaces for Blood Contacting Applications," Ph.D. Thesis, McMaster University, (2001).

Duinhoven, S., Poort, R., Vandervoet, G., Agterof, W. G., Norde, W., Lyklema, J., "Driving Forces for Enzyme Adsorption at Solid-Liquid Interfaces .1. The Serine-Protease Savinase," *J. Colloid Interface Sci.*, **170**, 340-350 (1995).

Emoto, K., Harris, J. M., Van Alstine, J. M., "Electrokinetic Analysis of Poly(Ethylene Glycol) Coating Chemistry," in *Poly(Ethylene Glycol): Chemistry and Biological Applications*, J. M. Harris, S. Zalipsky (eds), American Chemical Society, Washington, 1997, pp. 374-399.

Flory, P. J., "Principles of Polymer Chemistry," Cornell University Press, Ithaca, 1953.

Freij-Larsson, C., Wesslén, B., "Grafting of Polyurethane Surfaces with Poly(Ethylene Glycol)," *J. Appl. Polym. Sci.*, **50**, 345-352 (1993).

Fujimoto, K., Inoue, H., Ikada, Y., "Protein Adsorption and Platelet-Adhesion onto Polyurethane Grafted with Methoxy-Poly(Ethylene Glycol) Methacrylate by Plasma Technique," *J. Biomed. Mater. Res.*, **27**, 1559-1567 (1993).

Furness, E. L., Ross, A., Davis, T. P., King, G. C., "A Hydrophobic Interaction Site for Lysozyme Binding to Polyethylene Glycol and Model Contact Lens Polymers," *Biomaterials*, **19**, 1361-1369 (1998).

Goldstein, R. E., "On the Theory of Lower Critical Solution Points in Hydrogen-Bonded Mixtures," *J. Chem. Phys.*, **80**, 5340-5341 (1984).

Gombotz, W. R., Guanghui, W., Hoffman, A. S., "Immobilization of Poly(Ethylene Oxide) on Poly(Ethylene- Terephthalate) Using a Plasma Polymerization Process," *J. Appl. Polym. Sci.*, **37**, 91-107 (1989).

Gombotz, W. R., Guanghui, W., Horbett, T. A., Hoffman, A. S., "Protein Adsorption to Poly(Ethylene Oxide) Surfaces," *J. Biomed. Mater. Res.*, **25**, 1547-1562 (1991).

Gombotz, W. R., Guanghui, W., Horbett, T. A., Hoffman, A. S., "Protein Adsorption to and Elution from Polyether Surfaces," in *Poly(Ethylene Glycol) Chemistry: Biotechnical and Biomedical Applications*, J. M. Harris (ed), Plenum Press, New York, 1992, pp. 247-261.

Gölander, C. G., Eriksson, J. C., Vladkova, T., Stenius, P., "Preparation and Protein Adsorption Properties of Photopolymerized Hydrophilic Films Containing N-Vinylpyrrolidone (NVP), Acrylic Acid (AA) or Ethyleneoxide (EO) Units as Studied by ESCA," *Colloids Surfaces*, **21**, 149-165 (1986).

Gölander, C. G., Herron, J., Lim, K., Claesson, P. M., Stenius, P., Andrade, J. D., "Properties of Immobilized PEG Films and the Interaction with Proteins: Experiments

and Modeling," in *Biomedical Applications of Polyethyleneglycol Chemistry*, J. M. Harris (ed), Plenum Press, New York, 1992, pp. 221-245.

Halperin, A., "Polymer Brushes that Resist Adsorption of Model Proteins: Design Parameters," *Langmuir,* **15**, 2525-2533 (1999).

Han, D. K., Park, K. D., Ahn, K. D., Jeong, S. Y., Kim, Y. H., "Preparation and Surface Characterization of PEO-Grafted and Heparin-Immobilized Polyurethanes," *J. Biomed. Mater. Res. Appl. Biom.,* **23**, 87-104 (1989).

Han, D. K., Park, K. D., Ryu, G. H., Kim, U. Y., Min, B. G., Kim, Y. H., "Plasma Protein Adsorption to Sulfonated Poly(Ethylene Oxide)-Grafted Polyurethane Surface," *J. Biomed. Mater. Res.,* **30**, 23-30 (1996).

Harder, P., Grunze, M., Dahint, R., Whitesides, G. M., Laibinis, P. E., "Molecular Conformation in Oligo(Ethylene Glycol)-Terminated Self-Assembled Monolayers on Gold and Silver Surfaces Determines Their Ability to Resist Protein Adsorption," *J. Phys. Chem. B,* **102**, 426-436 (1998).

Harris, J. M., "Introduction to Biotechnical and Biomedical Applications of Poly(ethylene glycol)," in *Poly(ethylene glycol) Chemistry: Biotechnical and Biomedical Applications*, J. M. Harris (ed), Plenum Press, New York, 1992, pp. 1-14.

Harrison, P. M., Arosio, P., "The Ferritins: Molecular Properties, Iron Storage Function and Cellular Regulation," *Biochim. Biophys. Acta,* **1275**, 161-203 (1996).

Haynes, C. A., Norde, W., "Globular Proteins at Solid/liquid Interfaces," *Colloids Surfaces B: Biointerfaces,* **2**, 517 (1994).

He, X. M., Carter, D. C., "Atomic Structure and Chemistry of Human Serum-Albumin," *Nature,* **358**, 209-215 (1992).

Hellsing, K., "Gel Chromatography in Eluents Containing Polymers," *J. Chromatogr.,* **36**, 170-180 (1968).

Herde, K., Haupt, H., Schwick, H. B., "Plasma Protein Fractionation," Academic Press, New York, 1977.

Horbett, T. A., "Mass-Action Effects on Competitive Adsorption of Fibrinogen from Hemoglobin-Solutions and from Plasma," *Thromb. Haemost.,* **51**, 174-181 (1984).

Horbett, T. A., Brash, J. L., "Proteins at Interfaces: Current Issues and Future Prospects," in *Proteins at Interfaces: Physicochemical and Biochemical Studies*, J. L. Brash, T. A. Horbett (eds), American Chemical Society, Washington, 1987, pp. 1-33.

Horinaka, J., Amano, S., Funada, H., Ito, S., Yamamoto, M., "Local Chain Dynamics of Poly(Oxyethylene) Studied by the Fluorescence Depolarization Method," *Macromolecules,* **31**, 1197-1201 (1998).

Hunter, R. J., "Adsorption at Interfaces," in *Introduction to Modern Colloid Science,* Oxford University Press, 1993, pp. 164-193.

Jeon, S. I., Andrade, J. D., "Protein Surface Interactions in the Presence of Polyethylene Oxide .2. Effect of Protein Size," *J. Colloid Interface Sci.,* **142**, 159-166 (1991a).

Jeon, S. I., Lee, J. H., Andrade, J. D., De Gennes, P. G., "Protein Surface Interactions in the Presence of Polyethylene Oxide .1. Simplified Theory," *J. Colloid Interface Sci.,* **142**, 149-158 (1991b).

Johnson, R. D., Arnold, F. H., "The Temkin Isotherm Describes Heterogeneous Protein Adsorption," *Bba. Protein Struct. Mol. Enzym.,* **1247**, 293-297 (1995).

Karlström, G., "A New Model for Upper and Lower Critical Solution Temperatures in Poly(Ethylene Oxide) Solutions," *J. Phys. Chem.,* **89**, 4962-4964 (1985).

Kartha, G., Bello, J., Harker, D., "Tertiary Structure of Ribonuclease," *Nature,* **213**, 862-865 (1967).

Kendrew, J. C., "Myoglobin and the Structure of Proteins," *Science,* **139**, 1259-1266 (1963).

Kjellander, R., "Phase Separation of Non-Ionic Surfactant Solutions: A Treatment of the Micellar Interaction and Form," *J. Chem. Soc. ,Faraday Trans. 2,* **78**, 2025-2042 (1982).

Koutsoukos, P. G., Lyklema, J., Mummeyoung, C. A., Norde, W., "Effect of the Nature of the Substrate on the Adsorption of Human-Plasma Albumin," *Colloids Surfaces,* **5**, 93-104 (1982).

Lamba, N. M. K., Woodhouse, K. A., Cooper, S. L., "Polyurethanes in Biomedical Applications," CRC Press, Boca Raton, 1998.

Leckband, D., Sheth, S., Halperin, A., "Grafted Poly(ethylene oxide) Brushes as Nonfouling Surface Coatings," *J. Biomater. Sci. Polym. Ed.,* **10**, 1125-1147 (1999).

Lee, S.-W., Laibinis, P. E., "Protein-Resistant Coatings for Glass and Metal Oxide Surfaces Derived from Oligo(ethylne glycol)-Terminated Alkytrichlorosilanes," *Biomaterials,* **19** , 1669-1675 (1998).

Lelah, M. D., Cooper, S. L., "Polyurethanes in Medicine," CRC Press, Boca Raton, 1986.

Llanos, G. R., Sefton, M. V., "Immobilization of Poly(Ethylene Glycol) onto a Poly(Vinyl Alcohol) Hydrogel: 2. Evaluation of Thrombogenicity," *J. Biomed. Mater. Res.*, **27**, 1383-1391 (1993).

Lopez, G. P., Ratner, B. D., Tidwell, C. D., Haycox, C. L., Rapoza, R. J., Horbett, T. A., "Glow-Discharge Plasma Deposition of Tetraethylene Glycol Dimethyl Ether for Fouling-Resistant Biomaterial Surfaces," *J. Biomed. Mater. Res.*, **26**, 415-439 (1992).

Malmsten, M., Emoto, K., Van Alstine, J. M., "Effect of Chain Density on Inhibition of Protein Adsorption by Poly(Ethylene Glycol) Based Coatings," *J. Colloid Interface Sci.*, **202**, 507-517 (1998).

Marmur, A., "Contact-Angle Hysteresis on Heterogeneous Smooth Surfaces: Theoretical Comparison of the Captive Bubble and Drop Methods," *Colloids Surfaces A: Physicochem. Eng. Aspects*, **136**, 209-215 (1998).

McPherson, T., Kidane, A., Szleifer, I., Park, K., "Prevention of Protein Adsorption by Tethered Poly(Ethylene Oxide) Layers: Experiments and Single-Chain Mean-Field Analysis," *Langmuir*, **14**, 176-186 (1998).

Mcpherson, T. B., Lee, S. J., Park, K., "Analysis of the Prevention of Protein Adsorption by Steric Repulsion Theory," in *Proteins at Interfaces II: Fundamentals and Applications*, T. A. Horbett, J. L. Brash (eds), American Chemical Society, Washington, DC, 1995, pp. 395-404.

Mcpherson, T. B., Shim, H. S., Park, K., "Grafting of PEO to Glass, Nitinol, and Pyrolytic Carbon Surfaces by Gamma-Irradiation," *J. Biomed. Mater. Res.*, **38**, 289-302 (1997).

Mori, Y., Kikuchi, T., Nagaoka, S., Noguchi, N., Noishiki, Y., Takiuchi, H., Tanzawa, H., "A New Antithrombogenic Material with Long Polyethyleneoxide Chains," *Trans. Amer. Soc. Artif. Intern. O.*, **28**, 459-463 (1982).

Norde, W., "Adsorption of Proteins from Solution at the Solid-Liquid Interface," *Adv. Colloid Interface Sci.*, **25**, 267-340 (1986).

Norde, W., "Energy and Entropy of Protein Adsorption," *J. Disper. Sci. Tech.*, **13**, 363-377 (1992).

Norde, W., Haynes, C. A., "Reversibility and the Mechanism of Protein Adsorption," in *Proteins at Interfaces II: Fundamentals and Applications*, T. A. Horbett, J. L. Brash (eds), American Chemical Society, Washington, DC, 1995, pp. 26-40.

Norde, W., Lyklema, J., "Why Proteins Prefer Interfaces," *J. Biomater. Sci. Polym. Ed.*, **2**, 183 (1991).

Noshay, A., McGrath, J. E., "Block Copolymers," Academic Press, New York, 1977.

Palegrosdemange, C., Simon, E. S., Prime, K. L., Whitesides, G. M., "Formation of Self-Assembled Monolayers by Chemisorption of Derivatives of Oligo(Ethylene Glycol) of Structure Hs(CH2)11(Och2Ch2)Meta-OH on Gold," *J. Am. Chem. Soc.*, **113**, 12-20 (1991).

Prime, K. L., Whitesides, G. M., "Adsorption of Proteins Onto Surfaces Containing End-Attached Oligo(Ethylene Oxide) - A Model System Using Self-Assembled Monolayers," *J. Am. Chem. Soc.*, **115**, 10714-10721 (1993).

Rabe, T. E., Tilton, R. D., "Surface-Diffusion of Adsorbed Proteins in the Vicinity of the Substrate Glass-Transition Temperature," *J. Colloid Interface Sci.*, **159**, 243-245 (1993).

Reeke, G. N., Becker, J. W., Edelman, G. M., "The Covalent and Three-Dimensional Structure of Concanavalin A: Atomic Coordinates, Hydrogen Bonding, and Quaternary Structure," *J. Biol. Chem.*, **4**, 1525-1547 (1975).

Righetti, P. G., Caravaggio, T., "Isoelectric Points and Molecular Weights of Proteins," *J. Chromatogr.*, **127**, 1-28 (1976).

Ryle, A. P., "Behaviour of Polyethylene Glycol on Dialysis and Gel-Filtration," *Nature*, **206**, 1256-1256 (1965).

Saeki, S., Kuwahara, N., Nakata, M., Kaneko, M., "Upper and Lower Critical Solution Temperatures in Poly(ethylene glycol) Solutions," *Polymer*, **17**, 685 (1976).

Santerre, J.P., "Sulfonated and Derivatized Sulfonated Polyurethanes for Blood Contacting Applications," Ph.D., McMaster University, (1990).

Saunders, J. H., "Polyurethane Elastomers," in *Polymer Chemistry of Synthetic Elastomers Part II*, J. P. Kennedy, E. M. Torinquist (eds), Interscience Publishers, New York, 1969, pp. 727-765.

Schaaf, P., Talbot, J., "Surface Exclusion Effects in Adsorption Processes," *J. Chem. Phys.*, **91**, 4401-4409 (1989).

Skarja, G.A., "Investigation of Platelet-Surface Interactions Using a Novel Cone and Plate Device," Master's, McMaster University, (1994).

Sofia, S. J., Merrill, E. W., "Grafting of PEO to Polymer Surfaces Using Electron-Beam Irradiation," *J. Biomed. Mater. Res.*, **40**, 153-163 (1998a).

Sofia, S. J., Premnath, V., Merrill, E. W., "Poly(Ethylene Oxide) Grafted to Silicon Surfaces: Grafting Density and Protein Adsorption," *Macromolecules,* **31**, 5059-5070 (1998b).

Sun, X., "Peptide Modified Gold Coated Polyurethane Surfaces as Thrombin Scavengers," Master's, McMaster University, (1998).

Szleifer, I., "Protein Adsorption on Surfaces with Grafted Polymers: A Theoretical Approach," *Biophys. J.,* **72**, 595-612 (1997).

Tan, J. S., Butterfield, D. E., Voycheck, C. L., Caldwell, K. D., Li, J. T., "Surface Modification of Nanoparticles by Peo PPO Block- Copolymers to Minimize Interactions with Blood Components and Prolong Blood-Circulation in Rats," *Biomaterials,* **14**, 823-833 (1993).

Thomson, S. J., Webb, G., "Heterogeneous Catalysis," John Wiley & Sons, Inc., New York, 1968.

Van Tassel, P. R., Guemouri, L., Ramsden, J. J., Tarjus, G., Viot, P., Talbot, J., "A Particle-Level Model of Irreversible Protein Adsorption with a Postadsorption Transition," *J. Colloid Interface Sci.,* **207**, 317-323 (1998).

Vroman, L., Adams, A. L., "Identification of Rapid Changes at Plasma-Solid Interfaces," *J. Biomed. Mater. Res.,* **3**, 43 (1969).

Wesslén, B., Kober, M., Freij-Larsson, C., Ljungh, A., Paulsson, M., "Protein Adsorption of Poly(Ether Urethane) Surfaces Modified by Amphiphilic and Hydrophilic Polymers," *Biomaterials,* **15**, 278-284 (1994).

Wu, Y. J., Timmons, R. B., Jen, J. S., Molock, F. E., "Non-Fouling Surfaces Produced by Gas Phase Pulsed Plasma Polymerization of an Ultra Low Molecualr Weight Ethylene Oxide Containing Monomer," *Colloids Surfaces B: Biointerfaces,* **18**, 235-248 (2000).

Zhivkova, I. V., Zhivkov, A. M., Stoychev, D. S., "Electrostatic Behavior of Polyethylene Oxide," *Eur. Polym. J.,* **34**, 531-538 (1998).

10.0 APPENDIX A: SDS-PAGE AND IMMUNOBLOTS PROCEDURES

Polyacrylamide gel preparation (12% separating gel, 4% stacking gel)

The acrylamide/bis solution is prepared by dissolving the following reagents in distilled water, diluting to 100 mL and filtering the final solution:

Acrylamide	29.2 g
N,N'-Methylenebisacrylamide	0.8 g

The reagents for the 12% separating gel were mixed and degassed for 15 min at room temperature:

Distilled water	3.35 mL
1.5 M Tris, pH 8.8	2.5 mL
10% (w/v) SDS	0.1 mL
30% (w/v) Acrylamide/Bis	4.0 mL

Immediately prior to casting the gel, the following reagents are added to initiate polymerisation in the above mixture:

10% (w/v) ammonium persulfate (fresh)	50 µL
TEMED	5 µL

The casting plates were successively cleaned with distilled water and 95% ethanol. Once dry, the plates were inserted into the casting assembly. The assembly was then secured to the casting stand. Using a syringe, the gel plates were filled with polymerising 12% acrylamide solution, leaving enough space to pour the stacking gel. After 2 min, a small quantity of water was layered over the gel. The gel was allowed to polymerise for 1 h.

The reagents for the 4% stacking gel were mixed and degassed for 15 min at room temperature:

Distilled water	3.0 mL
0.5 M Tris, pH 6.8	1.2 mL
10% (w/v) SDS	0.1 mL
30% (w/v) Acrylamide/Bis	0.65 mL

Immediately prior to casting the gel, the following reagents are added to initiate polymerisation in the above mixture:

10% (w/v) ammonium persulfate (fresh)	25 µL
TEMED	5 µL

Using a syringe, the remainder of the gel plates was filled with polymerising 4% acrylamide solution. An appropriate comb was added and the gel allowed to polymerise for 1 h.

Sample preparation

The sample buffer used in sample preparation consists of the following reagents, mixed and stored at 4°C in 225 µL aliquots:

Distilled water	4.0 mL
0.5 M Tris, pH 6.8	1.0 mL
10% (w/v) SDS	1.6 mL
Glycerol	0.8 mL

Immediately prior to use, the following reagents are added to an aliquot, yielding tracking dye (TD):

2-Mercaptoethanol	30 µL
0.5% (w/v) Bromophenol blue	30 µL

Samples and standards used for SDS-PAGE only are prepared as follows:

0.5 µL SDS-PAGE MW Standards, Low Range, 10 µL TD
10 µL Protein sample, 10 µL TD
7.5 µL Prestained SDS-PAGE Standards, Low Range

Samples and standards used for immunobloting are prepared as follows:

1 µL SDS-PAGE MW Standards, Low Range, 10 µL TD
80-150 µL Protein sample, 10 µL TD
7.5 µL Prestained SDS-PAGE Standards, Low Range

Once mixed, the samples are placed in a 95°C water bath for 7.5 min.

Electrophoresis

Once the gel polymerisation was complete, the combs were gently removed and the wells rinsed with distilled water. The gels were removed from the casting stand and placed into the clamp assembly. The assembly was then placed into the buffer chamber. A 5X stock solution of electrophoresis buffer was prepared by mixing the following reagents in distilled water and diluting to 1 L (Note: the pH of this solution should be 8.3 ± 0.3):

Tris Base	15 g
Glycine	72 g
SDS	5 g

Just prior to use, the 5X stock solution was diluted to 1X with distilled water. The upper buffer chamber was filled to a level 3 mm below the edge of the outer (long) glass plate with electrophoresis buffer. The lower buffer chamber was filled to a level that covered the bottom 1 cm of the gel. The comb was subsequently removed and the well flushed with transfer buffer. The sample was then loaded into the wells and a potential difference of 200 V applied across the gel for approximately 1 h. When performing an immunoblot, a small quantity of pyronin Y dye (dissolved in sample buffer) was layered into the wells just before the tracking dye had reached the bottom of the separating gel. Electrophoresis was stopped once the pyronin Y dye had reached the top of the separating gel.

Gel equilibration

Transfer buffer was prepared by mixing the following reagents in distilled water and diluting to 1 L (Note: the pH of this solution should be 8.3 ± 0.3):

Tris Base	3.03 g
Glycine	14.4 g
Methanol (HPLC grade)	200 mL

The gels were removed from the electrophoresis assembly and equilibrated in fresh cold (4°C) transfer buffer for 30 min.

Electrophoretic transfer

Immobilon membranes were cut to gel-size, prewetted in methanol (1-3 seconds), incubated in water (1-2 min) and soaked in transfer buffer (15 min). The gels and membranes were loaded in the transfer cassettes according to specifications and placed in the transfer chamber. The chamber was then filled with transfer buffer so that the entire gel surface was covered. A potential difference of 100V (200 mA) was applied for 1 h.

The membranes can then immediately be stained with colloidal gold or dried and used for immunoblot analysis.

Gold staining

The PVDF membranes were washed two times in phosphate buffered saline (PBS), pH 7.4. PBS was prepared by mixing the following reagents in distilled water, adjusting the pH to 7.4 and diluting to 1 L:

Na_2HPO_4	1.32 g
$NaH_2PO_4 \cdot H_2O$	0.345 g
NaCl	8.5 g

The membranes were then incubated in 0.3% (v/v) Tween 20 solution in PBS for 1 h at 20°C to block unbound membrane sites. This was followed by three further washings of 5 min with this blocking solution. The membranes were then rinsed in water three times for 1 min.

The membranes were then placed in Protogold solution and stained for 1 to 4 h. Following the staining, the membranes were rinsed extensively with distilled water and air dried.

Immunoblotting

The sections of the membrane containing MW markers lanes and a small section of the sample lane were removed to be stained with the gold staining procedure described above.

The remainder of the membrane was sliced into 3 mm strips. The strips were prewet in methanol, rinsed in distilled water and placed into plastic wells. In order to block unbound membrane sites and prevent non-specific binding, the strips were incubated for 1 h in 5% (w/v) dry skim milk in TBS, pH 7.4 with gentle agitation. This treatment was followed by three 5 min rinses in 0.1% (w/v) dry skim milk in TBS.

Each strip was then incubated for 1 h in 1 mL 1% (w/v) dry skim milk and 0.05% (v/v) Tween 20 in TBS with a 1/1000 dilution of the primary antibody to the protein of interest. This treatment was followed by three 5 min rinses in 0.1% (w/v) dry skim milk in TBS. Each strip was then incubated for 1 h in 1 mL 1% (w/v) dry skim milk and 0.05% (v/v) Tween 20 in TBS with a 1/1000 dilution of the alkaline phosphatase-linked secondary antibody. Again followed three 5 min rinses in 0.1% (w/v) dry skim milk in TBS. Finally, the strips were incubated for up to 4 h with a solution to develop the colour reaction and

detect the bands. The buffer for this solution is prepared by dissolving the following reagents in distilled water, adjusting the pH to 9.8 and diluting to 100 mL:

$NaHCO_3$	840 mg
$MgCl_2 \cdot 6H_2O$	20 mg

The final solution is prepared by mixing 1 mL NBT stock (30 mg NBT in 1 mL 70% DMF in distilled water) and 1 mL BCIP stock (15 mg BCIP in 1 mL DMF) in 100 mL buffer: This reaction was terminated by rinsing the strips in distilled water twice for 5 min.

11.0 APPENDIX B: SUPPLEMENTAL FIGURES

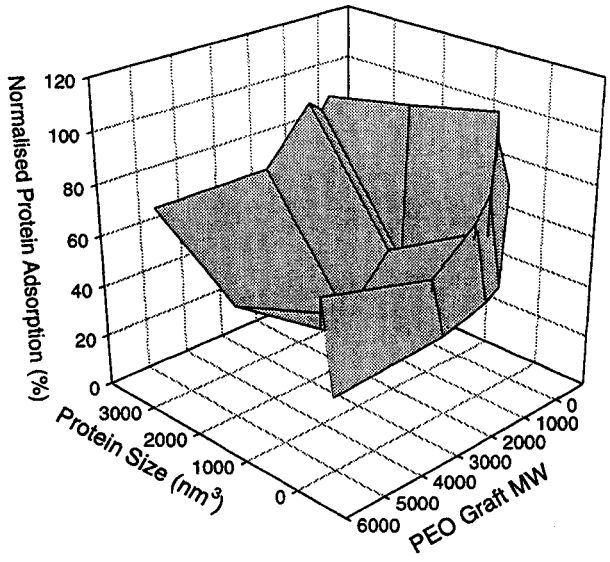

Figure 11.1: Protein adsorption response surface showing the effects of protein size and PEO graft MW on PUU-OPEO surfaces at 0.001 mg/mL protein concentration.

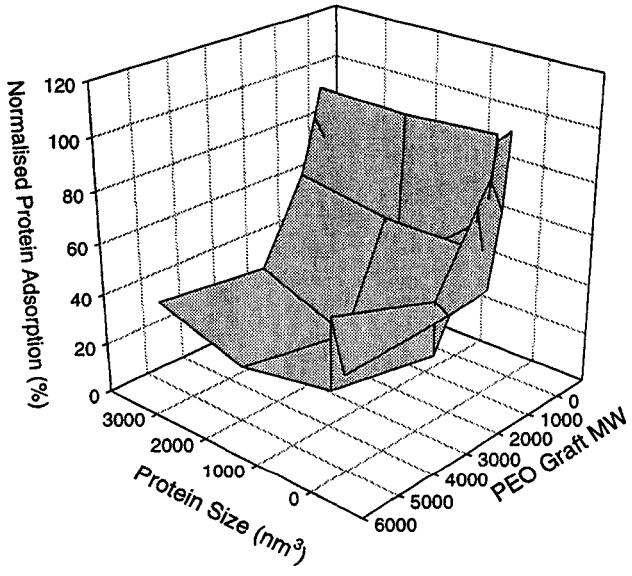

Figure 11.2: Protein adsorption response surface showing the effects of protein size and PEO graft MW on PUU-OPEO surfaces at 0.01 mg/mL protein concentration.

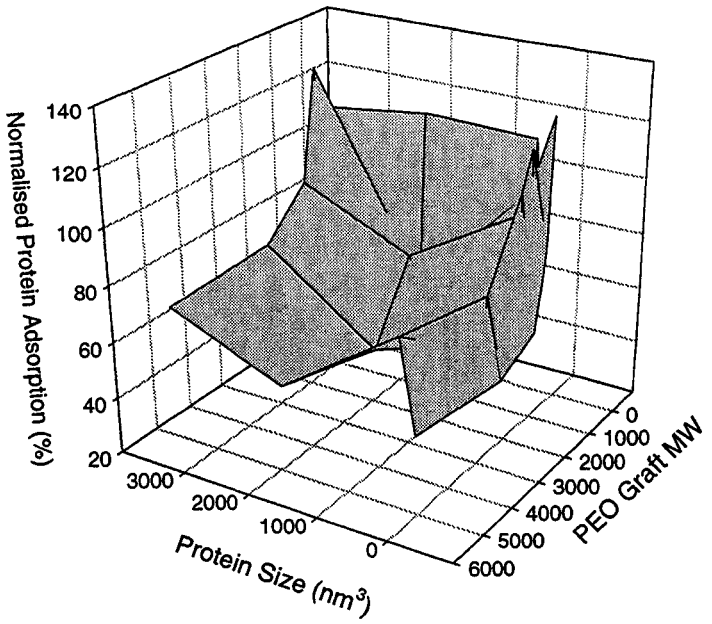

Figure 11.3: Protein adsorption response surface showing the effects of protein size and PEO graft MW on PUU-OPEO surfaces at 0.5 mg/mL protein concentration.

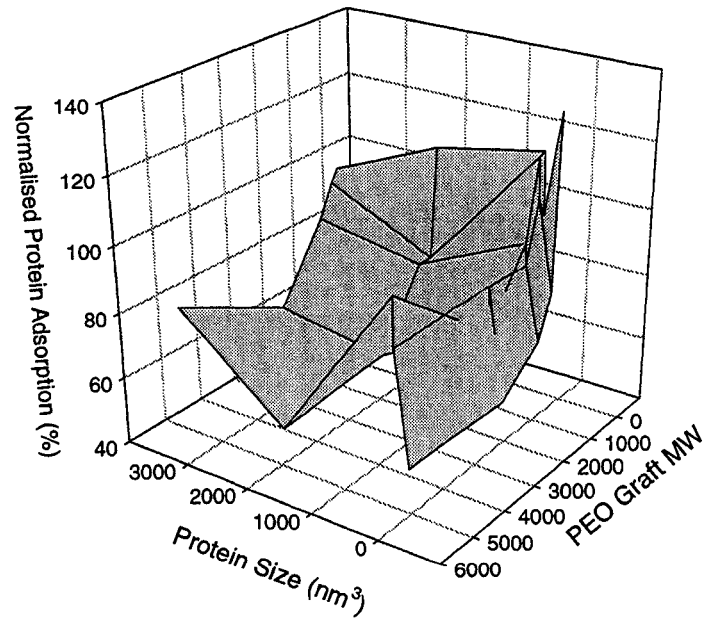

Figure 11.4: Protein adsorption response surface showing the effects of protein size and PEO graft MW on PUU-OPEO surfaces at 1.0 mg/mL protein concentration.

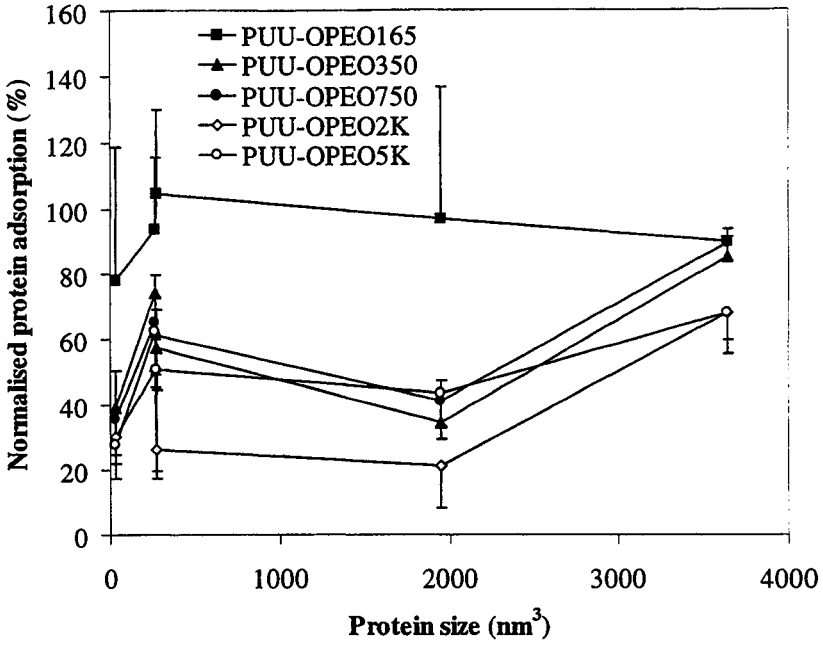

Figure 11.5: Protein adsorption as a function of protein size on the PUU-OPEO surfaces at 0.001 mg/mL protein concentration (± S.D., n=6 or 9).

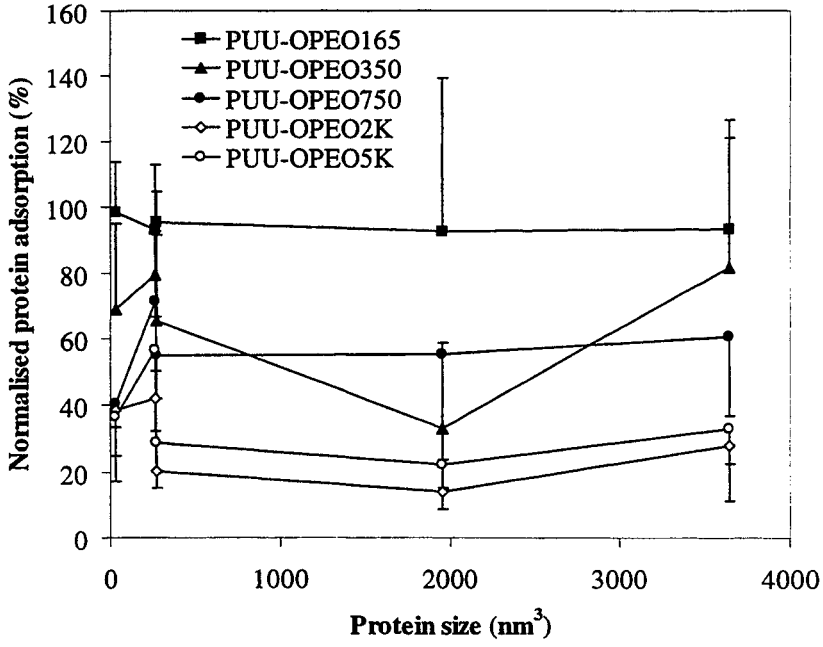

Figure 11.6: Protein adsorption as a function of protein size on the PUU-OPEO surfaces at 0.01 mg/mL protein concentration (± S.D., n=6 or 9).

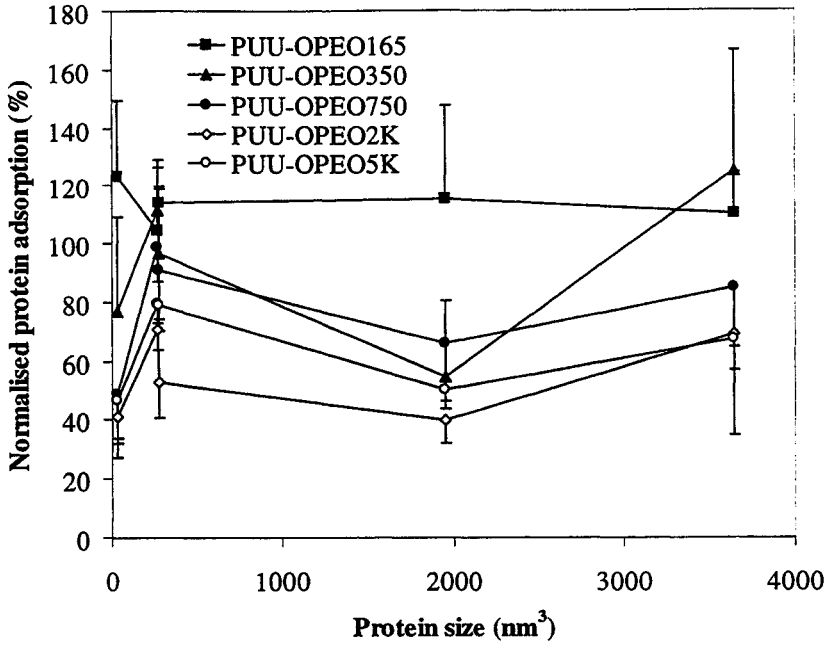

Figure 11.7: Protein adsorption as a function of protein size on the PUU-OPEO surfaces at 0.5 mg/mL protein concentration (±S.D., n=6 or 9).

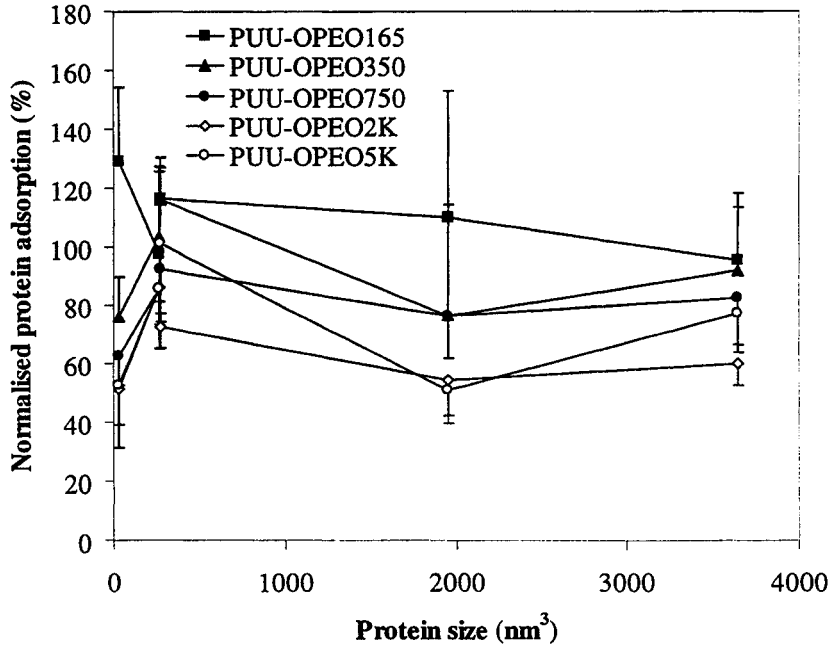

Figure 11.8: Protein adsorption as a function of protein size on the PUU-OPEO surfaces at 1.0 mg/mL protein concentration (±S.D., n=6 or 9).

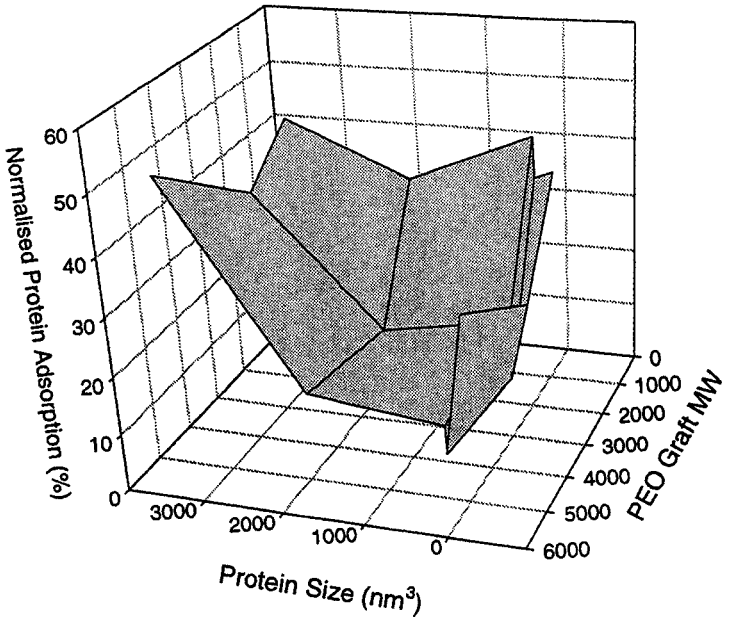

Figure 11.9: Protein adsorption response surface showing the effects of protein size and PEO graft MW on PUU-NPEO surfaces at 0.001 mg/mL protein concentration.

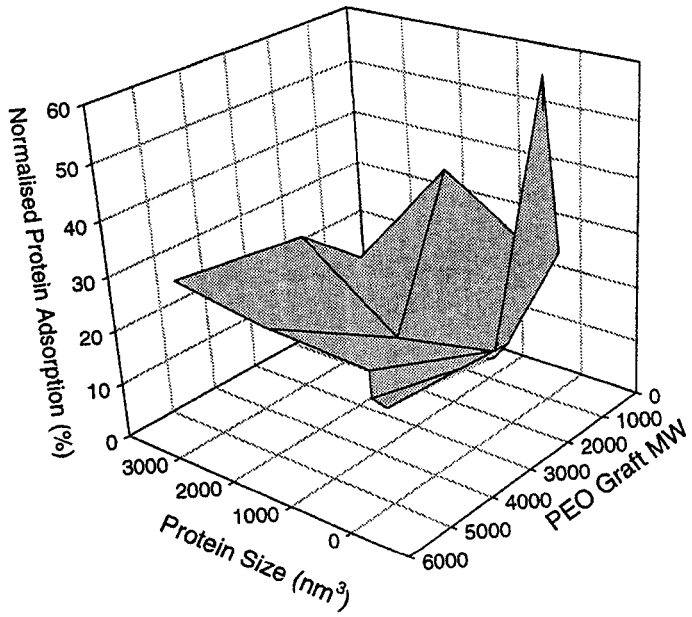

Figure 11.10: Protein adsorption response surface showing the effects of protein size and PEO graft MW on PUU-NPEO surfaces at 0.1 mg/mL protein concentration.

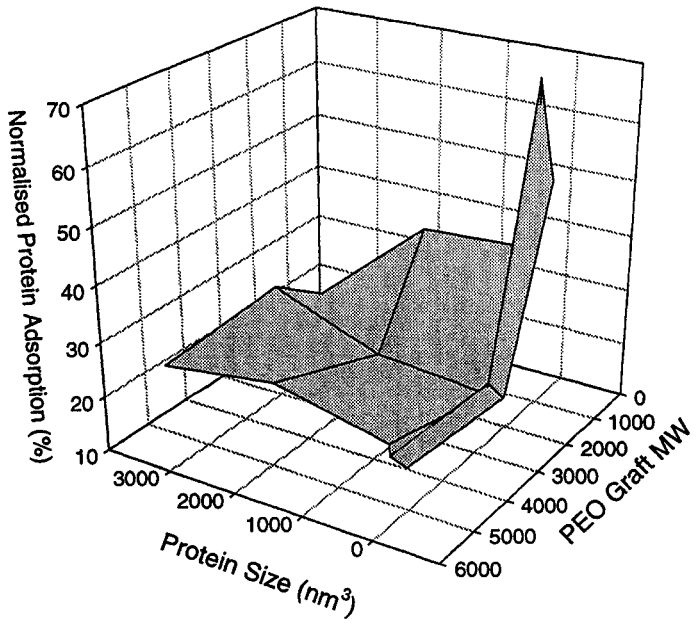

Figure 11.11: Protein adsorption response surface showing the effects of protein size and PEO graft MW on PUU-NPEO surfaces at 0.5 mg/mL protein concentration.

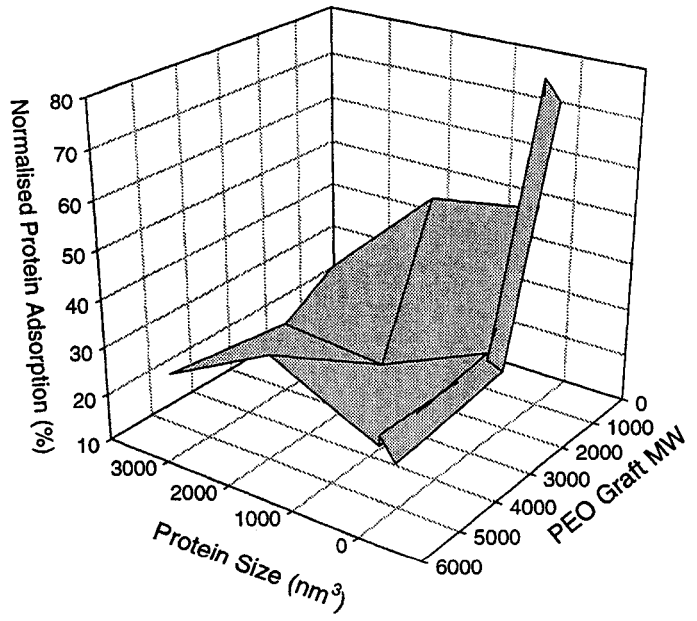

Figure 11.12: Protein adsorption response surface showing the effects of protein size and PEO graft MW on PUU-NPEO surfaces at 2.5 mg/mL protein concentration.

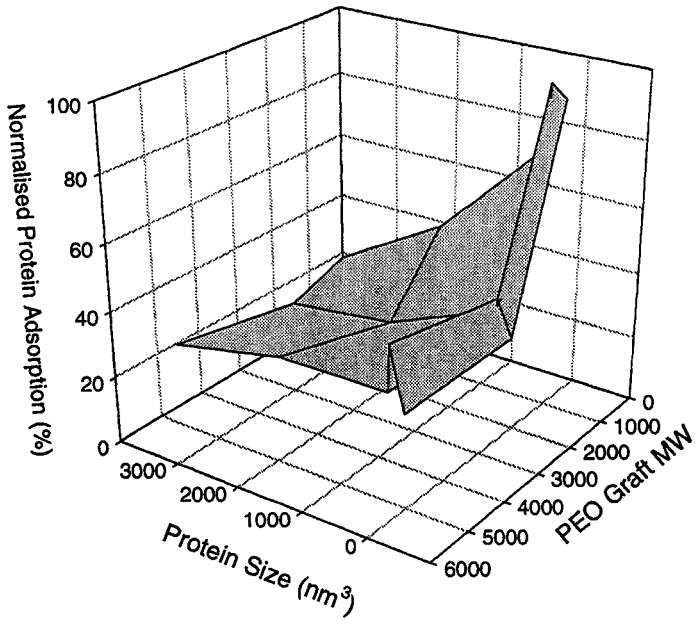

Figure 11.13: Protein adsorption response surface showing the effects of protein size and PEO graft MW on PUU-NPEO surfaces at 5.0 mg/mL protein concentration.

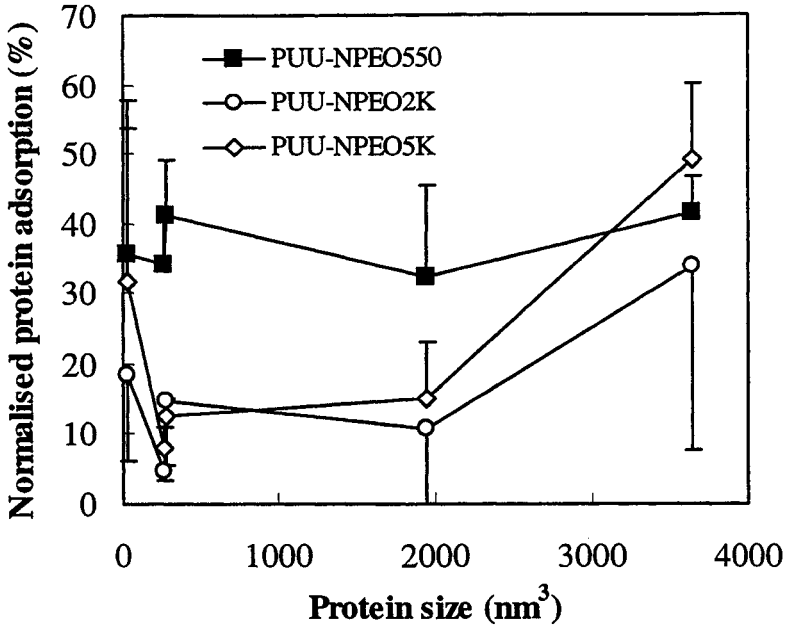

Figure 11.14: Protein adsorption as a function of protein size on the PUU-NPEO surfaces at 0.001 mg/mL protein concentration (±S.D., n=3, 6 or 9).

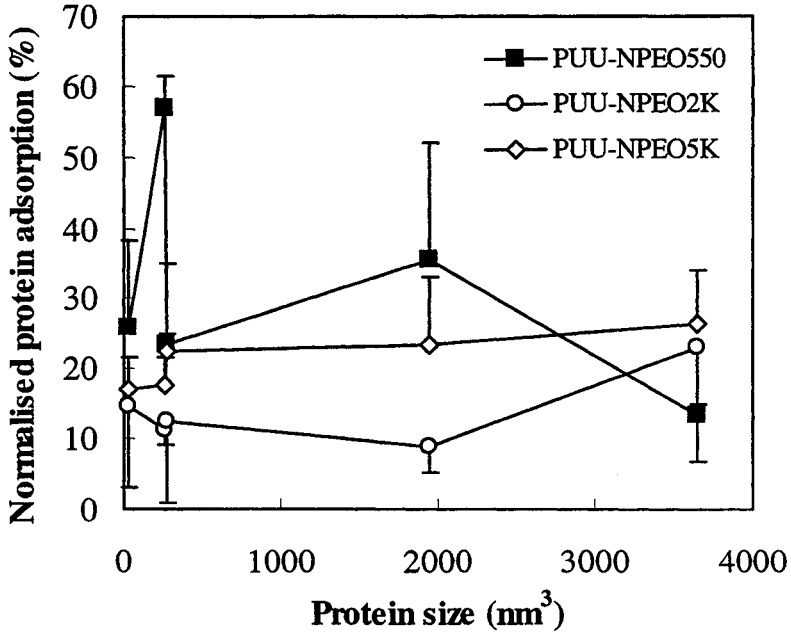

Figure 11.15: Protein adsorption as a function of protein size on the PUU-NPEO surfaces at 0.1 mg/mL protein concentration (±S.D., n=3, 6 or 9).

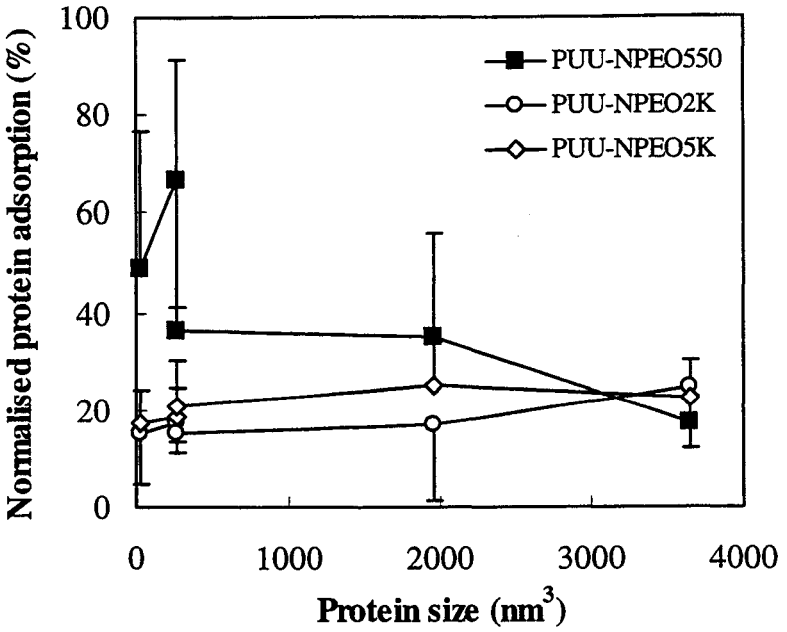

Figure 11.16: Protein adsorption as a function of protein size on the PUU-NPEO surfaces at 0.5 mg/mL protein concentration (±S.D., n=3, 6 or 9).

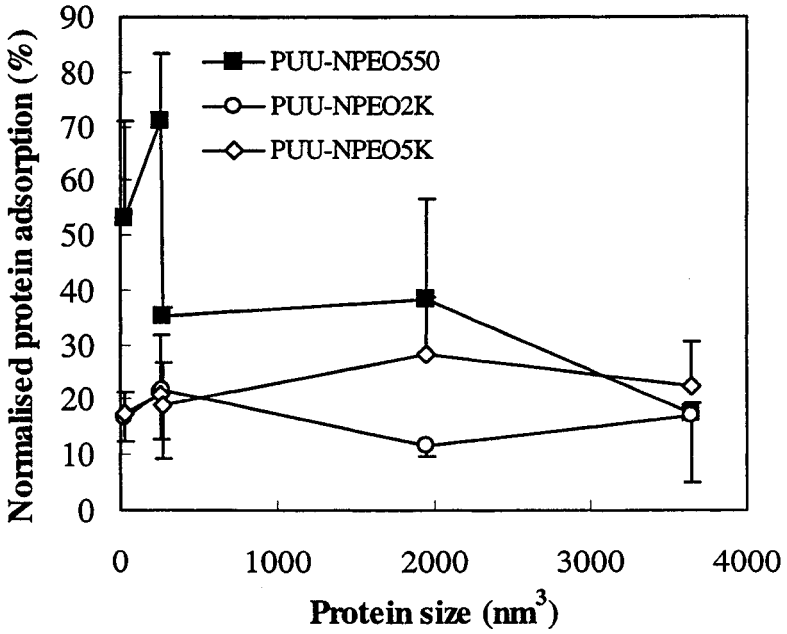

Figure 11.17: Protein adsorption as a function of protein size on the PUU-NPEO surfaces at 1.0 mg/mL protein concentration (±S.D., n=3, 6 or 9).

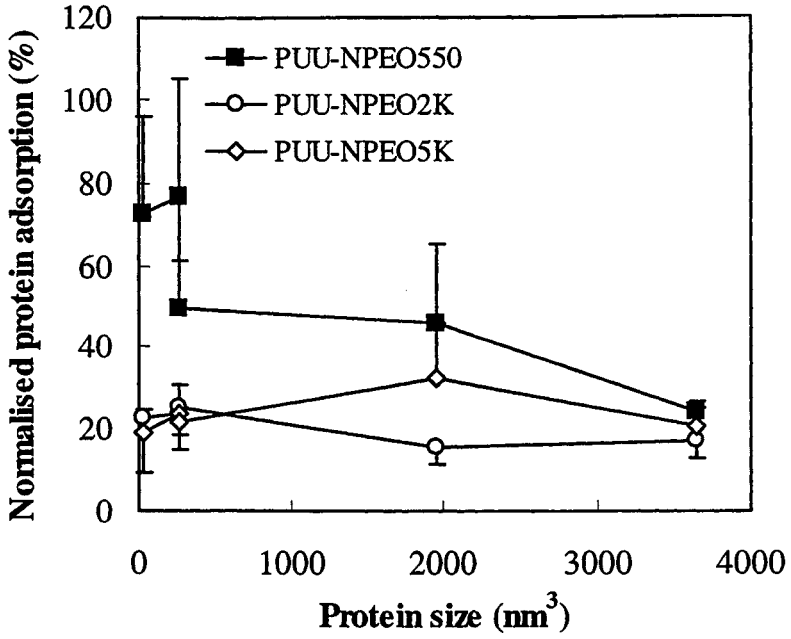

Figure 11.18: Protein adsorption as a function of protein size on the PUU-NPEO surfaces at 2.5 mg/mL protein concentration (±S.D., n=3, 6 or 9).

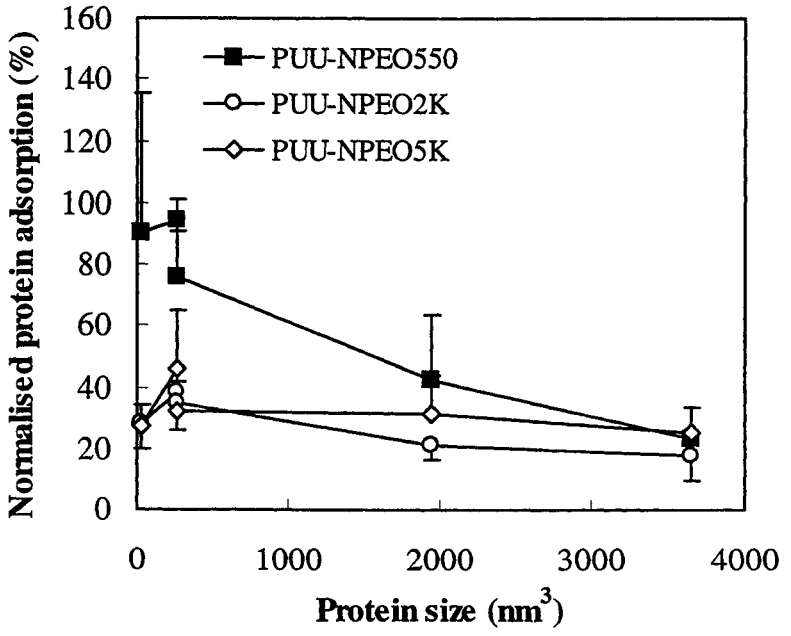

Figure 11.19: Protein adsorption as a function of protein size on the PUU-NPEO surfaces at 5.0 mg/mL protein concentration (±S.D., n=3, 6 or 9).

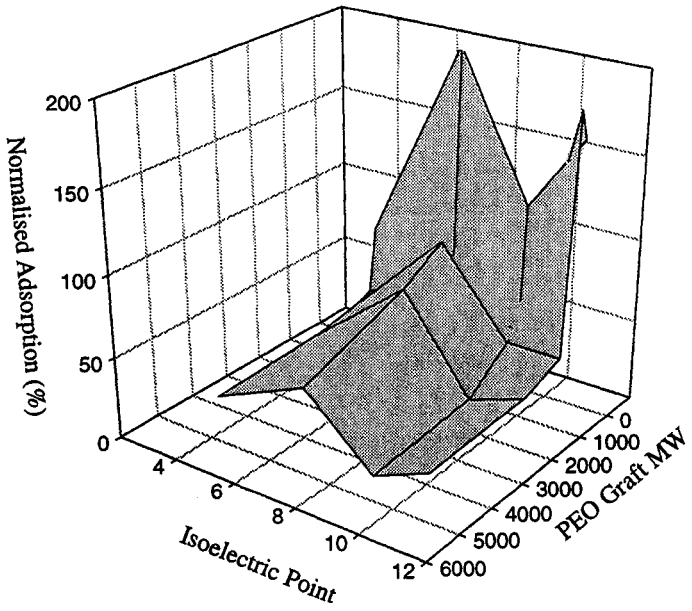

Figure 11.20: Protein adsorption response surface showing the effects of protein isoelectric point and PEO graft MW on PUU-OPEO surfaces at 0.001 mg/mL protein concentration.

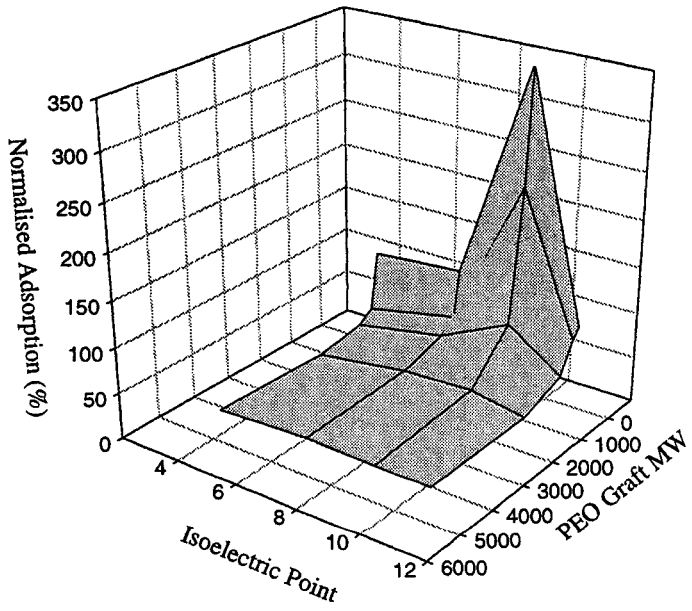

Figure 11.21: Protein adsorption response surface showing the effects of protein isoelectric point and PEO graft MW on PUU-OPEO surfaces at 0.1 mg/mL protein concentration.

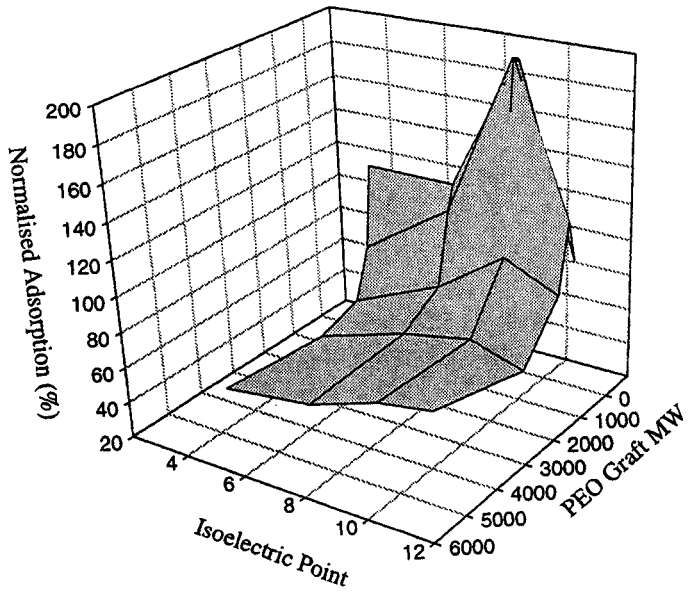

Figure 11.22: Protein adsorption response surface showing the effects of protein isoelectric point and PEO graft MW on PUU-OPEO surfaces at 0.5 mg/mL protein concentration.

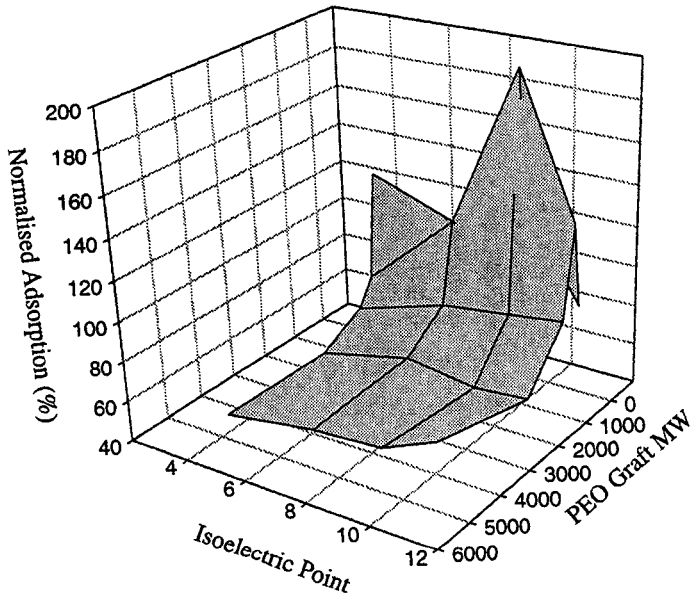

Figure 11.23: Protein adsorption response surface showing the effects of protein isoelectric point and PEO graft MW on PUU-OPEO surfaces at 1.0 mg/mL protein concentration.

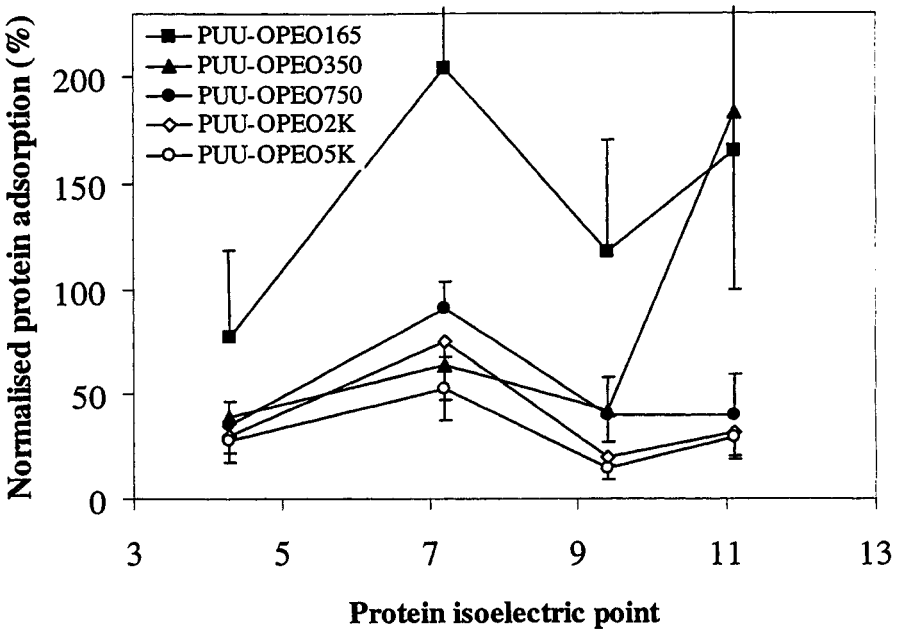

Figure 11.24: Protein adsorption as a function of isoelectric point on the PUU-OPEO surfaces at 0.001 mg/mL protein concentration (±S.D., n= 6 or 9).

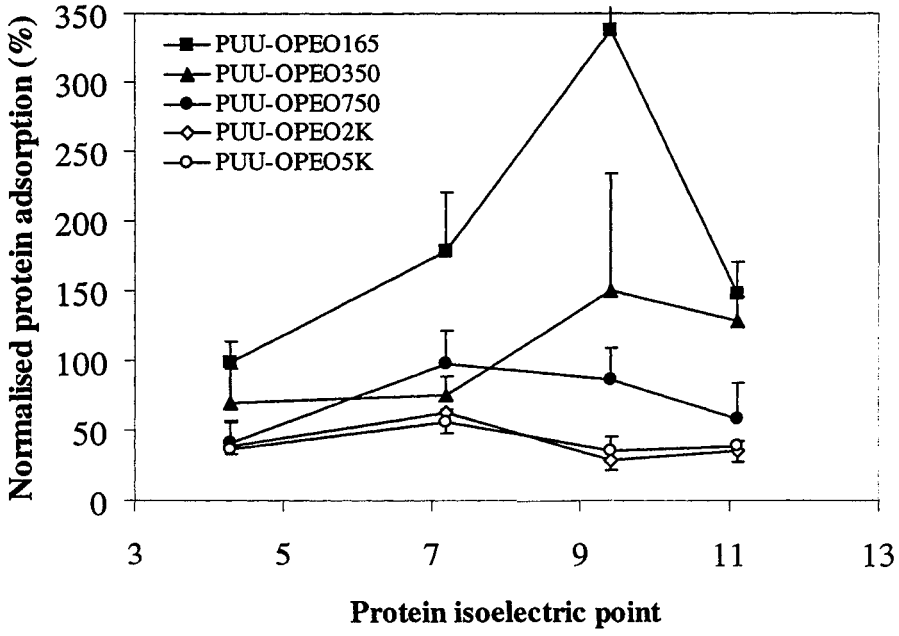

Figure 11.25: Protein adsorption as a function of isoelectric point on the PUU-OPEO surfaces at 0.01 mg/mL protein concentration (±S.D., n= 6 or 9).

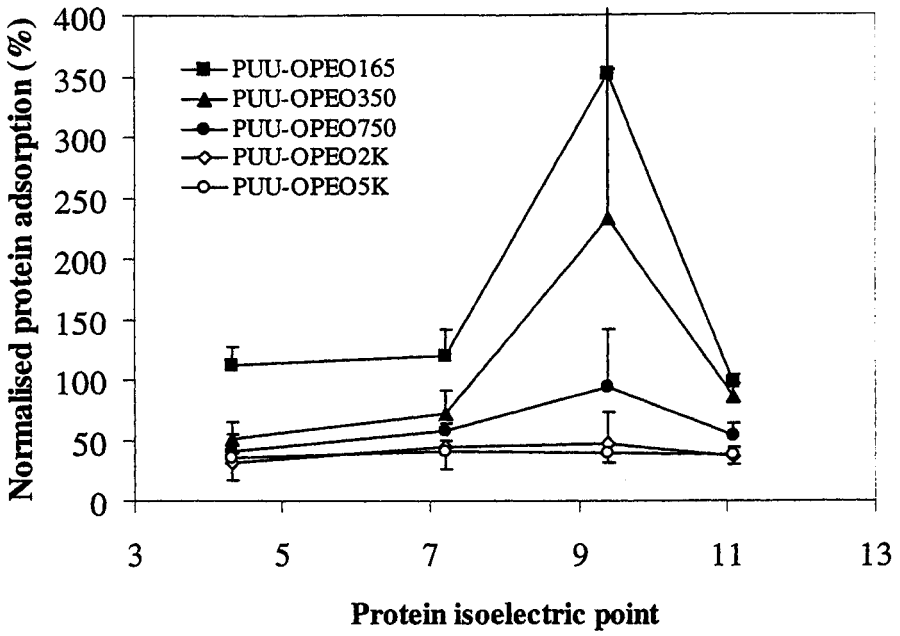

Figure 11.26: Protein adsorption as a function of isoelectric point on the PUU-OPEO surfaces at 0.1 mg/mL protein concentration (±S.D., n= 6 or 9).

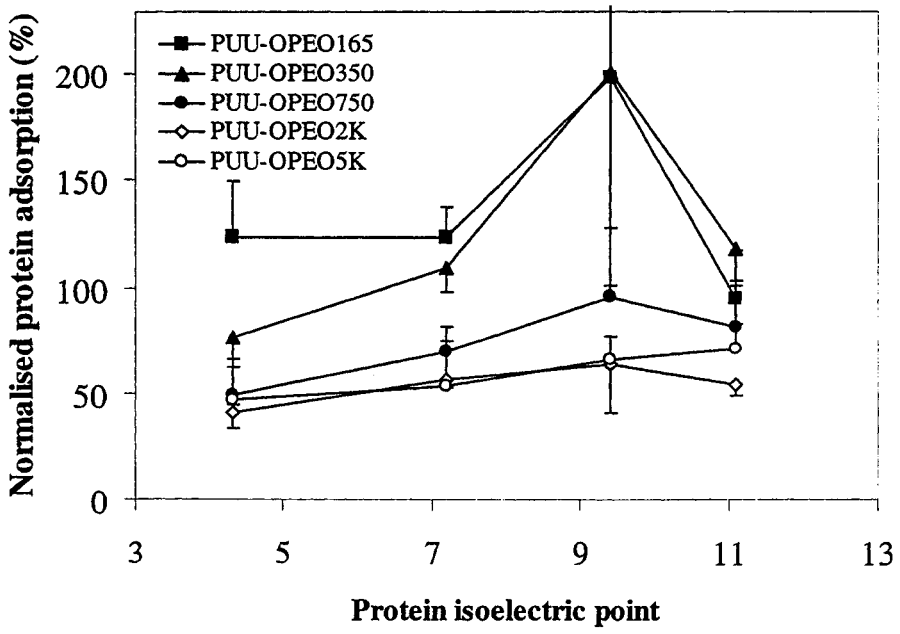

Figure 11.27: Protein adsorption as a function of isoelectric point on the PUU-OPEO surfaces at 0.5 mg/mL protein concentration (±S.D., n= 6 or 9).

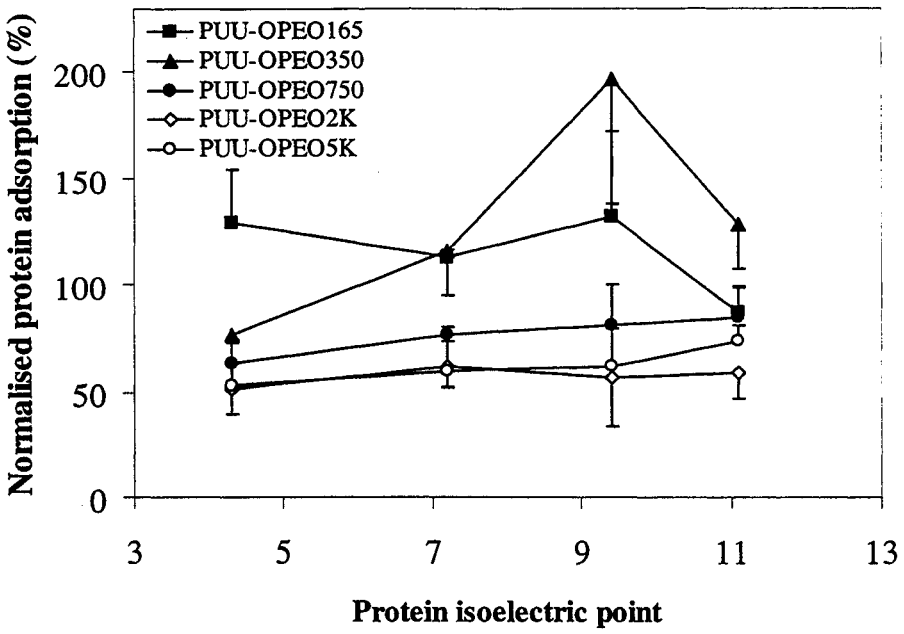

Figure 11.28: Protein adsorption as a function of isoelectric point on the PUU-OPEO surfaces at 1.0 mg/mL protein concentration (±S.D., n= 6 or 9).